

PALACKÝ UNIVERSITY OLOMOUČ

FACULTY OF SCIENCE

DEPARTMENT OF CHEMICAL BIOLOGY AND GENETICS



Study of molecular mechanism and biological activity of strigolactones

Ph.D. Thesis

Author: Mgr. Adéla Hýlová

Study programme: P1527/Biology

Study field: 1507V004/Botany

Supervisor: Mgr. Lukáš Spíchal, Ph.D.

Declaration

I hereby declare that the work presented in this PhD thesis is originally mine and the manuscript was written by myself with help of literature cited.

Olomouc, 4.5.2020

Acknowledgements

I would like to thank my supervisor Lukáš Spíchal for professional guidance and help with solving all the obstacles on the way to my PhD. Thank you to Tomáš Pospíšil and Binne Zwanenburg, for close collaboration and useful hints. Thanks also belongs to Nuria De Diego for guidance, never ending enthusiasm and motivation. Furthermore, I must not forget Jean-Bernard Pouvreau and the staff of the Plant Pathology lab of University in Nantes, for hosting and teaching me during my 3-month stay. I am grateful for the COST-FA1206 STREAM project, which financed this stay.

Thanks to my dear colleagues Lidia Ugena García-Consuegra, Kateřina Podlešáková, Alba Esteban Hernandiz and the staff of the Department of Chemical Biology and Genetics for creating a friendly atmosphere at the workplace. Lastly, big thanks belong to my friends and family for encouragement, support and putting their trust in me.

Contents

Bibliographical identification.....	6
Bibliografická identifikace.....	7
List of abbreviations.....	8
1. Introduction – the youngest group of plant hormones discovered	10
2. Aims of work	11
3. Various functions of SLs	12
3.1. Chemical properties	12
3.1.1. Natural SLS	12
3.1.2. Synthetic SLs	15
3.2. Similarity with karrikins	17
3.3. Biosynthesis	18
3.4. Perception of SL signal.....	21
3.4.1. Perception in non-parasitic plants	21
3.4.2. Perception in parasites.....	22
3.4.3. Mode of action of perception in parasites	23
4. Crosstalk with other hormones	24
4.1. Action in parasitic plants	25
5. Parasitic plants from <i>Orobanchaceae</i> family	26
5.1. Parasitic weeds – control by suicidal germination.....	29
5.2. Other methods of parasitic infestation control.....	30
6. Bioassays for testing strigolactone activity	32
6.1. Standard germination assay	32
6.2. Hyphal branching assay	33
6.3. Pea branching assay	34
6.4. A high-throughput germination assay for root parasitic plants	34
6.5. Adventitious rooting assay.....	36
6.6. A genetically encoded biosensor enabling quantitative analysis of strigolactone signalling.....	36
6.7. A reporter assay based on monitoring luminescence <i>in planta</i>	37

7. Material and methods.....	39
7.1. Plant material	39
7.2. Standard germination assay	39
7.3. High-throughput colorimetric germination assay	40
7.4. Pea branching assay	40
7.5. High-throughput colorimetric germination assay for <i>Arabidopsis</i> in salt conditions.....	40
8. Survey of results	42
8.1. Germination assays for parasitic weeds	42
8.2. Pea branching inhibition by SLs	47
8.3. <i>Arabidopsis</i> germination under salt stress	49
9. Conclusions and perspectives	52
10. References.....	54
10.1. Web references.....	67
11. Supplement	69
11.1. Hýlová, A., Pospíšil, T., Spíchal, L., Mateman, J. J., Blanco-Ania, D., and Zwanenburg, B. (2019). New hybrid type strigolactone mimics derived from plant growth regulator auxin. <i>N. Biotechnol.</i> 48:76–82.....	69
11.2. Dvořáková, M., Hýlová, A., Soudek, P., Retzer, K., Spíchal, L., and Vaněk, T. (2018). Resorcinol-Type Strigolactone Mimics as Potent Germinators of the Parasitic Plants <i>Striga hermonthica</i> and <i>Phelipanche ramosa</i> . <i>J. Nat. Prod.</i> 81(11):2321-2328. Dvořáková, M., Hýlová, A., Soudek, P., Retzer, K., Spíchal, L., and Vaněk, T. (2019). Correction to Resorcinol-Type Strigolactone Mimics as Potent Germinators of the Parasitic Plants <i>Striga hermonthica</i> and <i>Phelipanche ramosa</i> . <i>J. Nat. Prod.</i> 82:168–168.....	111
11.3. Dvořáková, M., Hýlová, A., Soudek, P., Petrová, Š., Spíchal, L., and Vaněk, T. (2019). Triazolidine strigolactone mimics as potent selective germinators of parasitic plant <i>Phelipanche ramosa</i> . <i>Pest Manag. Sci.</i> 75:2049–2056.....	133
11.4. Ugena, L., Hýlová, A., Podlešáková, K., Humplík, J. F., Doležal, K., De Diego, N., and Spíchal, L. (2018). Characterization of Biostimulant Mode of Action Using Novel Multi-Trait High-Throughput Screening of <i>Arabidopsis</i> Germination and Rosette Growth. <i>Front. Plant Sci.</i> 9:1327.....	159

BIBLIOGRAPHICAL IDENTIFICATION

First name and surname	Adéla Hýlová
Degree/Title	Mgr.
Type of thesis	Ph.D.
Department	Department of Chemical Biology and Genetics, CRH
Supervisor	Mgr. Lukáš Spíchal, Ph.D.
The year of presentation	2020
Abstract	<p>Strigolactones (SLs) have been recently discovered as signalling molecules and plant hormones. Apart from other functions in plants, they are active as germination stimulants for seeds of parasitic weeds, which are noxious pests causing a loss in yield of important crops. The work presented in this thesis includes optimization and implementation of bioassays aimed at germination of parasitic weeds upon application of SLs. A high-throughput bioassay, which is a colorimetric method based on spectrophotometric reading of absorbance, was successfully established. It was subsequently used to test the ability of newly synthesized SL derivatives (so-called SL mimics) to germinate severe parasites <i>Striga hermonthica</i>, <i>Phelipanche ramosa</i> and <i>Orobancha minor</i>. Several hybrid mimics combining structure of SL with an auxin moiety showed bioactivity as high as that of a standard, GR24, i.e. 0.5 nM. Triazolid and resorcinol type SL mimics showed considerable activity in nanomolar concentration, approximately 100-fold lower compared to GR24. In addition, general principle of the colorimetric method was used to develop high-throughput germination bioassay of <i>Arabidopsis thaliana</i> in salt stress conditions. The assay was validated by testing four compounds of natural origin, so-called biostimulants, with a proven effect on plants subjected to stress. It represents a high capacity tool suitable for analysis of many compounds within a single run of an experiment.</p>
Keywords	Strigolactone, SL mimics, parasitic weeds, <i>Striga</i> , <i>Phelipanche</i> , <i>Orobancha</i> , germination, bioassay, biostimulant, <i>Arabidopsis</i>
Number of pages	68
Number of appendices	4
Language	English

BIBLIOGRAFICKÁ IDENTIFIKACE

Jméno a příjmení	Adéla Hýlová
Titul	Mgr.
Typ práce	Ph.D.
Pracoviště	Oddělení chemické biologie a genetiky, CRH
Školitel	Mgr. Lukáš Spíchal, Ph.D.
Rok odevzdání	2020
Abstrakt	<p>Strigolaktony byly nedávno identifikovány jako signální molekuly a rostlinné hormony. Kromě jiných funkcí v rostlinném organismu vykazují aktivitu vůči klíčení semen parazitických rostlin, které jsou závažnými škůdci a způsobují velké ztráty ve výnosu hospodářských plodin. Výzkum prezentovaný v této dizertační práci zahrnuje optimalizaci a zavedení biotestů zaměřených na klíčení parazitů po aplikaci strigolaktonů. Do rutinního používání byl zaveden vysokokapacitní biotest (tzv. high-throughput), který je kolorimetrickou metodou založenou na spektrofotometrickém měření absorbance. Poté byl použit v testování schopnosti nových strigolaktonových derivátů (tzv. mimetik) indukovat klíčení parazitických rostlin <i>Striga hermonthica</i>, <i>Phelipanche ramosa</i> a <i>Orobancha minor</i>. Některá hybridní mimetika mající strukturu složenou částečně ze strigolaktonu a částečně z auxinu, vykazovala značnou bioaktivitu ve stejné koncentraci jako standard GR24, tj. 0,5 nM. Triazolidová a resorcinolová mimetika byla aktivní v nanomolární koncentraci, v porovnání s GR24 přibližně 100x méně. Obecný princip kolorimetrické metody byl použit k vývoji high-throughput biotestu, zaměřeného na klíčení <i>Arabidopsis thaliana</i> v solném stresu. Biotest byl validován pomocí čtyř látek přírodního původu, tzv. biostimulantů, majících prokázaný účinek na rostliny, které rostou ve stresových podmínkách. Tato metoda představuje vysokokapacitní nástroj vhodný k analýze mnoha látek v jednom experimentu.</p>
Klíčová slova	Strigolakton, SL mimetika, parazitické rostliny, <i>Striga</i> , <i>Phelipanche</i> , <i>Orobancha</i> , klíčení, biotest, biostimulant, <i>Arabidopsis</i>
Počet stran	68
Počet příloh	4
Jazyk	Anglický

LIST OF ABBREVIATIONS

5-DS – 5-deoxystigol

ABA – abscisic acid

AM – arbuscular mycorrhiza

BRC1 – BRANCHED1

CCD – CAROTENOID CLEAVAGE DIOXYGENASE

CK – cytokinin

CKX – CYTOKININ OXIDASE-DEHYDROGENASE

CL – carlactone

CLIM – covalently linked intermediate molecule

CO – CARLACTONE OXIDASE

Col-0 – Columbia-0, an ecotype of *Arabidopsis thaliana* L. Heyn

cv – cultivar

CYP711/CYP707 – cytochrome P450 from 711 or 707 clades

D14/D3/D27/D53 – DWARF14/3/27/53

DAD – DECREASED APICAL DOMINANCE

DMSO – dimethyl sulfoxide

EC₅₀ – half maximal effective concentration

FF – FIREFLY LUCIFERASE

HEPES - 4-(2-hydroxyethyl)-1-piperazineethanesulfonic acid

HTD – HIGH TILLERING DWARF

HTL – HYPOSENSITIVE TO LIGHT

HTS – high-throughput screening

IAA – indole-3-acetic acid

KAI2 – KARRIKIN INSENSITIVE 2

LBO – LATERAL BRANCHING OXIDOREDUCTASE

LC-MS – liquid chromatography-mass spectroscopy

LGS1 – LOW GERMINATION STIMULANT 1

LUC - LUCIFERASE

MAX – MORE AXILLARY GROWTH

MS – Murashige-Skoog

MTT - 3-(4,5-dimethylthiazol-2-yl)-2,5-diphenyltetrazolium bromide

MYA – million years ago

OS – OROBANCHOL SYNTHASE

PE – polyethylene

PEG – polyethylene glycol

PO₄⁻ - phosphate ions

Pro – proline

Put – putrescine

REN – RENILLA LUCIFERASE

RGB – red-green-blue

RMS – RAMOSUS (latin for “branched”)

SAR – structure-activity relationship

SCF – Skp1 – Cullin – F-box protein complex

Skp1 – S-PHASE KINASE ASSOCIATED PROTEIN 1

SL(s) – strigolactone(s)

SMAx-1 - SUPPRESSOR OF MAX2 1

SMAx2, SMAx1 – SIMILAR TO MAX2/1

SMXL – SIMILAR TO MAX2-LIKE

Spm – spermine

Spd – spermidine

1. INTRODUCTION – THE YOUNGEST GROUP OF PLANT HORMONES DISCOVERED

In the past several decades, plant hormones have been intensively studied in order to elucidate their functions within the plant body and to assess their usefulness as applied commercial products. Strigolactones (SLs) are carotenoid-derived plant secondary metabolites that comprise a group of recently discovered plant hormones. In 1966, the first SL molecule was identified in root exudates of cotton and was shown to stimulate seed germination of a parasitic plant *Striga* (Cook, 1966). The name Strigolactone is therefore derived from the word *Striga* and lactone, a structural unit present in all natural SLs. The first synthesis of artificial derivatives of SLs started 1981 (Johnson et al., 1981) and the newly developed branching mutants allowed the study of the formation of lateral branches in plants since 1992 (Arumingtyas et al., 1992, Beveridge et al., 1996). In 2005, SLs were found to be crucial for stimulating hyphal branching of symbiotic arbuscular mycorrhizal (AM) fungi, which are necessary for providing soil nutrients (Akiyama et al., 2006). More recently, SLs were found to be endogenous to plants involved in outgrowth of lateral buds (Gomez Roldan et al., 2008; Umehara et al., 2008). Eventually, the first SL receptor in plants, DWARF14 (D14), was described in rice and petunia (Arite et al., 2009; Hamiaux et al., 2012) and later in the parasitic plant *Striga hermonthica* (Conn et al., 2015; Toh et al., 2015; Tsuchiya et al., 2015). Fig. 1 summarizes the main milestones in SL research.

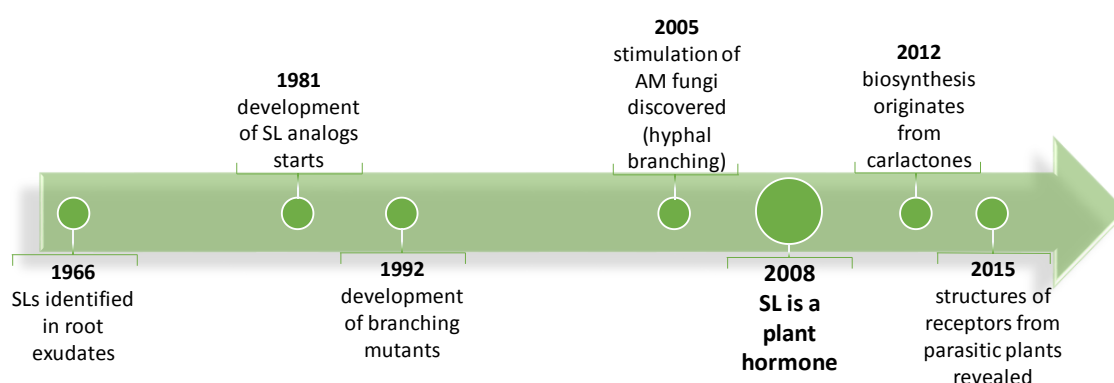


Fig. 1. An overview of important milestones in strigolactone research (according to Lumba et al., 2017).

SLs represent a group of exciting biologically active molecules, which offer a lot of research possibilities not only at a level of basic research but also have the potential to be applied in agriculture.

2. AIMS OF WORK

1. Literature search of the topic of the thesis
2. Implementation of standard germination assay for root parasitic plants
3. Optimization of high-throughput seed germination assay for root parasitic plants
4. Screening of biological activity and structure-activity relationship of new strigolactones
5. Optimization of physiological assay (pea bud outgrowth assay) and high-throughput phenotyping
6. Routine screening of biological activity of new strigolactones

3. VARIOUS FUNCTIONS OF SLs

From the evolutionary point of view, SLs origins date back to basal land plants (460 – 470 MYA), first identified in *Physcomitrella patens* (Proust et al., 2011), where they regulate protonema filament growth. In vascular plants they control several developmental processes, such as shaping root and shoot architecture and affecting leaf senescence (Gomez Roldan et al., 2008; Umehara et al., 2008; Ruyter-Spira et al., 2011; Kapulnik et al., 2011). SLs are exuded by plants via roots, in which their biosynthesis is mainly located to the rhizosphere, where they stimulate hyphal branching of arbuscular mycorrhizal (AM) fungi (Akiyama et al., 2006). It has been found that exudation of SLs is started in phosphate deficiency and is the way the plant seeks to establish a favorable symbiosis with AM fungus (López Ráez et al., 2008). The mechanism of sensing SLs in the soil was adapted by root parasitic plants, which require a signal to start seed germination. Another function is therefore stimulation of parasitic plant seed's germination (Cook et al., 1966; Cook et al., 1972), which is the primary focus of this thesis, as parasitic weeds display a threat to world's crop production.

3.1. CHEMICAL PROPERTIES

3.1.1. NATURAL SLs

SL's general structure is composed of four rings (Fig. 2). ABC tricyclic lactone is connected to a butenolide (D-ring), which is the bioactiphore of the SL molecule and is conserved among natural SLs. A biologically important structural feature is the connection of the D-ring to the C-ring via an enol ether bridge. Modifications of the A or B rings, e.g. methyl, hydroxyl or acetoxy substituents, are not critical for retaining the bioactivity (Zwanenburg and Pospíšil, 2013). Until now, 23 natural molecules have been identified (Yoneyama et al., 2018a). Several of them are shown in Fig. 2.

Natural SLs occur in two forms depending on stereochemistry – strigol and orobanchol. Spectral data have shown difference in the BC junction to the D-ring. While the strigol type SLs have the C ring β orientation (3aR, 8bS, 2'R), the orobanchol type SLs have the α orientation (3aR, 8bR, 2'R) (Fig. 2). Historically, (+)-strigol represents a parent molecule of the strigol type of SLs, which include sorgomol, 5-deoxystrigol (5-DS) or sorgolactone while the (–)-orobanchol represents a parent molecule of the orobanchol type of SLs, which include orobanchol acetate, solanacol or fabacyl acetate. Several

studies have described the synthesis and bioassaying of all possible stereoisomers of a compound, such as sorgolactone, strigol and synthetic GR7 (Mangnus and Zwanenburg 1992a; Reizelman et al., 2000; Sugimoto et al., 1997). The stereoisomer with the natural configuration at all chiral carbons was revealed to be the most active, pointing at the importance of the total stereochemistry of the SL molecule. Moreover, the configuration at carbon 2'R was found to be critical.

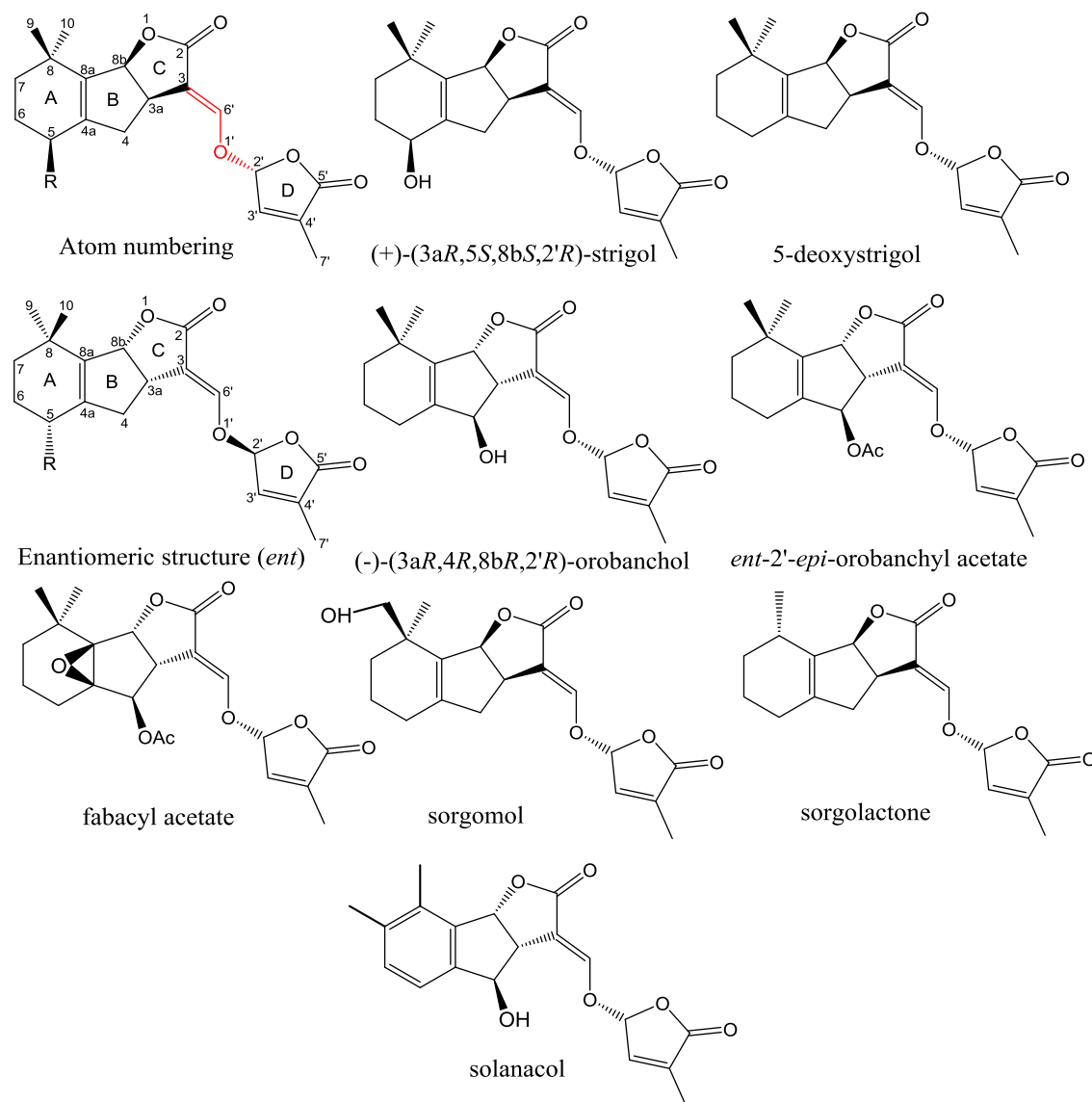


Fig. 2. Structures of common natural SLs. The enol ether bridge is highlighted in red in the general SL structure.

For elucidating the minimal structural unit needed for bioactivity, experiments with artificial SLs GR24, GR7 and GR5 (new compounds named after inventor Gerald Roseberry) were performed (Fig. 3). It has been revealed that the CD part of the molecule

is enough for bioactivity (Hassanali, 1984; Johnson et al., 1976). Butenolide (the D-ring) itself does not cause germination.

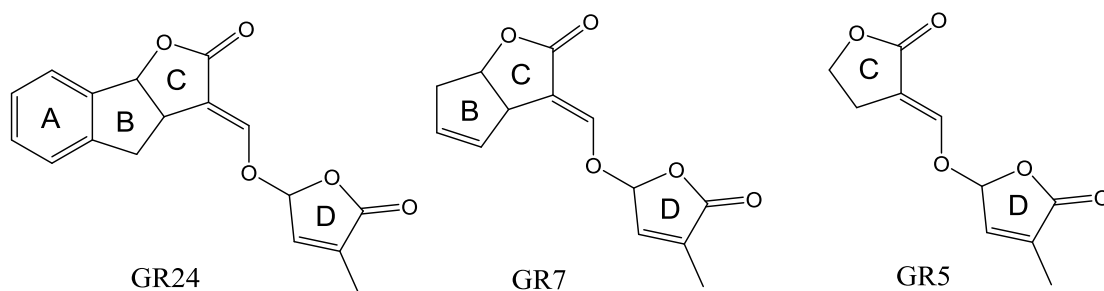


Fig. 3. GR series of synthetic SLs. GR5 is still active in germination assays, suggesting CD rings are enough for biological activity.

Another classification of SLs considers the less conserved moiety. Canonical SLs possess a tricyclic lactone (i.e. ABC rings), such as strigol, 5-DS, orobanchyl acetate and orobanchol (Fig. 2). On the contrary, non-canonical SLs vary significantly in the moiety connected to the D-ring and are produced by specific plant species, e.g. heliolactone, dehydrocostus lactone (*Helianthus annuus*), peagol (*Pisum sativum*) or zealactone (*Zea mays*) (Ueno et al., 2014; Joel et al., 2011; Evidente et al., 2009; Charnikhova et al., 2017). It has also been reported that compounds present in smoke after combustion of plant material, such as karrikinolide, which resembles SLs structurally, induce germination of non-parasitic plants (Baldwin 1994, Dixon et al., 1995, Flematti et al., 2004) (Fig. 4).

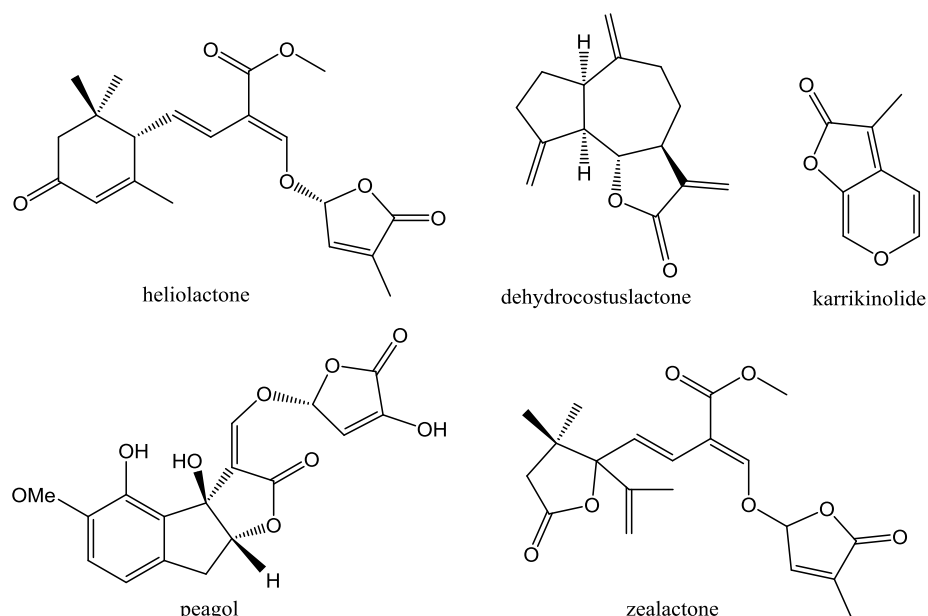
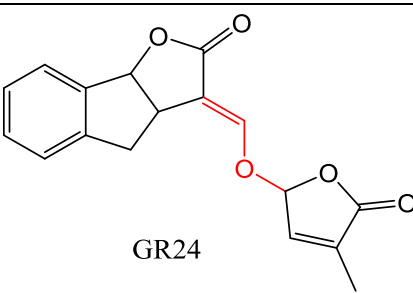
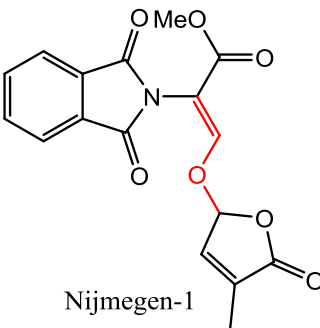
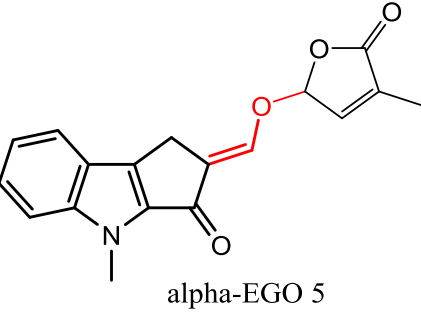
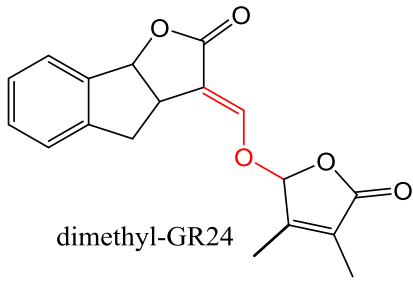
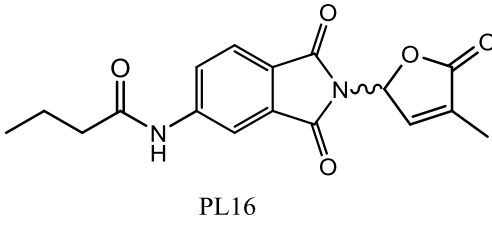


Fig. 4. Structurally different non-canonical SLs.

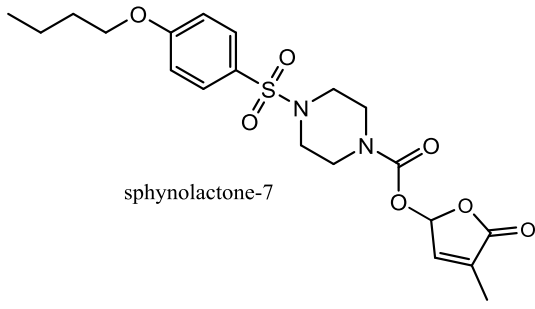
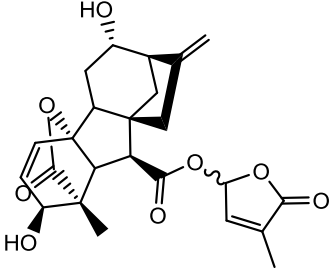
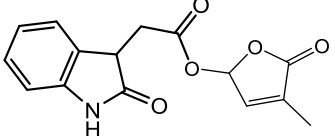
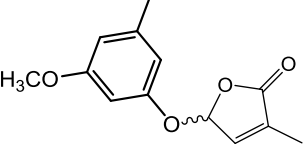
3.1.2. SYNTHETIC SLs

Total synthesis of natural SLs is linear procedure consisting of many steps and is very complicated. There has been an intensive search for synthetic molecules with simpler synthesis and retained bioactivity. Artificial compounds that have the enol ether bridge and the variable moiety connected to the D-ring like the natural SLs were successfully synthesized and are collectively called SL analogues. SL mimics represent another group of synthetic compounds, which have a much simpler structure, i.e. do not contain the canonical A, B, C rings and interestingly retain bioactivity despite the replacement of the enol ether bridge with a simpler linkage of the D-ring to the variable moiety. This emphasizes the important role of the D-ring. A variety of active SL analogues and mimics have been reported and assayed in bioassays and are described in chapter 6 and several of them are presented in Tab.1.

Tab.1. Synthetic SLs with proven bioactivity. Enol ether bridge in SL analogs is highlighted in red, the rest of the compounds represent SL mimics.

Structure	Activity in germination assay	Reference
 <p>GR24</p>	3.4×10^{-8} M 68 % <i>S. hermonthica</i> ; 3.4×10^{-6} M 78 % <i>O. crenata</i> , 3.3×10^{-10} M 70 % <i>P. ramosa</i> ; 10^{-6} M 90 % <i>P. aegyptiaca</i> ; 10^{-6} M 97 % <i>O. minor</i>	Mangnus et al., 1992b; Malik et al., 2011; Oancea et al., 2017; Xie et al., 2007;
 <p>Nijmegen-1</p>	3.4×10^{-6} M 40 % <i>S. hermonthica</i> , 3.4×10^{-7} M 35 % <i>O. crenata</i>	Nefkens et al., 1997
 <p>alpha-EGO 5</p>	10^{-12} M 60 % <i>P. aegyptiaca</i>	Prandi et al., 2011
 <p>dimethyl-GR24</p>	10^{-8} M 50% <i>P. ramosa</i> , <i>O. minor</i> , <i>S. hermonthica</i>	Boyer et al., 2012; Boyer et al., 2014
 <p>PL16</p>	10^{-5} M 70 % <i>O. minor</i>	Cala et al., 2016

Tab.1. Synthetic SLs with proven bioactivity. (Continued).

Structure	Activity in germination assay	Reference
 <p>sphynolactone-7</p>	10^{-11} M 60 % <i>S. hermonthica</i>	Uraguchi et al., 2018
 <p>Gibberelic hybrid SL mimic</p>	10^{-8} M 40 % <i>O. minor</i> , <i>P. aegyptiaca</i>	Pereira et al., 2017
 <p>Auxin hybrid SL mimic</p>	10^{-8} M 70% <i>P. ramosa</i> , 10^{-6} M 50 % <i>O. minor</i> , 10^{-6} M 80 % <i>S. hermonthica</i>	Hýlová et al., 2019 (this work)
 <p>resorcinol type SL mimic</p>	10^{-9} M 50 % <i>P. ramosa</i> , 10^{-7} M 50 % <i>S. hermonthica</i>	Dvořáková et al., 2018 (this work)

3.2. SIMILARITY WITH KARRIKINS

Several studies have shown that smoke from fire burnt areas triggers seed germination of more than 80 genera (Chiwocha et al., 2009; Dixon et al., 1995). An analysis of smoke water was performed and the first compound responsible for elicitation of germination was identified as butenolide (Flematti et al., 2004; Flematti et al., 2009; van Staden et al., 2004). The word “karrik”, which comes from aboriginal language and means “smoke”, was used to form a collective name for these compounds later – karrikins (Dixon et al., 2009). Although karrikins were not proven to be endogenous to plants, their structure is butenolide based and resemble SLs (Fig. 4).

Later it was discovered that karrikins and SLs share common features regarding signalling. Both receptors KAI2 (KARRIKIN INSENSITIVE 2) and D14 associate with the F-box protein encoded by the *MAX2* gene (*MORE AXILLARY GROWTH 2*) in *Arabidopsis* and transfer the signal further (Nelson et al., 2011; Waters et al., 2012). KAI2 perceives karrikins and is important in seed germination, as its transcripts are highly expressed in seeds. D14 is SL specific and plays a role in shoot branching inhibition, as suggested by higher transcription levels in seedlings (Waters et al., 2012).

KAI2 is involved in responses to stress. It has been found that *Arabidopsis* seeds with a *kai2* mutation showed inhibited germination upon exogenous treatment with karrikins under high temperature and osmotic stress. When favourable conditions were applied, karrikins stimulated germination of wild-type seeds. This suggests that karrikin-KAI2 signalling system offers protection against abiotic stresses (Wang et al., 2018).

3.3. BIOSYNTHESIS

SLs are derived from carotenoids, terpenoid pigments present in all plants (Matušová et al., 2005). Although biosynthesis has not been elucidated completely, several key steps are known. The initial step involves enzyme DWARF27 (D27), which is an isomerase catalysing conversion of all-trans- β -carotene to 9-cis- β -carotene. CAROTENOID CLEAVAGE DIOXYGENASE 7 (CCD7) is a stereospecific enzyme and forms two products, β -ionone and 9-cis- β -apo-10'-carotenal (Alder et al., 2012; Bruno et al., 2014). Cleavage of C27 product by CAROTENOID CLEAVAGE DIOXYGENASE 8 (CCD8) leads to an intermediate carlactone (CL), that contains a D-ring in the 2'R configuration (Alder et al., 2012; Seto et al., 2014). CL is widely considered as a direct precursor because it significantly resembles the SL structure and has the same number of carbon atoms as natural SLs. Further biosynthesis involves cytochromes P450 from 711 clade (CYP711), encoded by the *MORE AXILLARY GROWTH 1* (*MAX1*) gene, that are probably responsible for SL diversity (Abe et al., 2014; Alder et al., 2012; Zhang et al., 2014; Zhang et al., 2018). The *MAX1* expression product converts carlactone to carlactonoic acid in a conserved manner (Yoneyama et al., 2018b). Another enzyme that takes part in the final steps of biosynthesis is LATERAL BRANCHING OXIDOREDUCTASE (LBO), discovered recently in *Arabidopsis*

thaliana. It converts methyl carlactonoate to an unknown compound, that may be the final product of SL biosynthesis (Brewer et al., 2016) (Fig. 5).

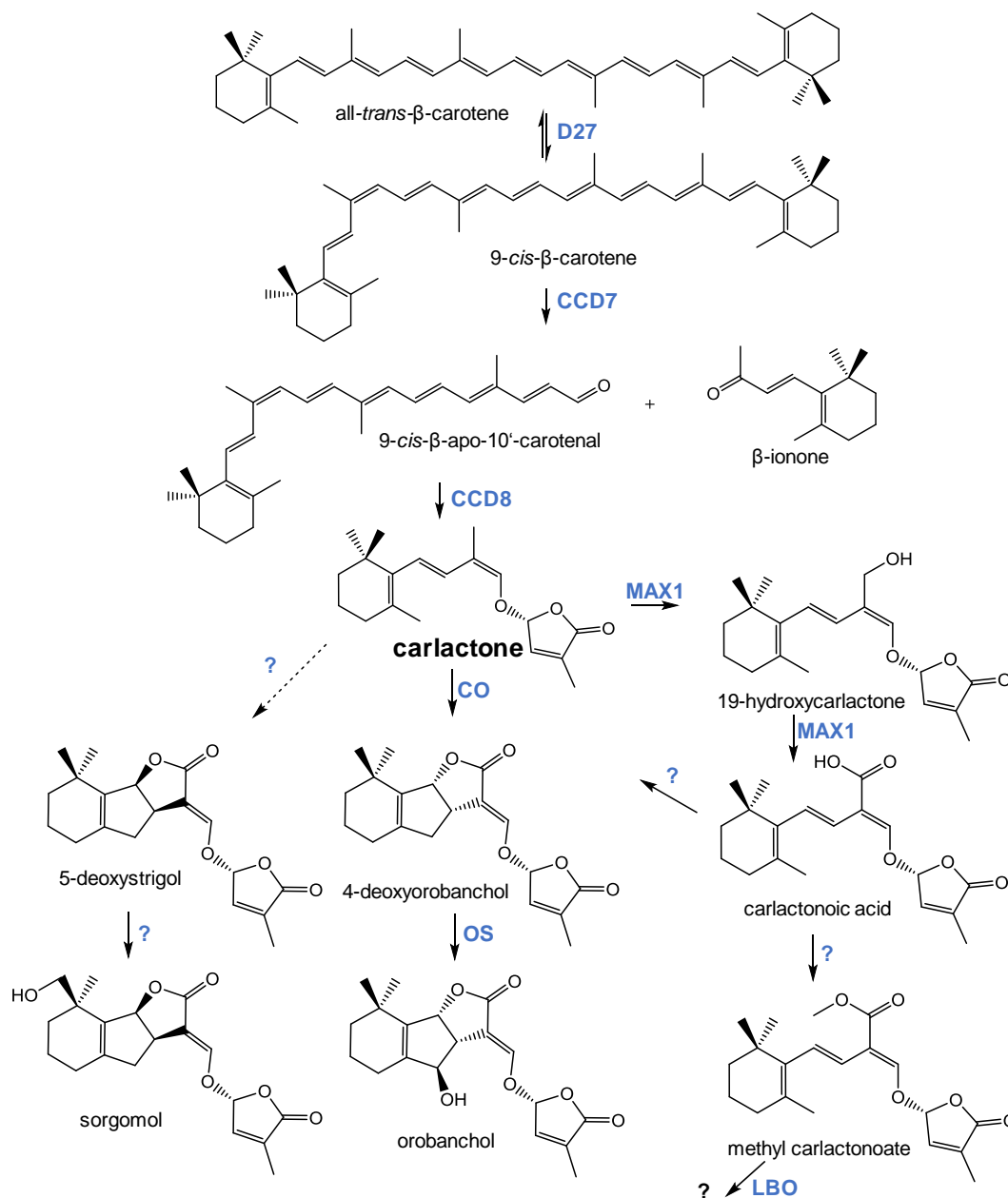


Fig. 5. SL biosynthesis pathway. (D27 = DWARF27, CCD7/8 = CAROTENOID CLEAVAGE DIOXYGENASE 7/8, CO = CARLACTONE OXIDASE, MAX1 = MORE AXILLARY GROWTH 1, OS = OROBANCHOL SYNTHASE, LBO = LATERAL BRANCHING OXIDOREDUCTASE) (according to Jia et al., 2018).

Some steps remain unresolved, e.g. the mechanism of carlactone generation by CCD8 or an enzyme responsible for formation of 5-DS from carlactone. However, the latter one has been recently studied and it was found that a sulfotransferase *LOW*

GERMINATION STIMULANT 1 (lgs1) mutant of sorghum (*Sorghum bicolor*) produced orobanchol in root exudates as the main SL and not 5-DS, which is typical for wild-type sorghum. This led to increased resistance of sorghum mutants to the parasitic plant *Striga hermonthica* (Gobena et al., 2017).

Moreover, the structural diversity of strigolactones is caused by the action of modifying enzymes that remain to be discovered. It is a non-conserved species-specific pathway (Iseki et al., 2018).

Historically, mutants of pea, *Arabidopsis* and rice that were impaired in carotenoid biosynthesis (genes encoding CCDs and CYP450, summarized in Tab. 2) were used to study the signal responsible for the inhibition of lateral shoot development. LC-MS analysis showed that the mutants had decreased production of SLs or did not produce SLs at all. All mutants having impaired SL biosynthesis or signalling showed a dwarf phenotype and increased branching (Fig. 6). Exogenous application of GR24 rescued the phenotype of wild-type plants (Gomez Roldan et al., 2008; Umehara et al., 2008). Since then, increased shoot branching mutants, e.g. *rms1* (*ramosus1*) of pea and *d27* of rice were used to develop bioassays based on testing compounds with potential SL activity on inhibition of bud outgrowth (Boyer et al., 2012).

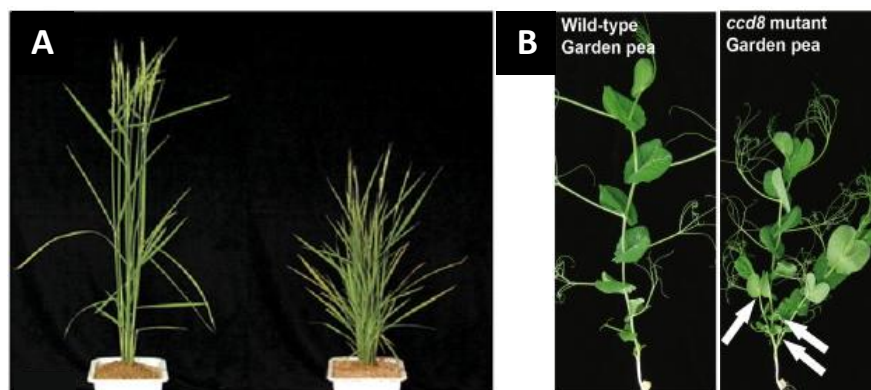


Fig. 6. SL mutants. (A) Dwarf over branched phenotypes of rice signalling mutant *d27* on the right compared to wild type (cultivar Shiokari) on the left. (B) Pea (*Pisum sativum* cv T  r  se) biosynthesis mutant *ccd8* compared to wild-type. (adapted from Dun et al., 2009; Lin et al., 2009).

Tab. 2. Overview of genes and enzymes from selected plants involved in SL biosynthesis.

<i>Arabidopsis</i>	pea	<i>Petunia hybrida</i>	rice	encoded enzyme
<i>AtD27</i>	-	-	<i>D27</i>	D27
<i>MAX3</i>	<i>RMS5</i>	<i>DAD3</i>	<i>HTD1/D17</i>	CCD7
<i>MAX4</i>	<i>RMS1</i>	<i>DAD1</i>	<i>D10</i>	CCD8
<i>MAX1</i>	-	<i>PhMAX1</i>	<i>Carlactone oxidase,</i> <i>carlactone synthase</i>	CYP711

Biosynthesis was found to be increased under phosphate starvation in important crops – tomato, rice, maize, sorghum and red clover, and also in some of them under nitrogen starvation (López Ráez et al., 2008; Jamil et al., 2011; Jamil et al., 2012; Yoneyama et al., 2007a; Yoneyama et al., 2007b). In non-mycotrophic plants, increased SL production under phosphate starvation and the presence of SLs in xylem sap contributes to shoot architecture, as described in *Arabidopsis* (Kohlen et al., 2011).

3.4. PERCEPTION OF SL SIGNAL

3.4.1. PERCEPTION IN NON-PARASITIC PLANTS

Components involved in signal transduction were identified through extensive mutant screening, which resulted in insensitivity to exogenously applied SLs and the axillary-branching phenotype. The protein responsible for SL perception, D14, was originally identified in rice (*Oryza sativa*) (Arite et al., 2009). The *Arabidopsis* ortholog is also D14 (Waters et al., 2012), the *Pisum sativum* ortholog was shown as RAMOSUS 3 (RMS3) (de Saint Germain et al., 2016) and the other rice signalling mutants were identified and named HIGH TILLERING DWARF (HTD) (Liu et al., 2009). Another ortholog has been found in *Petunia hybrida* and is known as DECREASED APICAL DOMINANCE 2 (DAD2) (Hamiaux et al., 2012).

The receptors belong to group of α/β hydrolase enzymes. They bind to SL molecules and catalyse their hydrolysis, using the conserved catalytic triad of serine-histidine-aspartate in their active site (Kagiyama et al., 2013). SL is perceived by binding to the active site and consequently the receptor associates with the F-box protein AtMAX2/OsD3/PsRMS4. This leads to the assembly of Skp1 (S-PHASE KINASE ASSOCIATED PROTEIN 1) and Cullin proteins and the formation of the SCF complex (Skp1 – Cullin – F-box protein complex), which targets specific proteins for

ubiquitination and degradation in the proteasome (Stirnberg et al., 2007). These downstream effectors were identified as SUPPRESSOR OF MAX2 1 (SMAX-1)-LIKE (SMXL) in *Arabidopsis* and DWARF53 (D53) in rice and their role is signalling repression unless they are degraded upon treatment of GR24 (Jiang et al., 2013, Stanga et al., 2013, Zhou et al., 2013).

It must be noted that paralogous receptors present in angiosperms, HYPOSENSITIVE TO LIGHT and KARRIKIN INSENSITIVE 2 (HTL, KAI2), are almost identical in sequence and have the same catalytic triade (Bythell-Douglas et al., 2013; Zhao et al., 2013). Karrikins, butenolide compounds produced by combustion of plant material, are signals for KAI2. KAI2 is capable of binding to GR24 in *Arabidopsis* and *Brassica tournefortii*, although with a lower affinity and neglectable germination induction. Similarly, HTL can bind karrikin, but does not result in germination (Nelson et al., 2009). Interestingly, KAI2 signalling involves complex formation with MAX2 and the signal transduction is very similar to that of the D14 receptor (Nelson et al., 2011). It is believed that different clades of SMXL proteins play a role as effectors in SL/karrikin signalling (Soundappan et al., 2015; Wallner et al., 2017).

3.4.2. PERCEPTION IN PARASITES

The orthologous genes present in parasitic plant *Striga hermonthica* are HTL/KAI2 and occur in 11 variants (Conn et al., 2015; Toh et al., 2015; Tsuchiya et al., 2015). Experiments on *Arabidopsis htl* mutants (loss-of-function) complemented with *ShHTL1* – *ShHTL11* genes showed differing sensitivity to a range of SLs, *ShHTL7* being sensitive at picomolar concentrations to 5-DS and nanomolar to strigol. Such a wide receptor genetic background supported by residue variability in the active site could be a reason for substrate preferences of distinct parasitic species. Moreover, expression levels of individual genes may play a role in sensing SLs among species (Toh et al., 2015).

All the ShHTLs possess the conserved catalytic triad Ser-His-Asp with a highly similar amino acid sequence. Loss-of-function/Complementation mutant experiments unravelled that ShHTL1 and ShHTL2-3 perceive KARs and not SLs, forming a “conserved” and “intermediate” clade of receptors, respectively (Fig. 7). Similarly, ShHTL4-9 are sensitive to SLs and do not respond to karrikins and were identified as a “divergent” clade of receptors in parasitic plants. Recently, a D14 paralogue (ShD14) was identified and found to be also SL sensitive. Comparative analysis of the crystal structures

of ShHTLs showed differing sizes of catalytical pockets. ShHTL7 has the largest pocket with unbulky residues, which correlates with the sensitivity to distinct SLs mentioned above. The spatial orientation of helix α D1 also plays a role in SL preference (Toh et al., 2015; Xu et al., 2018).

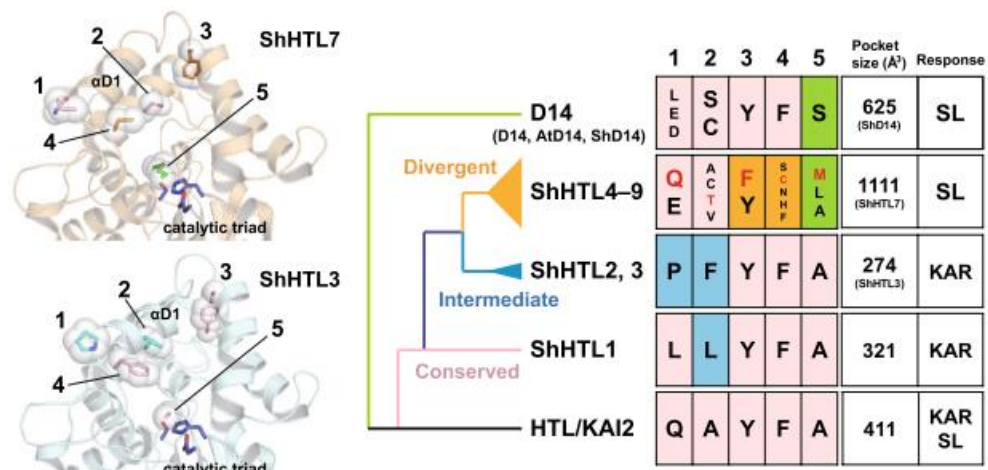


Fig. 7. Catalytical sites of the receptors from parasitic plant *Striga hermonthica* are on the left. ShHTL7 with a large pocket binds SLs, whereas the shape of the ShHTL3 active site is suitable for karrikins and not SLs. The table on the right shows evolution of the groups of receptors, dividing them into conserved, intermediate and divergent clades according to the amino acid residues present. The residue at position 1 influences α D1 helix. The residues in the blue boxes make the active site narrow and prevent SL binding, whereas the orange boxes cause expansion of the pocket. Green boxed residues are responsible for sterical hindrance and prevent D14 and ShHTL4-9 from binding KARs (Miyakawa et al., 2019).

3.4.3. MODE OF ACTION OF PERCEPTION IN PARASITES

As previously described, the structural element responsible for bioactivity in SLs is the D-ring. The mode of action has been suggested by experiments with nucleophilic hydrolysis of the synthetic SL GR24. As the receptors contains nucleophilic residues in their active sites, it was thought that they attack the enol-ether bridge and an elimination of D-ring follows (Mangnus and Zwanenburg, 1992a). It was discovered that modified molecules at 1' position - dihydro-GR24 and carbaGR24 – shown no germination (Thuring et al., 1997; Zwanenburg and Pospíšil, 2013).

However, SL mimics are capable of germination induction but do not possess an enol-ether bridge. Therefore, it was suggested that perception is initiated by a nucleophile with an acyl attack of the D-ring carbonyl (Scaffidi et al., 2012). Then it binds to the catalytical serine (Ser95) and the ABC moiety is cleaved. The His246 is modified and a covalently linked intermediate molecule (CLIM) is formed. The detachment of hydroxy

butenolide leads to a conformational change of ShHTL7 receptor which opens for interaction with ShMAX2 and ShSMAX1 to transfer the signal further by the ubiquitination of suppressor proteins, their proteolysis activates gene expression and triggers germination (Fig. 8) (Yao et al., 2017).

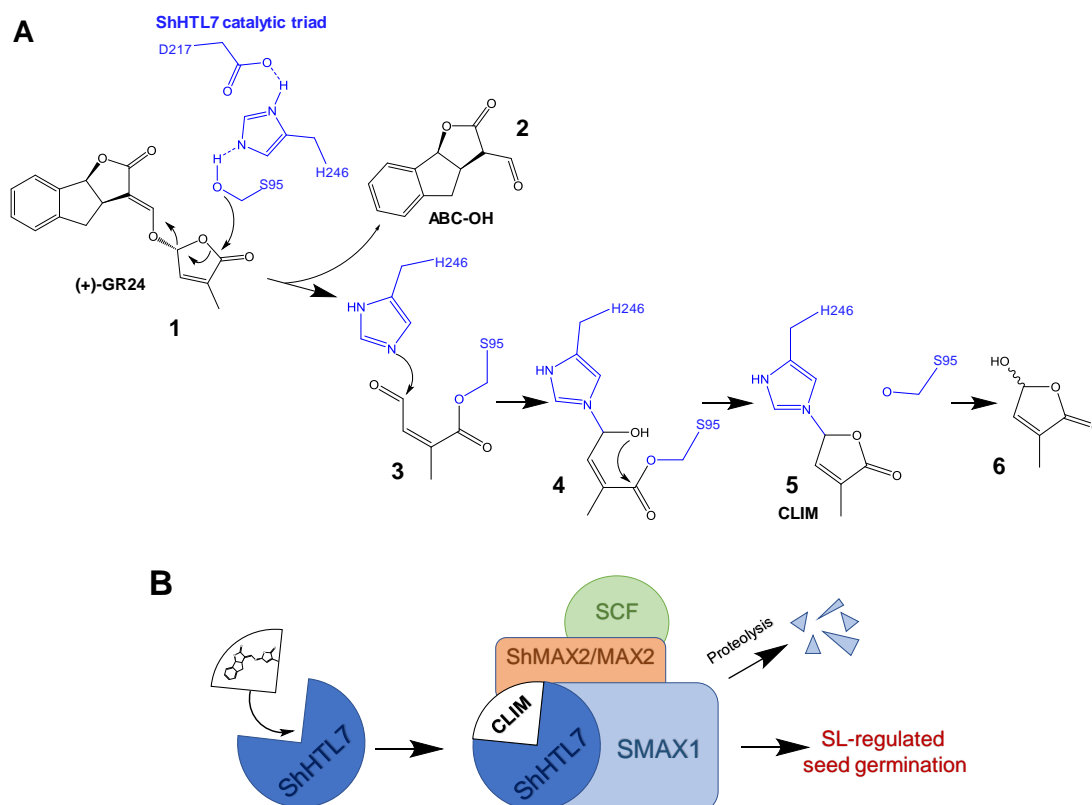


Fig. 8. Scheme of molecular mechanism of SL perception in *Striga hermonthica*. (according to Yao et al., 2017). **(A)** 1 – ShHTL7 binds GR24 by nucleophilic attack of D-ring by catalytic triad's serine. 2 – detachment of hydroxylated ABC rings happens followed by 3 – binding of histidine residue. 4 – intramolecular nucleophilic attack leads to 5 - formation of covalently linked intermediate molecule (CLIM). 6 – subsequent hydrolysis produces hydroxylated D-ring. **(B)** SL is perceived by ShHTL7 receptor, which is an α/β hydrolase and causes a conformational change of HTL7. Interaction with proteins SMAX1 and MAX2 is now enabled and mediates binding to SCF complex, needed for ubiquitination of suppressor proteins, which are subsequently degraded in proteasome and expression of genes involved in germination starts.

4. CROSSTALK WITH OTHER HORMONES

Interaction with many other hormones has been studied. Ethylene has been found to act synergistically with SLs, as well as with auxins, in root-hair elongation (Kapulnik

et al., 2011) and the suppression by gibberelins has been observed on the level of SL biosynthesis (Ito et al., 2017). Nevertheless, auxins and cytokinins (CKs) represent the most intensively examined hormones and are described in more detail.

Auxins play important role in shoot branching and are responsible for apical dominance. Together with SLs they are involved in lateral bud outgrowth inhibition. Auxin positively regulates the biosynthesis of SLs, which then act directly in buds by up-regulating the expression of *BRC1* (*BRANCHED1*) gene, which codes for the transcription factor and suppresses bud outgrowth. SLs are also able to prevent branching in decapitated pea plants when applied exogenously (Brewer et al., 2009). *BRC1* is also CK responsive, down-regulation by exogenous CK allows for branching in several dicots (Aguilar-Martínez et al., 2007; Braun et al., 2012; Dun et al., 2012). The function of CKs and SLs in bud outgrowth is antagonistic.

Very little is known about the action of auxins and CK in monocots. Nevertheless, a recent study showed that GR24 induces degradation of CK via transcriptional activation of *CYTOKININ OXIDASE-DEHYDROGENASE 9* in rice (*OsCKX9*), suggesting that CK homeostasis in monocots could also be controlled by SLs (Duan et al., 2019).

4.1. ACTION IN PARASITIC PLANTS

Research on hormonal crosstalk in parasitic plants is still in its infancy. Yet, *CYP707A* genes were found to be part of the signalling pathway in *Arabidopsis* as well as in parasitic plants (Brun et al., 2019). *CYP707A1* codes for cytochrome P that catabolizes abscisic acid (ABA) and is strongly upregulated by GR24 treatment in *Phelipanche ramosa* seeds. GR24 is therefore responsible for breaking seed dormancy maintained by ABA (Lechat et al., 2012; Lechat et al., 2015).

CKs are also involved in formation of haustorium. In *P. ramosa* seeds pre-germinated by GR24, *cis*-zeatin, *trans*-zeatin and CK-containing root exudates of *Brassica napus* triggered establishment of early haustorial structures (swelling of radicle apex) and increased aggressiveness of the parasite, i.e. number of attachments to the host plant's roots (Goyet et al., 2017).

5. PARASITIC PLANTS FROM *OROBANCHACEAE* FAMILY

One of the functions of SLs is induction of the germination of root parasitic plants from *Orobanchaceae* family. This family consists of 99 genera and about 2060 species (<https://www.britannica.com/plant/Lamiales/Orobanchaceae>). Two groups of parasites can be distinguished, obligate and facultative. Obligate parasites (e.g. *Orobanche*, *Phelipanche*, *Striga*) need presence of the host plant to finish their life cycle, whereas facultative parasites (e.g. *Triphysaria*, *Odontites*, *Rhinantus*, *Rhamphicarpa*) can reproduce under specific conditions without the host. Another differentiation of parasites based on nutrition can be made – hemiparasites (*Striga*) are green and photosynthetically independent on the host, whereas holoparasites (*Cistanche*, *Orobanche*, *Phelipanche*) rely completely on the host for water and assimilates. Some of the species from this *Orobanchaceae* family are called weedy parasites, having wide host range and/or ability to propagate rapidly. These species can be found in many publications under common English name, *Orobanche* and *Phelipanche* spp. are called “broomrapes” and *Striga* genus “witchweeds”.

It is important to note that the species names *Orobanche ramosa* and *Orobanche aegyptiaca* was used in the past, namely in publications released before 2009. It has been suggested by one of the leading parasitology research groups to distinct these two species from other *Orobanche* genera based on e.g. morphological features (branched stems above ground) or chromosome number and use a new genus name – *Phelipanche* (Joel, 2009). This work respects and follows the new naming.

The life cycle of parasitic plants starts with seed imbibition in a moist and warm environment, a requirement for dormancy breakage (Fig. 9). Furthermore, an exogenous host-derived stimulant is needed to trigger germination of many *Orobanchaceae* species. SLs represent the most studied group of such compounds. Some species are specific to the stimulant – *Orobanche foetida* Poir. germinates upon exposure to orobanchol type SLs (Fernández-Aparicio et al., 2011; Trabelsi et al., 2017), while *Striga hermonthica* prefers strigol or 5-DS over orobanchol (Awad et al., 2006; Yoneyama et al., 2015; Yoneyama et al., 2010). A radical protrudes out of the seed coat and an important stage of the parasite’s development follows – attachment to the host root, which is conditioned by the development of radicle’s apical cells into papillae in broomrapes or root hairs in

witchweeds. This structure is able to adhere to the host root creating the “haustorium” formation. Haustorium is a specialized organ needed in attachment to host roots and later it connects to the hosts xylem and enables the transfer of nutrients and water to the parasite., as defined by most of the researchers in the field and summarized in Joel et al., 2013. The haustorium formation is triggered by host-derived compounds and it has been reported, that plant hormones, cytokinins, take part in this action in *Phelipanche ramosa* (Goyet et al., 2017). The next step in the life cycle is development of the tubercle, which later develops into the stem. In *Striga* it happens after emergence from the soil followed by the formation of leafy green shoot. In broomrapes, the stem is formed under the ground and a flowering spike appears above the ground. Pollination is specific to the species, but a common ability is the production of thousands of minute seeds (summarized in Delavault et al., 2017).

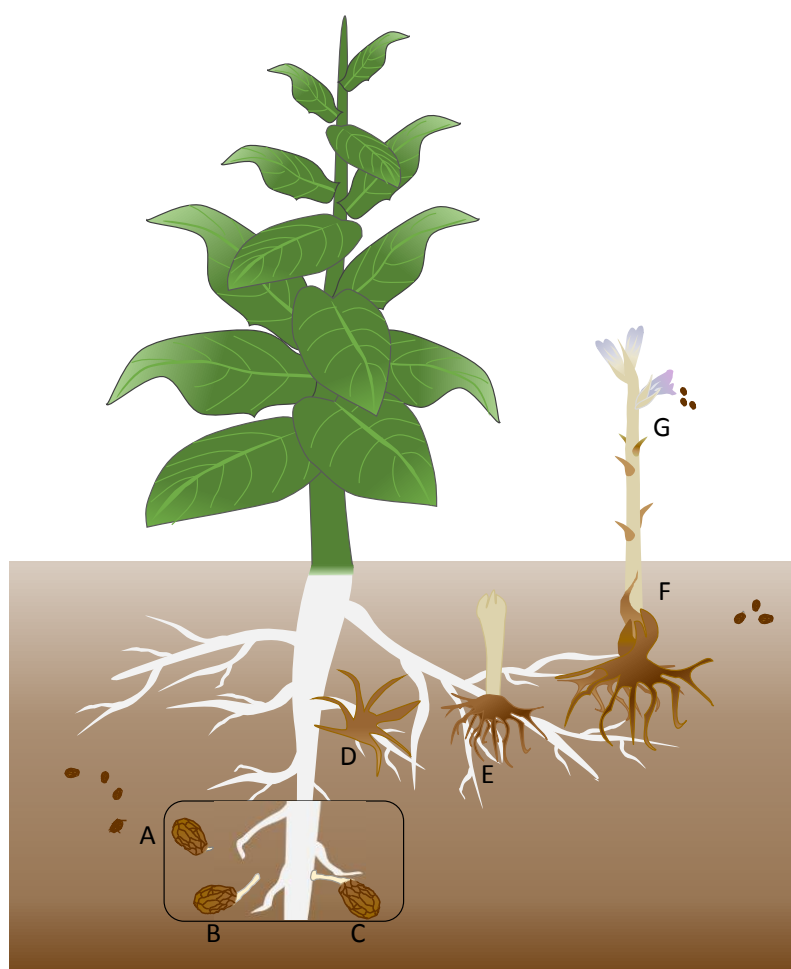


Fig. 9. Life cycle of parasitic weeds. (A) Seeds start to germinate upon a signal exuded from the host, (B) a radicle grows in a chemotropic manner, (C) the radicle attaches to the host root via a specialized organ called the haustorium, (D) a tubercle develops, (E) a shoot emerges, (F) the maturation of the plant occurs, (G) flowering and seed production follows.

As previously mentioned, the life cycle of *Orobanchaceae* parasites is dependent on host plants, which include economically important crops, such as faba bean (*Vicia faba*), pea (*Pisum sativum*), maize (*Zea mays*), rice (*Oryza sativa*), tomato (*Solanum lycopersicum*), sorghum (*Sorghum bicolor*), pearl millet (*Pennisetum glaucum*), sugarcane (*Saccharum officinarum*), tobacco (*Nicotiana tabacum*) or oilseed rape (*Brassica napus*). As the growing parasite steals nutrients from the host and is eventually lethal, large losses in the yield result. Species that represent a major threat to agriculture include *Orobanche cumana* Wallr. (Fig. 10), *O. crenata* Forsk., *Phelipanche ramosa* (L.) Pomel. (Fig. 10), *P. aegyptiaca* (Pers.) Pomel, *Striga hermonthica* (Del.) Benth. (Fig. 10), *S. asiatica* (L.) Kuntze and *S. gesnerioides* (Willd.) Vatke (Parker, 2009; Parker, 2012). Parasites have different specificities to various crops. For example, *O. cumana* is a sunflower (*Helianthus annuus* L.) specific parasite, whereas *Phelipanche* or *Striga* genera can parasitize many host species (Fernández-Martínez et al., 2015). *Orobanche minor* Sm. mostly occurs on red clover (*Trifolium pratense*), but its contribution to economic damage in Europe is not serious, as populations are not dense. It decreases the inflorescence of the host, causing harm only when red clover is grown for seed. However, damaging infestation by *O. minor* has been recorded in USA, reducing the host weight by 15-50 % (Colquhoun et al., 2006). Geographical distribution of these species varies, some of them are dominant in the Mediterranean (*O. crenata*), Near and Middle East (*P. ramosa*, *P. aegyptiaca*), South and Western Asia (*S. asiatica*) and Africa (*S. hermonthica*) (Parker, 2012). Economically, parasitic weeds cause a loss of approximately US \$200 million with an annual increase of \$30M (Rodenburg et al., 2016a).

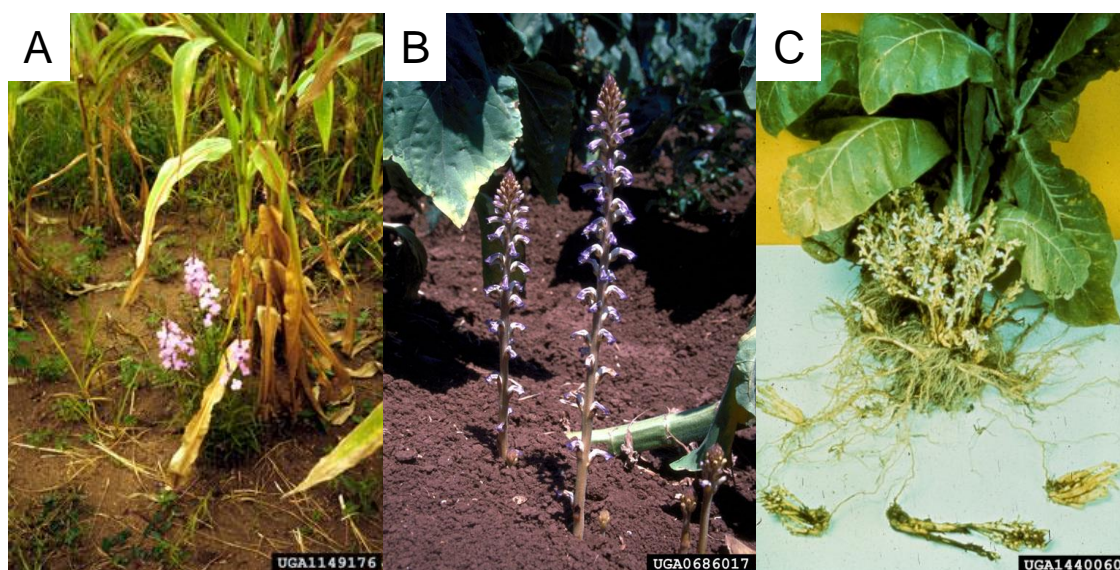


Fig. 10. Selected species from *Orobanchaceae* family. (A) *Striga* sp. parasitizing maize (<https://www.weedimages.org/browse/detail.cfm?imgnum=1149176>); (B) *Orobanche cumana* in a sunflower field (<https://www.weedimages.org/browse/detail.cfm?imgnum=0686017>); (C) *Phelipanche ramosa* attached to a tobacco plant (<https://www.weedimages.org/browse/detail.cfm?imgnum=1440060>).

5.1. PARASITIC WEEDS – CONTROL BY SUICIDAL GERMINATION

As infestation by parasitic weeds rises annually and threatens world food security, there is a need to manage seed banks in soil, mainly by prevention of distribution and restraint of infested areas. Enormous numbers of dust-like seeds, long viability in soil and easy dispersal are a very problematic features of the parasites. Several strategies using SLs to combat harmful parasites have been developed.

SLs are attractive for agriculture use. They could help to reduce parasitic seed banks in soil by a process called suicidal germination. With this method, SLs are applied in a formulated solution to a field prior to planting a crop (Johnson et al., 1976), inducing germination artificially resulting in the parasite's death in the absence of the host roots.

The structural diversity of SLs gave inspiration for designing much simpler molecules. Synthesis of natural SLs is a linear process consisting of many steps. Any mistakes make finishing the synthesis impossible which results in poor yield and high cost of production. Therefore, the aim of current research is to synthesize new SL

analogues that retain biological activity towards parasite seed germination. An ideal synthetic stimulant would be universal for all the major aggressive weed species with hydrolysis-resistance at higher pH levels, as chemical instability is a common feature of SLs (Halouzka et al., 2018; Johnson et al., 1976).

Successful field and pot trials have been performed, where SL analogues or mimics were applied in formulated form, i.e. dissolved in an emulsifier to improve stability (Zwanenburg et al., 2016). Pot experiments with *S. hermonthica* and *S. asiatica* showed up to a 98% parasite reduction on sorghum and pearl millet (Kgosi et al., 2012). One of the compounds, Nijmegen-1, was also used in field trials with tobacco (*Nicotiana tabacum*) infested by *P. ramosa*. The results confirmed feasibility of this approach, as reduction of emergence reached 95 % (Zwanenburg et al., 2016). Experiments with SL mimic T-010 on *S. hermonthica* artificially infested sorghum field showed delayed and reduced emergence of the parasite as well as improved growth of the host (Samejima et al., 2016). Jamil et al. (2019) recorded significant decrease of emerging *S. hermonthica* – in pot experiments by 52 – 82 % and in field experiments by 41 %. Kountche et al. (2019) further validated the suicidal germination approach under natural rain-fed and harsh (40 °C) conditions on sorghum and pearl millet farmer's fields in Burkina Faso. The parasitic reduction by three different SL analogues ranged from 39 % (= 32 g ha⁻¹) to 65 % in the pearl millet field, however, in the case of sorghum, reduction was only by 12 to 20 %. These differences could be caused by varying soil types or susceptibility to the host. This study suggests that suicidal germination must be the main component of *Striga* control combined with other approaches – fallow, crop rotation and intercropping with non-host crops, such as cowpea (*Vigna unguiculata*) or sesame (*Sesamum* spp.).

5.2. OTHER METHODS OF PARASITIC INFESTATION CONTROL

There are more approaches to combat parasitic weed problem. However, a lot of them are ineffective or insufficient.

Manual weeding is an obvious method and common control, which helps to reduce future infestation. However, it is laborious and since most of the parasite's development happens under the ground, damage to the host is inevitable. Hand weeding after emergence is ineffective (N'cho et al., 2019).

Since phosphate or nitrogen deficiency starts SL biosynthesis, supply of fertilizers could be an effective control. In pot experiments, the application of PO_4^- reduced *Striga* colonization in rice (Jamil et al., 2011) and *P. aegyptiaca* in tomato (Jain and Foy, 1992; López-Ráez et al., 2008), while borax and/or urea stopped *O. crenata* emergence in tomato (Kannan et al. 2015) and nitrate reduced *S. hermonthica* infestation in sorghum (Ayongwa et al., 2006). In general, *Striga* is linked with low soil fertility (Parker, 2009), therefore application of fertilizers suggests itself to be useful in combating infestation (Showemimo et al., 2002; Jamil et al., 2012).

The use of fumigants, i.e. gaseous pesticides applied to soil, was also shown to be effective. Methyl bromide was applied in a national eradication project of *P. ramosa* in California but was later found to be environmentally toxic and banned. Furthermore, a mixture of fumigants (metham sodium, chloropicrin, methyl iodide, dimethyl disulphide) were tested in Israel on *P. aegyptiaca* with positive results. However, due to high costs this approach is not preferably used (Goldwasser and Rodenburg, 2013). Interestingly, non-toxic ethylene was proved to be an effective fumigant against *S. hermonthica* in Mali (Rodenburg et al., 2005) and it was partly used in USA *Striga asiatica* eradication project (Eplee, 1992; Tasker and Westwood, 2012), but it also is a costly method.

Another chemical control introduces compounds that inhibit germination of parasites, mainly herbicides. Several foliar and soil applications were tested successfully (Eizenberg et al., 2012; Hershenhorn et al., 1998), although some results lead to decreased crop yield (Aly et al., 2001). Instead, seed coating (surface incorporation of herbicide) or priming (imbibition in herbicide solution) are methods that lower the amounts of herbicide used and were shown to be a much better option and the usage of imazapyr or pyrithiobac were commercialized (Ransom et al., 2012). Still, the main limitations of herbicide usage are low selectivity, metabolization to non-toxic compounds by hosts or non-resistance of host plants. Interestingly, reduced germination of parasites was observed under treatment by natural compounds. Amino acids, namely methionine, reduced *O. minor* emergence on red clover by 67 % without affecting the host (Fernández-Aparicio et al., 2017). However, it is questionable if the parasites could evolve resistance to herbicides.

Environmentally friendly or biocontrol approaches have also been introduced. Intercropping with allelopathic plant *Desmodium uncinatum* has been adapted by farmers

in Kenya, resulting in suppression on *Striga* emergence by allelochemicals (Khan et al., 2010; Pickett et al., 2010).

Another possibility is parasite control by microorganisms. Treatment with many bacterial or fungal species showed decreased infection by *Striga* spp., *Fusarium oxysporum* being the most potent (Nzioki et al., 2016). The fungi strain Foxy 2 not only decreased *Striga* emergence by 98 %, but also increased sorghum yield by 26 % (Kroschel et al., 1996). The study of the fungi *Trichoderma harzianum* in conjunction with with *F. oxysporum* revealed the mechanism of action – degradation of SLs and/or pathogenicity to developing parasite’s tubercles (Boari et al., 2016).

Breeding of crop cultivars with low susceptibility to parasites is one of the most promising strategies. Tolerant or resistant cultivars of crops have been selected, to include rice (Rodenburg et al., 2016b; Rodenburg et al., 2017), faba bean (Abbes et al., 2007; Fernández-Aparicio et al., 2014; Rubiales et al., 2014), sorghum (Mohemed et al., 2016), pea (Pavan et al., 2016) and pearl millet (Kountche et al., 2013) and are characterized by differing SL emission (Yoneyama et al., 2015).

Nevertheless, it is widely suggested to combine several control measures to combat parasitic weeds in order to achieve elimination of the parasite’s attachment and development. Yet, these approaches do not resolve depletion of seed banks in soil.

6. BIOASSAYS FOR TESTING STRIGOLACTONE ACTIVITY

Several studies describing methodology for testing strigolactone bioactivity *in vitro* or *in vivo* have been published by researchers. They represent a useful tool in primary investigation of biological activity of compounds, e.g. new synthetic SL analogues and mimics.

6.1. STANDARD GERMINATION ASSAY

Historically, the first detailed protocol that summarized and described a reproducible germination bioassay for parasitic weed seeds was published by Mangnus

et al. (Mangnus et al., 1992b). Previously, there were imperfectly reported procedures that were not easily repeatable.

The bioassay starts with surface sterilization of seeds with 5 min of agitation in a new sterilization solution that includes a detergent, i.e. 1% Triton X-100 in 2% sodium hypochlorite. Seeds were filtered with distilled water and dried overnight. Conditioning (i.e. warm stratification) in glass Petri dishes followed – two moistened filter papers were placed per each dish and 5 glass fibre filter paper discs were placed in the case of *S. hermonthica*, for *O. crenata*, 45 discs were used. Seeds were put on each disc with a paint brush and covered by another disc. Dishes were closed in polyethylene (PE) bags and incubated for two weeks at the appropriate temperature. Following the incubation, the discs were taken out to a filter paper to remove additional moisture, Petri dishes were dried and 2 rings of filter paper (Ø 9 cm outer, 7 cm inner) were placed in dishes and wetted. “Sandwiches” with seeds were placed back and stimulation solution was applied in three replicates per treatment (= 3 Petri dishes). PE bags were used to cover the dishes, which were subsequently placed back in their respective incubators. An evaluation was completed by counting germinated seeds under a microscope after a 5-day (*S. hermonthica*) or 5-7-days (*O. crenata*) incubation.

6.2. HYPHAL BRANCHING ASSAY

The assay was performed on spores of AM fungus *Gigaspora rosea* Becker and Hall using the disc diffusion method. The spores were surface sterilized by sodium hypochlorite with Triton X-100, washed with water and placed in a 6 cm Petri dish with medium containing phytigel and MgSO₄. They were then grown under 2% CO₂ and 32 °C. After a secondary hypha emerged from the primary one, two paper discs supplied with 5-DS solution were placed next to the tip of hypha, one on each side. After 24 h, the assay was evaluated by observation of newly formed hyphae in close proximity to the discs and compared to negative control (70% ethanol in water) (Akiyama *et al.*, 2006). Some studies use *Glomus intraradices* or *Gigaspora margarita* Becker and Hall as biological material (Artuso et al., 2015; Cohen et al., 2013).

6.3. PEA BRANCHING ASSAY

As mentioned in section 3.2., SLs negatively regulate lateral bud outgrowth in plants. A bioassay performed on an increased branching *rms1* mutant of pea (*Pisum sativum*) cv. T  r  se, which has disrupted SL synthesis, was published to assess whether putative SLs have the ability to restore phenotype of wild-type (Boyer *et al.*, 2012).

At first, pots are filled with substrate, placed on a tray and seeds are planted in each pot. After 10 days, when buds at node 3 and/or 4 were visible, 10 µl of SL solution was applied directly onto the bud. Prior to that, buds at nodes 1 and 2 (alternatively 3) were cut with a scalpel to promote strength of the experimental bud. Application solution consisted of 0.1% acetone, 0.4% dimethyl sulfoxide (DMSO), 2% polyethylene glycol (PEG) 1450, 50% ethanol and SL in desired concentration. The assay was performed in 24 biological replicates per treatment. After 8-10 days, outgrowing branches were measured and compared with negative control.

6.4. A HIGH-THROUGHPUT GERMINATION ASSAY FOR ROOT PARASITIC PLANTS

Pouvreau *et al.* (2013) published a convenient, rapid and reliable high-throughput method able to screen much more compounds for germination stimulatory activity than in the standard germination assay (Mangnus *et al.*, 1992b). The assay is a colorimetric method based on a redox reaction of yellow tetrazolium salt MTT [3-(4,5-dimethylthiazol-2-yl)-2,5-diphenyltetrazolium bromide] to purple formazan, which happens only in living cells and is done by mitochondrial enzymes (Mosmann, 1983). The protocol is summarized in Fig. 11.

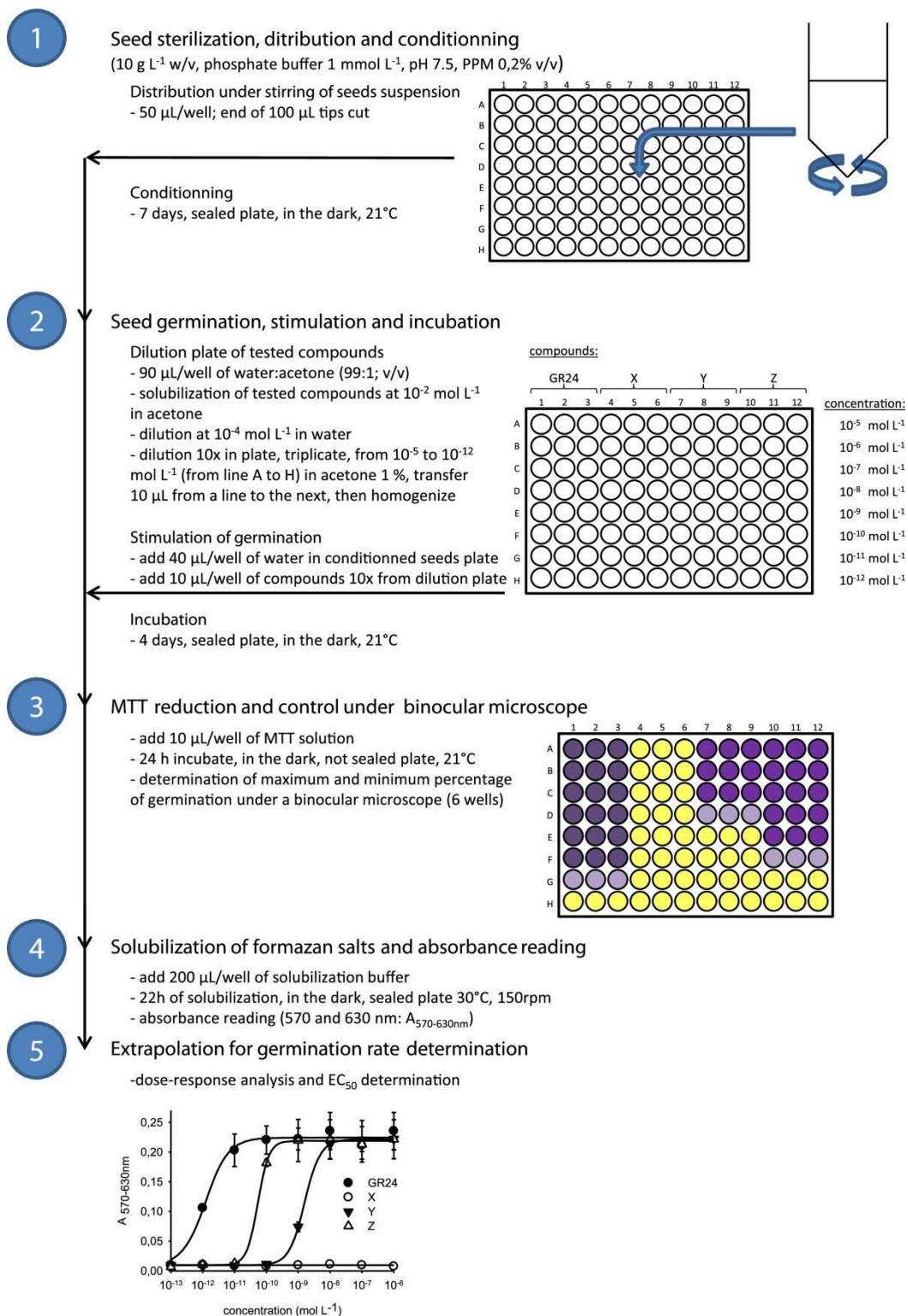


Fig. 11. Step by step protocol of high-throughput seed germination assay for root parasitic weeds (Pouvreau et al., 2013).

6.5. ADVENTITIOUS ROOTING ASSAY

SLs are involved in shaping root architecture, therefore bioassay for screening adventitious root formation has been developed (Rasmussen et al., 2012). SLs suppress lateral root formation. The SL biosynthesis mutants of *Arabidopsis max1*, *max3* and *max4*, and SL response mutant *max2* display higher adventitious root production. Application of GR24 reduced the number of roots in all the synthesis mutants and wild-type, but not in *max2*, in a dose-dependent manner. The same results were observed in the pea synthesis mutant *rms5* and response mutant *rms4* in three genetic backgrounds. This study gave a foundation to use a bioassay performed on *max* mutants of *Arabidopsis* (Rasmussen et al., 2013; Boyer et al., 2014).

Arabidopsis seeds were surface sterilized with 70% ethanol (1 min) and 30% bleach with 0.1% Triton X-100 (20 min), sown on solid MS medium with sucrose supplemented with SL (GR24 in several concentrations) and cold stratified for 3 d. After that, plants were exposed to light for 8 h, etiolated for 4 d and grown under long day conditions at 22 °C for 7 d. Adventitious roots were counted above the root-shoot junction using an image-analysis software.

6.6. A GENETICALLY ENCODED BIOSENSOR ENABLING QUANTITATIVE ANALYSIS OF STRIGOLACTONE SIGNALLING

The perception system of SLs based on the degradation of a signalling complex has been used to design a luminescent ratiometric SL sensor and was named “StrigoQuant” (Samodelov *et al.*, 2016). The molecular tool composes of *SMXL6* gene from *Arabidopsis*, the mediator of SL signalling. *SMXL6* is fused to *FIREFLY LUCIFERASE* (*FF*) and enables monitoring of luminescence. The *RENILLA LUCIFERASE* gene (*REN*) was also introduced as a part of the sensor system and normalization element. The self-processing 2A peptide serves as a link between *REN* and *SMXL6-FF* and allows for co-translational cleavage and stoichiometric expression of the sensor elements from a single transcript. While the *FF* signal upon the addition of SL decreases in time, due to the degradation of the *SMXL6*-mediated complex, the *REN* remains unchanged. The ratio of the two signals can then be calculated (Fig. 12). The “CtrlQuant” construct, which

exchanges the *SMXL6* gene for a short-repeated sequence of guanine and adenine is used as the negative control.

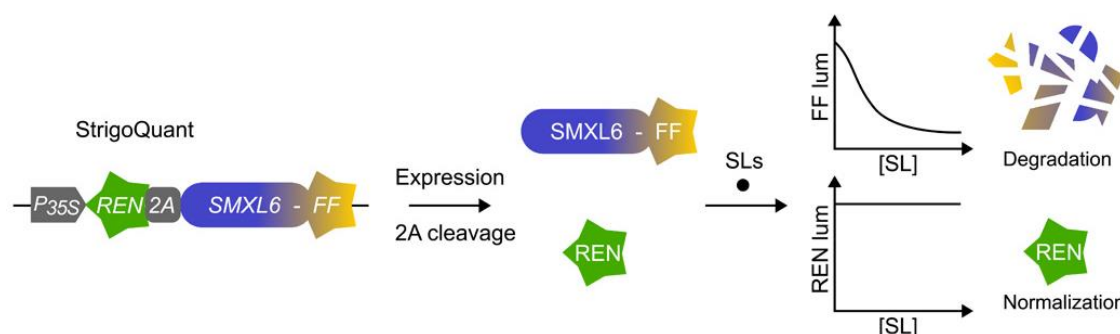


Fig. 12. Scheme of StrigoQuant, genetically encoded tool for quantitative SL signalling (Samodelov et al., 2016). Perception of SL involves assembly of a protein complex, of which SMXL6 is a part of, and its subsequent degradation which results in diminishing FIREFLY LUCIFERASE (FF) luminescence. The RENILLA LUCIFERASE (REN) signal serves as normalization element.

Plasmid carrying the StrigoQuant construct was used to transiently transform *A. thaliana* Col-0 protoplasts. The study showed that structurally different strigol- and orobanchol-type SLs both triggered SMXL6 dependent degradation, while 5-DS was effective even in femtomolar concentration.

The advantage of this genetically encoded sensor is that it allows for quantitative analysis and can enable studies of substrate specificity of receptors from different plant species. This was confirmed in an experiment with *d14 Arabidopsis* mutant complemented with construct carrying *D14* gene from rice (*OsD14*) (Samodelov et al., 2016).

6.7. A REPORTER ASSAY BASED ON MONITORING LUMINESCENCE IN PLANTA

Another quantitative assay was published by Sánchez et al. (2018). It is based on quenching luminescence of D14 fused with LUCIFERASE (D14::LUC) after SL perception in transgenic *A. thaliana* plants. In other words, AtD14::LUC is constitutively expressed in seedlings placed in 96-well plate filled with growth medium supported with luciferin. A biochemical reaction is started by the addition of a SL solution. Degradation of the fusion receptor happens after binding of the hormone resulting in diminution of

luminescence. The assay allows the testing of a variety of compounds and therefore can be used for structure-activity relationship (SAR) studies.

7. MATERIAL AND METHODS

This chapter briefly summarizes the material and methods used in this work. For detailed description see following publications:

Hýlová, A., Pospíšil, T., Spíchal, L., Mateman, J. J., Blanco-Ania, D., and Zwanenburg, B. (2019). New hybrid type strigolactone mimics derived from plant growth regulator auxin. *N. Biotechnol.* **48**:76–82.

Ugena, L., Hýlová, A., Podlešáková, K., Humplík, J. F., Doležal, K., De Diego, N., and Spíchal, L. (2018). Characterization of Biostimulant Mode of Action Using Novel Multi-Trait High-Throughput Screening of *Arabidopsis* Germination and Rosette Growth. *Front. Plant Sci.* **9**:1327.

7.1. PLANT MATERIAL

Seeds of parasitic weeds *Striga hermonthica* (Delile) Benth. (collected in Sudan, 2007), *Phelipanche ramosa* (L.) Pomel (population collected from *Cannabis sativa* in St. Martin de Bossenay, France, 2012 and population from *Brassica napus*, in St. Jean d'Angely, France, 2015) and *Orobanche minor* Sm. (from *Hypochaeris* sp. in Golfo Aranci, Sardinia, Italy, 2011) were used in germination assays.

Arabidopsis thaliana L. Heynht seeds, accession Col-0, were used in development of the high-throughput screening (HTS) germination assay.

The mutant *rms1* of the garden pea (*Pisum sativum* cv Tèreše) was obtained from Dr. Catherine Rameau's group in INRA, Versailles, France, and used in the "Branching" assay.

7.2. STANDARD GERMINATION ASSAY

Method published by Mangnus et al. (1992b) was simplified and optimized.

Sterilized seeds of parasitic weeds were spread on glass fiber filter paper discs (ø10 mm, Whatman, GE Healthcare) placed in 6-well plates (three per well), moistened and conditioned (warm stratified) for 6-14 days under controlled conditions in the dark. The discs with seeds were then placed on a filter paper to remove moisture, placed back into the 6-well plates and a solution of a putative stimulant was pipetted onto each disc in

triplicates per treatment. Seeds were observed under a binocular after 6 days and the percentage of germinated seeds was calculated.

7.3. HIGH-THROUGHPUT COLORIMETRIC GERMINATION ASSAY

Sterilized seeds suspended in buffer were conditioned for 4-14 days under controlled conditions in the dark. The seed suspension was supplied with 0.05% (w/w) agarose to evenly distribute the seeds into each well of a 96-well plate and stimulant solution in a wide concentration range was added. After 4 days of germination, 10 µl of MTT solution was added, which caused a reduction to purple formazan in non-dormant and germinating seeds. Germination rate was counted for the highest concentration of positive control. Formazan was solubilized by acidified isopropanol and the absorbance was measured on a multiwell plate reader. Absorbance was recalculated to germination percentage.

7.4. PEA BRANCHING ASSAY

Peas were sown into pots (1 seed per pot) filled with clay substrate (Substrate 4 with clay, Klasmann-Deilmann, Germany) to 1 cm depth and placed on a tray. Each tray was watered (1 L), covered with a transparent lid to enhance moisture and fasten germination. Peas were grown in a phytotron under irradiance 150 µmol m⁻² s⁻¹ for 5 or 8 days, until a bud at 1st or 3rd node emerged, respectively. The plant population was homogenized – only well-developed seedlings were chosen for the experiment. Lower bud(s) were cut off with a scalpel to promote outgrowth of the bud of interest. Solution of SL formulated in DMSO, PEG and EtOH was applied directly on the bud (10 µl) in 24 replicates per treatment. Plants were placed back in the phytotron and the outgrowth was observed after 8 days. Percentage of outgrowing plants was estimated, and mean length of a branch calculated.

7.5. HIGH-THROUGHPUT COLORIMETRIC GERMINATION ASSAY FOR *ARABIDOPSIS* IN SALT CONDITIONS

Arabidopsis thaliana seeds were separated on Retsch sieves according to size (280-299 µm seeds were used in the experiment). Seeds were weighed into microtubes evenly,

surface sterilized and 1 mM HEPES [4-(2-hydroxyethyl)-1-piperazineethanesulfonic acid], pH 7.5, was added. Seeds were primed by biostimulants proline (Pro), spermine (Spm), spermidine (Spd) and putrescine (Put), added to the seed suspension in various concentrations followed by a 4-days long cold stratification. Biostimulants were removed by washing with buffer and an agarose solution was added to 0.05% (w/w). Seeds were pipetted into 96-well plates, salt stress was applied by adding 75 or 150 mM NaCl and the plates were put to phytotron for 24 h/48 h of germination under irradiance $150 \mu\text{mol m}^{-2} \text{s}^{-1}$. Following germination MTT solution was added, emerged formazan was solubilized by acidified isopropanol and absorbance was measured on a multiwell plate reader.

8. SURVEY OF RESULTS

In order to study the molecular mechanisms and biological activity of SLs and their SAR, HTS bioassays or those with potential for optimization to high capacity were chosen. Bioassays were optimized and simplified. The standard germination assay for root parasitic weeds was integrated and used to validate an MTT high-throughput assay. The objective of this assay was to develop a high capacity tool for screening many SL derivatives in a single experiment (publications in Supplements I – III), with the goal of eventually identifying compounds for practical use in controlling of parasitic plants by the suicidal germination approach.

The branching assay was chosen as another system for testing biological activity of SLs with the aim of optimization to high-throughput phenotyping of plants and deciphering a role of SLs in stress conditions. Unfortunately, the branching assay turned out to be unsuitable for high-throughput application. Instead, the MTT assay principle was applied to develop a germination assay of *Arabidopsis* to use as a tool for testing the impact of biostimulants on seedling development in stress conditions (Supplementary article IV).

8.1. GERMINATION ASSAYS FOR PARASITIC WEEDS

In order to assess the effects of SL stimulation on parasitic weeds we began by optimizing the published germination bioassay. The glass Petri dishes, which are inconvenient to handle manually, were replaced with plastic 6-well plates. Moreover, replicates were reduced from 5 to 3, having consistent results with a reasonable standard deviation. This also reduced the total number of plates and amount of seeds required for each test. Due to the high price of the glass fiber filter paper discs, the affordability of the assay was further improved when it was found that covering the first disc with a second one is not needed, as the germination rate was not changed, although it is contradictory to the method published before (Mangnus et al., 1992b). Furthermore, PE bags were replaced with wrapping in aluminium foil, which reduced harmful exposure to light. Finally, the conditioning time was optimized for individual species, especially for *S. hermonthica*, where it was found that 7 days are enough to ensure a high germination rate after SL application. Since the drying of the discs on a filter paper was not defined in

detail in the original protocol, the drying time under a flow hood was therefore set to 30 min when one disc with seeds was covered by another one or 15 min in the case of uncovered seeds (Fig. 13).

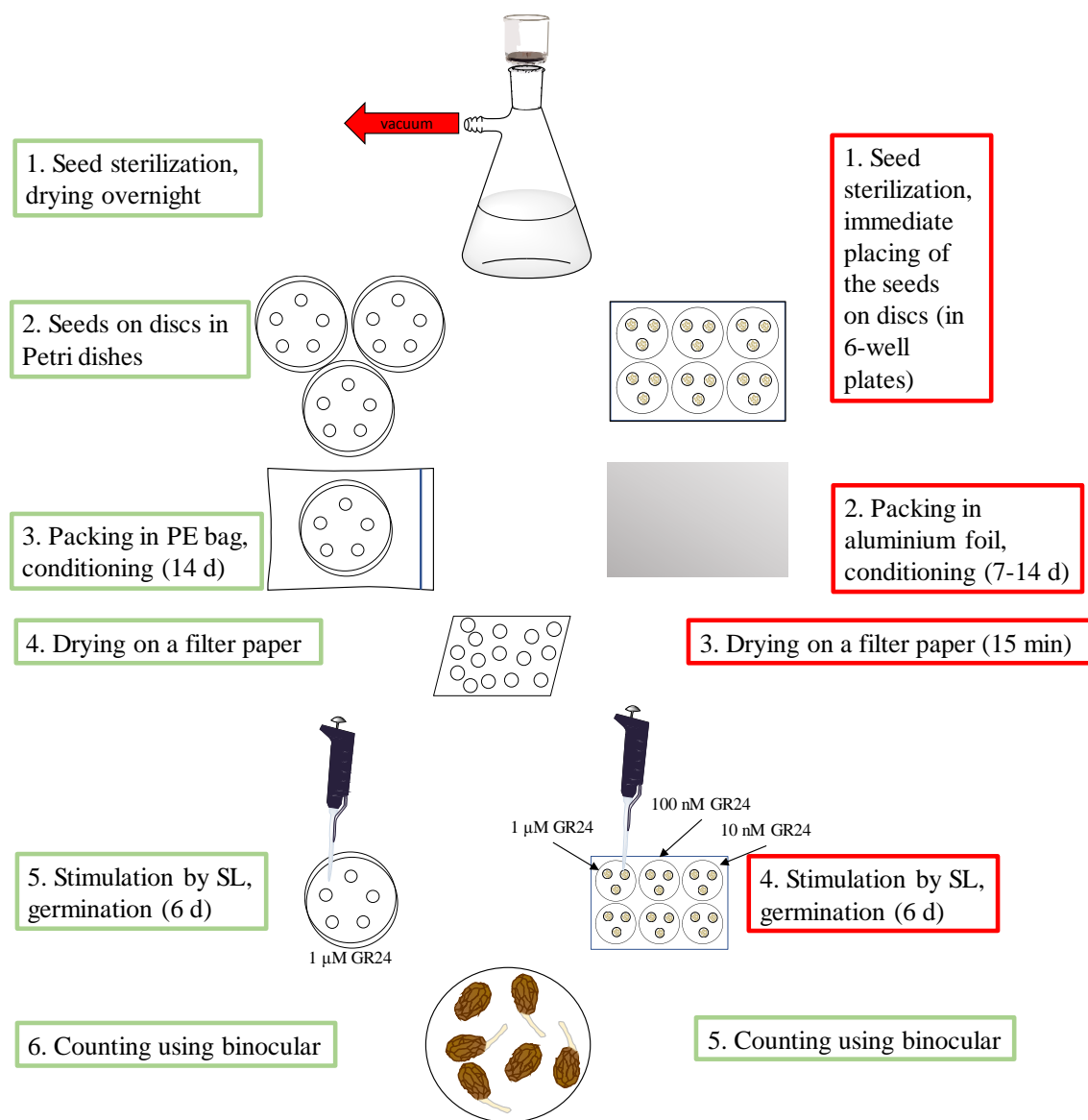


Fig. 13. Protocol of standard (green) germination bioassay illustrated in a diagram. Enhanced steps are highlighted in red.

Surface seed sterilization in the MTT high-throughput assay performed by Pouvreau et al. (2013) involved shaking the seeds manually in a falcon tube for 5 min in 2% sodium hypochlorite followed by washing and filtering out the liquid through a nylon mesh. This step was performed the same way in our optimized assay, but by stirring the seeds in 2% sodium hypochlorite and subsequently washing them using a vacuum filtration system, which resulted in speeding up the step. A major enhancement was made

in seed distribution. Instead of constantly shaking the seeds on a vortex during pipetting, which is technically demanding and requires practice to achieve even seed number per well, a sterile agarose was added to the seed suspension to a final concentration of 0.05%. Seeds in 0.05% agarose do not immediately sediment and the suspension remains homogeneous for several minutes, which enables fast and precise pipetting with a multistep pipette (Fig. 14).

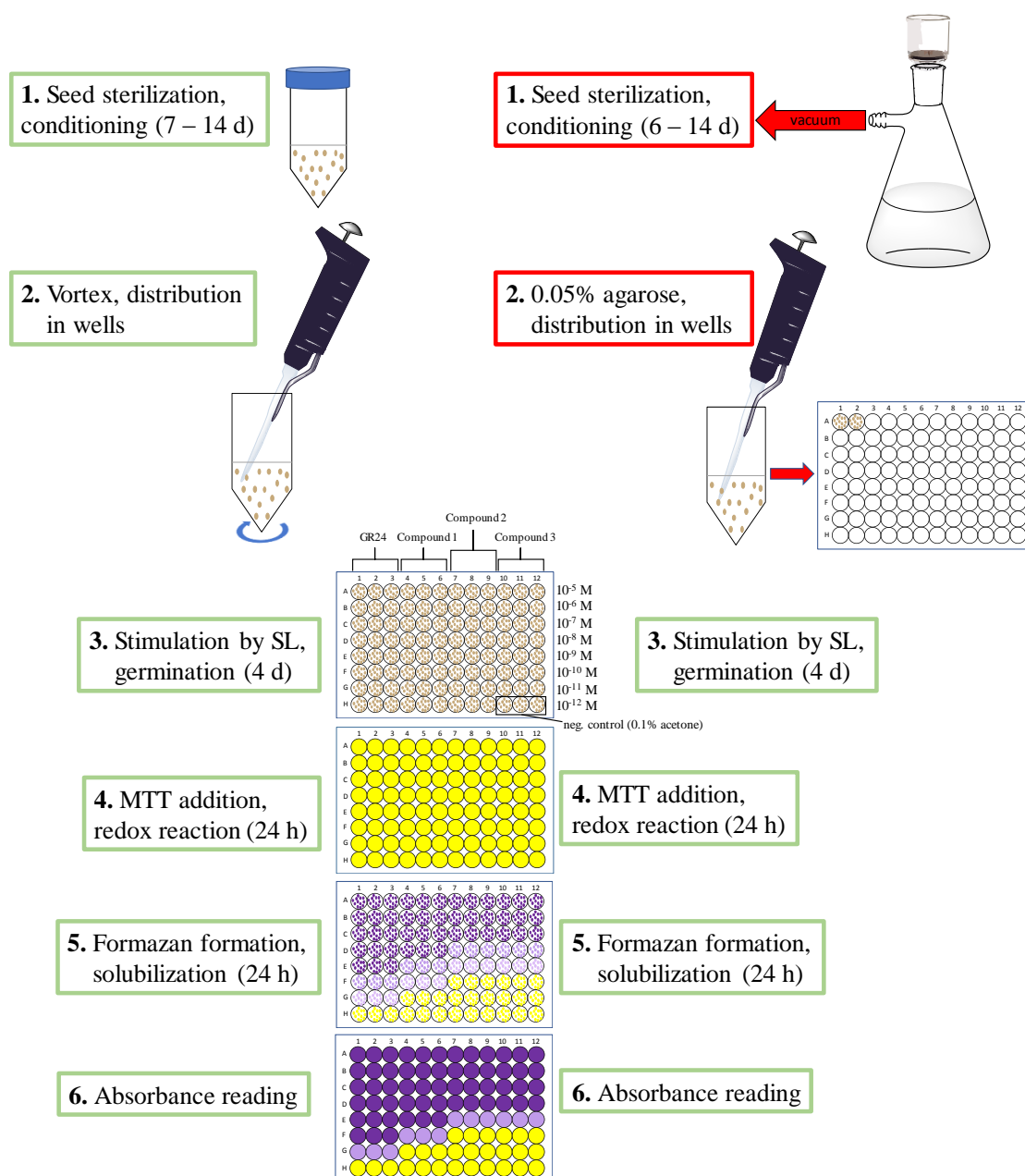


Fig. 14. Protocol of the high-throughput germination assay (MTT assay) illustrated in a diagram. Enhanced steps are highlighted in red.

Once the assay was optimized and provided reliable repeatable data, an array of SLs was tested for seed germination stimulating activity towards *Striga hermonthica*, *Phelipanche ramosa* and *Orobancha minor*. Maximal average germination rates with standard *rac*-GR24 reached 80%, 82% and 50%, respectively (Supplementary article I, Fig.4). We then assayed newly designed SL mimics whose structures possess a variety of chemically distinct non-conserved moieties attached to the D-ring. For clarity, numbering of the compounds in this thesis remains the same as in their original articles.

New SL mimics are derived from natural plant hormones auxins, i.e. from indole-3-acetic acid (IAA), oxo-IAA and phenylacetic acid (Supplementary article I, Fig. 3). Several compounds were revealed to be slightly more sensitive than standard GR24 towards *P. ramosa* and *O. minor* germination (Supplementary article I, Fig. 5). Such remarkable activity was never published before. Auxins as structural moieties carrying the D-ring appear to be promising candidates for design of new SL derivatives. The dose-response curves of the most active compounds are displayed in Fig. 15 and their structures in Fig. 16. Compound 5, having oxo-IAA attached to the D-ring, reached almost 100 pM EC₅₀ (half maximal effective concentration). Compound 9, a phenylacetic acid derivative, exhibited 50 nM EC₅₀ towards *S. hermonthica*. Another group of chemically distinct compounds representing resorcinol derivatives showed significant activity towards *P. ramosa* with the EC₅₀ value two to three orders of magnitude higher than that of GR24, and slightly worse activity towards *S. hermonthica* (Supplementary article II, Tab. 2). Triazolide type mimics showed similar germination stimulation of *P. ramosa* as resorcinol mimics, but poor results towards *S. hermonthica* (μM or higher) (Supplementary article III, Tab. 1). These findings indicate species selectivity. For a detailed discussion, see corresponding articles in supplements.

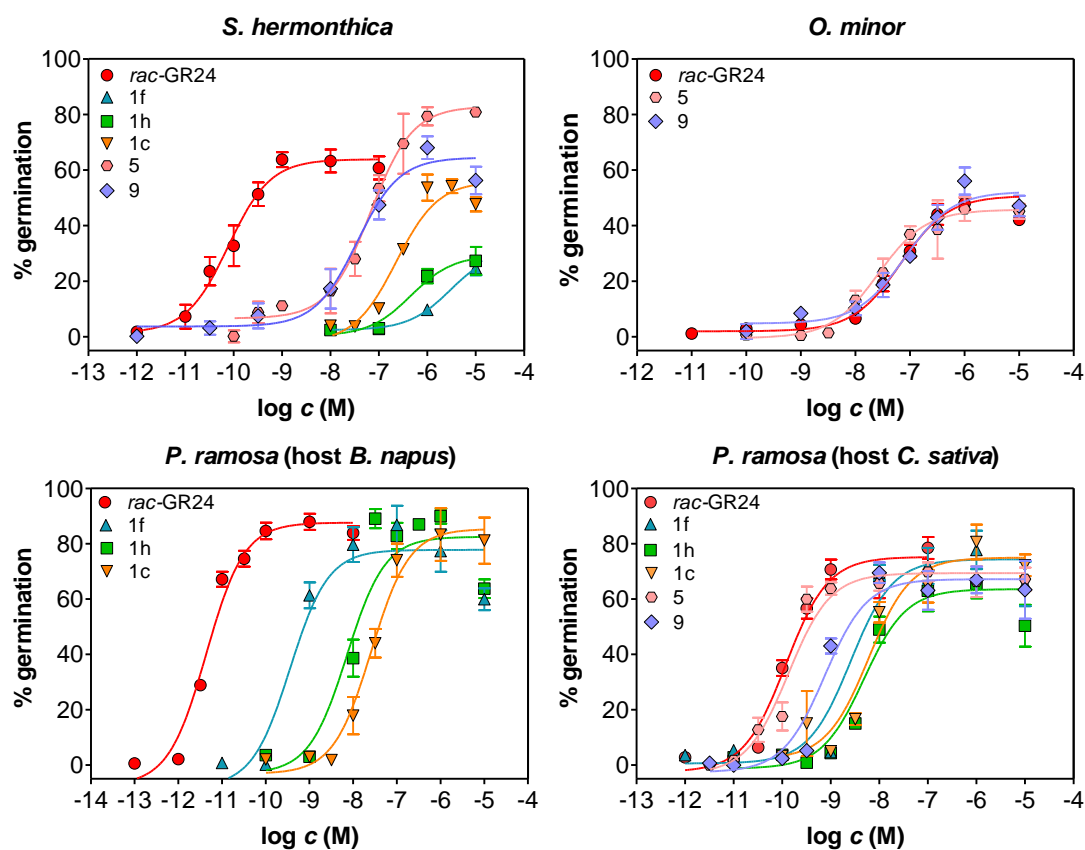


Fig. 15. Representative graph comparing several of the most biologically active SL mimics. 1f = triazolid type mimic, 1c and 1h = resorcinol type mimic, 5 = oxo-IAA-derived mimic, 9 = phenylacetic acid derivative.

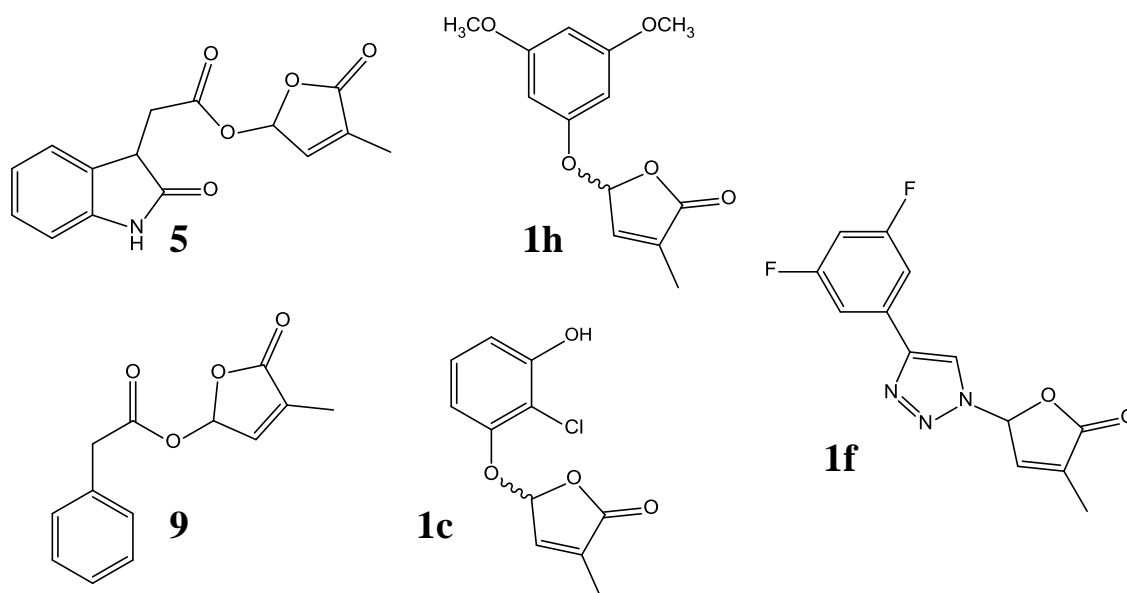


Fig. 16. Structures of new SL mimics, which showed high activity in germination assays. Compound 5 is an oxo-IAA-derived mimic and 9 is a phenylacetic acid derivative. Compounds 1h and 1c are derived from resorcinol. Compound 1f incorporates a triazole connected to the D-ring.

Stability of the new compounds at pH 6.5 to 8.5 was evaluated and compound 5 was found to be slightly more stable than GR24 at pH 8.5, whereas compound 9 showed lower stability (Supplementary article I, Supplementary Fig.4). It is a desirable feature for potential field application, as pH of soil can be elevated, and natural SLs decompose rapidly under high pH.

In conclusion, our new mimics display high bioactivity with respect to stimulating seed germination and could be possibly applied as suicidal germination activators. Despite this, compounds being moderately or less active in *in vitro* germination assays can exhibit better results in field trials when factors such as soil adhesion to particles or varying mobility in soil are encountered., as suggested by Samejima et. al. (2016), which requires wider complex research.

8.2. PEA BRANCHING INHIBITION BY SLs

High-throughput plant phenotyping is non-invasive method using image analysis for studying plant growth and performance (Humplík et al., 2015). A growth chamber-based phenotyping platform installed at Palacký University enables e.g.

monitoring of chlorophyll fluorescence (photosynthesis performance), thermoimaging (transpiration performance) or red-green-blue (RGB) imaging of plant shoots (biomass analysis). Several publications shown that SLs play a role in plant's response to environmental stresses (Ha et al., 2013; Ma et al., 2017; Lu et al., 2019). The garden pea, a representative of cultural crops, was intended to be employed in branching assays as a high capacity tool to study the inhibition of lateral bud outgrowth by SLs and newly developed SL derivatives. It could also exhibit interesting response during abiotic stresses, which could be analysed by monitoring changes in the above physiological traits.

However, the protocol of the branching assay described in the original article (Boyer et al., 2012) was found hard to reproduce, as many technical details are missing; amount of water, irradiance intensity and temperature. Furthermore, the cutting off of the lower buds and the application of the SL solution turned out to be a too difficult and time-consuming obstacle for large scale operations (Fig. 17).

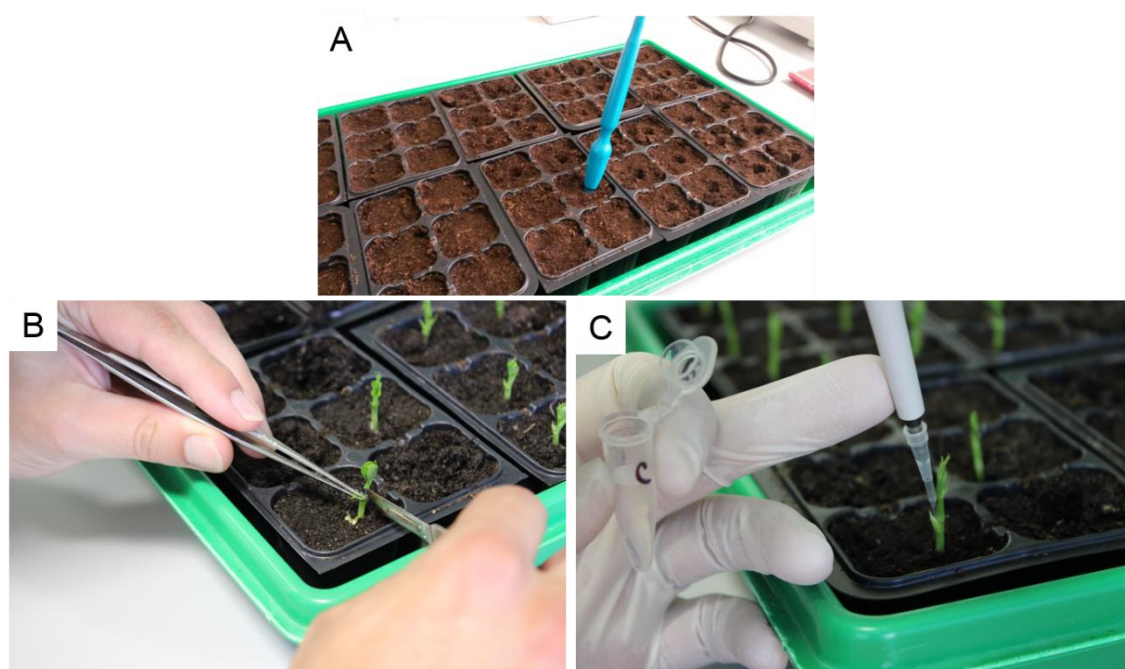


Fig. 17. Selected steps of the pea branching bioassay. (A) Seed sowing into pots filled with substrate. (B) Cutting off of a lower bud. (C) Application of SL solution onto tested bud.

Moreover, the results showed poor repeatability as represented with a high standard deviation (SD) and contribution of SD to each mean (Tab. 3). Therefore, the aim of re-scaling the bioassay to a plant phenotyping platform was not further followed.

Tab. 3. Branching assay parameters. Results are presented as mean \pm standard deviation from four runs and percentage contribution of the SD to the mean. C = 0.1% acetone.

	3 rd bud				1 st bud			
	% of outgrowth		Mean length of a branch		% of outgrowth		Mean length of a branch	
	C	1 μ M GR24	C	1 μ M GR24	C	1 μ M GR24	C	1 μ M GR24
Mean	92	52	4.3	1.3	80	37	18.6	6.8
SD	3	18	1.4	0.3	15	14	4.2	4.5
%	3.3	35.6	32.6	23.7	17.6	37.9	22.6	66.2

8.3. ARABIDOPSIS GERMINATION UNDER SALT STRESS

Excitingly, due to the versatile principle of the MTT assay, the colorimetric method was used to develop an assay on model plant *Arabidopsis thaliana* and monitor germination under control and salt stress conditions (Supplementary article IV, Fig. 1). Biostimulants, which are compounds of a natural origin and are present in commercial products for plant growth enhancement, were used to validate the assay. Amino acid proline (Pro) and three polyamines – spermine (Spm), spermidine (Spd) and putrescin (Put) – were added to the medium and so-called priming during cold stratification was performed. Priming is a procedure where seeds imbibe the liquid and chemicals they are placed in, which improves subsequent plant growth and performance, e.g. in elevated salinity.

The protocol was refined in several steps (Fig. 18):

- Seed size was found to influence ability to germinate, therefore seeds were separated using Retsch sieves with 250, 280 and 300 μ m mesh size. Seeds of 280-299 μ m had the highest germination rate and were used in subsequent experiments.
- Seeds were distributed in a suspension of 0.05% agarose into 96-well plates by multistep pipetting, similarly as described in the improved germination assay for parasitic plants.
- A critical point for accurate results is knowing the exact number of seeds in each well. A simple code for image analysis was developed in MATLAB software (MathWorks, USA), using a picture of the plate to identify wells,

seeds in them and calculating seed number per well. This enabled the recalculation of absorbance per seed and reduced the standard deviation by three times (Supplementary article IV, Fig. 2, Tab. 1).

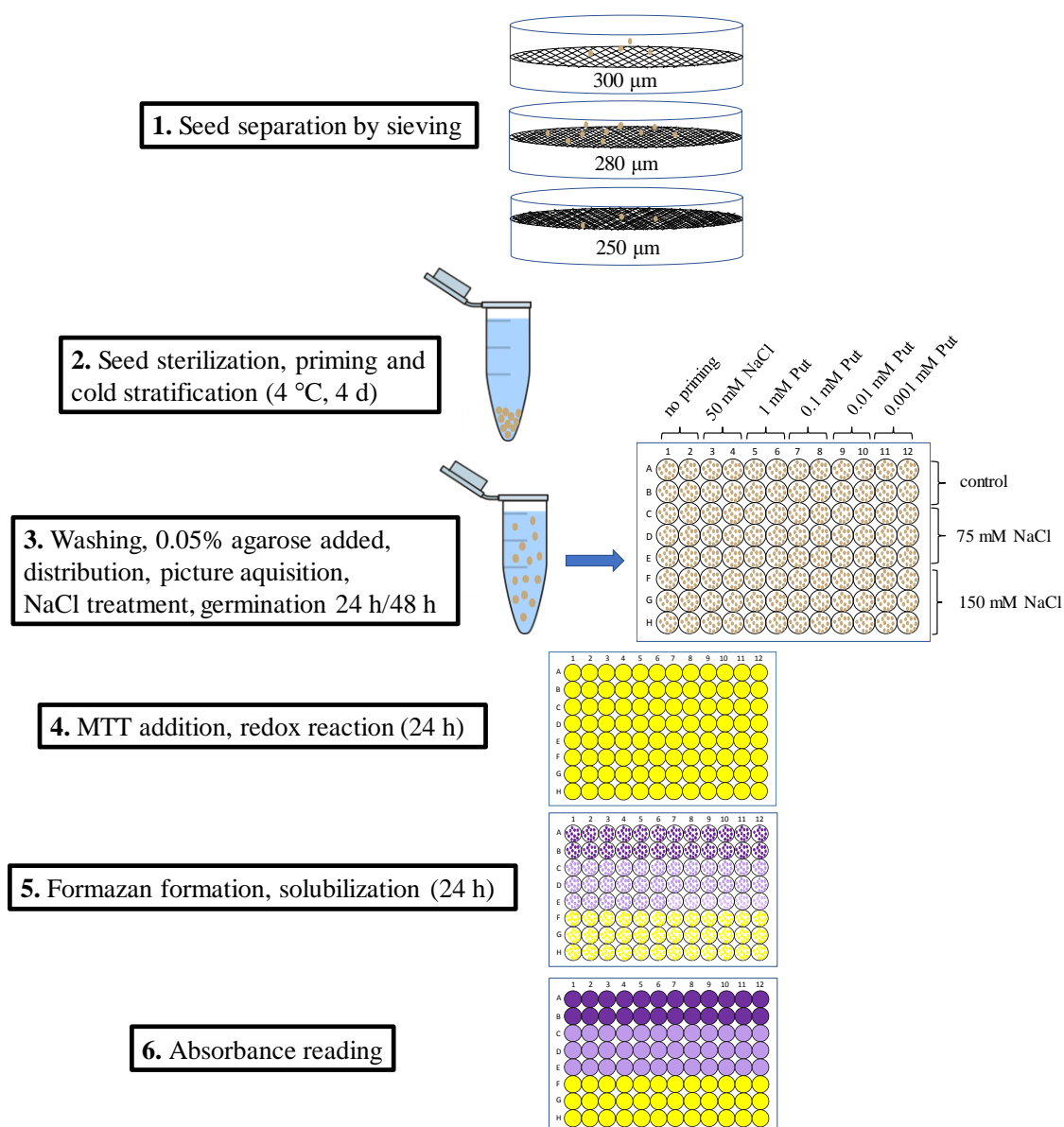


Fig. 18. Scheme of protocol for *Arabidopsis* MTT germination assay in stress conditions.

After solving the technical issues of the protocol, the effects of priming with biostimulants on early seedling development were evaluated. Results calculated at 24 h of germination did not show substantial differences between control and treatments, whereas after 48 h, Put in 0.1 and 0.01 mM concentrations significantly enhanced germination in moderate and severe salinity. 1 mM Pro had the same effect as Put at

severe conditions (Supplementary article IV, Fig. 3). The effect of Spm and Spd was concentration dependent at control and moderate salt stress conditions, showing inhibition at 1 mM Spm or Spd. In severe salt stress conditions priming with Spm/Spd showed no significant differences in comparison with non-primed seeds (Supplementary article IV, Fig. 3).

High capacity of the protocol consists in testing one compound (e.g. putative biostimulant) in 4 concentrations at two salinity strengths per one time point in a single 96-well plate. With this assay, it is therefore manageable to assess the effect of 8 – 12 compounds per a single run, which lasts one week.

9. CONCLUSIONS AND PERSPECTIVES

The scope of this work covers development, optimization and/or enhancement of protocols serving for study of germination of parasitic plants or *Arabidopsis* under salinity stress.

In summary, the following results were obtained:

- An assay of parasitic weed germination as well as a high-throughput MTT based germination assay has been optimized and put into routine testing.
- A complex array of SL mimics has been tested for seed germination stimulation. Compounds composed of oxo-IAA and the SL's D-ring exhibited very low EC₅₀ values, able to stimulate *P. ramosa* at nanomolar concentrations. Some of the SL mimics reached the same stimulatory activity as the standard GR24.
- An MTT based high-throughput assay of *Arabidopsis* germination in salt stress was developed and validated using four natural compounds (proline, spermine, spermidine and putrescine), which are common components of commercial biostimulants.
- Proline and putrescine elicited germination, whereas Spm and Spd had an opposite effect – inhibition of germination, although only at high concentration.

Chemically different SL mimics were evaluated for their biological effect on germination, which can lead to the future development of improved strategies in reducing parasitic weeds infestation, as they display a big threat to agriculture and food security. Furthermore, ongoing climate change can cause the spreading of these noxious weeds to new areas of the world and affect more and more people.

However, it is important to note that parasitic plants include not only noxious weeds, but also endangered species present in The Red List of Threatened Species. Researching ideal germination conditions and developing germination protocols could lay the foundation for cultivation of these plants in pots to multiply the seed bank, which could help save these species.

The *Arabidopsis* MTT based germination assay represents a fast and elegant tool for evaluation of this crucial phase of plant development. Many studies have dealt with seed germination and stress tolerance, but this assay presents an easily employable, high capacity protocol which to our knowledge has never been published before. Robotization

of the protocol at the step of pipetting could increase the capacity and lead to testing large libraries of compounds. For example, as karrikins were shown to play a role in stress protection (see chapter 3.2.), testing of these butanolide compounds and their derivatives in high salinity could provide interesting results.

10. REFERENCES

- Abbes, Z., Kharrat, M., Simier, P., and Chaïbi, W. (2007). Characterization of resistance to crenate broomrape (*Orobancha crenata*) in a new small-seeded line of Tunisian faba beans. *Phytoprotection* **88**:83–92.
- Abe, S., Sado, A., Tanaka, K., Kisugi, T., Asami, K., Ota, S., Kim, H. II, Yoneyama, K., Xie, X., Ohnishi, T., et al. (2014). Carlactone is converted to carlactonoic acid by MAX1 in *Arabidopsis* and its methyl ester can directly interact with AtD14 in vitro. *Proc. Natl. Acad. Sci.* **111**:18084–18089.
- Aguilar-Martínez, J. A., Poza-Carrión, C., and Cubas, P. (2007). *Arabidopsis* Branched1 acts as an integrator of branching signals within axillary buds. *Plant Cell* **19**:458–472.
- Akiyama, K., and Hayashi, H. (2006). Strigolactones: Chemical signals for fungal symbionts and parasitic weeds in plant roots. *Ann. Bot.* **97**:925–931.
- Alder, A., Jamil, M., Marzorati, M., Bruno, M., Vermathen, M., Bigler, P., Ghisla, S., Bouwmeester, H., Beyer, P., and Al-Babili, S. (2012). The Path from β -Carotene to Carlactone, a Strigolactone-Like Plant Hormone. *Science*. **335**:1348–1351.
- Aly, R., Goldwasser, Y., Eizenberg, H., Hershenhorn, J., Golan, S., and Kleifeld, Y. (2001). Broomrape (*Orobancha cumana*) Control in Sunflower (*Helianthus annuus*) with Imazapic1. *Weed Technol.* **15**:306–309.
- Arite, T., Umehara, M., Ishikawa, S., Hanada, A., Maekawa, M., Yamaguchi, S., and Kyoizuka, J. (2009). d14, a Strigolactone-Insensitive Mutant of Rice, Shows an Accelerated Outgrowth of Tillers. *Plant Cell Physiol.* **50**:1416–1424.
- Artuso, E., Ghibaudi, E., Lombardi, C., Koltai, H., Kapulnik, Y., Novero, M., Occhiato, E. G., Scarpi, D., Parisotto, S., Deagostino, A., et al. (2015). Stereochemical Assignment of Strigolactone Analogues Confirms Their Selective Biological Activity. *J. Nat. Prod.* **78**:2624–2633.
- Awad, A. A., Sato, D., Kusumoto, D., Kamioka, H., Takeuchi, Y., and Yoneyama, K. (2006). Characterization of strigolactones, germination stimulants for the root parasitic plants *Striga* and *Orobancha*, produced by maize, millet and sorghum. *Plant Growth Regul.* **48**:221–227.
- Ayongwa, G. C., Stomph, T. J., Emechebe, A. M., and Kuyper, T. W. (2006). Root nitrogen concentration of sorghum above 2 % produces least *Striga hermonthica* seed stimulation. *Ann. Appl. Biol.* **149**:255–262.
- Arumingtyas, E., Floyd, R., Gregory, M., and Murfet, I. (1992). Branching in *Pisum*: inheritance and allelism tests with 17 ramosus mutants. *Pisum Genet.* **24**:17–31.

- Baldwin, I. T., Staszak-Kozinski, L., and Davidson, R.** (1994). Up in smoke: I. Smoke-derived germination cues for postfire annual, *Nicotiana attenuata* torr. Ex. Watson. *J. Chem. Ecol.* **20**:2345–2371.
- Beveridge, C. A., Ross, J. J., and Murfet, I. C.** (1996). Branching in Pea: Action of Genes Rms3 and Rms4. *Plant Physiol.* **110**:859–865.
- Boari, A., Ciasca, B., Pineda-Martos, R., Lattanzio, V. M., Yoneyama, K., and Vurro, M.** (2016). Parasitic weed management by using strigolactone-degrading fungi. *Pest Manag. Sci.* **72**:2043–2047.
- Boyer, F.-D., de Saint Germain, A., Pillot, J.-P., Pouvreau, J.-B., Chen, V. X., Ramos, S., Stévenin, A., Simier, P., Delavault, P., Beau, J.-M., et al.** (2012). Structure-Activity Relationship Studies of Strigolactone-Related Molecules for Branching Inhibition in Garden Pea: Molecule Design for Shoot Branching. *Plant Physiol.* **159**:1524–1544.
- Boyer, F., Saint, A. De, Pouvreau, J., and Clavé, G.** (2014). New Strigolactone Analogs as Plant Hormones with Low Activities in the Rhizosphere. *Mol. Plant* **7**:675–690.
- Braun, N., de Saint Germain, A., Pillot, J.-P., Boutet-Mercey, S., Dalmais, M., Antoniadi, I., Li, X., Maia-Grondard, A., Le Signor, C., Bouteiller, N., et al.** (2011). The Pea TCP Transcription Factor PsBRC1 Acts Downstream of Strigolactones to Control Shoot Branching. *Plant Physiol.* **158**:225–238.
- Brewer, P. B., Yoneyama, K., Filardo, F., Meyers, E., Scaffidi, A., Frickey, T., Akiyama, K., Seto, Y., Dun, E. A., Cremer, J. E., et al.** (2016). *LATERAL BRANCHING OXIDOREDUCTASE* acts in the final stages of strigolactone biosynthesis in *Arabidopsis*. *Proc. Natl. Acad. Sci.* **113**:201601729.
- Brewer, P. B., Dun, E. A., Ferguson, B. J., Rameau, C., and Beveridge, C. A.** (2009). Strigolactone acts downstream of auxin to regulate bud outgrowth in pea and *Arabidopsis*. *Plant Physiol.* **150**:482–93.
- Brun, G., Thoiron, S., Braem, L., Pouvreau, J., Montiel, G., Lechat, M., Simier, P., Gevaert, K., Goormachtig, S., and Delavault, P.** (2019). CYP707As are effectors of karrikin and strigolactone signalling pathways in *Arabidopsis thaliana* and parasitic plants. *Plant. Cell Environ.* **42**:2612–2626.
- Bruno, M., Hofmann, M., Vermathen, M., Alder, A., Beyer, P., Al-Babili, S., and Schroeder, J.** (2014). On the substrate-and stereospecificity of the plant carotenoid cleavage dioxygenase 7. *FEBS Lett.* **588**:1802-1807.
- Bythell-Douglas, R., Waters, M. T., Scaffidi, A., Flematti, G. R., Smith, S. M., and Bond, C. S.** (2013). The Structure of the Karrikin-Insensitive Protein (KAI2) in *Arabidopsis thaliana*. *PLoS One* **8**.
- Cala, A., Ghooray, K., Fernández-Aparicio, M., Molinillo, J. M. G., Galindo, J. C. G., and Macías, F. A.** (2016). Phthalimide-derived strigolactone mimics as germinating agents for seeds of parasitic weeds. *Pest Manag. Sci.* **72**:2069–2081.

- Charnikhova, T. V., Gaus, K., Lumbroso, A., Sanders, M., Vincken, J.-P., De Mesmaeker, A., Ruyter-Spira, C. P., Screpanti, C., and Bouwmeester, H. J.** (2017). Zealactones. Novel natural strigolactones from maize. *Phytochemistry* **137**:123–131.
- Chiwocha, S., Dixon, K., Flematti, G., Ghisalberti, E., Merritt, D., Nelson, D., Riseborough, J. M., Smith, S., Stevens, J.** (2009). Karrikins: A new family of plant growth regulators in smoke. *Plant Science* **177**:4, 252-256.
- Cohen, M., Prandi, C., Occhiato, E. G., Tabasso, S., Wininger, S., Resnick, N., Steinberger, Y., Koltai, H., and Kapulnik, Y.** (2013). Structure-Function Relations of Strigolactone Analogs: Activity as Plant Hormones and Plant Interactions. *Mol. Plant* **6**:141–152.
- Colquhoun, J. B., Eizenberg, H., and Mallory-Smith, C. A.** (2006). Herbicide Placement Site Affects Small Broomrape (*Orobanche minor*) Control in Red Clover. *Weed Technol.* **20**:356–360.
- Conn, C. E., Bythell-Douglas, R., Neumann, D., Yoshida, S., Whittington, B., Westwood, J. H., Shirasu, K., Bond, C. S., Dyer, K. A., and Nelson, D. C.** (2016). Convergent evolution of strigolactone perception enabled host detection in parasitic plants. *Science*. **349**:540–543.
- Cook, C. E., Whichard, L. P., Turner, B., Wall, M. E., and Egley, G. H.** (1966). Germination of Witchweed (*Striga lutea* Lour.): Isolation and Properties of a Potent Stimulant. *Science*. **154**:1189–1190.
- Cook, C. E., Whichard, L. P., Wall, M., Egley, G. H., Coggon, P., Luhan, P. A., and McPhail, A. T.** (1972). Germination stimulants. II. Structure of strigol, a potent seed germination stimulant for witchweed (*Striga lutea*). *J. Am. Chem. Soc.* **94**:6198–6199.
- Delavault, P., Montiel, G., Brun, G., Pouvreau, J.-B., Thoiron, S., and Simier, P.** (2017). Communication Between Host Plants and Parasitic Plants. *Adv. Bot. Res.* **82**:55–82.
- de Saint Germain, A., Clavé, G., Badet-Denisot, M.-A., Pillot, J.-P., Cornu, D., Le Caer, J.-P., Burger, M., Pelissier, F., Retailleau, P., Turnbull, C., et al.** (2016). An histidine covalent receptor and butenolide complex mediates strigolactone perception. *Nat. Chem. Biol.* **12**:787–794.
- Dixon, K. W., Roche, S., and Pate, J. S.** (1995). The promotive effect of smoke derived from burnt native vegetation on seed germination of Western Australian plants. *Oecologia* **101**:185–192.
- Dixon, K. W., Merritt, D. J., Flematti, G. R., and Ghisalberti, E. L.** (2009). Karrikinolide – A Phytoreactive Compound Derived from Smoke with Applications in Horticulture, Ecological Restoration and Agriculture. *Acta Hort.* **813**:155-170.

- Duan, J., Yu, H., Yuan, K., Liao, Z., Meng, X., Jing, Y., and Liu, G.** (2019). Strigolactone promotes cytokinin degradation through transcriptional activation of CYTOKININ OXIDASE / DEHYDROGENASE 9 in rice. *Proc. Natl. Acad. Sci. U. S. A.* **116**:2–7.
- Dun, E. a., Brewer, P. B., and Beveridge, C. A.** (2009). Strigolactones: discovery of the elusive shoot branching hormone. *Trends Plant Sci.* **14**:364–372.
- Dun, E. a., de Saint Germain, a., Rameau, C., and Beveridge, C. A.** (2012). Antagonistic Action of Strigolactone and Cytokinin in Bud Outgrowth Control. *Plant Physiol.* **158**:487–498.
- Dvořáková, M., Hýlová, A., Soudek, P., Retzer, K., Spíchal, L., and Vaněk, T.** (2018). Resorcinol-Type Strigolactone Mimics as Potent Germinators of the Parasitic Plants *Striga hermonthica* and *Phelipanche ramosa*. *J. Nat. Prod.* **81**(11):2321–2328.
- Dvořáková, M., Hýlová, A., Soudek, P., Retzer, K., Spíchal, L., and Vaněk, T.** (2019). Correction to Resorcinol-Type Strigolactone Mimics as Potent Germinators of the Parasitic Plants *Striga hermonthica* and *Phelipanche ramosa*. *J. Nat. Prod.* **82**:168–168.
- Dvořáková, M., Soudek, P., and Vaněk, T.** (2017). Triazolide Strigolactone Mimics Influence Root Development in *Arabidopsis*. *J. Nat. Prod.* **80**:1318–1327.
- Eizenberg, H., Aly, R., and Cohen, Y.** (2012). Technologies for Smart Chemical Control of Broomrape (*Orobanch* spp. and *Phelipanche* spp.). *Weed Sci.* **60**:316–323.
- Eplee, R. E.** (1992). Witchweed (*Striga asiatica*): an overview of management strategies in the USA. *Crop Prot.* **11**:3–7.
- Evidente, A., Fernández-Aparicio, M., Cimmino, A., Rubiales, D., Andolfi, A., and Motta, A.** (2009). Peagol and peagoldione, two new strigolactone-like metabolites isolated from pea root exudates. *Tetrahedron Lett.* **50**:6955–6958.
- Fernández-Aparicio, M., Bernard, A., Falchetto, L., Marget, P., Chauvel, B., Steinberg, C., Morris, C. E., Gibot-Leclerc, S., Boari, A., Vurro, M., et al.** (2017). Investigation of Amino Acids As Herbicides for Control of *Orobanch* minor Parasitism in Red Clover. *Front. Plant Sci.* **8**:1–12.
- Fernández-Aparicio, M., Kisugi, T., Xie, X., Rubiales, D., and Yoneyama, K.** (2014). Low strigolactone root exudation: A novel mechanism of broomrape (*Orobanch* and *Phelipanche* spp.) resistance available for faba bean breeding. *J. Agric. Food Chem.* **62**:7063–7071.
- Fernández-Aparicio, M., Yoneyama, K., and Rubiales, D.** (2011). The role of strigolactones in host specificity of *Orobanch* and *Phelipanche* seed germination. *Seed Sci. Res.* **21**:55–61.

- Fernández-Martínez, J. M., Pérez-Vich, B., and Velasco, L.** (2015). Sunflower Broomrape (*Orobancha cumana* Wallr.). In *Sunflower*, pp. 129–155. Elsevier.
- Flematti, G. R., Ghisalberti, E. L., Dixon, K. W., and Trengove, R. D.** (2009). Identification of Alkyl Substituted 2 *H* -Furo[2,3- *c*]pyran-2-ones as Germination Stimulants Present in Smoke. *J. Agric. Food Chem.* **57**:9475–9480.
- Flematti, G. R., Ghisalberti, E. L., Dixon, K. W., and Trengove, R. D.** (2004). A compound from smoke that promotes seed germination. *Science* **305**:977.
- Gobena, D., Shimels, M., Rich, P. J., Ruyter-Spira, C., Bouwmeester, H., Kanuganti, S., Mengiste, T., and Ejeta, G.** (2017). Mutation in sorghum LGS1 alters strigolactones and causes *Striga* resistance. *Proc. Natl. Acad. Sci.* **114**:4471–76.
- Goldwasser, Y., and Rodenburg, J.** (2013). Integrated Agronomic Management of Parasitic Weed Seed Banks. In *Parasitic Orobanchaceae*, pp. 393–413. Berlin, Heidelberg: Springer Berlin Heidelberg.
- Gomez Roldan, V., Fermas, S., Brewer, P. B., Puech-Pagès, V., Dun, E. A., Pillot, J.-P., Letisse, F., Matušová, R., Danoun, S., Portais, J.-C., et al.** (2008). Strigolactone inhibition of shoot branching. *Nature* **455**:189–94.
- Goyet, V., Billard, E., Pouvreau, J.-B., Lechat, M.-M., Pelletier, S., Bahut, M., Monteau, F., Spíchal, L., Delavault, P., Montiel, G., et al.** (2017). Haustorium initiation in the obligate parasitic plant *Phelipanche ramosa* involves a host-exuded cytokinin signal. *J. Exp. Bot.* **68**:5539–5552.
- Ha, C. V., Leyva-Gonzalez, M. A., Osakabe, Y., Tran, U. T., Nishiyama, R., Watanabe, Y., Tanaka, M., Seki, M., Yamaguchi, S., Dong, N. V., et al.** (2013). Positive regulatory role of strigolactone in plant responses to drought and salt stress. *Proc. Natl. Acad. Sci.* **111**:851–856.
- Halouzka, R., Tarkowski, P., Zwanenburg, B., Cavar, S., and Zeljković, Z.** (2017). Stability of strigolactone analog GR24 toward nucleophiles. *Pest Manag. Sci.* **74**:896–904.
- Hamiaux, C., Drummond, R. S. M., Janssen, B. J., Ledger, S. E., Cooney, J. M., Newcomb, R. D., and Snowden, K. C.** (2012). DAD2 is an α/β hydrolase likely to be involved in the perception of the plant branching hormone, strigolactone. *Curr. Biol.* **22**:2032–6.
- Hassanali, A., Ayensu, E. S., Doggett, H., Keynes, R. D., Marton-Lefevre, J., Musselman, L. J., Parker, C., and Pickering, A.** (1984). *Striga: Biology and Control*.
- Hershenhorn, J., Goldwasser, Y., Plakhine, D., Ali, R., Blumenfeld, T., Bucsbaum, H., Herzlinger, G., Golan, S., Chilf, T., Eizenberg, H., et al.** (1998). *Orobancha aegyptiaca* control in tomato fields with sulfonylurea herbicides. *Weed Res.* **38**:343–349.

- Humplík, J. F., Lazár, D., Husičková, A., and Spíchal, L.** (2015). Automated phenotyping of plant shoots using imaging methods for analysis of plant stress responses – a review. *Plant Methods* **11**:1–10.
- Hýlová, A., Pospíšil, T., Spíchal, L., Mateman, J. J., Blanco-Ania, D., and Zwanenburg, B.** (2019). New hybrid type strigolactone mimics derived from plant growth regulator auxin. *N. Biotechnol.* **48**:76–82.
- Iseki, M., Shida, K., Kuwabara, K., Wakabayashi, T., Mizutani, M., Takikawa, H., and Sugimoto, Y.** (2018). Evidence for species-dependent biosynthetic pathways for converting carlactone to strigolactones in plants. *J. Exp. Bot.* **69**:2305–2318.
- Ito, S., Yamagami, D., Umehara, M., Hanada, A., Yoshida, S., Sasaki, Y., Yajima, S., Kyojuka, J., Ueguchi-Tanaka, M., Matsuoka, M., et al.** (2017). Regulation of Strigolactone Biosynthesis by Gibberellin Signaling. *Plant Physiol.* **174**:1250–1259.
- Jain, R., and Foy, C. L.** (1992). Nutrient Effects on Parasitism and Germination of Egyptian Broomrape (*Orobanchae aegyptiaca*). *Weed Technol.* **6**:269–275.
- Jamil, M., Charnikhova, T., Cardoso, C., Jamil, T., Ueno, K., Verstappen, F., Asami, T., and Bouwmeester, H. J.** (2011). Quantification of the relationship between strigolactones and *Striga hermonthica* infection in rice under varying levels of nitrogen and phosphorus. *Weed Res.* **51**:373–385.
- Jamil, M., Kanampiu, F. K., Karaya, H., Charnikhova, T., and Bouwmeester, H. J.** (2012). *Striga hermonthica* parasitism in maize in response to N and P fertilisers. *F. Crop. Res.* **134**:1–10.
- Jamil, M., Kountche, B. A., Haider, I., Wang, J. Y., Aldossary, F., Zarban, R. A., Jia, K.-P., Yonli, D., Shahul Hameed, U. F., Takahashi, I., et al.** (2019). Methylation at the C-3' in D-Ring of Strigolactone Analogs Reduces Biological Activity in Root Parasitic Plants and Rice. *Front. Plant Sci.* **10**:353.
- Jia, K.-P., Baz, L., and Al-Babili, S.** (2018). From carotenoids to strigolactones. *J. Exp. Bot.* **69**:2189–2204.
- Jiang, L., Liu, X., Xiong, G., Liu, H., Chen, F., Wang, L., Meng, X., Liu, G., Yu, H., Yuan, Y., et al.** (2013). DWARF 53 acts as a repressor of strigolactone signalling in rice. *Nature* **504**:401–405.
- Joel, D. M.** (2009). The new nomenclature of *Orobanchae* and *Phelipanche*: Editors' note. *Weed Res.* **49**:6–7.
- Joel, D. M., Chaudhuri, S. K., Plakhine, D., Ziadna, H., and Steffens, J. C.** (2011). Dehydrocostus lactone is exuded from sunflower roots and stimulates germination of the root parasite *Orobanchae cumana*. *Phytochemistry* **72**:624–634.
- Joel, D. M. (Daniel M.), Gressel, J., and Musselman, L. J.** (2013). Parasitic *Orobanchaceae*: parasitic mechanisms and control strategies. Berlin, Heidelberg: Springer.

- Joel, D. M.** (2013). The Haustorium and the Life Cycles of Parasitic *Orobanchaceae*. In *Parasitic Orobanchaceae*, pp. 21–23. Berlin, Heidelberg: Springer Berlin Heidelberg.
- Johnson, A. W., Roseberry, G., and Parker, C.** (1976). A novel approach to *Striga* and *Orobanche* control using synthetic germination stimulants. *Weed Res.* **16**:223–227.
- Johnson, A. W., Gowada, G., Hassanali, A., Knox, J., Monaco, S., Razavi, Z., and Rosebery, G.** (1981). The preparation of synthetic analogues of strigol. *J. Chem. Soc. Perkin Trans. 1.* **6**:1734-1743.
- Kagiyama, M., Hirano, Y., Mori, T., Kim, S.-Y., Kyojuka, J., Seto, Y., Yamaguchi, S., and Hakoshima, T.** (2013). Structures of D14 and D14L in the strigolactone and karrikin signaling pathways. *Genes to Cells* **18**:147–160.
- Kannan, C., Aditi, P., and Zwanenburg, B.** (2015). Quenching the action of germination stimulants using borax and thiourea, a new method for controlling parasitic weeds: A proof of concept. *Crop Prot.* **70**:92–98.
- Kapulnik, Y., Resnick, N., Mayzlish-Gati, E., Kaplan, Y., Wininger, S., Hershenhorn, J., and Koltai, H.** (2011). Strigolactones interact with ethylene and auxin in regulating root-hair elongation in *Arabidopsis*. *J. Exp. Bot.* **62**:2915–2924.
- Kgosi, R. L., Zwanenburg, B., Mwakaboko, A. S., and Murdoch, A. J.** (2012). Strigolactone analogues induce suicidal seed germination of *Striga* spp. in soil. *Weed Res.* **52**:197–203.
- Khan, Z. R., Midega, C. A. O., Bruce, T. J. A., Hooper, A. M., and Pickett, J. A.** (2010). Exploiting phytochemicals for developing a “push-pull” crop protection strategy for cereal farmers in Africa. *J. Exp. Bot.* **61**:4185–4196.
- Kohlen, W., Charnikhova, T., Liu, Q., Bours, R., Domagalska, M. A., Beguerie, S., Verstappen, F., Leyser, O., Bouwmeester, H., and Ruyter-Spira, C.** (2011). Strigolactones are transported through the xylem and play a key role in shoot architectural response to phosphate deficiency in nonarbuscular mycorrhizal host *Arabidopsis*. *Plant Physiol.* **155**:974–87.
- Kountche, B. A., Hash, C. T., Dodo, H., Laoualy, O., Sanogo, M. D., Timbeli, A., Vigouroux, Y., This, D., Nijkamp, R., and Haussmann, B. I. G.** (2013). Development of a pearl millet *Striga*-resistant genepool: Response to five cycles of recurrent selection under *Striga*-infested field conditions in West Africa. *F. Crop. Res.* **154**:82–90.
- Kountche, B. A., Jamil, M., Yonli, D., Nikiema, M. P., Blanco-Ania, D., Asami, T., Zwanenburg, B., and Al-Babili, S.** (2019). Suicidal germination as a control strategy for *Striga hermonthica* (Benth.) in smallholder farms of sub-Saharan Africa. *Plants, People, Planet* **1**:107–118.
- Kroschel, J., Hundt, A., Abbasher, A. A., and Sauerborm, J.** (1996). Pathogenicity of fungi collected in northern Ghana to *Striga hermonthica*. *Weed Res.* **36**:515–520.

- Lechat MM, Pouvreau JB, Péron T, Gauthier M, Montiel G, Véronési C, Todoroki Y, Le Bizec B, Monteau F, Macherel D, Simier P, Thoiron S, D. P.** (2012). PrCYP707A1, an ABA catabolic gene, is a key component of *Phelipanche ramosa* seed germination in response to the strigolactone analogue GR24. *J. Exp. Bot.* **63**:695–709.
- Lechat, M.-M., Brun, G., Montiel, G., Véronési, C., Simier, P., Thoiron, S., Pouvreau, J.-B., and Delavault, P.** (2015). Seed response to strigolactone is controlled by abscisic acid-independent DNA methylation in the obligate root parasitic plant, *Phelipanche ramosa* L. Pomel. *J. Exp. Bot.* **66**:3129–40.
- Lin, H., Wang, R., Qian, Q., Yan, M., Meng, X., Fu, Z., Yan, C., Jiang, B., Su, Z., Li, J., et al.** (2009). DWARF27, an Iron-Containing Protein Required for the Biosynthesis of Strigolactones, Regulates Rice Tiller Bud Outgrowth. *Plant Cell Online* **21**:1512–1525.
- Liu, W., Wu, C., Fu, Y., Hu, G., Si, H., Zhu, L., Luan, W., He, Z., and Sun, Z.** (2009). Identification and characterization of HTD2: a novel gene negatively regulating tiller bud outgrowth in rice. *Planta* **230**:649–658.
- López-Ráez, J. A., Charnikhova, T., Gómez-Roldán, V., Matusova, R., Kohlen, W., De Vos, R., Verstappen, F., Puech-Pages, V., Bécard, G., Mulder, P., et al.** (2008). Tomato strigolactones are derived from carotenoids and their biosynthesis is promoted by phosphate starvation. *New Phytol.* **178**:863–874.
- Lu, T., Yu, H., Li, Q., Chai, L., and Jiang, W.** (2019). Improving Plant Growth and Alleviating Photosynthetic Inhibition and Oxidative Stress From Low-Light Stress With Exogenous GR24 in Tomato (*Solanum lycopersicum* L.) Seedlings. *Front. Plant Sci.* **10**:490.
- Lumba, S., Holbrook-Smith, D., and McCourt, P.** (2017). The perception of strigolactones in vascular plants. *Nat. Chem. Biol.* **13**.
- Ma, N., Hu, C., Wan, L., Hu, Q., Xiong, J., and Zhang, C.** (2017). Strigolactones Improve Plant Growth , Photosynthesis , and Alleviate Oxidative Stress under Salinity in Rapeseed (*Brassica napus* L .) by Regulating Gene Expression. *Front. Plant Sci.* **8**:1–15.
- Malik, H., Kohlen, W., Jamil, M., Rutjes, F. P. J. T., and Zwanenburg, B.** (2011). Aromatic A-ring analogues of orobanchol, new germination stimulants for seeds of parasitic weeds. *Org. Biomol. Chem.* **9**:2286–93.
- Mangnus, E. M., and Zwanenburg, B.** (1992a). Synthesis, structural characterization, and biological evaluation of all four enantiomers of strigol analog GR7. *J. Agric. Food Chem.* **40**:697–700.
- Mangnus, E. M., Stommen, P. L. A., and Zwanenburg, B.** (1992b). A standardized bioassay for evaluation of potential germination stimulants for seeds of parasitic weeds. *J. Plant Growth Regul.* **11**:91–98.

- Matušová, R., Kumkum, R., Verstappen, F. W. A., Franssen, M. C. R., Beale, M. H., and Bouwmeester, H. J.** (2005). The Strigolactone Germination Stimulants of the Plant-Parasitic *Striga* and *Orobanch*e spp. Are Derived from the Carotenoid Pathway. *Plant Physiol.* **139**:920–934.
- Miyakawa, T., Xu, Y., and Tanokura, M.** (2019). Molecular basis of strigolactone perception in root-parasitic plants: aiming to control its germination with strigolactone agonists/antagonists. *Cell. Mol. Life Sci.*
- Mohemed, N., Charnikhova, T., Bakker, E. J., van Ast, A., Babiker, A. G., and Bouwmeester, H. J.** (2016). Evaluation of field resistance to *Striga hermonthica* (Del.) Benth. in *Sorghum bicolor* (L.) Moench. The relationship with strigolactones. *Pest Manag. Sci.* **72**:2082–2090.
- Mosmann, T.** (1983). Rapid colorimetric assay for cellular growth and survival: Application to proliferation and cytotoxicity assays. *J. Immunol. Methods* **65**:55–63.
- Nelson, D. C., Riseborough, J.-A., Flematti, G. R., Stevens, J., Ghisalberti, E. L., Dixon, K. W., and Smith, S. M.** (2009). Karrikins Discovered in Smoke Trigger *Arabidopsis* Seed Germination by a Mechanism Requiring Gibberellic Acid Synthesis and Light. *Plant Physiol.* **149**:863–873.
- Nelson, D. C., Scaffidi, A., Dun, E. A., Waters, M. T., Flematti, G. R., Dixon, K. W., Beveridge, C. A., Ghisalberti, E. L., and Smith, S. M.** (2011). F-box protein MAX2 has dual roles in karrikin and strigolactone signaling in *Arabidopsis thaliana*. *Proc. Natl. Acad. Sci. U. S. A.* **108**:8897–902.
- N’cho, S. A., Mourits, M., Rodenburg, J., and Oude Lansink, A.** (2019). Inefficiency of manual weeding in rainfed rice systems affected by parasitic weeds. *Agric. Econ.* **50**:151–163.
- Nzioki, H. S., Oyosi, F., Morris, C. E., Kaya, E., Pilgeram, A. L., Baker, C. S., and Sands, D. C.** (2016). *Striga* Biocontrol on a Toothpick : A Readily Deployable and Inexpensive Method for Smallholder Farmers. *Front. Plant Sci.* **7**:1–8.
- Oancea, F., Georgescu, E., Matusova, R., Georgescu, F., Vladulescu, L., and Deleanu, C.** (2017). New Strigolactone Mimics as Exogenous Signals for Rhizosphere Organisms. *Molecules* **22**:1–15.
- Parker, C.** (2012). Parasitic Weeds: A World Challenge. *Weed Sci.* **60**:269–276.
- Parker, C.** (2009). Observations on the current status of *Orobanch*e and *Striga* problems worldwide. *Pest Manag. Sci.* **65**:453–9.
- Pavan, S., Schiavulli, A., Marcotrigiano, A. R., Bardaro, N., Bracuto, V., Ricciardi, F., Charnikhova, T., Lotti, C., Bouwmeester, H., and Ricciardi, L.** (2016). Characterization of Low-Strigolactone Germplasm in Pea (*Pisum sativum* L.) Resistant to Crenate Broomrape (*Orobanch*e crenata Forsk.). *Mol. Plant-Microbe Interact.* **29**:743–749.

- Pereira, R. G., Cala, A., Fernández-aparicio, M., Molinillo, J. M. G., Boaventura, A. D., and Macías, F. A.** (2017). Gibberellic and kaurenoic hybrid strigolactone mimics for seed germination of parasitic weeds. *Pest Manag. Sci.* **73**(12):2529–2537.
- Pickett, J. A., Hamilton, M. L., Hooper, A. M., Khan, Z. R., and Midega, C. A. O.** (2010). Companion Cropping to Manage Parasitic Plants. *Annu. Rev. Phytopathol.* **48**:161–177.
- Pouvreau, J.-B., Gaudin, Z., Auger, B., Lechat, M.-M., Gauthier, M., Delavault, P., and Simier, P.** (2013). A high-throughput seed germination assay for root parasitic plants. *Plant Methods* **9**:32.
- Prandi, C., Occhiato, E. G., Tabasso, S., Bonfante, P., Novero, M., Scarpi, D., Bova, M. E., and Miletto, I.** (2011). New Potent Fluorescent Analogues of Strigolactones: Synthesis and Biological Activity in Parasitic Weed Germination and Fungal Branching. *European J. Org. Chem.* **20-21**:3781-3793.
- Proust, H., Hoffmann, B., Xie, X., Yoneyama, K., Schaefer, D. G., Yoneyama, K., Nogué, F., and Rameau, C.** (2011). Strigolactones regulate protonema branching and act as a quorum sensing-like signal in the moss *Physcomitrella patens*. *Development* **138**:1531–9.
- Ransom, J., Kanampiu, F., Gressel, J., De Groote, H., Burnet, M., and Odhiambo, G.** (2012). Herbicide Applied to Imidazolinone Resistant-Maize Seed as a *Striga* Control Option for Small-Scale African Farmers. *Weed Sci.* **60**:283–289.
- Rasmussen, A., Mason, M. G., De Cuyper, C., Brewer, P. B., Herold, S., Agusti, J., Geelen, D., Greb, T., Goormachtig, S., Beeckman, T., et al.** (2012). Strigolactones Suppress Adventitious Rooting in *Arabidopsis* and Pea. *Plant Physiol.* **158**:1976–1987.
- Rasmussen, A., Heugebaert, T., Matthys, C., Deun, R. Van, Boyer, F. D., Goormachtig, S., Stevens, C., and Geelen, D.** (2013). A fluorescent alternative to the synthetic strigolactone GR24. *Mol. Plant* **6**:100–112.
- Reizelman, A., Scheren, M., Nefkens, G. H. L., and Zwanenburg, B.** (2000). Synthesis of all eight stereoisomers of the germination stimulant strigol. *Synthesis (Stuttg.)* **13**:1944-1951.
- Rodenburg, J., Bastiaans, L., Weltzien, E., and Hess, D. E.** (2005). How can field selection for *Striga* resistance and tolerance in sorghum be improved? *F. Crop. Res.* **93**:34–50.
- Rodenburg, J., Demont, M., Zwart, S. J., and Bastiaans, L.** (2016a). Parasitic weed incidence and related economic losses in rice in Africa. *Agric. Ecosyst. Environ.* **235**:306–317.

- Rodenburg, J., Cissoko, M., Dieng, I., Kayeke, J., and Bastiaans, L.** (2016b). Rice yields under *Rhizophragma fistulosa*-infested field conditions, and variety selection criteria for resistance and tolerance. *F. Crop. Res.* **194**:21–30.
- Rodenburg, J., Cissoko, M., Kayongo, N., Dieng, I., Bisikwa, J., Irakiza, R., Masoka, I., Midega, C. A. O., and Scholes, J. D.** (2017). Genetic variation and host-parasite specificity of *Striga* resistance and tolerance in rice: the need for predictive breeding. *New Phytol.* **214**:1267–1280.
- Rubiales, D., Flores, F., Emeran, A. A., Kharrat, M., Amri, M., Rojas-Molina, M. M., and Sillero, J. C.** (2014). Identification and multi-environment validation of resistance against broomrapes (*Orobancha crenata* and *Orobancha foetida*) in faba bean (*Vicia faba*). *F. Crop. Res.* **166**:58–65.
- Ruyter-Spira, C., Kohlen, W., Charnikhova, T., Van Zeijl, A., Van Bezouwen, L., De Ruijter, N., Cardoso, C., Antonio López-Ráez, J., Matušová, R., Bours, R., et al.** (2011). Physiological Effects of the Synthetic Strigolactone Analog GR24 on Root System Architecture in *Arabidopsis*: Another Belowground Role for Strigolactones? *Plant Physiol.* **155**:721–734.
- Sánchez, E., Artuso, E., Lombardi, C., Visentin, I., Lace, B., Saeed, W., Lolli, M. L., Kobauri, P., Ali, Z., Spyraakis, F., et al.** (2018). Structure–activity relationships of strigolactones via a novel, quantitative in planta bioassay. *J. Exp. Bot.* **69**:2333–43.
- Samejima, H., Babiker, G., Takikawa, H., and Sugimoto, Y.** (2016). Practicality of the suicidal germination approach for controlling *Striga hermonthica*. *Pest Manag. Sci.* **72**:2035–42.
- Samodelov, S. L., Beyer, H. M., Guo, X., Augustin, M., Jia, K.-P., Baz, L., Ebenhoeh, O., Beyer, P., Weber, W., Al-Babili, S., et al.** (2016). StrigoQuant: A genetically encoded biosensor for quantifying strigolactone activity and specificity. *Sci. Adv.* **2**:e1601266.
- Scaffidi, A., Waters, M. T., Bond, C. S., Dixon, K. W., Smith, S. M., Ghisalberti, E. L., and Flematti, G. R.** (2012). Exploring the molecular mechanism of karrikins and strigolactones. *Bioorg. Med. Chem. Lett.* **22**:3743–3746.
- Seto, Y., Sado, A., Asami, K., Hanada, A., Umehara, M., Akiyama, K., and Yamaguchi, S.** (2014). Carlactone is an endogenous biosynthetic precursor for strigolactones. *Proc. Natl. Acad. Sci. U. S. A.* **111**:1640–5.
- Showemimo, F., Kimbeng, C., and Alabi, S.** (2002). Genotypic response of sorghum cultivars to nitrogen fertilization in the control of *Striga hermonthica*. *Crop Prot.* **21**:867–870.
- Soundappan, I., Bennett, T., Morffy, N., Liang, Y., Stanga, J. P., Abbas, A., Leyser, O., and Nelson, D. C.** (2015). SMAX1-LIKE/D53 Family Members Enable Distinct MAX2-Dependent Responses to Strigolactones and Karrikins in *Arabidopsis*. *Plant Cell* **14**:1–18.

- Stanga, J. P., Smith, S. M., Briggs, W. R., and Nelson, D. C.** (2013). SUPPRESSOR OF MORE AXILLARY GROWTH2 1 controls seed germination and seedling development in *Arabidopsis*. *Plant Physiol.* **163**:318–30.
- Stirnberg, P., Furner, I. J., and Leyser, O. H. M.** (2007). MAX2 participates in an SCF complex which acts locally at the node to suppress shoot branching. *Plant J.* **50**:80–94.
- Sugimoto, Y., Wigchert, S. C. M., Thuring, J. W. J. F., and Zwanenburg, B.** (1997). The first total synthesis of the naturally occurring germination stimulant sorgolactone. *Tetrahedron Lett.* **38**:2321–2324.
- Tasker, A. V., and Westwood, J. H.** (2012). The U.S. Witchweed Eradication Effort Turns 50: A Retrospective and Look-Ahead on Parasitic Weed Management. *Weed Sci.* **60**:267–268.
- Thuring, J. W. J. F., Nefkens, G. H. L., and Zwanenburg, B.** (1997). Synthesis and Biological Evaluation of the Strigol Analogue Carba-GR24. *J. Agric. Food Chem.* **45**:1409–14.
- Toh, S., Holbrook-Smith, D., Stogios, P. J., Onopriyenko, O., Lumba, S., Tsuchiya, Y., Savchenko, A., and McCourt, P.** (2015). Structure-function analysis identifies highly sensitive strigolactone receptors in *Striga*. *Science.* **350**:203–207.
- Trabelsi, I., Yoneyama, K., Abbes, Z., Amri, M., Xie, X., Kisugi, T., Kim, H. I., Kharrat, M., and Yoneyama, K.** (2017). Characterization of strigolactones produced by *Orobanche foetida* and *Orobanche crenata* resistant faba bean (*Vicia faba* L.) genotypes and effects of phosphorous, nitrogen, and potassium deficiencies on strigolactone production. *South African J. Bot.* **108**:15–22.
- Tsuchiya, Y., Yoshimura, M., Sato, Y., Kuwata, K., Toh, S., Holbrook-Smith, D., Zhang, H., McCourt, P., Itami, K., Kinoshita, T., et al.** (2015). Probing strigolactone receptors in *Striga hermonthica* with fluorescence. *Science* (80). **349**:864–868.
- Ueno, K., Furumoto, T., Umeda, S., Mizutani, M., Takikawa, H., Batchvarova, R., and Sugimoto, Y.** (2014). Heliolactone, a non-sesquiterpene lactone germination stimulant for root parasitic weeds from sunflower. *Phytochemistry* **108**:122–8.
- Umehara, M., Hanada, A., Yoshida, S., Akiyama, K., Arite, T., Takeda-Kamiya, N., Magome, H., Kamiya, Y., Shirasu, K., Yoneyama, K., et al.** (2008). Inhibition of shoot branching by new terpenoid plant hormones. *Nature* **455**:195–200.
- Uraguchi, D., Kuwata, K., Hijikata, Y., Yamaguchi, R., Imaizumi, H., Am, S., Rakers, C., Mori, N., Akiyama, K., Irle, S., et al.** (2018). A femtomolar-range suicide germination stimulant for the parasitic plant *Striga hermonthica*. *Science.* **1305**:1301–1305.

- van Staden, J., Jäger, A. K., Light, M. E., Burger, B. V., Brown, N. A. C., and Thomas, T. H. (2004). Isolation of the major germination cue from plant-derived smoke. *South African J. Bot.* **70**:654–659.
- Wallner, E.-S., López-Salmerón, V., Belevich, I., Agustí, J., Lebovka, I., and Greb, T. (2017). Strigolactone- and Karrikin-Independent SMXL Proteins Are Central Regulators of Phloem Formation. *Curr. Biol.* **27**:1–7.
- Wang, L., Waters, M. T., and Smith, S. M. (2018). Karrikin-KAI2 signalling provides *Arabidopsis* seeds with tolerance to abiotic stress and inhibits germination under conditions unfavourable to seedling establishment. *New Phytol.* **219**:605–618.
- Waters, M. T., Nelson, D. C., Scaffidi, A., Flematti, G. R., Sun, Y. K., Dixon, K. W., and Smith, S. M. (2012). Specialisation within the DWARF14 protein family confers distinct responses to karrikins and strigolactones in *Arabidopsis*. *Development* **139**:1285–1295.
- Xie, X., Kusumoto, D., Takeuchi, Y., Yoneyama, K., Yamada, Y., and Yoneyama, K. (2007). 2'-Epi-orobanchol and solanacol, two unique strigolactones, germination stimulants for root parasitic weeds, produced by tobacco. *J. Agric. Food Chem.* **55**:8067–8072.
- Xu, Y., Miyakawa, T., Nosaki, S., Nakamura, A., Lyu, Y., Nakamura, H., Ohto, U., Ishida, H., Shimizu, T., Asami, T., et al. (2018). Structural analysis of HTL and D14 proteins reveals the basis for ligand selectivity in *Striga*. *Nat. Commun.* **9**:3947.
- Yao, R., Wang, F., Ming, Z., Du, X., Chen, L., Wang, Y., Zhang, W., Deng, H., and Xie, D. (2017). ShHTL7 is a non-canonical receptor for strigolactones in root parasitic weeds. *Cell Res.* **27**:838–841.
- Yoneyama, K., Xie, X., Kusumoto, D., Sekimoto, H., Sugimoto, Y., Takeuchi, Y., and Yoneyama, K. (2007a). Nitrogen deficiency as well as phosphorus deficiency in sorghum promotes the production and exudation of 5-deoxystrigol, the host recognition signal for arbuscular mycorrhizal fungi and root parasites. *Planta* **227**:125–132.
- Yoneyama, K., Yoneyama, K., Takeuchi, Y., and Sekimoto, H. (2007b). Phosphorus deficiency in red clover promotes exudation of orobanchol, the signal for mycorrhizal symbionts and germination stimulant for root parasites. *Planta* **225**:1031–1038.
- Yoneyama, K., Awad, A. A., Xie, X., Yoneyama, K., and Takeuchi, Y. (2010). Strigolactones as germination stimulants for root parasitic plants. *Plant Cell Physiol.* **51**:1095–1103.
- Yoneyama, K., Arakawa, R., Ishimoto, K., Kim, H. II, Kisugi, T., Xie, X., Nomura, T., Kanampiu, F., Yokota, T., Ezawa, T., et al. (2015). Difference in *Striga*-susceptibility is reflected in strigolactone secretion profile, but not in compatibility and host preference in arbuscular mycorrhizal symbiosis in two maize cultivars. *New Phytol.* **206**:983–989.

- Yoneyama, K., Xie, X., Yoneyama, K., Kisugi, T., Nomura, T., Nakatani, Y., Akiyama, K., and McErlean, C. S. P.** (2018a). Which are the major players, canonical or non-canonical strigolactones? *J. Exp. Bot.* **69**:2231–2239.
- Yoneyama, K., Mori, N., Sato, T., Yoda, A., Xie, X., Okamoto, M., Iwanaga, M., Ohnishi, T., Nishiwaki, H., Asami, T., et al.** (2018b). Conversion of carlactone to carlactonoic acid is a conserved function of MAX1 homologs in strigolactone biosynthesis. *New Phytol.* **218**:1522–1533.
- Zhang, Y., van Dijk, A. D. J., Scaffidi, A., Flematti, G. R., Hofmann, M., Charnikhova, T., Verstappen, F., Hepworth, J., van der Krol, S., Leyser, O., et al.** (2014). Rice cytochrome P450 MAX1 homologs catalyze distinct steps in strigolactone biosynthesis. *Nat. Chem. Biol.* **10**:1028–1033.
- Zhang, Y., Cheng, X., Wang, Y., Díez-Simón, C., Floková, K., Bimbo, A., Bouwmeester, H. J., and Ruyter-Spira, C.** (2018). The tomato MAX1 homolog, SIMAX1, is involved in the biosynthesis of tomato strigolactones from carlactone. *New Phytol.* **219**:297–309.
- Zhao, L.-H., Zhou, X. E., Wu, Z.-S., Yi, W., Xu, Y., Li, S., Xu, T.-H., Liu, Y., Chen, R.-Z., Kovach, A., et al.** (2013). Crystal structures of two phytohormone signal-transducing α/β hydrolases: karrikin-signaling KAI2 and strigolactone-signaling DWARF14. *Cell Res.* **23**:436–9.
- Zhou, F., Lin, Q., Zhu, L., Ren, Y., Zhou, K., Shabek, N., Wu, F., Mao, H., Dong, W., Gan, L., et al.** (2013). D14-SCF D3-dependent degradation of D53 regulates strigolactone signalling. *Nature* **504**:406–410.
- Zwanenburg, B., and Pospíšil, T.** (2013). Structure and activity of strigolactones: New plant hormones with a rich future. *Mol. Plant* **6**:38–62.
- Zwanenburg, B., Mwakaboko, A. S., and Kannan, C.** (2016). Suicidal germination for parasitic weed control. *Pest Manag. Sci.* **72**:2016–25.

10.1. WEB REFERENCES

1. Encyclopaedia Britannica, 2019 [online]. [cit. 22. 1. 2020]. Available at: <https://www.britannica.com/plant/Lamiales/Orobanchaceae>
2. USDA APHIS PPQ - Oxford, North Carolina, USDA APHIS PPQ, Bugwood.org [online]. *Weed images*, 2018 [cit. 22. 1. 2020]. Available at: <https://www.weedimages.org/browse/detail.cfm?imgnum=1149176>
3. Dr. Reuven Jacobsohn, Agricultural Research Organization, Bugwood.org [online]. *Weed images*, 2018 [cit. 22. 1. 2020]. Available at: <https://www.weedimages.org/browse/detail.cfm?imgnum=0686017>

4. R.J. Reynolds Tobacco Company Slide Set, R.J. Reynolds Tobacco Company, Bugwood.org [online]. *Weed images*, 2018 [cit. 22. 1. 2020]. Available at: <https://www.weedimages.org/browse/detail.cfm?imgnum=1440060>

11. SUPPLEMENT

- 11.1. HÝLOVÁ, A., POSPÍŠIL, T., SPÍCHAL, L., MATEMAN, J. J., BLANCO-ANIA, D., AND ZWANENBURG, B. (2019). NEW HYBRID TYPE STRIGOLACTONE MIMICS DERIVED FROM PLANT GROWTH REGULATOR AUXIN. *N. BIOTECHNOL.* 48:76–82.



Full length Article

New hybrid type strigolactone mimics derived from plant growth regulator auxin

Adéla Hýlová^a, Tomáš Pospíšil^{a,*}, Lukáš Spíchal^a, Jurgen J. Mateman^b, Daniel Blanco-Ania^b, Binne Zwanenburg^{a,b}^a Palacký University, Faculty of Science, Centre of the Region Haná for Biotechnological and Agricultural Research, Department of Chemical Biology and Genetics, Šlechtitelů 241/27, CZ-783 71 Olomouc, Czech Republic^b Radboud University, Institute for Molecules and Materials, Cluster of Organic Chemistry, Heyendaalsweg 135, 6525AJ Nijmegen, The Netherlands

ARTICLE INFO

Keywords:

Strigolactones
SL mimics
Suicidal germinations
Auxins
Parasitic weeds
S. hermonthica
O. minor
P. ramosa

ABSTRACT

Strigolactones (SLs) constitute a new class of plant hormones of increasing importance in plant science. The structure of natural SLs is too complex for ready access by synthesis. Therefore, much attention is being given to design of SL analogues and mimics with a simpler structure but with retention of bioactivity. Here new hybrid type SL mimics have been designed derived from auxins, the common plant growth regulators. Auxins were simply coupled with the butenolide D-ring using bromo (or chloro) butenolide. D-rings having an extra methyl group at the vicinal C-3' carbon atom, or at the C-2' carbon atom, or at both have also been studied. The new hybrid type SL mimics were bioassayed for germination activity of seeds of the parasitic weeds *S. hermonthica*, *O. minor* and *P. ramosa* using the classical method of counting germinated seeds and a colorimetric method. For comparison SL mimics derived from phenyl acetic acid were also investigated. The bioassays revealed that mimics with a normal D-ring had appreciable to good activity, those with an extra methyl group at C-2' were also appreciably active, whereas those with a methyl group in the vicinal C-3' position were inactive (*S. hermonthica*) or only slightly active. The new hybrid type mimics may be attractive as potential suicidal germination agents in agronomic applications.

Introduction

Strigolactones (SLs) constitute a new family of plant hormones that is currently receiving much attention [1–5]. Their most noteworthy bioproperty is that they function as germination stimulants for seeds of parasitic weeds. This can be used to reduce infection of harvest by parasitic plants, for example using a so-called suicidal germination approach [2,3]. Other bioproperties of SLs are their performance as branching factors for arbuscular mycorrhizal (AM) fungi and as inhibitors of shoot branching and bud outgrowth. Naturally occurring SLs are present in the root exudates of many plants, especially hosts of parasitic weeds. Canonical SLs invariably contain three annulated rings, the ABC scaffold, connected to a butenolide (D-ring) via an enol-ether unit conjugated with a carbonyl group (Fig. 1). Non-canonical SLs, which lack the A, B or C part but have an enol ether D-ring moiety, were also described recently [6]. The first SL was isolated as early as 1966

from the false host cotton [7] and was named strigol. The isolation and structure elucidation of SLs require an elaborate effort. Initially assigned structures of some SLs needed to be corrected. Typical examples are the structural corrections of alectrol [8,9], orobanchol [10] and solanacol [11]. At present two families of SLs are known, namely one having the stereochemistry as in (+)-strigol and the other with the stereochemistry as in (–)-orobanchol (Fig. 1).

The total synthesis of natural SLs requires a linear sequence of several steps [2,12,13] and as a consequence they cannot be prepared in multigram quantities. Logically, there has been an active search for SL analogues with a simplified structure, but retention of activity. Such analogues were constructed using the common SL structural unit, namely the D-ring connected to a carbonyl group via an enol ether [12]. Typical examples of bioactive SL analogues (Fig. 1) are GR24, widely used as standard in bioassays, Nijmegen-1 [2,14,15] successfully used in field experiments to control parasitic weeds in tobacco [12,16], and

Abbreviations: AtD14, arabidopsis DWARF14 orthologue; AtHLT/KAI2, arabidopsis HYPOSENSITIVE TO LIGHT/KARRIKIN/INSENSITIVE2; CDCl₃, deuterated chloroform; DMSO, dimethyl sulfoxide; DR5::GUS, *arabidopsis* auxin-responsive reporter line; EtOAc, ethyl acetate; HEPES, 4-(2-hydroxyethyl)-1-piperazineethanesulfonic acid; IAA, indole-3-acetic acid; MTT, 3-(4,5-dimethylthiazol-2-yl)-2,5-diphenyltetrazolium bromide; NMR, nuclear magnetic resonance

* Corresponding author.

E-mail address: tomas.pospisil@upol.cz (T. Pospíšil).<https://doi.org/10.1016/j.nbt.2018.08.001>

Available online 02 August 2018

1871-6784/ © 2018 Elsevier B.V. All rights reserved.

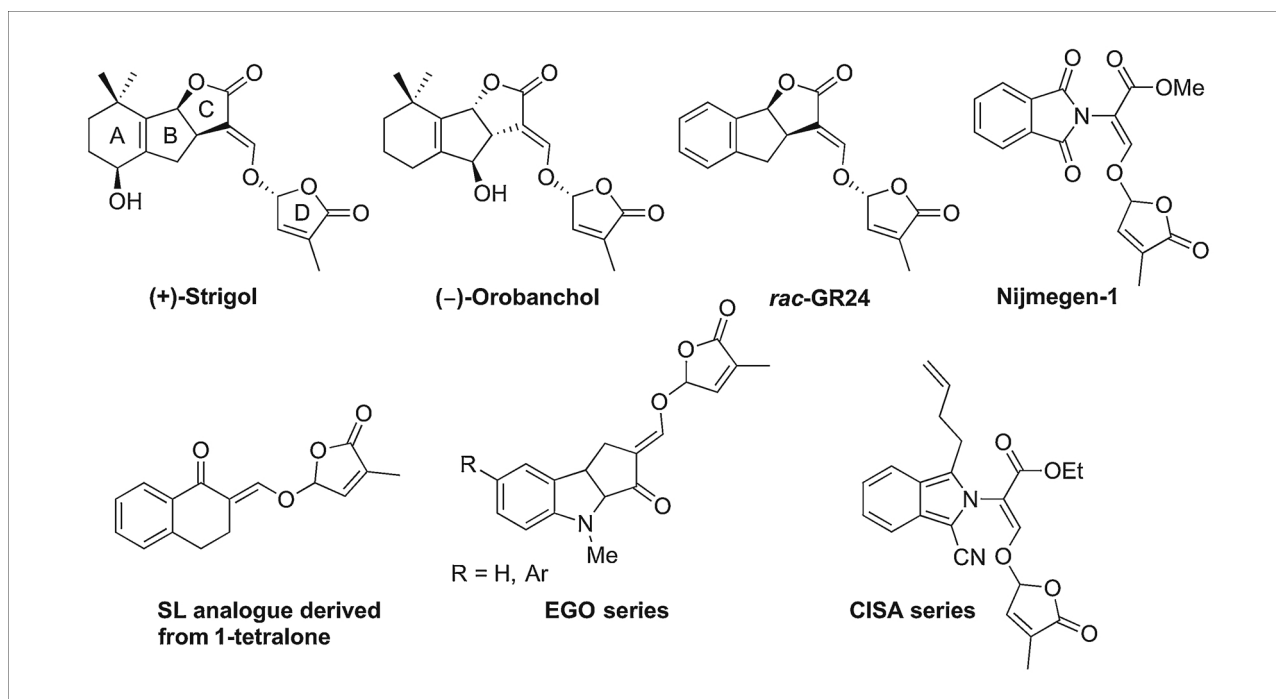


Fig. 1. Natural SLs and some synthetic analogues.

the SL analogue derived from 1-tetralone [17] tested in pot experiments [18]. In addition, SL analogues containing a heterocyclic unit in the ABC scaffold are also known. Examples are SL analogues with an indolyl group (EGO series [19,20]) and an isindolyl unit (CISA series [21]) in the ABC scaffold (Fig. 1).

New bioactive compounds with similar biofunctions to SL analogues, but lacking the ABC scaffold and only having a butenolide with a substituent at C-5, are collectively called *SL mimics* (Fig. 2). The first reported type of SL mimic is a butenolide with a phenoxy substituent at C-5. *para*-Bromophenoxy butenolide is modestly active as a germinating agent for seeds of *Striga hermonthica*, but interestingly is highly active as an inhibitor of shoot branching. For the latter reason, Asami et al. named these phenoxy compounds *debranones* (branching furanones; Fig. 2) [22–25]. The second reported type has an aryloxy substituent at C-5 of the butenolide. These compounds exhibit a modest to good germination activity towards seeds of *Striga hermonthica* and *Orobancha cernua*, with the activity in the latter case being remarkably high [26]. These aryloxy butenolides have not yet been tested for inhibition of shoot branching. A particular observation was made when, in such mimics, an extra methyl group was introduced at C-4. For the phenoxy type compounds, especially in the case of 4-Cl thiadebranone, the inhibition of shoot branching was boosted (Fig. 2) [27]. In contrast, an extra C-4 methyl in the aryloxy butenolides reduced germination activity practically to zero [28,29]. This remarkable finding provides a clue to the mode of action [3,28]. It is relevant to note that these SL

mimics are easy to prepare from either bromo butenolide or from hydroxy butenolide [15,18,22].

Although interesting bioproperties of SL mimics have been uncovered, knowledge concerning them is still in its infancy. Some new SL mimics have been prepared and bioassayed for germination activity based on the idea of incorporating the structural moiety of common plant growth regulators. Recently, Pereira et al. [30] published SL hybrid type mimics derived from the plant hormone gibberellic acid (GA_3) and their activity as germination stimulants. Because SL analogues with incorporated indolyl group exhibited bioactivity [19,20], we have focused on SL hybrid mimics derived from the natural auxins indole-3-acetic acid (IAA) and oxo-IAA, which contain the same group, and for comparison also on mimics derived from phenylacetic acid. Note that these SL mimics that are essentially derived from aryl alkanic acids are new types of potential germination stimulants.

Auxins are common plant hormones that play an important role as plant growth regulators and are involved in many essential processes in plants, such as stimulation of cell growth and cell expansion, and division or meristem generation and organization [31].

Although an SL receptor was isolated recently from *Arabidopsis thaliana* (AtD14) [32], direct translation to parasitic plants is difficult, because loss of function of AtD14 does not cause defects in *Arabidopsis* seed germination. The discovery of a second pathway in *Arabidopsis* where the AtHTL/AtKAI2 protein regulates seed germination has resulted in a search and discovery of similar proteins in *Striga hermonthica*

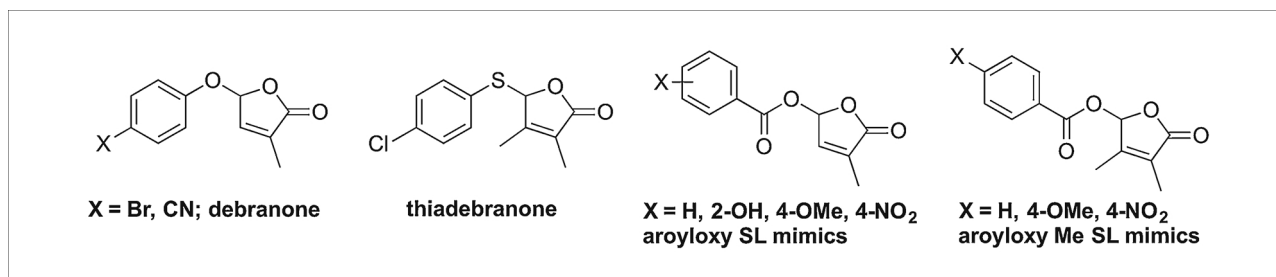


Fig. 2. Various SL mimics.

(ShHTL). The binding assay of 10 ShHTL proteins revealed that each has a unique profile of SL binding. This can be explained by variation in the amino acid composition of the binding pocket, causing differences in SL recognition. This finding implies that the diversification of SL receptors may enable the parasite to recognise the preferred host according to SL composition [33–36]. In this case, the docking studies with only one ShHTL could lead to unsatisfactory results. On the other hand, screening a library of SLs might be a useful means to discover compounds either very active towards specific parasitic plants or generally active against the whole family. This is the ideal place for simple, easily prepared compounds such as SL mimics. With readily accessible compounds, a wide variety of structural motives can be tested and their properties easily tuned.

The mode of action of SL mimics involves detachment of the hydroxy D-ring (HO–D). The remaining part of the SL mimic normally has no further function, but when auxin is released the situation may be very different, because auxin has an activity of its own. Here, we concentrate on the synthesis of auxin derived SL mimics and bioassay them as germination stimulants for seeds of parasitic weeds.

Materials and methods

Synthesis

The synthesis of the hybrid type SL mimics proceeded by coupling of auxin (or oxo-auxin) with the appropriate bromo (or chloro) butenolide as shown in Scheme 1.

Typical synthetic procedure

In a flame dried two-neck round-bottom flask (25 mL), indol-3-ylacetic acid (0.10 g, 0.57 mmol, 1.0 equiv.) was dissolved in dry acetone (2 mL) under an argon atmosphere. 5-Bromo-3-methylfuran-2(5H)-one (0.11 g, 0.62 mmol, 1.1 equiv.) [28] was added to this mixture followed by triethylamine (0.087 mL, 0.62 mmol, 1.1 equiv.) and the mixture was stirred at room temperature for 12 h. The mixture was diluted with water (5 mL) and extracted with dichloromethane (3 × 10 mL). The combined organic layers were washed with water (10 mL), brine (10 mL), dried over Na₂SO₄, filtered and concentrated under a vacuum. The residue was purified by column chromatography (silica gel, gradient of petroleum ether/EtOAc) to furnish a white solid compound 94 mg, 61%. The purity of the product was ascertained with HPLC.

Note on the naming of the compounds in the experimental section: According to IUPAC rules, the compounds must be named as esters of indolyl acetic acids. However, in the text of the paper we use the numbering of the butenolides as shown in Scheme 1 with the auxin unit attached to C-5.

The spectral data of newly prepared compounds are reported in the supplementary material.

Structure determination

Nuclear magnetic resonance (¹H and ¹³C NMR) spectra were obtained with Jeol ECA-500, Bruker Avance III 400 MHz or Bruker Avance III 500 MHz spectrometers and are reported as chemical shifts in parts per million (ppm, δ). Chemical shifts were calibrated to residual and solvent peak (CDCl₃ ¹H = 7.26 and ¹³C = 77.0 ppm; DMSO-*d*₆ ¹H = 2.49 and ¹³C = 39.5 ppm). Mass spectra (MS) were recorded with a Waters Q-TOF micro mass spectrometer. High-resolution mass spectra (HRMS) were recorded with JEOL AccuTOF mass spectrometer. FT-IR spectra were recorded on a Thermo Nicolet iS5 FTIR spectrometer. Flash column chromatography was performed using silica gel (Aldrich Silica gel 60 Å, 230–400 mesh particle size). The purity of the final compounds was determined using a Waters 2695 series HPLC system with Waters DAD PDA 996 detector using an Waters Symmetry C18 column (5 µm, 2.1 mm × 150 mm) with the solvent system consisting of methanol (mobile phase A) and water containing ammonium formate (pH 4) (mobile phase B). Thin-layer chromatography was carried out on Merck Silica 60 F254 plates. Chemicals used during the synthesis were purchased from Acros Organics, Fluka, Sigma-Aldrich, and LachNer s.r.o and used without further purification.

Bioassays

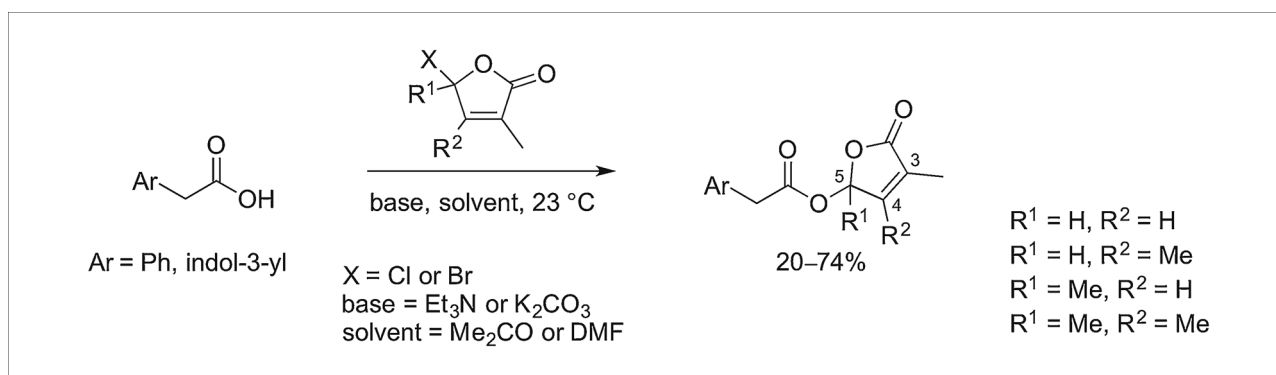
Seeds of the following parasitic weeds were used to assay the germination stimulatory activity of the new hybrid type SL mimics: *Striga hermonthica* (Sudan, collected in 2007), *Phelipanche ramosa* (Poitou-Charentes, France, collected from *Cannabis sativa* in 2012) and *Orobancha minor* (Golfo Aranci, Sardinia, Italy, collected from *Hypochaeris* sp. in 2011).

Germination assays

Standard germination assays, i.e. classical germination assay using glass fibre filter paper discs [37] and a high-throughput seed germination assay for root parasitic plants (MTT assay) [38] were employed with some important modifications as described below. The effect of SL mimics on germination was assayed in a dose-dependent manner using a concentration range of 10^{−5} to 10^{−13} M. *rac*-GR24 was used as a positive control. The corresponding auxins and 0.1% acetone served as negative controls. Dose-response curves and EC₅₀ values were computed using non-linear regression in GraphPad Prism 5.0 software. The bioassay was performed at least two times in three replicates.

Classical germination assay

Seeds were surface sterilized by intensive stirring for 6 min in an aqueous solution of 2% (v/v) sodium hypochlorite and 1% (v/v) Triton X-100. Sterile seeds were washed with 200 mL of sterile MilliQ water using glass frit and vacuum. Sterile 6-well plates were used instead of commonly used glass Petri dishes. Three round-shaped filter papers (diameter 32 mm) were placed into each well and moistened with



Scheme 1. Synthesis of hybrid type mimics from auxins.

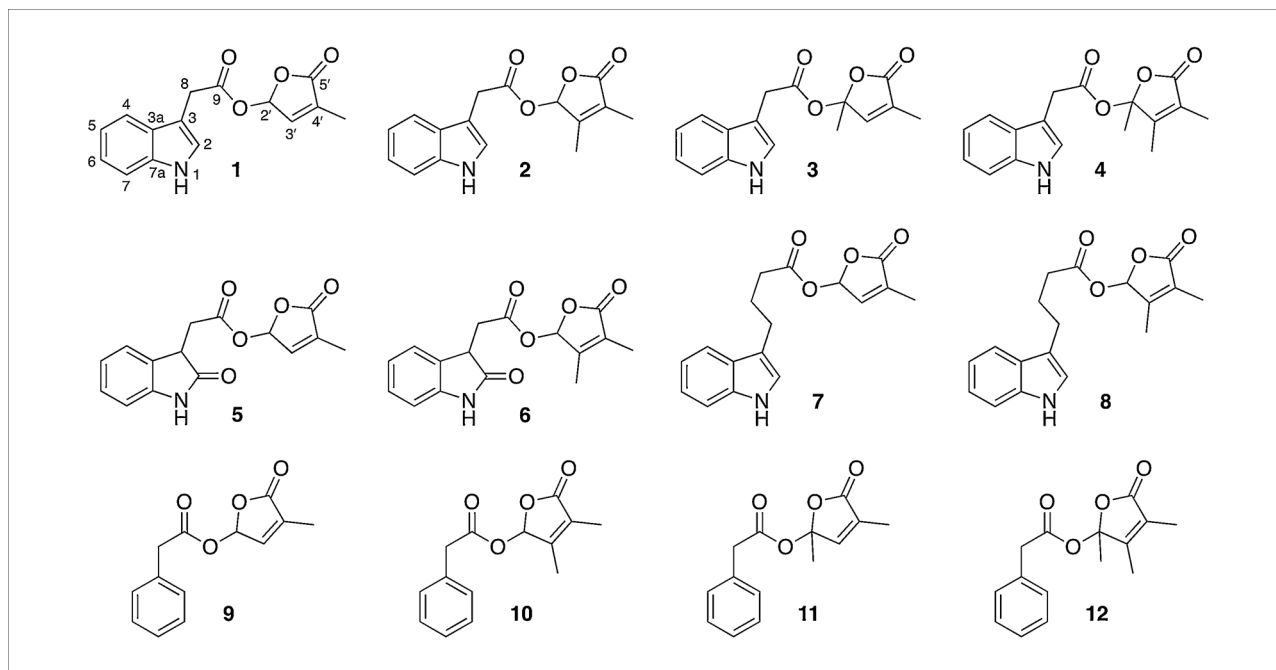


Fig. 3. Structures of the newly prepared SL mimics.

0.8 mL of sterile MilliQ water. Three glass fibre filter paper discs (10 mm, Grade GF/D, Whatman, GE Healthcare) were placed into each well and approximately 25 seeds per disc were spread evenly with a toothpick. The seeds were covered with another glass fibre disc and put into incubation chamber for conditioning. The conditioning period for *S. hermonthica* was 7–10 d at 27 °C; for *O. minor* 14 d at 21 °C and *P. ramosa* 7–10 d at 21 °C. Subsequently, discs with seeds were dried for 30 min in a laminar flow cabinet. Wells were dried, discs were placed back and germination was induced by adding 100 µL of solutions of the test and control compounds. Plates were sealed and put into incubation chambers for another 6 d. Germinated seeds were counted under a binocular microscope and percentages of germination were calculated.

MTT germination assay

The first step of the MTT assay consisted of seed sterilization using the same technique as described above. Seeds were conditioned at a density of 10 g/L in 1 mM HEPES buffer pH 7.5 and 0.1% PPM (Plant Preservative Mixture, Diagonation Technologies, NY, USA) for 3–4 d at 27 °C for *S. hermonthica*, 14 d for *O. minor* at 21 °C and at least 7 d for *P. ramosa* at 21 °C. Maintaining the same seed density, sterile agarose was added to 0.05% (w/v) to prevent sedimentation and achieve homogenous seed distribution. Seeds were distributed into 96-well plates (Microplate P tissue culture, GAMA Group, Czech Republic), using 50 µL of the seed suspension per well. Germination was induced with 10 µL of test and control compounds and total volume was adjusted to 100 µL with water. The plates were sealed with Parafilm and placed in an incubator for 4 d. Sterile filtered MTT solution (5 g/L) was then added, 10 µL per well. The following day, maximal germination rate was determined by counting under a binocular microscope and 100 µL of lysing solution (10% Triton X-100 and 0.04% HCl in isopropanol) was added to each well to solubilize formazan salts. Absorbance was measured after 22 h at 570 and 690 nm according to the In vitro toxicology assay kit (Sigma) on an EL800 Absorbance Microplate Reader (Biotek, Winooski, USA). Finally, the difference in absorbance between wavelengths was calculated for each well ($A_{570-690}$).

Since the classical germination assay and MTT assay provided the same results as revealed by linear correlation (Supplementary Fig. S1),

the data obtained from both bioassays were summarized and averages were calculated.

Auxin DR5::GUS bioassay

Transgenic seeds of *Arabidopsis thaliana* carrying a DR5::GUS fusion were used for the assay. The procedure was carried out according to [39], with only minor modifications: the assay was performed in 24-well plates and fluorescence was measured on a Synergy H4 hybrid reader (Biotek, USA) at excitation/emission wavelengths 365/460 nm. Compounds were tested at concentrations of 10^{-6} and 10^{-7} M. IAA and 0.1% acetone were used as positive and negative controls respectively. Mean values and standard deviations were computed using GraphPad Prism 5.0 software.

Stability study

The test compound (1 mg) was dissolved in DMSO (100 µL). The solution (2 µL) was added to HEPES buffer (10 µL of 100 mM stock at pH 6.5, 7.5 or 8.5) and diluted with water (988 µL). The solution was analysed by HPLC (Waters 2695 series HPLC system with Waters DAD PDA 996 detector using an Waters Symmetry C18 column (5 µm, 2.1 mm × 150 mm) with the solvent system consisting of methanol (mobile phase A) and water containing ammonium formate (pH 4) (mobile phase B)) in given time period. The relative concentration of the compound was determined from peak area. (See Supplementary data Fig. S4)

Results and discussion

Synthesis of the library

To explore the idea mentioned in the Introduction, two commonly used growth regulating agents were selected, namely indole-3-acetic acid (IAA) and 2-oxindole-3-acetic acid (oxo-IAA). These compounds are essentially aliphatic carboxylic acids, hence structurally different from the aromatic carboxylic acids used previously, see Fig. 2. All these acids were coupled straightforwardly with the D-ring by using bromo [28] or chloro [40] butenolide and triethylamine as a base. A second series was prepared by coupling the bromo butenolide having an extra methyl group at C-3' (Scheme 1). Other molecular variants have an

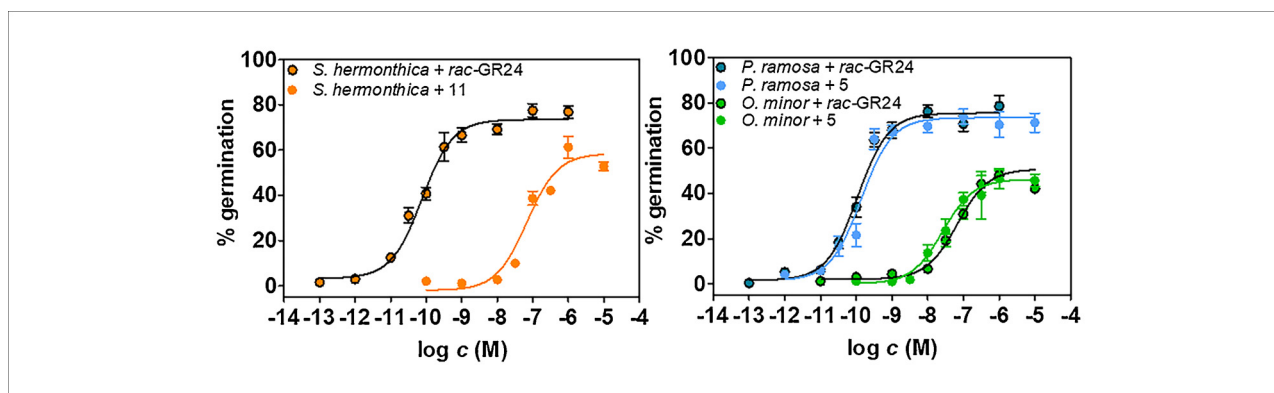


Fig. 4. Dose-response curves of germination of parasitic weeds stimulated with *rac*-GR24 or new SL mimics 5 and 11 in concentration range of 10^{-5} – 10^{-13} M. Data represent averages with standard error ($n \geq 4$).

extra methyl at C-2' or two extra methyl groups, one at C-2' and one at C-3'. For comparison, a series derived from phenylacetic acid was also prepared with the same variations in the D-ring. The structures of all newly prepared hybrid type SL mimics are shown in Fig. 3. The structures of all compounds were confirmed by spectral analysis and their purity assessed by HPLC.

Germination activity

Germination data are presented as dose-response curves. The examples of positive control and one stimulant out of the compounds tested for each species are shown in Fig. 4. For dose-response curves of the remaining compounds, see supplementary Figure S2. Average maximal germination rates of *S. hermonthica*, *P. ramosa* and *O. minor* with 1 μ M *rac*-GR24 were 80%, 82% and 50%, respectively. Spontaneous germination was not observed for any parasitic species. A non-linear regression was employed to compute EC_{50} values from dose-response curves. Graphical presentation of EC_{50} values is shown in Fig. 5.

Generally, the mimics with the best activity towards the three species were those having the “normal natural” D-ring (compounds 1,

5, 7 and 9), i.e., monomethylated at C-4' as in natural SLs. On the other hand, mimics methylated at both C-3' and C-4' were inactive (8) or less active (2, 10) than the corresponding ones with the natural D-ring. *S. hermonthica* did not respond at all to SL mimics methylated at both C-3' and C-4' (2, 8, 10) or at C-2', C-3' as well as C-4' (4, 12). On the contrary, mimics with methyl groups at both C-2' and C-4' (3, 11) showed activity on *S. hermonthica* which was similar to their monomethylated analogues (1, 9). *O. minor* responded to polymethylated mimics derived only from IAA and phenylacetic acid.

Several compounds exhibited interesting behaviour. Hybrids of IAA, oxo-IAA, and phenylacetic acid (1, 5, 9) were highly active towards *P. ramosa*, almost as active as *rac*-GR24. Compounds 3, 7 and 11 showed an activity only slightly lower than that of *rac*-GR24. 3, 5 and 9 showed significant activity towards *S. hermonthica* at approximately 100 nM. Remarkably, 5 was an even better stimulant for *O. minor* than *rac*-GR24. Compound 9 showed the same bioactivity as the standard and 1, 7 and 10 had a slightly higher EC_{50} . This analysis of the germination data reveals that the best activity is observed for mimics having the “normal natural” D-ring. When an extra methyl is introduced at C-2' the activity is slightly reduced. However, when an extra vicinal methyl is present at C-3', the germination response for *S. hermonthica* seeds is practically nil, and that for the other two seed types very much reduced. This observation is in line with earlier results with a vicinal methyl group at C-3' [28] and confirms the mechanism for the mode action shown in [3].

It is of interest to compare the germination data of the auxin type hybrid SL mimics with those reported for gibberellin (GA_3) type hybrid mimics [30]. Triggering by GA_3 type hybrid at concentrations comparable to *rac*-GR24 was only observed for *O. minor*. In general, the activity of GA_3 mimics was moderate. In summary, the synthesis of hybrid mimics from common plant hormones is an effective tool in the search for new germination stimulants for parasitic weed control. It should be noted that the mimics derived from auxin exhibit a higher activity profile than debranones [24,25] and phthalimide derived SL mimics [41]. None of these exhibit such a significant stimulatory activity as the new auxin hybrid type SL mimics with a “natural” D-ring.

Our results demonstrate that new auxin type SL mimics are species specific. For example, 1 and 3 are very good stimulants for *P. ramosa*, but only moderate for *S. hermonthica* and *O. minor*. Mimics with two methyls, namely 2 and 6, stimulate only *P. ramosa*, albeit only at considerably higher concentrations. This selectivity could be interesting for practical application in controlling certain weed species that infect various crops [42], for example *S. hermonthica* occurs in Sub-Saharan Africa, *P. ramosa* especially in the Mediterranean part of Europe and *O. minor* in the Middle East or Ethiopia. In these areas, the new SL mimics may potentially be useful for suicidal seed germination [16].

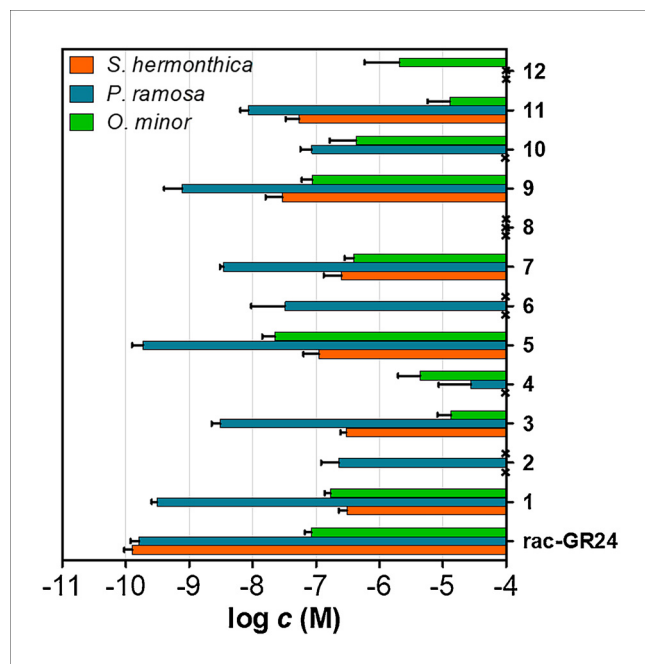


Fig. 5. Bioactivity of new SL mimics expressed as EC_{50} values. Crosses indicate no stimulatory activity. Data represent averages with standard error ($n \geq 2$).

Chemical stability

The stability of the most active compounds **1**, **5** and **9** in aqueous solution at various pH values (from 6.5 to 8.5) was compared with that of *rac*-GR24. Since it is known that stability of SLs depends on the medium used [43,44], the test was performed in similar conditions as those used for the germination bioassay and all compounds proved to be reasonably stable at given conditions. Typical behaviour of SLs was also observed, when their stability decreased with increasing pH. In this respect, it is interesting to note a result with compound **5**, which exhibited similar stability to *rac*-GR24 at pH values 6.5 and 7.5, but better stability in solution at pH 8.5 (Supplementary Figure S4).

Auxins activity

To investigate whether the hybrid mimics act as auxins, an assay employing *Arabidopsis* seedlings expressing the auxin responsive reporter DR5::GUS was employed [39,45]. Compounds **1–4** representing all 4 variants of D-ring methylation with different SL activity (Fig. 5) were tested. All showed high activity at 1 μ M concentration (Supplementary Figure S3), apart from **4**, which has triple methylation on the D-ring. Taking into account that the tested SL mimic representatives are esters of IAA, oxo-IAA and phenylacetic acid, it is likely that the reason for the auxin activity is activity of the free auxin released through cleavage of the ester bond by plant esterases [46]. Nevertheless, the general mode of SL action is hydrolysis of the D-ring and release of the ABC scaffold. Auxin seems to be a good candidate as a “carrier” for the D-ring, as supported by our results regarding bioactivity. The results confirmed the assumption stated in the Introduction.

Conclusion

New hybrid type SL mimics of auxin and having the ‘natural’ D-ring showed a considerable germination activity on parasitic weed seeds, some with EC₅₀ values in the nM range. Some of these mimics, namely compounds **5** and **9**, were the most effective germination stimulants. The germination data also suggest that some of the new mimics are species specific. Activity was strongly influenced by introducing a methyl group at the vicinal C-3’ position of the D-ring. The new mimics, which are easy to prepare, are of potential interest for agronomic applications.

Acknowledgements

This work was supported by grant IGA_PrF_2018_023 of Palacký University in Olomouc and grant No. LO1204 (Sustainable development of research in the Centre of the Region Haná) from the National Program of Sustainability I, MEYS, Czech Republic.

We thank Prof. Philippe Delavault for providing *Phelipanche ramosa* and Prof. Renata Piwowarczyk for *Orobancha minor* seeds.

Appendix A. Supplementary data

Supplementary material related to this article can be found, in the online version, at doi:<https://doi.org/10.1016/j.nbt.2018.08.001>.

References

- [1] Tsuchiya Y, McCourt P. Strigolactones: a new hormone with a past. *Curr Opin Plant Biol* 2009;12:556–61.
- [2] Zwanenburg B, Pospisil T. Structure and activity of strigolactones: new plant hormones with a rich future. *Mol Plant* 2013;6:38–62.
- [3] Zwanenburg B, Pospisil T, Zeljkovic SC. Strigolactones: new plant hormones in action. *Planta* 2016;243:1311–26.
- [4] Al-Babili S, Bouwmeester HJ. Strigolactones, a novel carotenoid-derived plant hormone. *Annu Rev Plant Biol* 2015;66:161–86.
- [5] Screpanti C, Yoneyama K, Bouwmeester HJ. Strigolactones and parasitic weed management 50 years after the discovery of the first natural strigolactone strigol-

- status and outlook. *Pest Manage Sci* 2016;72:2013–5.
- [6] Xie XN. Structural diversity of strigolactones and their distribution in the plant kingdom. *J Pestic Sci* 2016;41:175–80.
- [7] Cook CE, Whichard LP, Turner B, Wall ME, Egley GH. Germination of witchweed (*Striga lutea* Lour.): isolation and properties of a potent stimulant. *Science* 1966;154:1189–90.
- [8] Mueller S, Hauck C, Schildknecht H. Germination stimulants produced by *Vigna unguiculata* Walp cv Saunders Upright. *J Plant Growth Regul* 1992;11:77–84.
- [9] Ueno K, Sugimoto Y, Zwanenburg B. The genuine structure of aletrrol: end of a long controversy. *Phytochem Rev* 2015;14:835–47.
- [10] Ueno K, Nomura S, Muranaka S, Mizutani M, Takikawa H, Sugimoto Y. *Ent-2'-epi-Orobanchol* and its acetate, As germination stimulants for *Striga gesnerioides* seeds isolated from Cowpea and red clover. *J Agric Food Chem* 2011;59:10485–90.
- [11] Chen VX, Boyer F-D, Rameau C, Retaillieu P, Vors J-P, Beau J-M. Stereochemistry, Total Synthesis, and Biological Evaluation of the New Plant Hormone Solanacol. *Chem Eur J* 2010;16:13941–5.
- [12] Zwanenburg B, Mwakaboko AS, Reizelman A, Anilkumar G, Sethumadhavan D. Structure and function of natural and synthetic signalling molecules in parasitic weed germination. *Pest Manage Sci* 2009;65:478–91.
- [13] Bromhead LJ, McErlean CSP. Accessing Single Enantiomer Strigolactones: Progress and Opportunities. *Eur J Org Chem* 2017:5712–23.
- [14] Zwanenburg B, Cavar Zeljkovic S, Pospisil T. Synthesis of strigolactones, a strategic account. *Pest Manage Sci* 2016;72:15–29.
- [15] Neffkens GHL, Thuring JWJF, Beenackers MFM, Zwanenburg B. Synthesis of a phthaloylglycine-derived strigol analog and its germination-stimulatory activity toward seeds of the parasitic weeds *Striga hermonthica* and *Orobancha crenata*. *J Agric Food Chem* 1997;45:2273–7.
- [16] Zwanenburg B, Mwakaboko AS, Kannan C. Suicidal germination for parasitic weed control. *Pest Manage Sci* 2016;72:2016–25.
- [17] Mwakaboko AS, Zwanenburg B. Strigolactone analogs derived from Ketones using a working model for germination stimulants as a blueprint. *Plant Cell Physiol* 2011;52:699–715.
- [18] Kgosi RL, Zwanenburg B, Mwakaboko AS, Murdoch AJ. Strigolactone analogues induce suicidal seed germination of *Striga* spp. in soil. *Weed Res* 2012;52:197–203.
- [19] Artuso E, Ghibaudi E, Lace B, Marabell D, Vinciguerra D, et al. Stereochemical assignment of strigolactone analogs confirms their selective biological activity. *J Nat Prod* 2015;78:2624–33.
- [20] Bhattacharya C, Bonfante P, Deagostino A, Kapulnik Y, Larini P, et al. A new class of conjugated strigolactone analogues with fluorescent properties: synthesis and biological activity. *Org Biomol Chem* 2009;7:3413–20.
- [21] Rasmussen A, Heugebaert T, Matthys C, Van Deun R, Boyer F-D, et al. A fluorescent alternative to the synthetic strigolactone GR24. *Mol Plant* 2013;6:100–12.
- [22] Fukui K, Ito S, Ueno K, Yamaguchi S, Kyoizuka J, Asami T. New branching inhibitors and their potential as strigolactone mimics in rice. *Bioorg Med Chem Lett* 2011;21:4905–8.
- [23] Fukui K, Ito S, Asami T. Selective mimics of strigolactone actions and their potential use for controlling damage caused by root parasitic weeds. *Mol Plant* 2013;6:88–99.
- [24] Takahashi I, Fukui K, Asami T. Chemical modification of a phenoxyfuranone-type strigolactone mimic for selective effects on rice tillering or *Striga hermonthica* seed germination. *Pest Manage Sci* 2016;72:2048–53.
- [25] Fukui K, Yamagami D, Ito S, Asami T. A Taylor-made design of phenoxyfuranone-type strigolactone mimic. *Front Plant Sci* 2017;8:936.
- [26] Zwanenburg B, Mwakaboko AS. Strigolactone analogues and mimics derived from phthalimide, saccharine, p-tolylmalondialdehyde, benzoic and salicylic acid as scaffolds. *Bioorg Med Chem* 2011;19:7394–400.
- [27] Boyer F-D, de Saint Germain A, Pillot J-P, Pouvreau J-B, Chen VX, et al. Structure-activity relationship studies of strigolactone-related molecules for branching inhibition in garden pea: molecule design for shoot branching. *Plant Physiol* 2012;159:1524–44.
- [28] Zwanenburg B, Nayak SK, Charnikhova TV, Bouwmeester HJ. New strigolactone mimics: structure-activity relationship and mode of action as germinating stimulants for parasitic weeds. *Bioorg Med Chem Lett* 2013;23:5182–6.
- [29] Boyer F-D, de Saint Germain A, Pouvreau J-B, Clave G, Pillot J-P, et al. New strigolactone analogs as plant hormones with low activities in the rhizosphere. *Mol Plant* 2014;7:675–90.
- [30] Pereira RG, Cala A, Fernandez-Aparicio M, Molinillo JMG, Boaventura MAD, et al. Gibberellic and kaurenic hybrid strigolactone mimics for seed germination of parasitic weeds. *Pest Manage Sci* 2017;73:2529–37.
- [31] Mockaitis K, Estelle M. Auxin receptors and plant development: a new signaling paradigm. *Annu Rev Cell Dev Biol* 2008;24:55–80.
- [32] Yao R, Ming Z, Yan L, Li S, Wang F, et al. DWARF14 is a non-canonical hormone receptor for strigolactone. *Nature (London, U K)* 2016;536:469–73.
- [33] Tsuchiya Y, Yoshimura M, Sato Y, Kuwata K, Toh S, et al. Probing strigolactone receptors in *Striga hermonthica* with fluorescence. *Science (Washington, DC, U S)* 2015;349:864–8.
- [34] Toh S, Holbrook-Smith D, Stogios PJ, Onoprienko O, Lumba S, et al. Structure-function analysis identifies highly sensitive strigolactone receptors in *Striga*. *Science (Washington, DC, U S)* 2015;350:203–7.
- [35] Yao RF, Wang F, Ming ZH, Du XX, Chen L, et al. ShHTL7 is a non-canonical receptor for strigolactones in root parasitic weeds. *Cell Res* 2017;27:838–41.
- [36] Lumba S, Holbrook-Smith D, McCourt P. The perception of strigolactones in vascular plants. *Nat Chem Biol* 2017;13:599–606.
- [37] Mangnus EM, Stommen PLA, Zwanenburg B. A standardized bioassay for evaluation of potential germination stimulants for seeds of parasitic weeds. *J Plant Growth Regul* 1992;11:91–8.
- [38] Pouvreau J-B, Gaudin Z, Auger B, Lechat M-M, Gauthier M, et al. A high-throughput

- seed germination assay for root parasitic plants. *Plant Methods* 2013;9:32.
- [39] Pospisilova H, Nisler J, Spichal L, Frebort I. Nebularine affects plant growth and development but does not interfere with cytokinin signaling. *J Plant Growth Regul* 2009;28:321–30.
- [40] Johnson AW, Gowda G, Hassanali A, Knox J, Monaco S, et al. The preparation of synthetic analogs of strigol. *J Chem Soc Perkin Trans* 1981;1:1734–43.
- [41] Cala A, Ghooray K, Fernandez-Aparicio M, Molinillo JMG, Galindo JCG, et al. Phthalimide-derived strigolactone mimics as germinating agents for seeds of parasitic weeds. *Pest Manage Sci* 2016;72:2069–81.
- [42] Parker C. Observations on the current status of *Orobanch*e and *Striga* problems worldwide. *Pest Manage Sci* 2009;65:453–9.
- [43] Kannan C, Zwanenburg B. A novel concept for the control of parasitic weeds by decomposing germination stimulants prior to action. *Crop Prot* 2014;61:11–5.
- [44] Halouzka R, Tarkowski P, Zwanenburg B, Zeljkovic SC. Stability of strigolactone analog GR24 toward nucleophiles. *Pest Manage Sci* 2018;74:896–904.
- [45] Ulmasov T, Murfett J, Hagen G, Guilfoyle TJ. Aux/IAA proteins repress expression of reporter genes containing natural and highly active synthetic auxin response elements. *Plant Cell* 1997;9:1963–71.
- [46] Yang Y, Xu R, C-j Ma, Vlot AC, Klessig DF, Pichersky E. Inactive methyl indole-3-acetic acid ester can be hydrolyzed and activated by several esterases belonging to the AtMES esterase family of Arabidopsis. *Plant Physiol* 2008;147:1034–45.

Supporting information

New Hybrid Type Strigolactone Mimics Derived from Plant Growth Regulator Auxin

Adéla Hýlová^a, Tomas Pospíšil^{*a}, Lukáš Spíchal^a, Jurgen J. Mateman^b, Daniel Blanco-Ania^b and Binne Zwanenburg^{*a,b}

^aPalacký University, Faculty of Science, Centre of the Region Haná for Biotechnological and Agricultural Research, Department of Chemical Biology and genetics, Slechtitelu 241/27, CZ-783 71 Olomouc, Czech Republic

^bRadboud University, Institute for Molecules and Materials, Cluster of Organic Chemistry, Heyendaalsweg 135, 6525AJ Nijmegen, the Netherlands

Table of contents

Fig. S1: Linear correlation of MTT bioassay and classical germination assay.	2
Fig. S2: Dose response curves of germination of parasitic weeds <i>Striga hermonthica</i> (A), <i>Phelipanche ramosa</i> (B) and <i>Orobancha minor</i> (C).	3
Fig. S3: Auxin activity in reporter assay DR5::GUS.	4
Fig. S4. Stability of compounds 1, 5, 9 and (+/-)-GR-24 in HEPES buffer at different pH.	5
Characterisation of compounds 1-12.	6-10
¹H and ¹³C NMR spectra of compounds 1–12.	11–34

Fig. S1

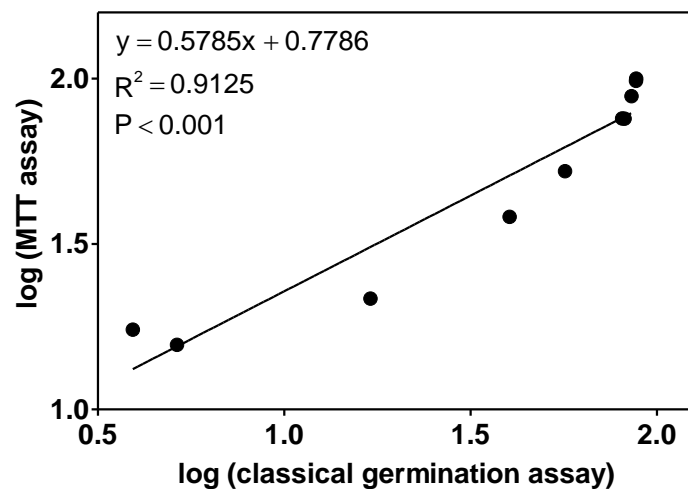


Fig. S1. Linear correlation of MTT bioassay and classical germination assay. The data represent averages of *S. hermonthica* and GR24 concentration range of 10^{-6} – 10^{-13} M (n = 9).

Fig. S2

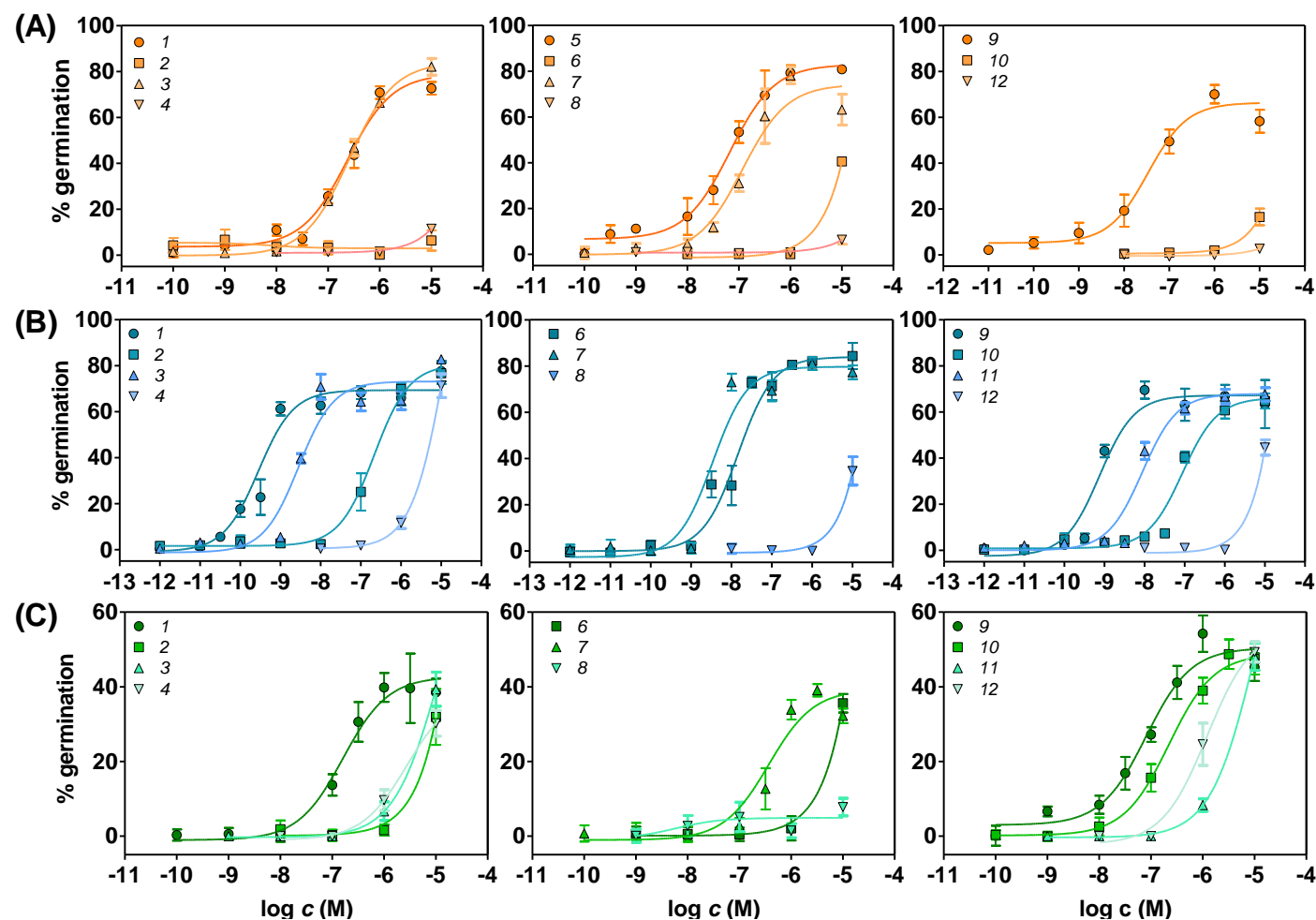


Fig. S2. Dose response curves of germination of parasitic weeds *Striga hermonthica* (A), *Phelipanche ramosa* (B) and *Orobanche minor* (C). The seeds were stimulated with compounds **1–12** in concentration range of 10^{-5} – 10^{-12} M. Data represent averages with standard error ($n \geq 2$).

Fig. S3

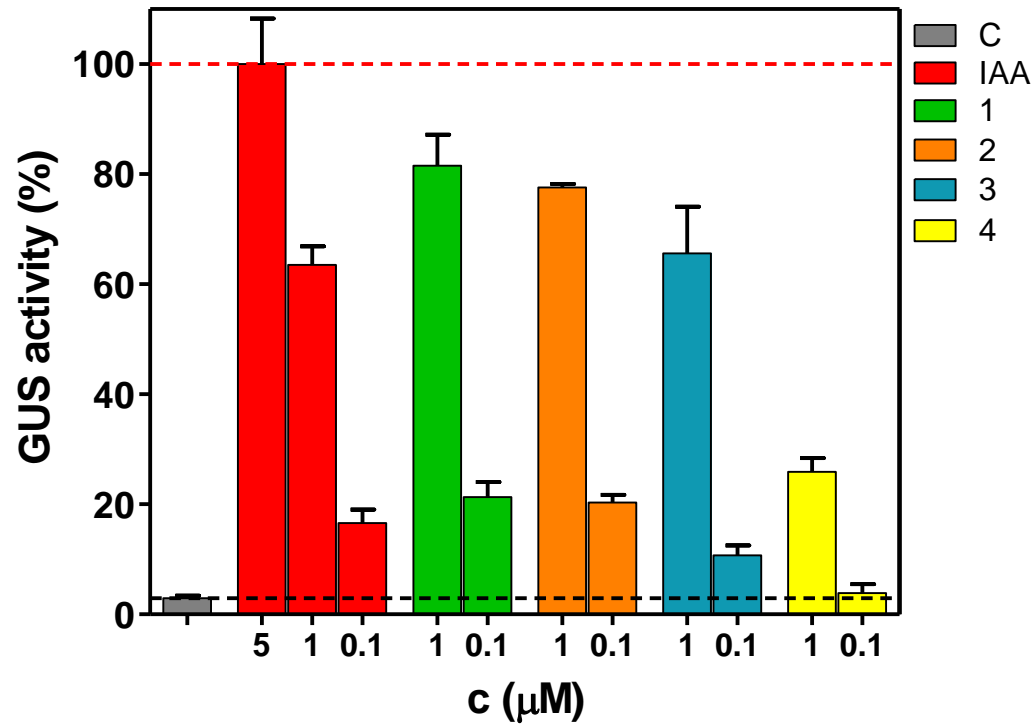


Fig. S3. Auxin activity in reporter assay DR5::GUS. Fluorescence of β -glucuronidase (GUS) is expressed relatively to 5 μM IAA. C = 0.1% acetone. Data represent averages of three replicates with SD ($n = 2$).

Fig. S4

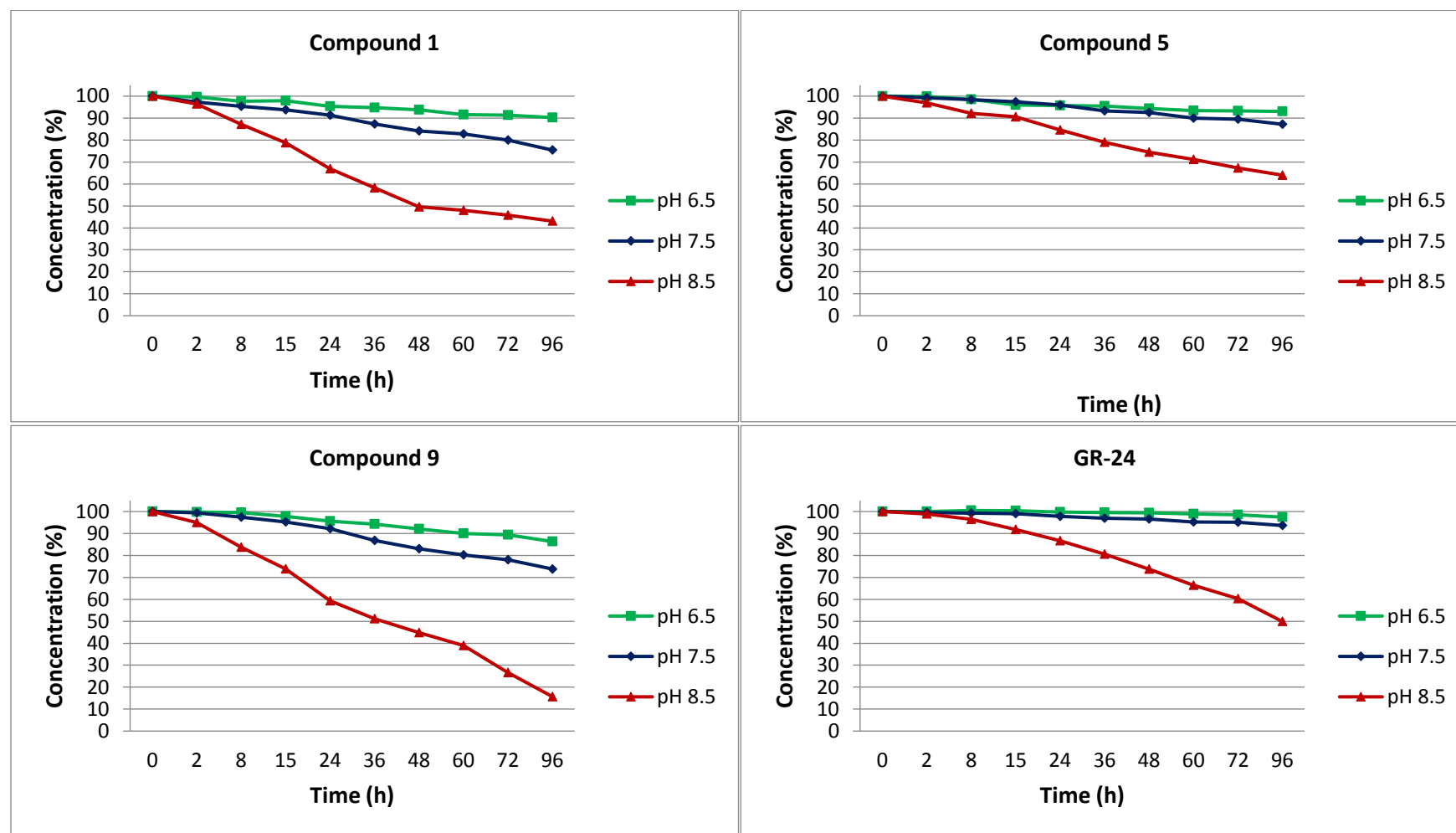


Fig. S4. Stability of compounds 1, 5, 9 and (+/-)-GR-24 in HEPES buffer at different pH.

Characterisation of compounds 1–12.

4-Methyl-5-oxo-2,5-dihydrofuran-2-yl 2-(1*H*-indol-3-yl)acetate (1)

Yield 94 mg (61%). White solid. ¹H NMR (500 MHz, CDCl₃, δ) 1.98 (t, *J* = 1.4 Hz, 3H, CH₃), 3.86 (s, 2H, CH₂), 6.87 (bs, 1H, OCHO), 6.90 (bs, 1H, CH=), 7.14–7.24 (m, 3H, H_{Ar}), 7.38 (d, *J* = 7.9 Hz, 1H, H_{Ar}), 7.58 (d, *J* = 7.6 Hz, 1H, H_{Ar}), 8.16 (s, 1H, NH). ¹³C NMR (126 MHz, CDCl₃, δ) 10.8 (CH₃), 31.1 (CH₂), 92.8 (CH), 107.2 (Cq), 111.4 (CH), 118.8 (CH), 120.0 (CH), 122.6 (CH), 123.4 (CH), 127.1, (Cq), 134.6 (Cq), 136.2 (Cq), 142.2 (CH), 170.3 (C=O), 171.3 (C=O). FT-IR (cm⁻¹): 3421, 1780, 1765, 1329, 1296, 1137, 1002, 966, 742. MS (ES+) *m/z* (%): 272.4 (*M* + 1, 86), 273.7 (*M* + 2, 100), 289.4 (*M* + NH₄, 39), 310.5 (*M* + K, 36). HRMS [ESI⁺ (*m/z*)] calcd for (C₁₅H₁₃NO₄ + Na)⁺ 294.07423, found 294.07419. HPLC purity 99%.

3,4-Dimethyl-5-oxo-2,5-dihydrofuran-2-yl 2-(1*H*-indol-3-yl)acetate (2)

Yield 113 mg (74%). Yellowish solid. ¹H NMR (500 MHz, CDCl₃, δ) 1.83 (s, 3H, CH₃), 1.85 (s, 3H, CH₃), 3.88 (d, *J* = 2.1 Hz, 2H, CH₂), 6.75 (s, 1H, OCHO), 7.15 (d, *J* = 7.9 Hz, 1H, H_{Ar}), 7.20–7.22 (m, 2H, H_{Ar}), 7.38 (d, *J* = 8.3 Hz, 1H, H_{Ar}), 7.58 (d, *J* = 7.9 Hz, 1H, H_{Ar}), 8.12 (s, 1H, NH). ¹³C NMR (126 MHz, CDCl₃, δ) 8.6 (CH₃), 11.4 (CH₃), 31.2 (CH₂), 94.0 (CH), 107.4 (Cq), 111.4 (CH), 118.8 (CH), 120.0 (CH), 122.6 (CH), 123.4 (CH), 127.1 (Cq), 136.2 (Cq), 153.6 (Cq), 170.6 (C=O), 171.8 (C=O). FT-IR (cm⁻¹): 3385, 3344, 1754, 1694, 1457, 1406, 1132, 980, 759. MS (ES+) *m/z* (%): 286.5 (*M* + 1, 93), 287.5 (*M* + 2, 100), 303.3 (*M* + NH₄, 86), 324.6 (*M* + K, 53). HRMS [ESI⁺ (*m/z*)] calcd for (C₁₆H₁₅NO₄ + Na)⁺ 308.08988, found 308.08979. HPLC purity 99%.

2,4-Dimethyl-5-oxo-2,5-dihydrofuran-2-yl 2-(1*H*-indol-3-yl)acetate (3)

Yield 32 mg (20%). White solid. ¹H NMR (400 MHz, CDCl₃, δ) 1.70 (s, 3H, CH₃), 1.81 (d, *J* = 1.7 Hz, 3H, CH₃), 3.67 (dd, *J* = 16.3, 0.9 Hz, 1H, CH_αH_β), 3.70 (dd, *J* = 16.3, 0.8 Hz, 1H, CH_αH_β), 7.02–7.07 (m, 2H, H_{Ar}), 7.10–7.14 (m, 2H, CH= +

H_{Ar}), 7.26 (d, $J = 8.1$ Hz, 1H, H_{Ar}), 7.49 (d, $J = 7.8$ Hz, 1H, H_{Ar}), 8.12 (br s, 1H, NH). ¹³C NMR (101 MHz, CDCl₃, δ) 10.4, 23.0, 31.7, 105.9, 107.3, 111.3, 118.6, 119.7, 122.2, 123.4, 127.0, 132.0, 136.1, 145.8, 169.9, 170.9. HRMS [ESI⁺ (m/z)] calcd for (C₁₆H₁₅NO₄ + Na)⁺ 308.08988, found 308.08977.

2,3,4-Trimethyl-5-oxo-2,5-dihydrofuran-2-yl 2-(1*H*-indol-3-yl)acetate (4)

Yield 95 mg (56%). White solid. ¹H NMR (500 MHz, CDCl₃, δ) 1.67 (s, 3H, CH₃), 1.76 (q, $J = 1.1$ Hz, 3H, CH₃), 1.79 (q, $J = 1.1$ Hz, 3H, CH₃), 3.72 (d, $J = 16.2$ Hz, 1H, CH _{α} H _{β}), 3.77 (d, $J = 16.2$ Hz, 1H, CH _{α} H _{β}), 7.07–7.15 (m, 2H, H_{Ar}), 7.16–7.22 (m, 1H, H_{Ar}), 7.34 (d, $J = 8.1$ Hz, 1H, H_{Ar}), 7.54–7.58 (m, $J = 7.9$ Hz, 1H, H_{Ar}), 8.34 (br s, 1H, NH). ¹³C NMR (126 MHz, CDCl₃, δ) 8.6, 10.4, 23.1, 31.9, 106.0, 107.4, 111.5, 118.6, 119.7, 122.2, 123.5, 125.6, 127.1, 136.2, 156.7, 169.5, 171.4. HRMS [ESI⁺ (m/z)] calcd for (C₁₇H₁₇NO₄ + Na)⁺ 322.10553, found 322.10508.

4-Methyl-5-oxo-2,5-dihydrofuran-2-yl 2-(2-oxoindolin-3-yl)acetate (5)

Yield 60 mg (40%). White solid. ¹H NMR (500 MHz, CDCl₃, δ) 1.96–1.97 (m, 3H, CH₃), 2.89 (dd, $J = 17.1, 7.9$ Hz, CH _{α} H _{β} CO, diastereomer A), 2.96 (dd, $J = 17.1, 7.6$ Hz, CH _{α} H _{β} CO, diastereomer B), 3.11 (dd, $J = 14.3, 4.6$ Hz, CH _{α} H _{β} CO, diastereomer A), 3.11 (dd, $J = 14.3, 4.9$ Hz, CH _{α} H _{β} CO, diastereomer B), 3.80 (dd, $J = 7.5, 4.8$ Hz, 1H, CHCH₂, diastereomer A), 3.80 (dd, $J = 7.6, 4.8$ Hz, 1H, CHCH₂, diastereomer B), 6.83–6.92 (m, 3H, H_{Ar} + CH=), 7.02–7.05 (m, 1H, OCHO), 7.22–7.27 (m, 2H, H_{Ar}), 8.55 (s, 1H, NH). ¹³C NMR (126 MHz, CDCl₃, δ) 10.8, 34.6, 34.7, 42.0, 42.1, 92.7, 92.8, 110.1, 122.8, 122.9, 124.2, 124.5, 128.1, 128.7, 128.8, 134.7, 141.8, 141.9, 169.4, 169.4, 171.1. FT-IR (cm⁻¹): 3182, 3082, 2910, 1784, 1698, 1621, 1470, 1336, 1196, 978, 749. MS (ES⁺) m/z (%): 288.4 (M + 1, 100), 289.3 (M + 2, 48), 290.2 (M + 3, 22). HRMS [ESI⁺ (m/z)] calcd for (C₁₅H₁₃NO₅ + Na)⁺ 310.06944, found 310.06936. HPLC purity 99%.

3,4-Dimethyl-5-oxo-2,5-dihydrofuran-2-yl 2-(2-oxoindolin-3-yl)acetate (6)

Yield 96 mg (61%). White solid. ^1H NMR (500 MHz, CDCl_3 , δ) 1.85 (s, 3H, CH_3 , diastereomer A and B), 1.91 (s, 3H, CH_3 , diastereomer B), 1.94 (s, 3H, CH_3 , diastereomer A), 2.89 (dd, $J = 17.1, 7.9$ Hz, 1H, $\text{CH}_\alpha\text{H}_\beta\text{CO}$, diastereomer A), 2.99 (dd, $J = 17.1, 7.6$ Hz, 1H, $\text{CH}_\alpha\text{H}_\beta\text{CO}$, diastereomer B), 3.12 (dd, $J = 9.5, 4.8$ Hz, 1H, $\text{CH}_\alpha\text{H}_\beta\text{CO}$, diastereomer A), 3.16 (dd, $J = 9.5, 4.8$ Hz, 1H, $\text{CH}_\alpha\text{H}_\beta\text{CO}$, diastereomer B), 3.81 (dd, $J = 7.5, 5.0$ Hz, 1H, CHCH_2 , diastereomer B), 3.89 (dd, $J = 7.8, 5.0$ Hz, 1H, CHCH_2 , diastereomer A), 6.73 (s, 1H, OCHO, diastereomer B), 6.76 (s, 1H, OCHO, diastereomer A), 6.88–6.91 (m, 1H, H_{Ar} , diastereomer A and B), 7.03–7.06 (m, 1H, H_{Ar} , diastereomer A and B), 7.21–7.29 (m, 3H, H_{Ar} , diastereomer A and B), 8.13 (s, 1H, NH, diastereomer A and B). ^{13}C NMR (126 MHz, CDCl_3 , δ) 8.7, 11.4, 34.6, 34.8, 42.0, 42.2, 94.1, 94.1, 110.1, 110.1, 122.9, 123.0, 124.2, 124.5, 127.3, 128.0, 128.1, 128.3, 128.8, 128.8, 129.2, 141.5, 153.4, 169.6, 170.3, 171.6, 178.6, 178.6. Diastereomer A: MS (ES+) m/z (%): 302.4 ($M + 1$, 100), 303.9 ($M + 2$, 88), 304.4 ($M + 3$, 66). Diastereomer B: MS (ES+): 302.4 ($M + 1$, 100), 303.9 ($M + 2$, 89), 304.4 ($M + 3$, 60). HRMS [ESI $^+$ (m/z)] calcd for $(\text{C}_{16}\text{H}_{15}\text{NO}_5 + \text{Na})^+$ 324.08479, found 324.08448. HPLC purity 96%.

4-Methyl-5-oxo-2,5-dihydrofuran-2-yl 4-(1*H*-indol-3-yl)butanoate (7)

Yield 71 mg (48%). Brownish oil. ^1H NMR (500 MHz, CDCl_3 , δ) 1.96 (d, $J = 1.2$ Hz, 3H, CH_3), 2.06–2.11 (m, 2H, $\text{CH}_2\text{CH}_2\text{CH}_2$), 2.45 (t, $J = 7.3$ Hz, 2H, CH_2CO), 2.84 (t, $J = 7.2$ Hz, 2H, ArCH_2), 6.75 (bs, 1H, OCHO), 6.80 (bs, 1H, CH=), 6.98 (s, 1H, H_{Ar}), 7.12 (t, $J = 7.9$ Hz, 1H, H_{Ar}), 7.19 (t, $J = 7.9$ Hz, 1H, H_{Ar}), 7.36 (d, $J = 7.9$ Hz, 1H, H_{Ar}), 7.60 (d, $J = 7.6$ Hz, 1H, H_{Ar}), 8.06 (s, 1H, NH). ^{13}C NMR (126 MHz, CDCl_3 , δ) 10.8 (CH_3), 24.4 (CH_2), 24.9 (CH_2), 33.6 (CH_2), 92.4 (CH), 111.3(CH), 115.2 (Cq), 119.0 (CH), 119.4 (CH), 121.9 (CH), 122.2 (CH), 127.5 (Cq), 134.4 (Cq), 136.5 (Cq), 142.2 (CH), 171.3 (C=O), 172.0 (C=O). FT-IR (cm^{-1}): 3412, 2927, 1762, 1457, 1336, 1205, 1132, 962, 739. MS (ES+) m/z (%): 300.5 ($M + 1$, 95), 301.4 ($M + 2$, 100), 302.3 ($M + 3$, 68). HRMS [ESI $^+$ (m/z)] calcd for $(\text{C}_{17}\text{H}_{17}\text{NO}_4 + \text{Na})^+$ 322.10553, found 322.10550. HPLC purity 99%.

3,4-Dimethyl-5-oxo-2,5-dihydrofuran-2-yl 4-(1*H*-indol-3-yl)butanoate (8)

Yield 63 mg (41%). White solid. ^1H NMR (500 MHz, CDCl_3 , δ) 1.86 (s, 3H, CH_3), 1.93 (s, 3H, CH_3), 2.08 (pent, $J = 7.34$ Hz, 2H, $\text{CH}_2\text{CH}_2\text{CH}_2$), 2.47 (t, $J = 7.5$ Hz, 2H, CH_2CO), 2.84 (td, $J = 7.4, 1.7$ Hz, 2H, ArCH_2), 6.74 (s, 1H, OCHO), 7.00 (d, $J = 1.2$ Hz, 1H, H_{Ar}), 7.11 (t, $J = 7.0$ Hz, 1H, H_{Ar}), 7.19 (t, $J = 7.0$ Hz, 1H, H_{Ar}), 7.37 (d, $J = 7.9$ Hz, 1H, H_{Ar}), 7.59 (d, $J = 7.9$ Hz, 1H, H_{Ar}), 8.00 (s, 1H, NH). ^{13}C NMR (126 MHz, CDCl_3 , δ) 8.7 (CH_3), 11.5 (CH_3), 24.4 (CH_2), 25.1 (CH_2), 33.6 (CH_2), 93.7 (CH), 111.3 (CH), 115.2 (Cq), 118.9 (CH), 119.4 (CH), 121.8 (CH), 122.2 (CH), 127.2 (Cq), 127.5 (Cq), 136.5 (Cq), 153.6 (Cq), 171.8 (C=O), 172.3 (C=O). FT-IR (cm^{-1}): 3360, 2930, 1759, 1459, 1317, 1085, 990, 826, 746. MS (ES+) m/z (%): 314.5 ($M + 1$, 100), 315.5 ($M + 2$, 69), 316.5 ($M + 3$, 57). HRMS [ESI $^+$ (m/z)] calcd for $(\text{C}_{18}\text{H}_{19}\text{NO}_4 + \text{Na})^+$ 336.12118, found 336.12110. HPLC purity 99%.

4-Methyl-5-oxo-2,5-dihydrofuran-2-yl 2-phenylacetate (9)

Yield 67 mg (39%). White solid. ^1H NMR (500 MHz, CDCl_3 , δ) 1.96 (s, 3H, CH_3), 3.68 (ABq, $\Delta\nu_{\text{AB}} = 8$ Hz, $J_{\text{AB}} = 15.2$ Hz, 2H, CH_2), 6.85–6.86 (m, 2H, OCHO and CH=), 7.24–7.34 (m, 5H, H_{Ar}). ^{13}C NMR (126 MHz, CDCl_3 , δ) 10.8 (CH_3), 40.9 (CH_2), 92.8 (CH), 127.6 (CH), 128.9 (CH), 129.4 (CH), 132.7 (Cq), 134.6 (Cq), 142.0 (CH), 169.9 (C=O), 171.2 (C=O). FT-IR (cm^{-1}): 3357, 3098, 2924, 1775, 1756, 1498, 1415, 1322, 1140, 1011, 826, 708. MS (ES+) m/z (%): 233.3 ($M + 1$, 12), 250.4 ($M + \text{NH}_4$, 100), 271.3 ($M + \text{K}$, 25). HRMS [ESI $^+$ (m/z)] calcd for $(\text{C}_{13}\text{H}_{12}\text{O}_4 + \text{Na})^+$ 255.06333, found 255.06328. HPLC purity 99%.

3,4-Dimethyl-5-oxo-2,5-dihydrofuran-2-yl 2-phenylacetate (10)

Yield 119 mg (66%). White solid. ^1H NMR (500 MHz, CDCl_3 , δ) 1.83–1.84 (m, 3H, CH_3), 1.85–1.86 (m, 3H, CH_3), 3.70 (s, 2H, CH_2), 6.71 (s, 1H, OCHO), 7.25–7.34 (m, 5H, H_{Ar}). ^{13}C NMR (126 MHz, CDCl_3 , δ) 8.6 (CH_3), 11.3 (CH_3), 41.1 (CH_2), 94.0 (CH), 127.2 (Cq), 127.6 (CH), 128.8 (CH), 129.3 (CH), 132.8 (Cq), 153.5 (Cq), 170.2 (C=O), 171.7 (C=O). FT-IR (cm^{-1}): 3370, 3031, 2923, 1758, 1692, 1498, 1408, 1335, 1195, 1085, 966, 698. MS (ES+) m/z (%): 247.3 ($M + 1$, 100), 248.4

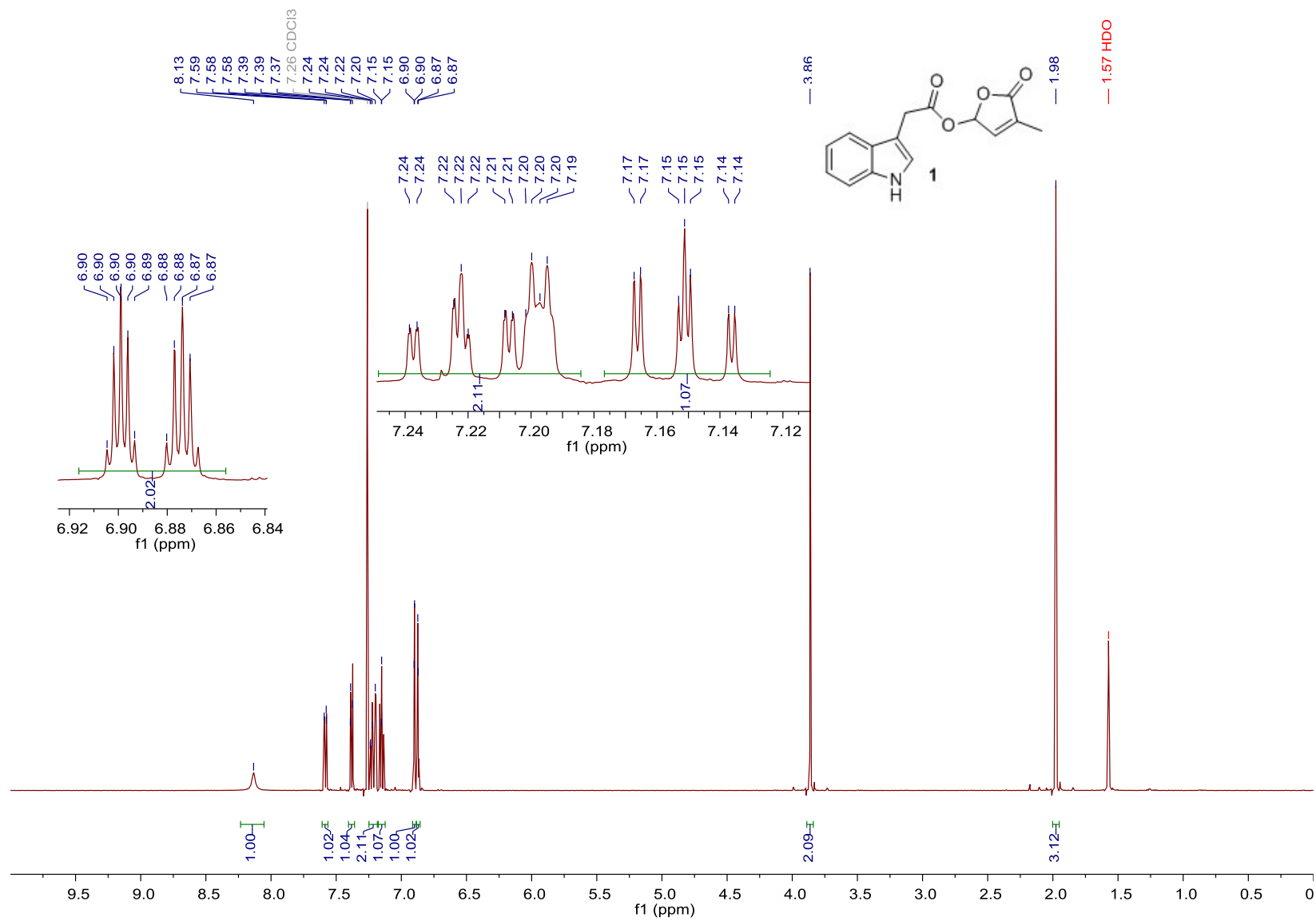
(M + 2, 92), 264.4 (M + NH₄, 83), 285.4 (M + K, 29). HRMS [ESI⁺ (m/z)] calcd for (C₁₄H₁₄O₄ + Na)⁺ 269.07898, found 269.07836. HPLC purity 96%.

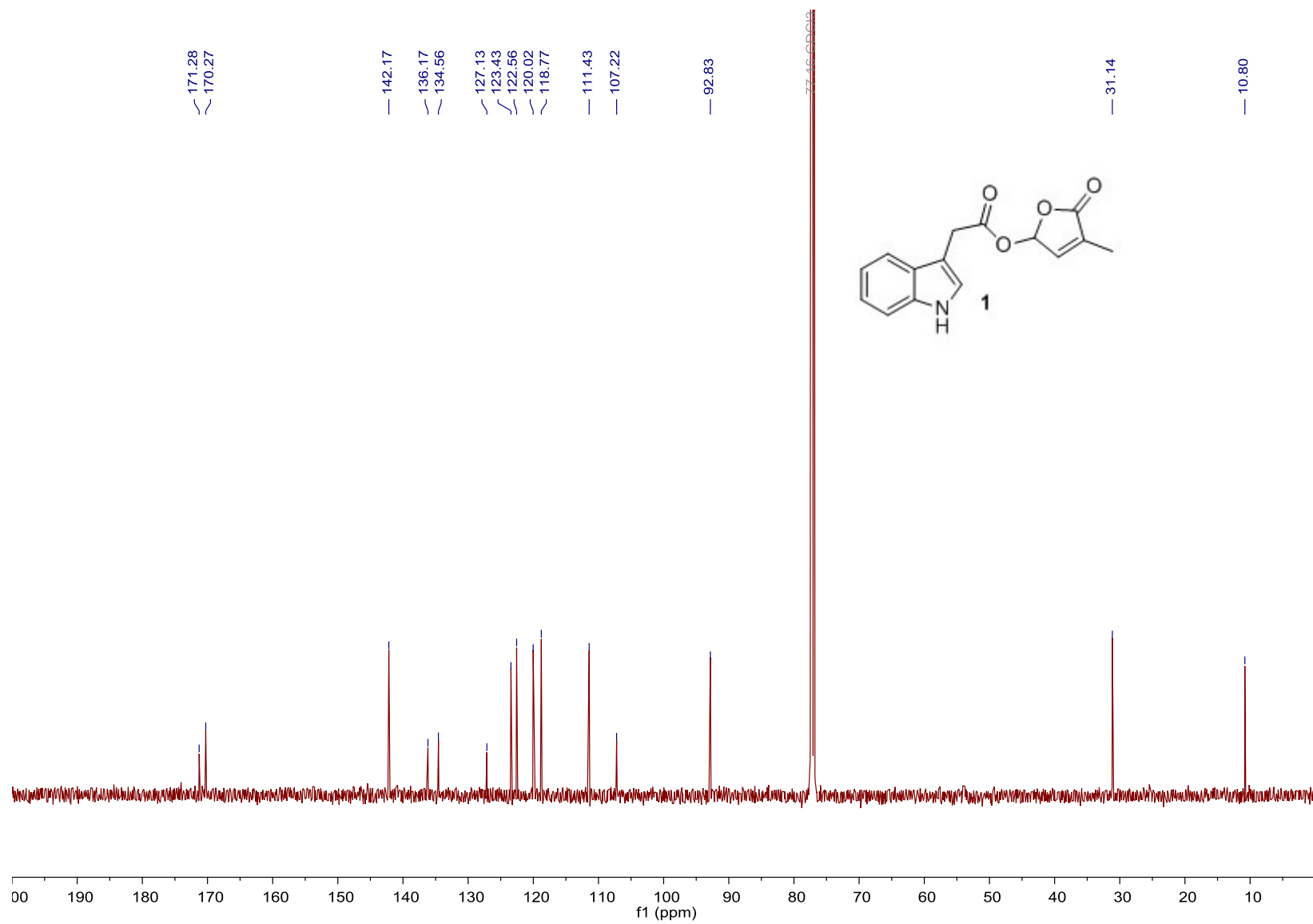
2,4-Dimethyl-5-oxo-2,5-dihydrofuran-2-yl 2-phenylacetate (11)

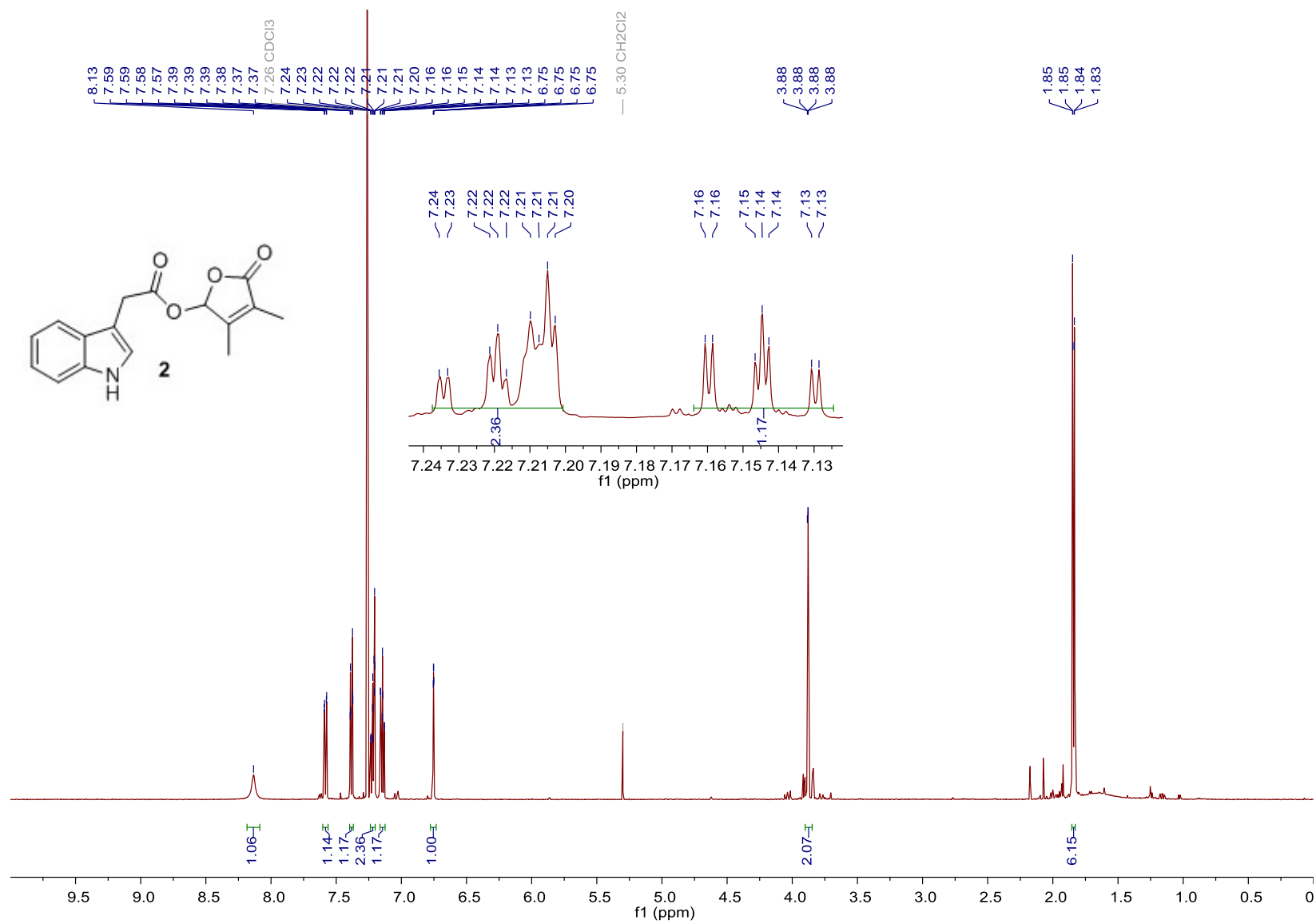
Yield 87 mg (48%). White solid. ¹H NMR (500 MHz, CDCl₃, δ) 1.77 (s, 3H, CH₃), 1.91 (d, *J* = 1.8 Hz, 3H, CH₃), 3.61 (s, 2H, CH₂), 7.20 (q, *J* = 1.7 Hz, 1H, CH=), 7.22–7.35 (m, 5H, H_{Ar}). ¹³C NMR (126 MHz, CDCl₃, δ) 10.4, 23.0, 41.5, 105.9, 127.4, 128.7, 129.3, 132.2, 133.0, 145.6, 169.5, 170.7. HRMS [ESI⁺ (m/z)] calcd for (C₁₄H₁₄O₄ + Na)⁺ 269.07898, found 269.07821.

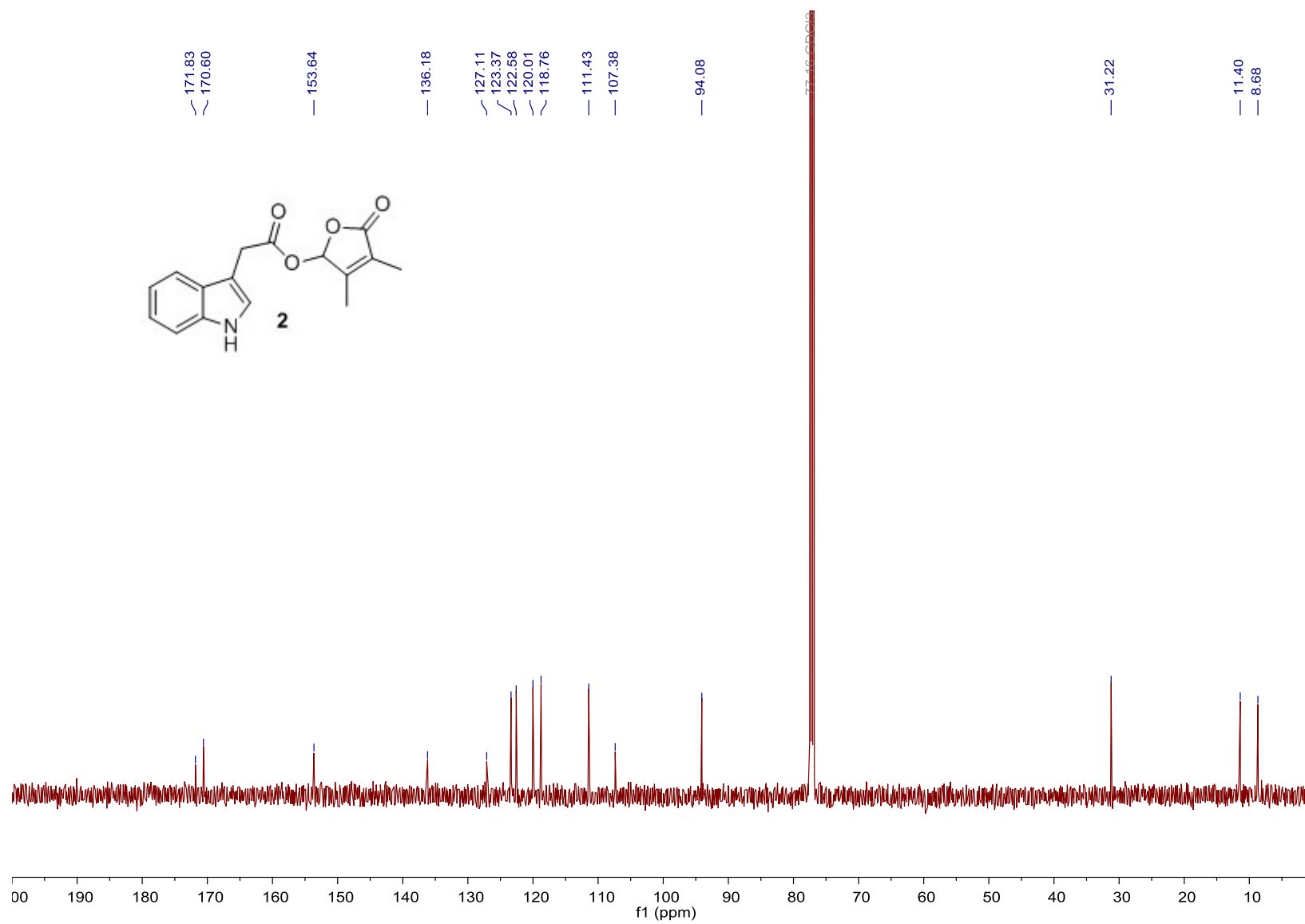
2,3,4-Trimethyl-5-oxo-2,5-dihydrofuran-2-yl 2-phenylacetate (12)

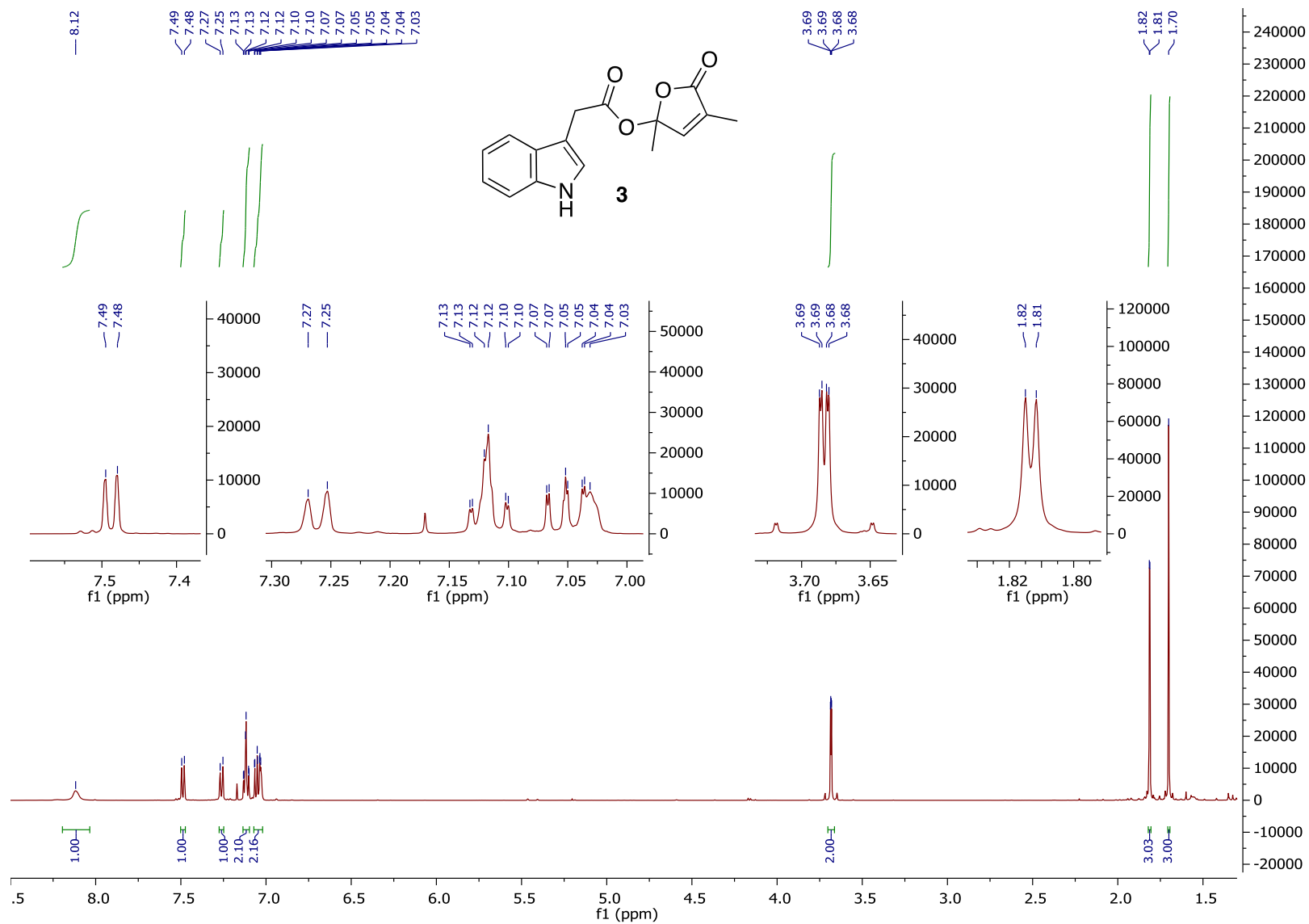
Yield 118 mg (62%). White solid. ¹H NMR (500 MHz, CDCl₃, δ) 1.65 (s, 3H, CH₃), 1.77–1.82 (m, 6H, 2 × CH₃), 3.59 (s, 2H, CH₂), 7.36–7.20 (m, 5H, H_{Ar}). ¹³C NMR (126 MHz, CDCl₃, δ) 8.5, 10.3, 23.0, 41.8, 105.8, 125.7, 127.3, 128.7, 129.2, 133.2, 156.1, 168.8, 171.0. HRMS [ESI⁺ (m/z)] calcd for (C₁₅H₁₆O₄ + Na)⁺ 283.09463, found 283.09375.

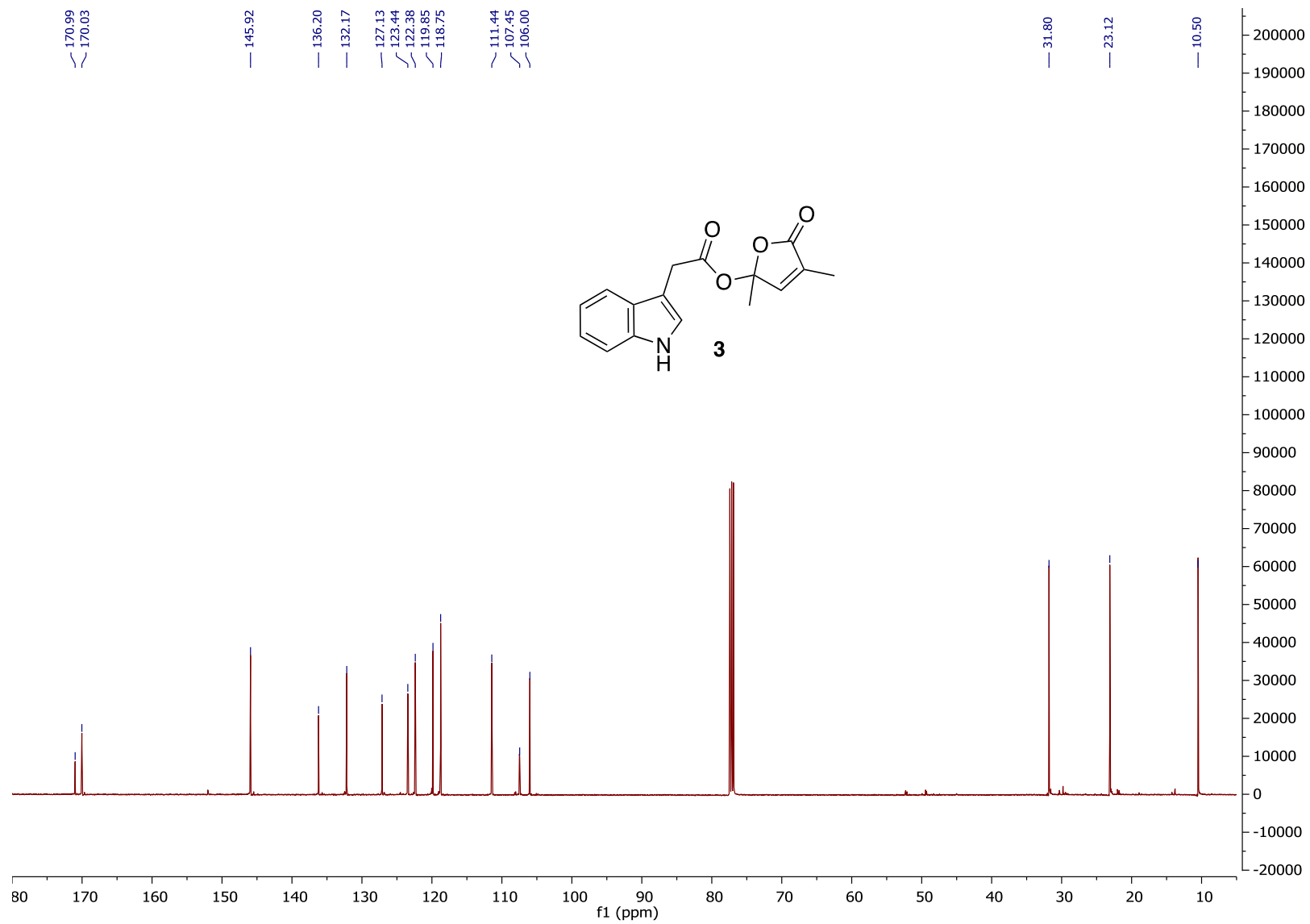


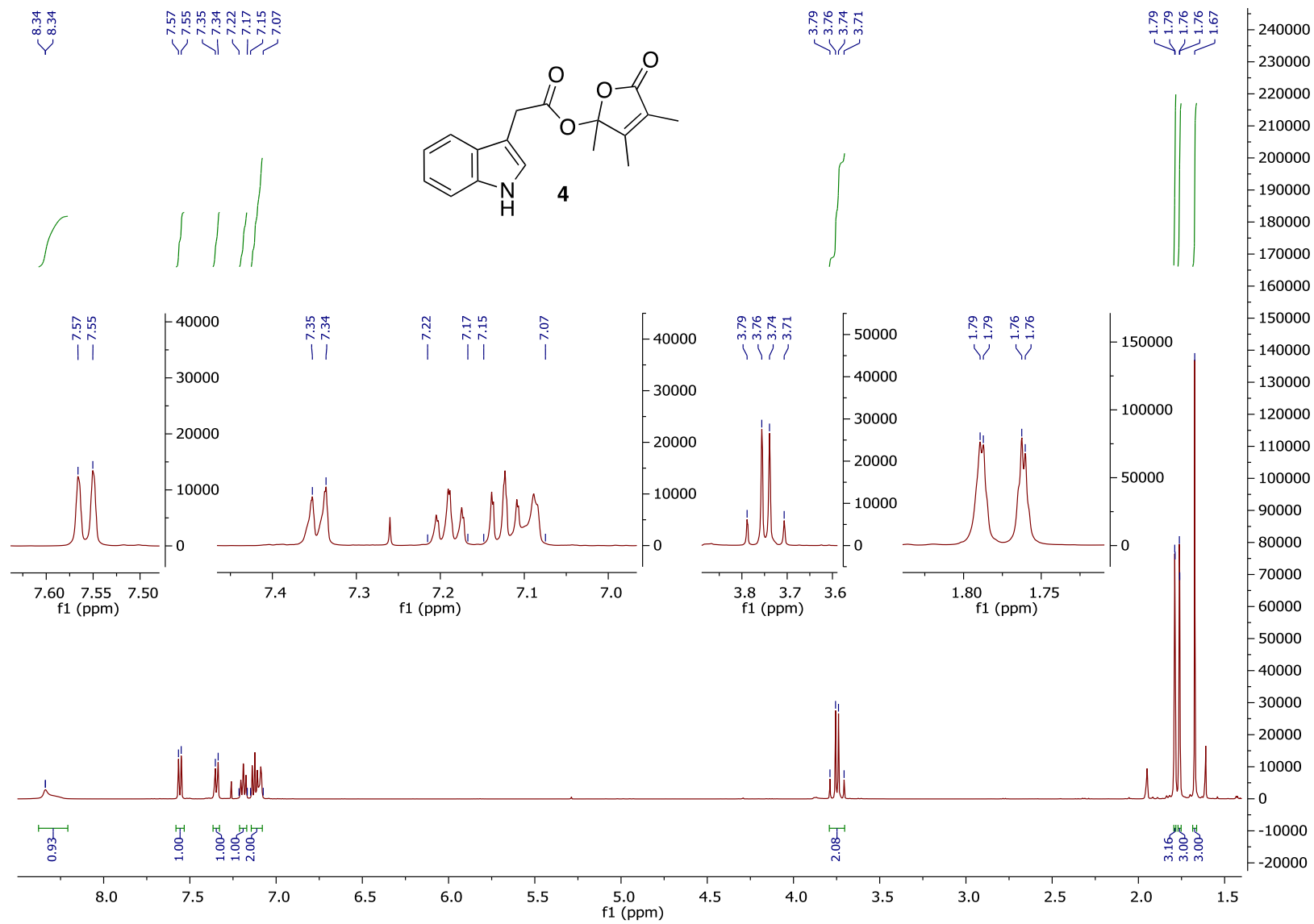


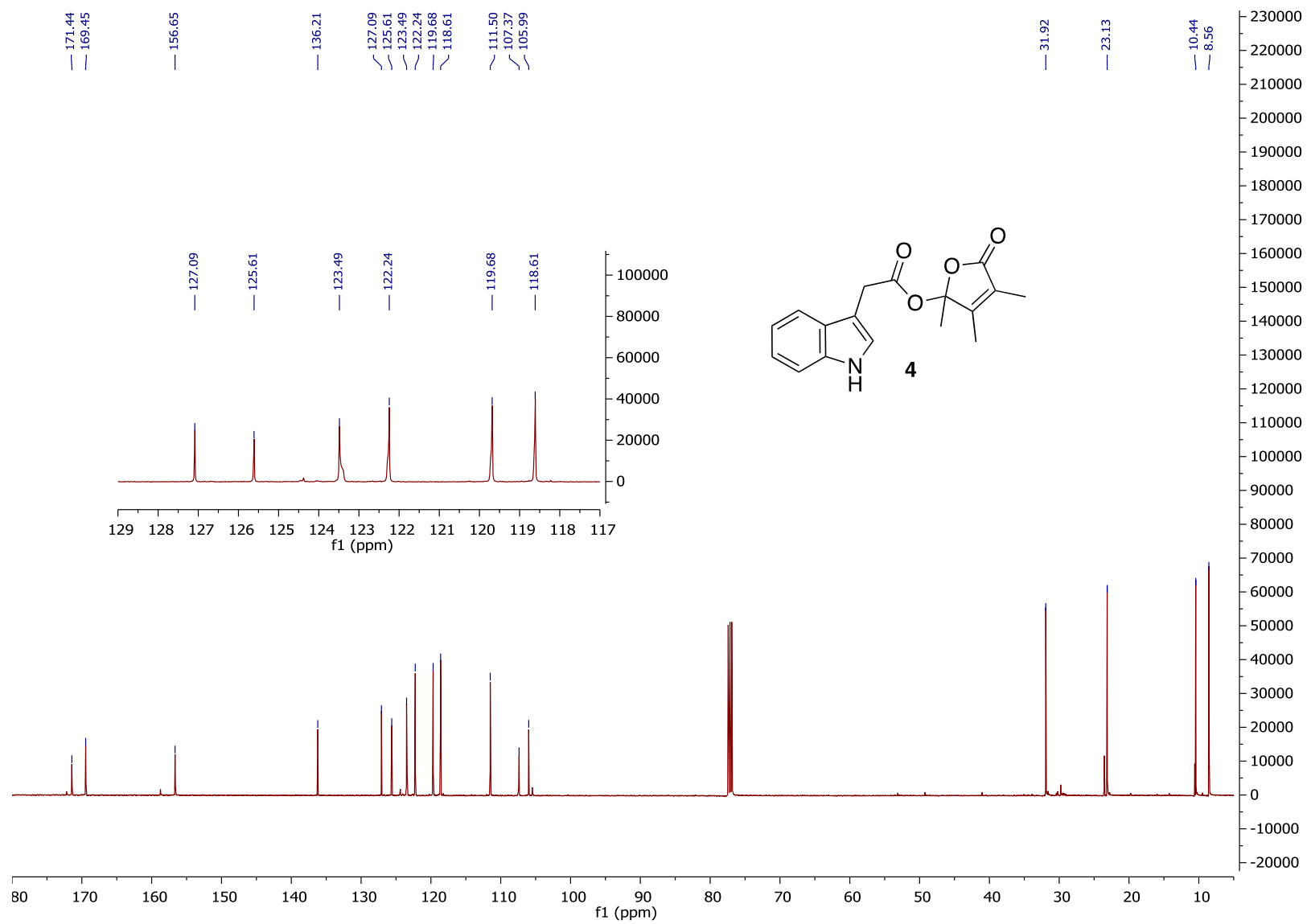


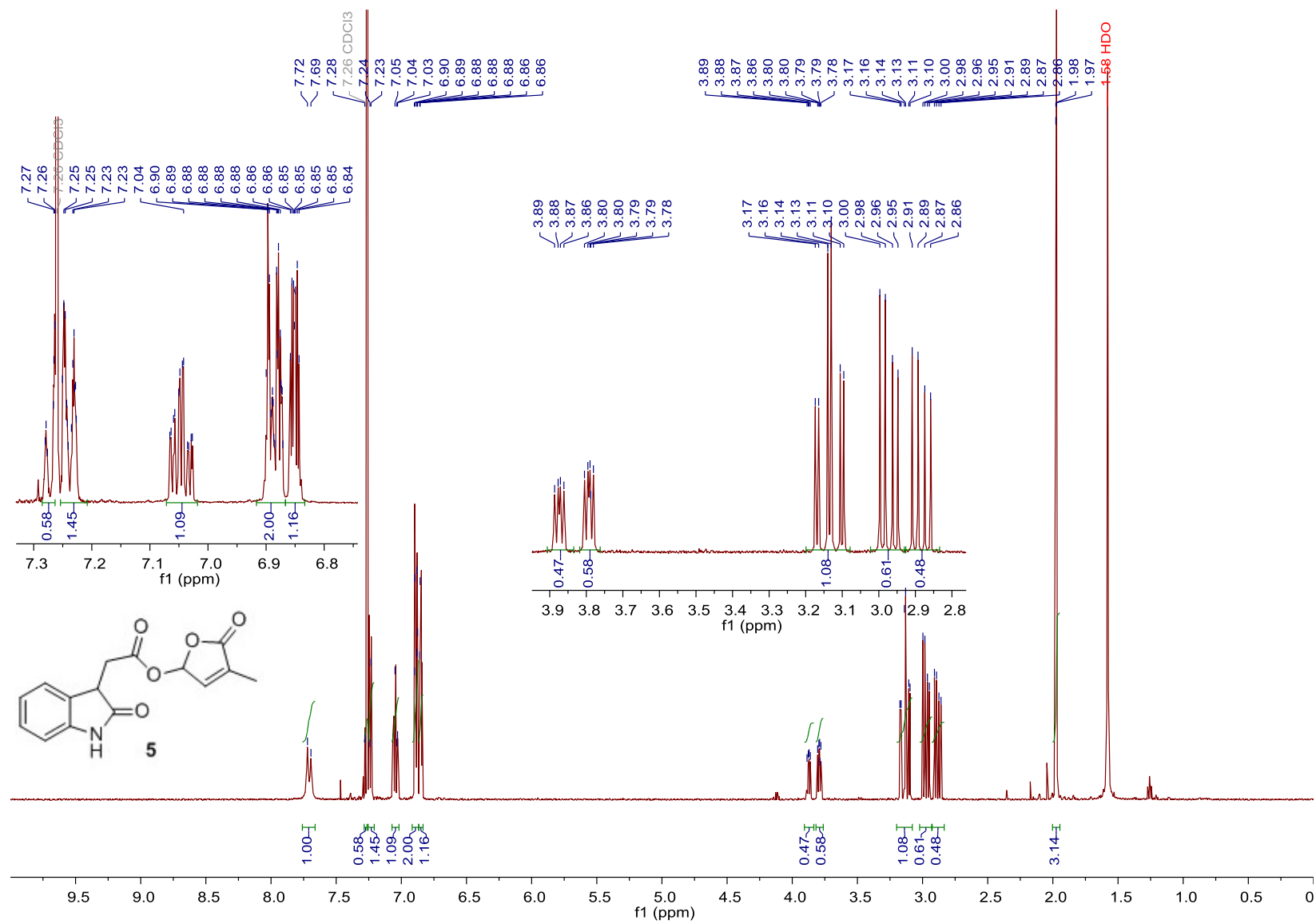


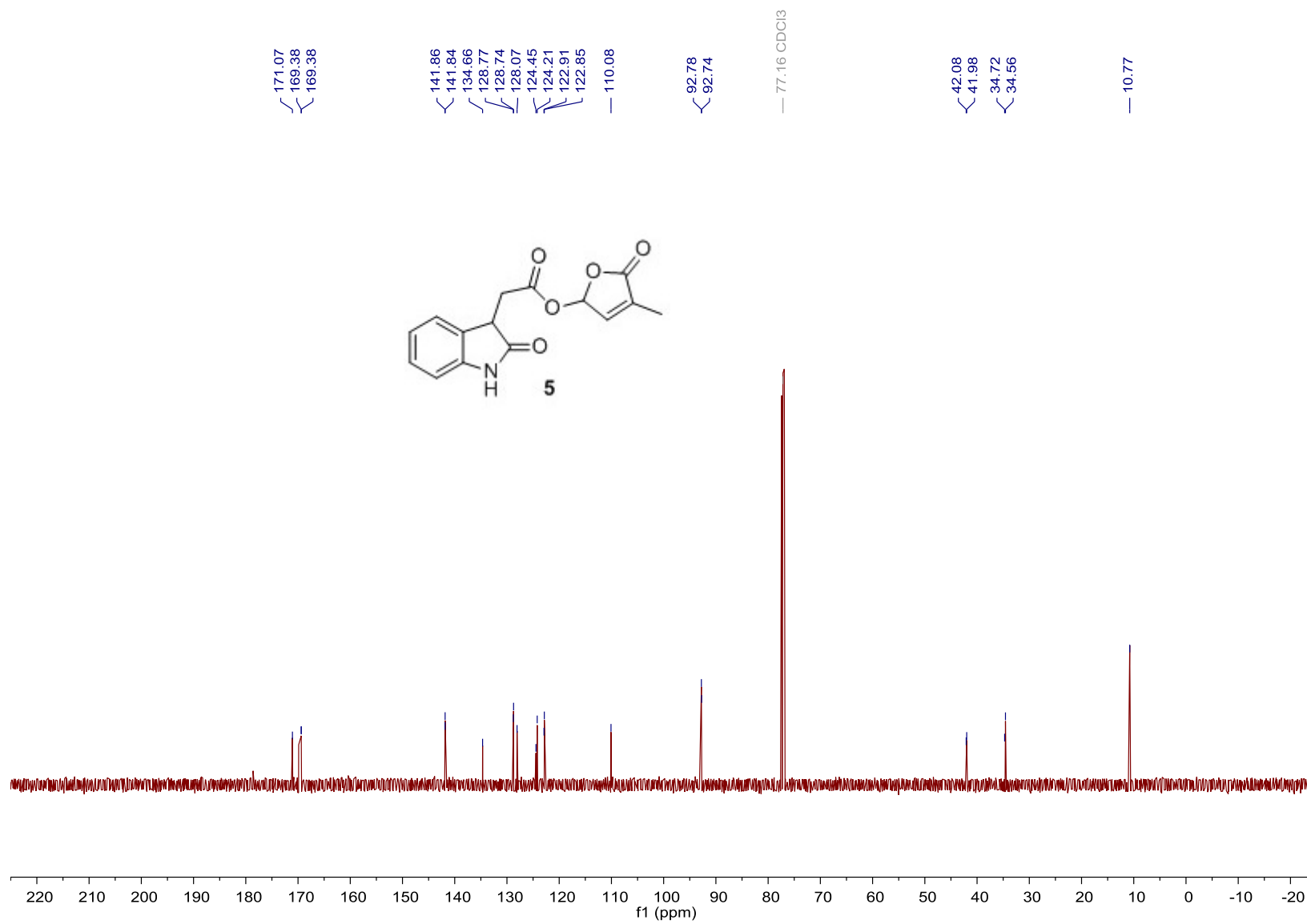


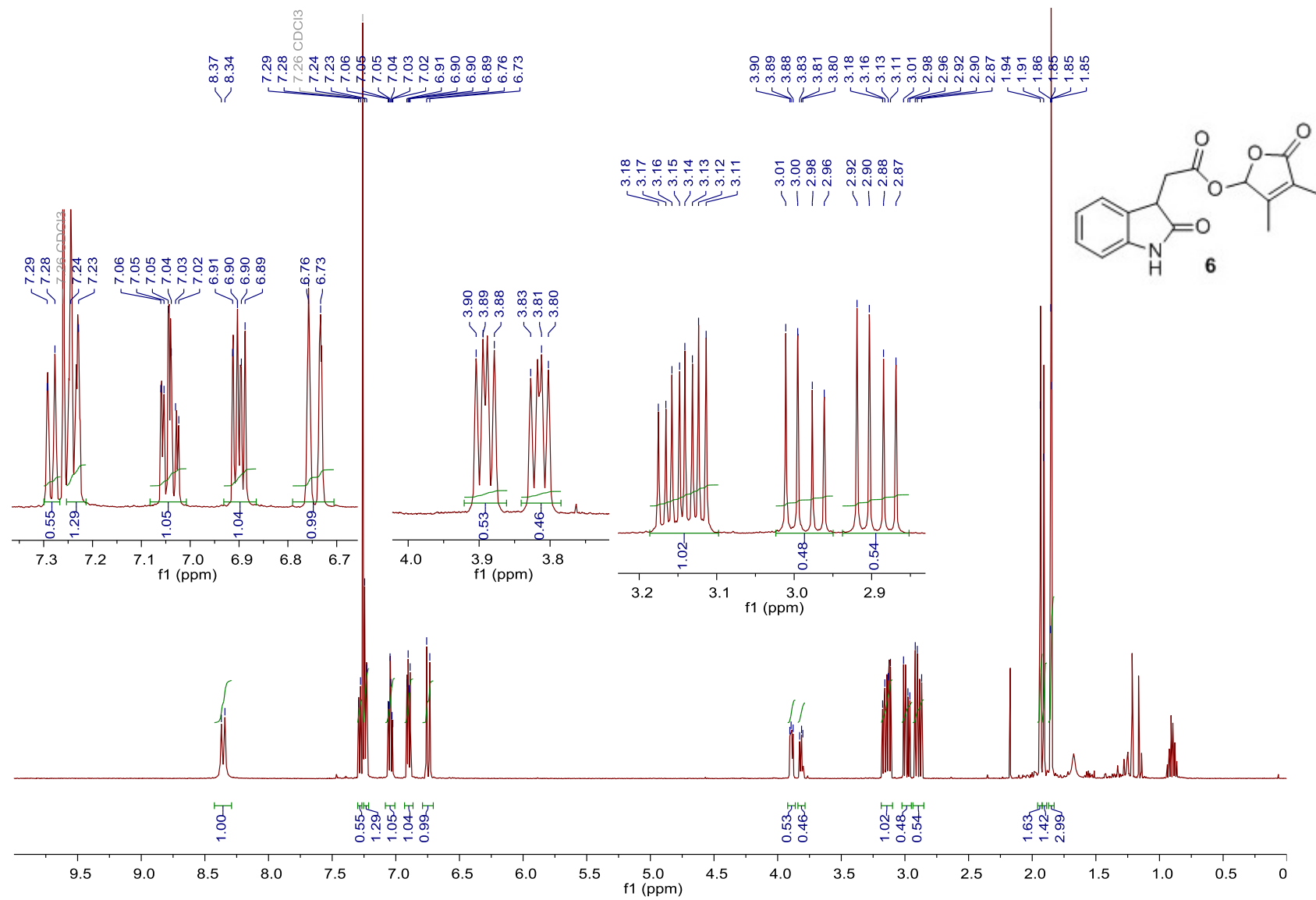


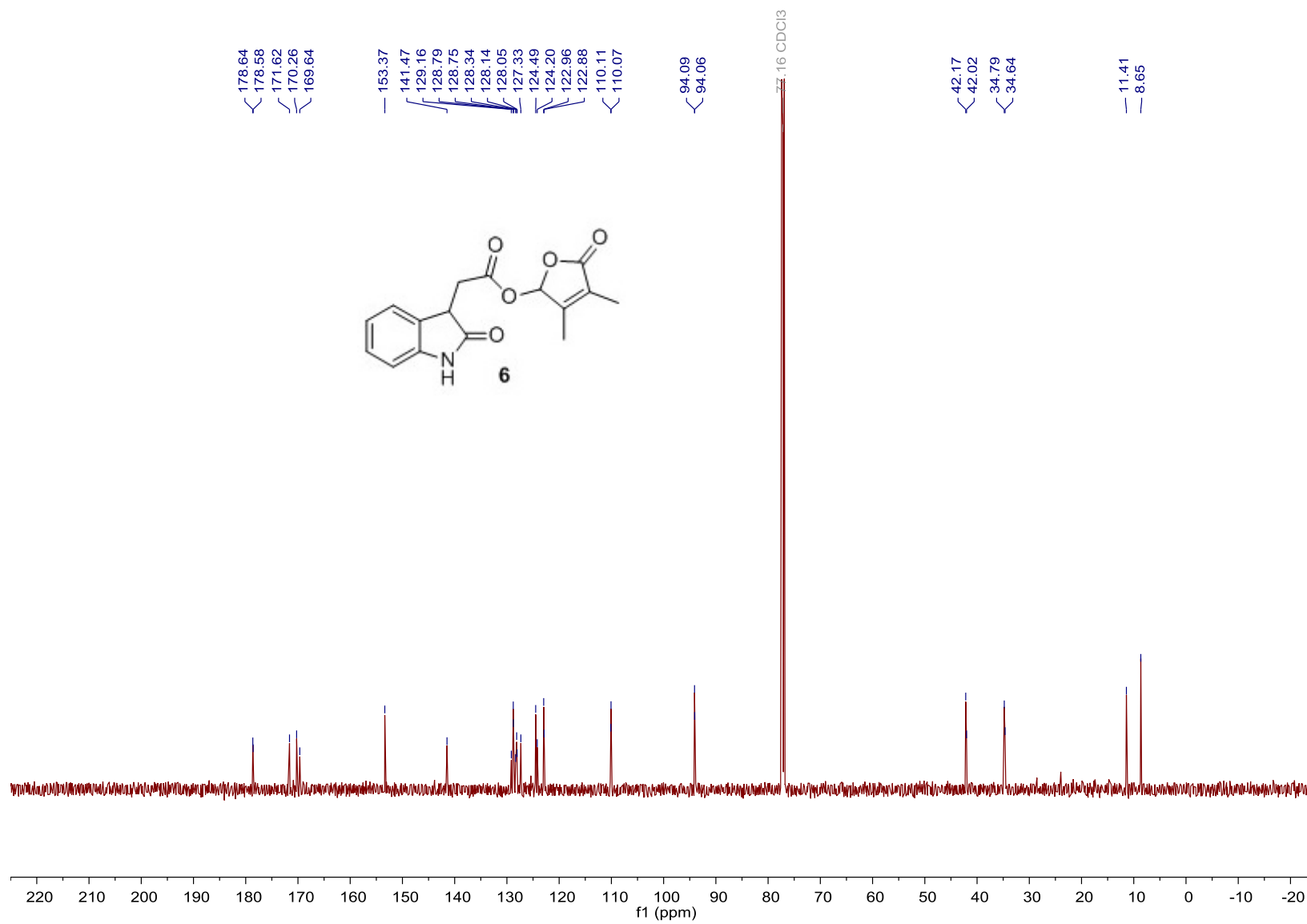


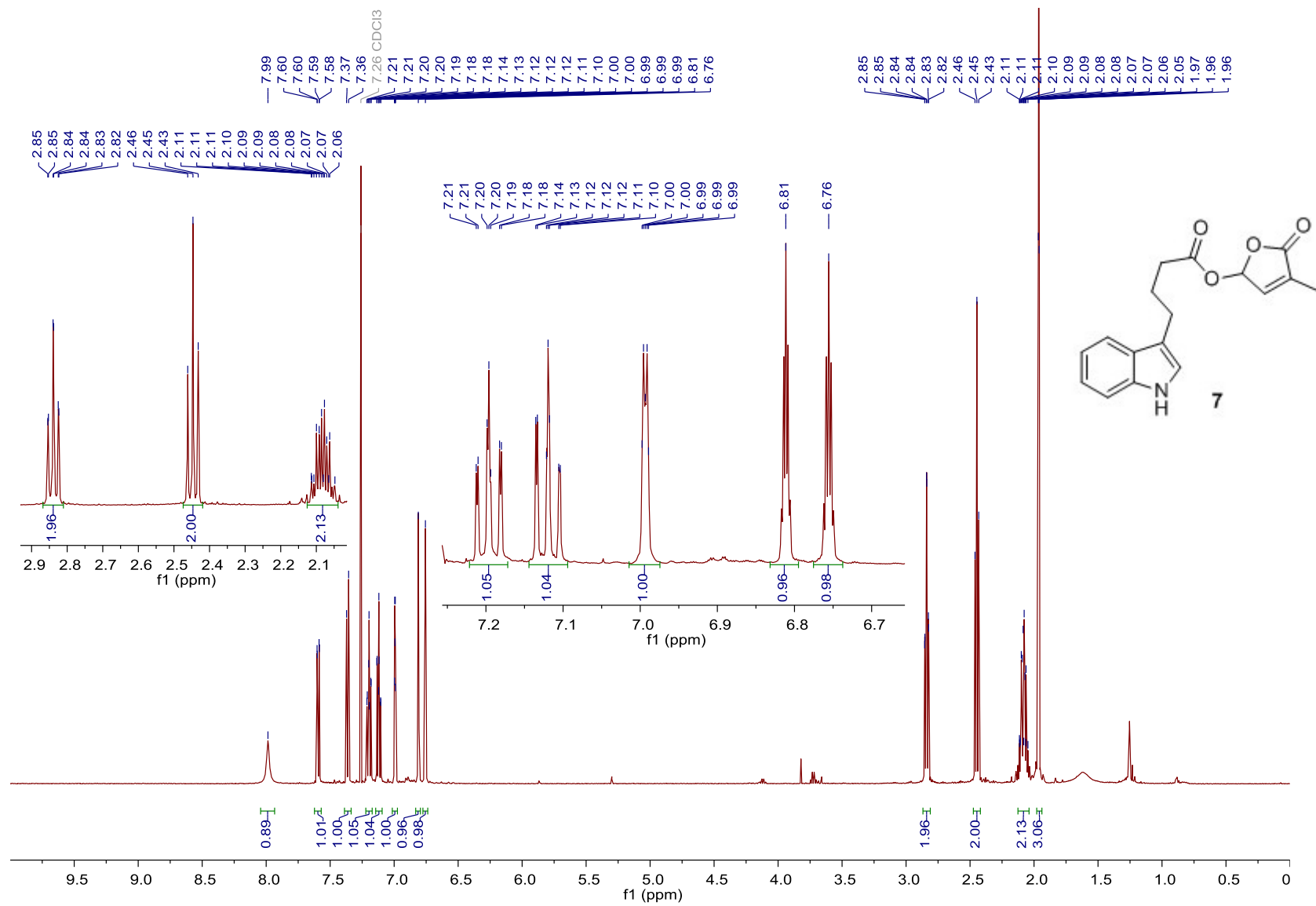


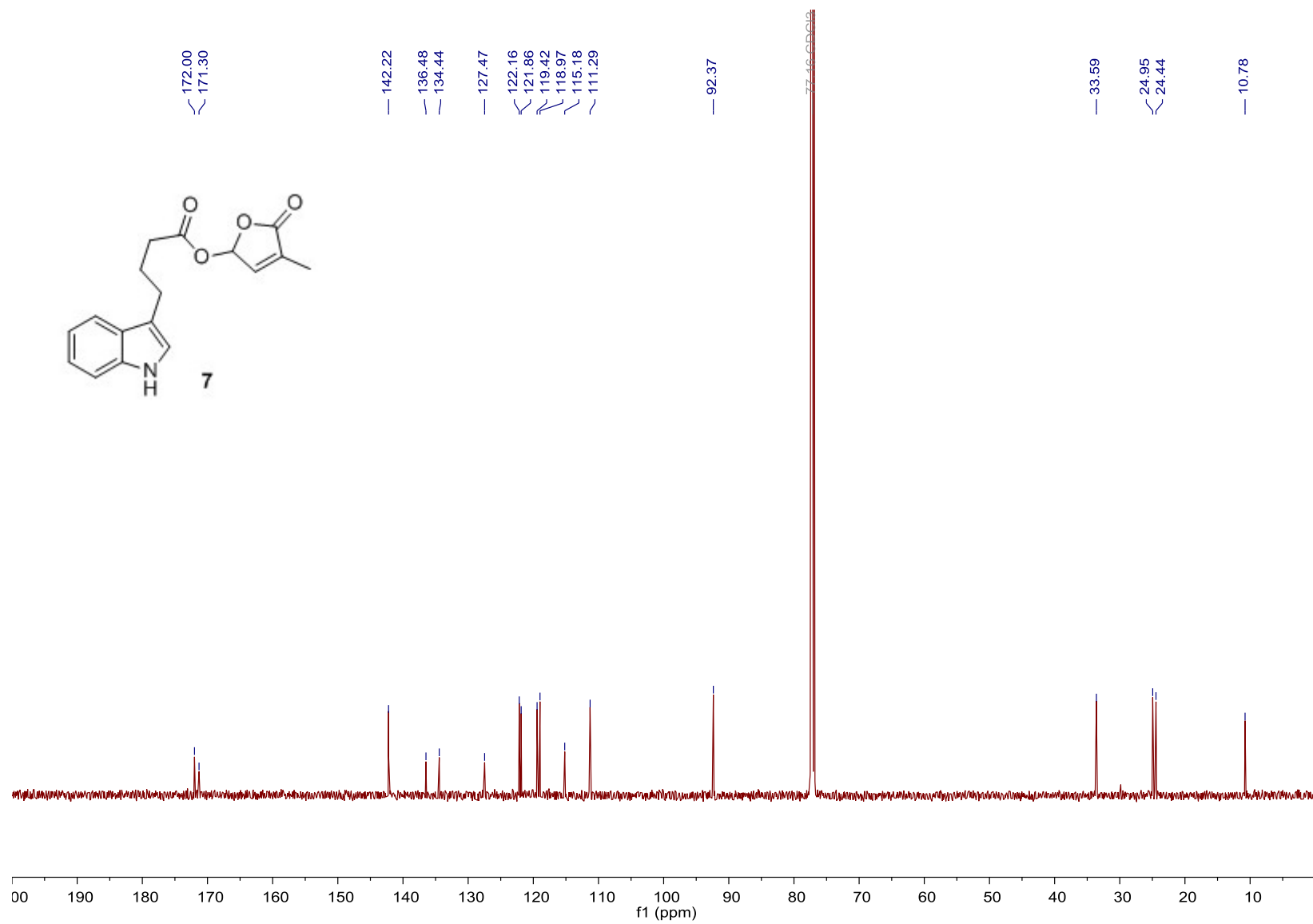


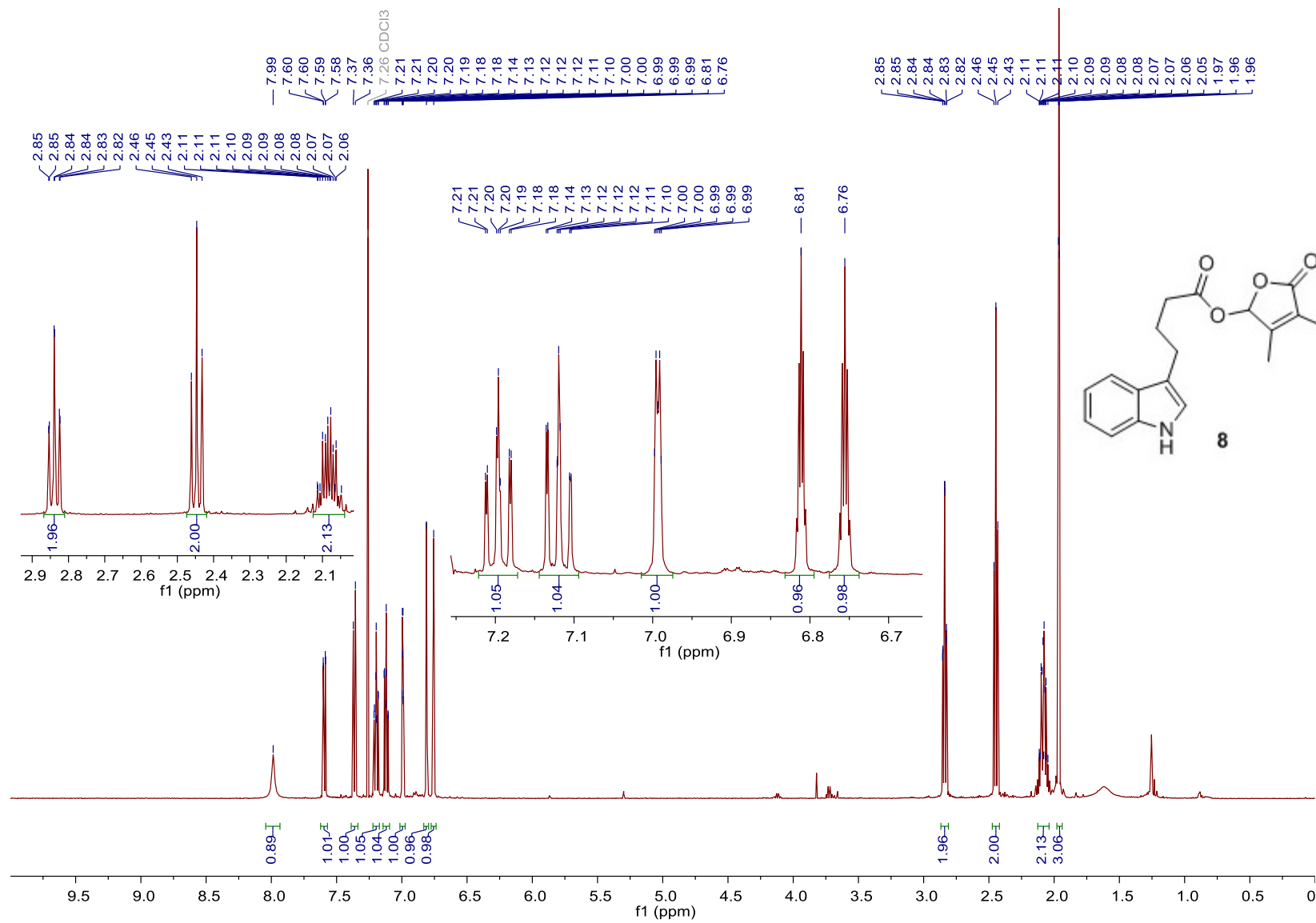


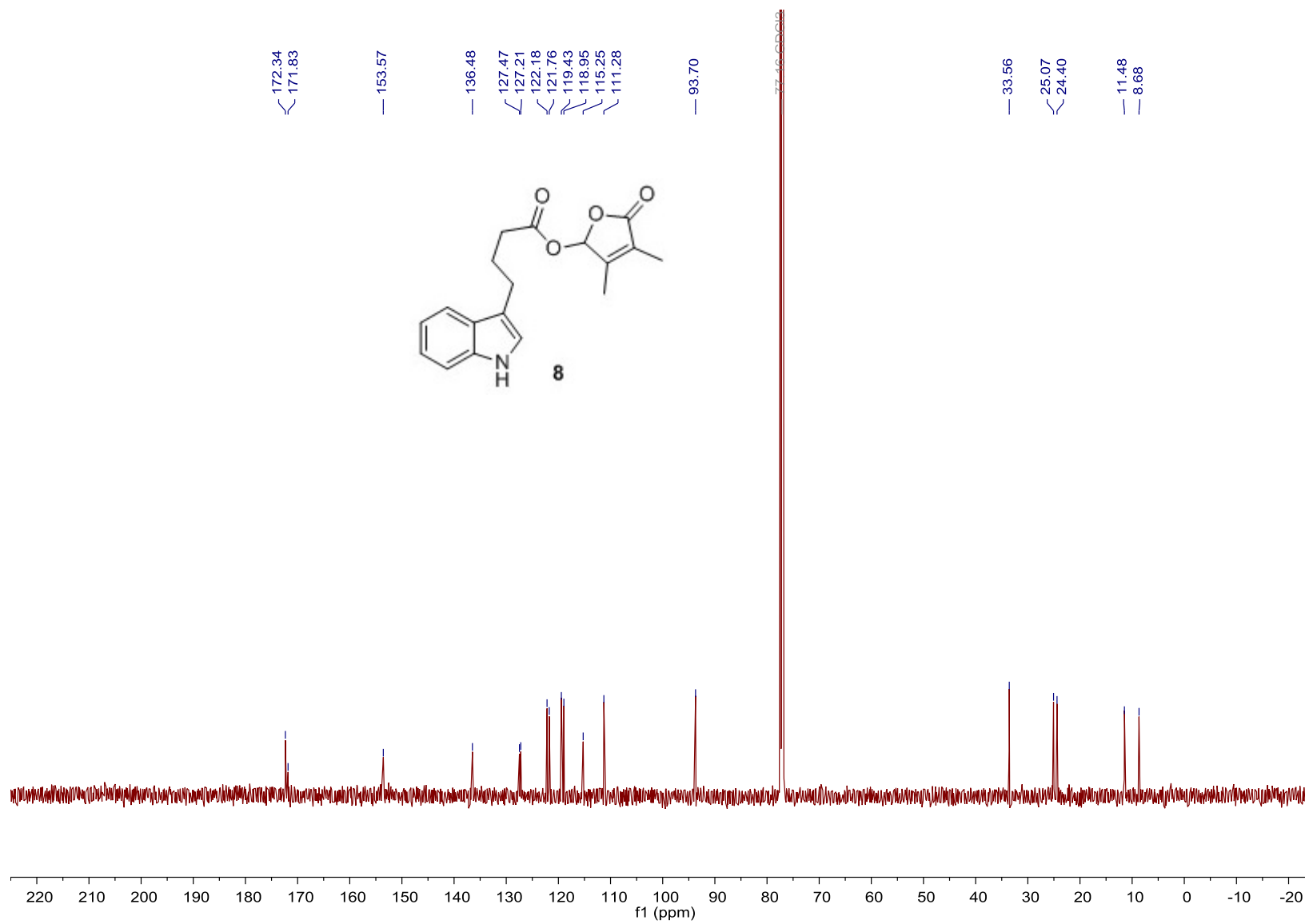


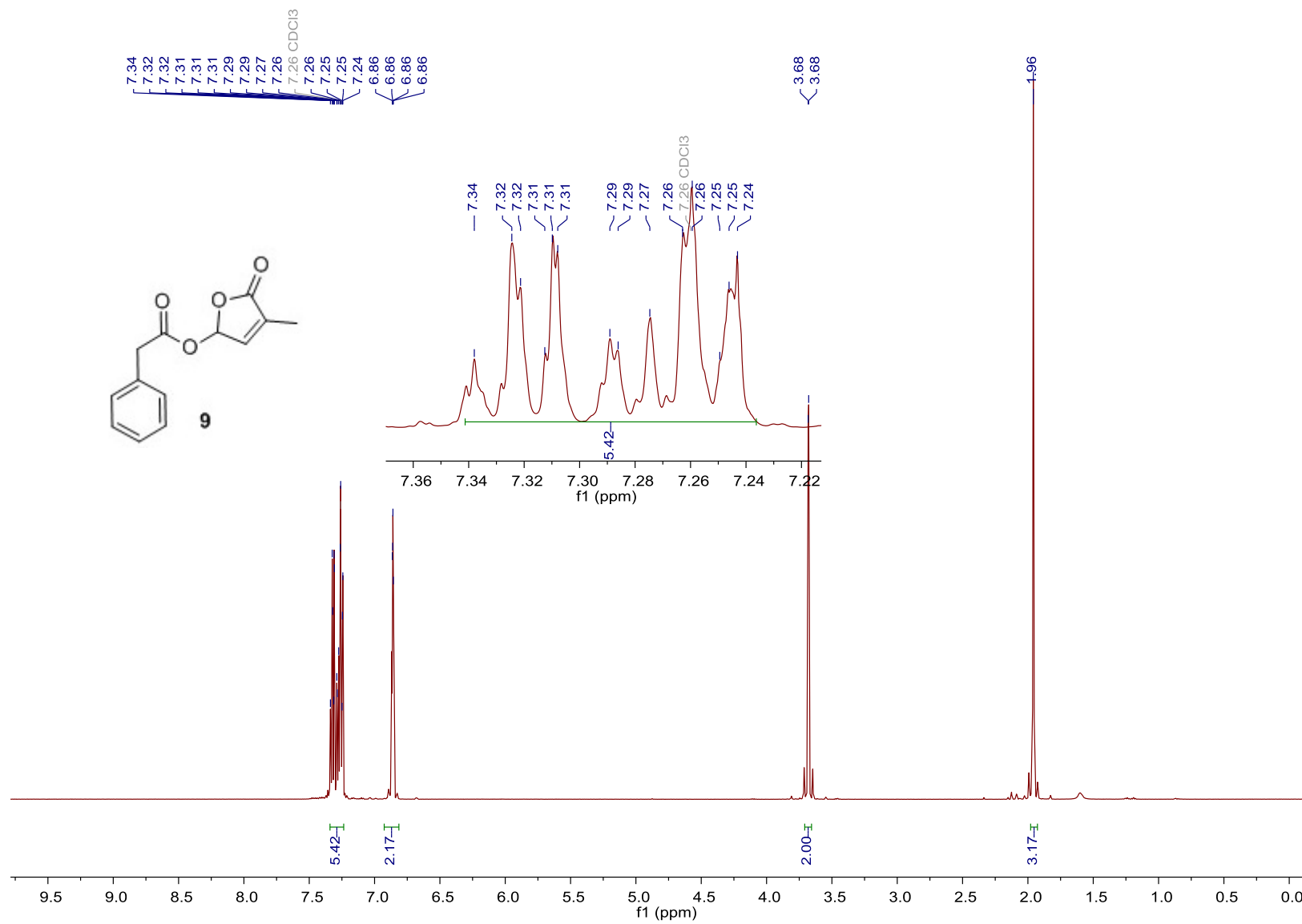


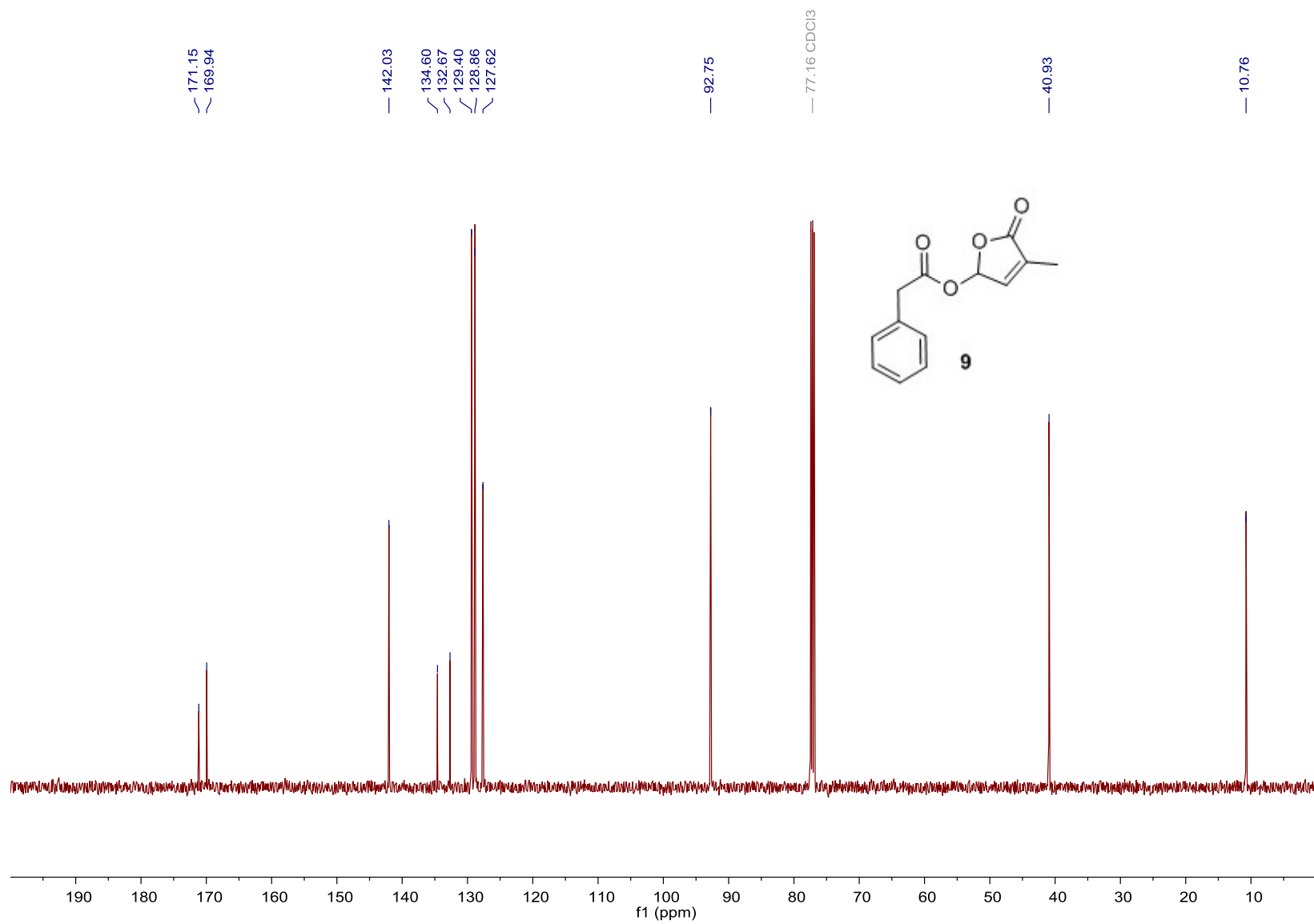


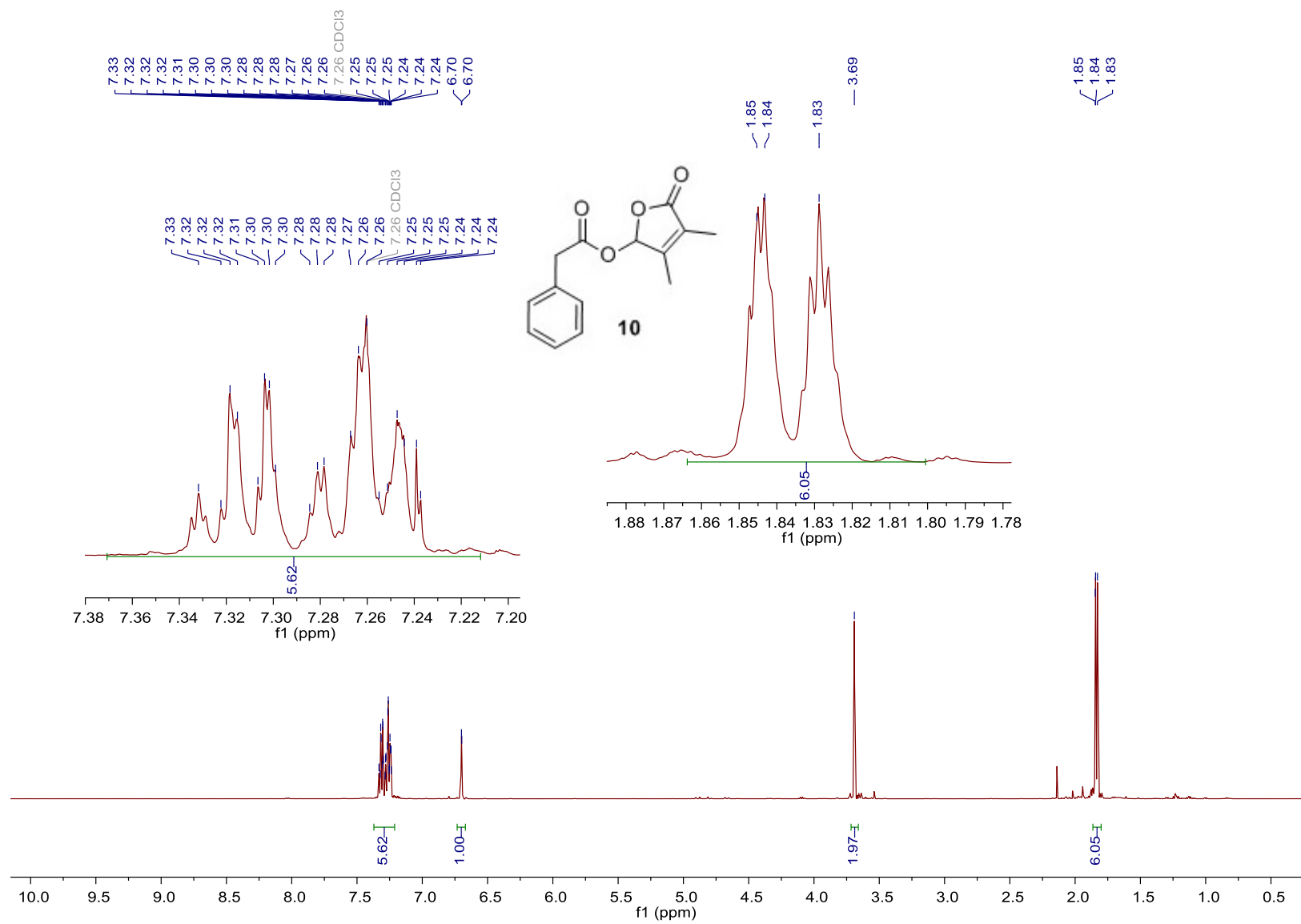


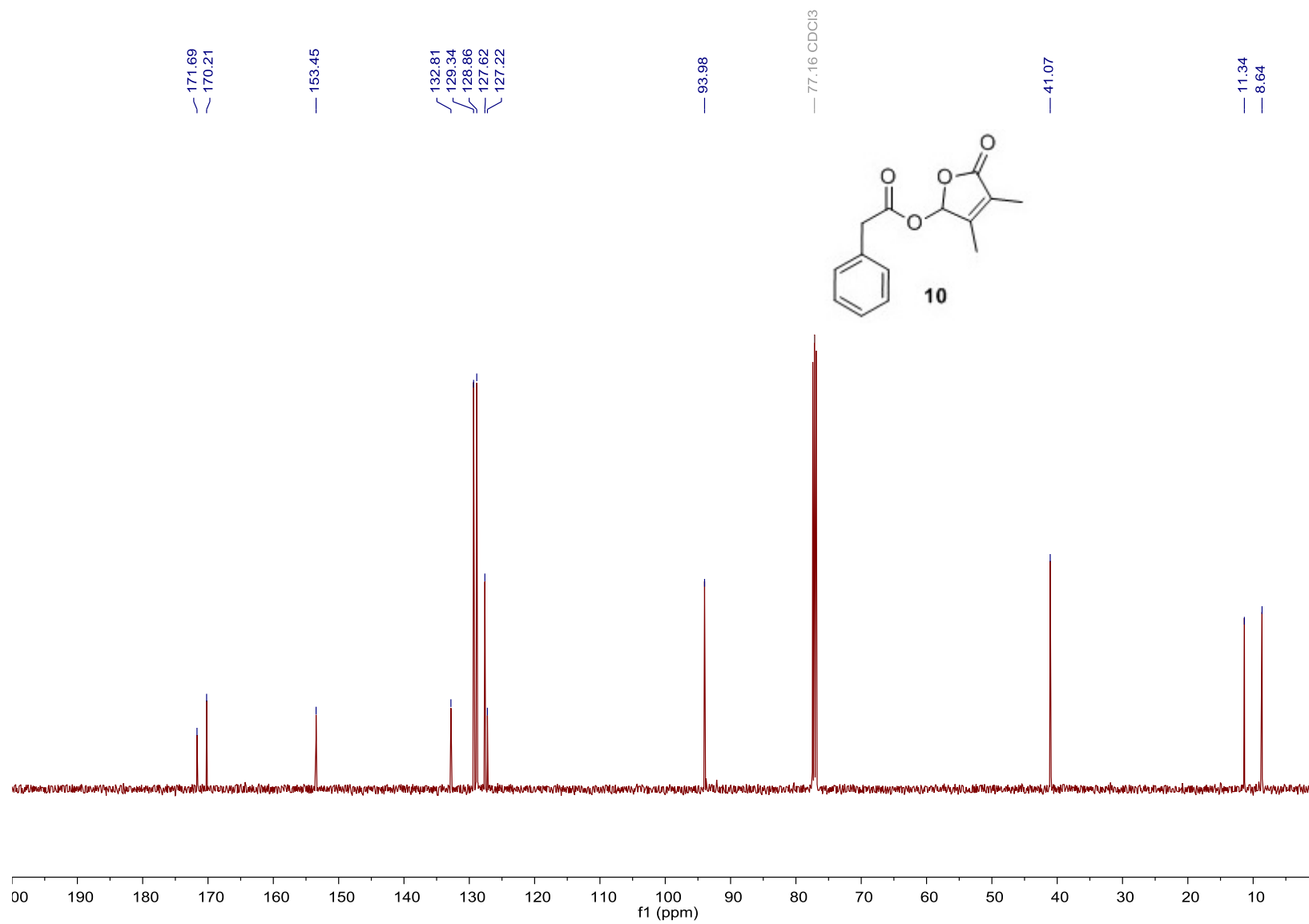


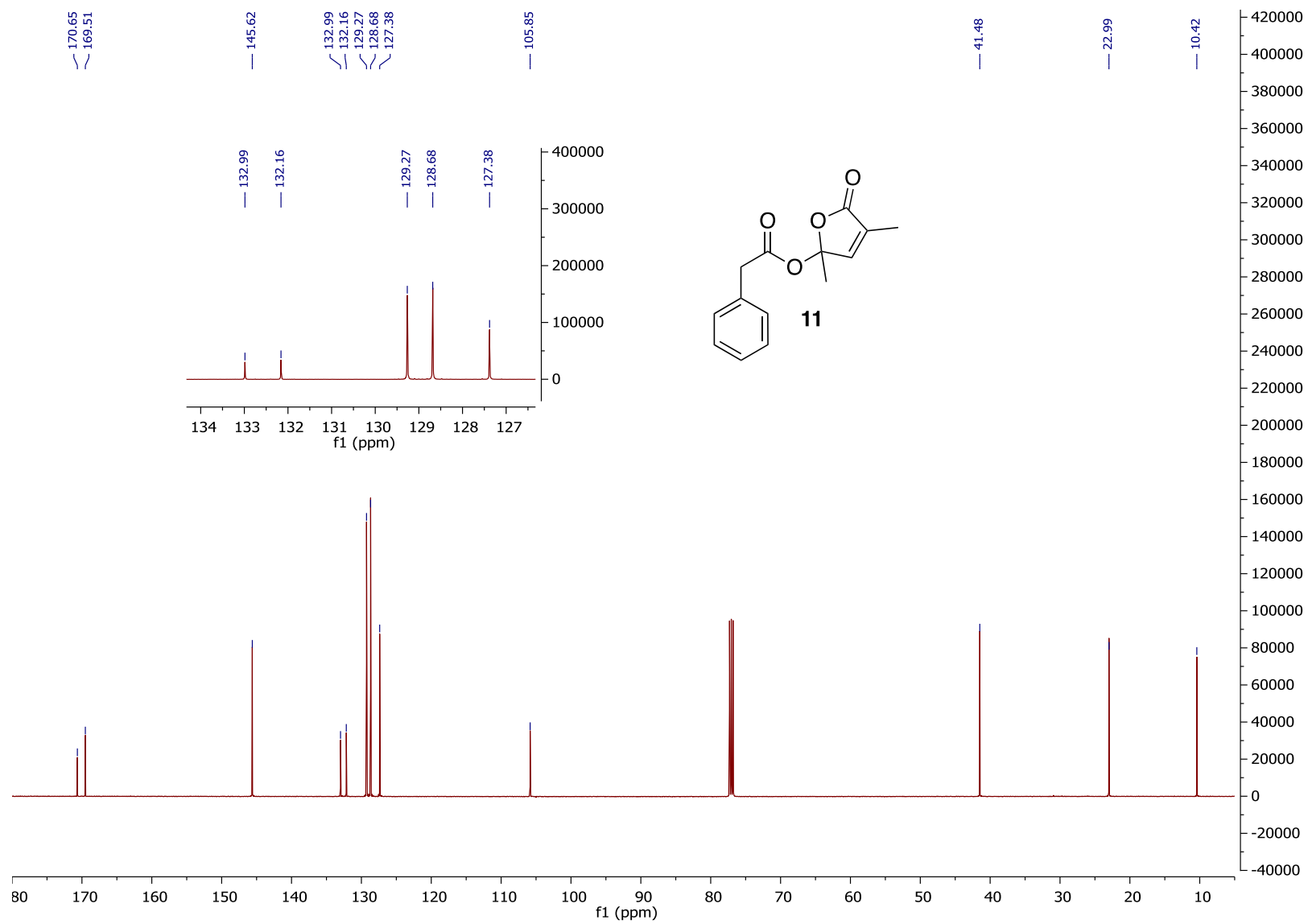


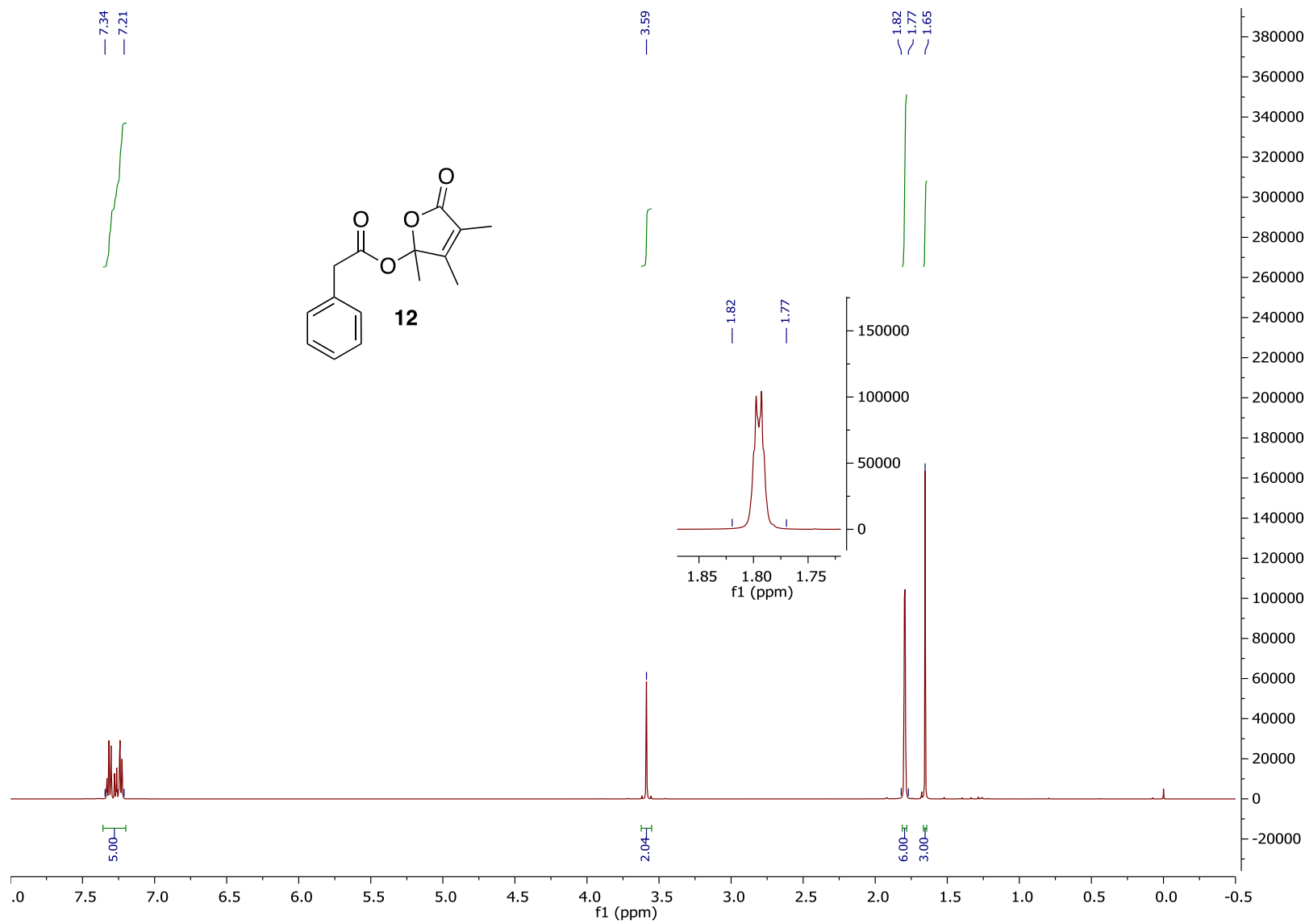


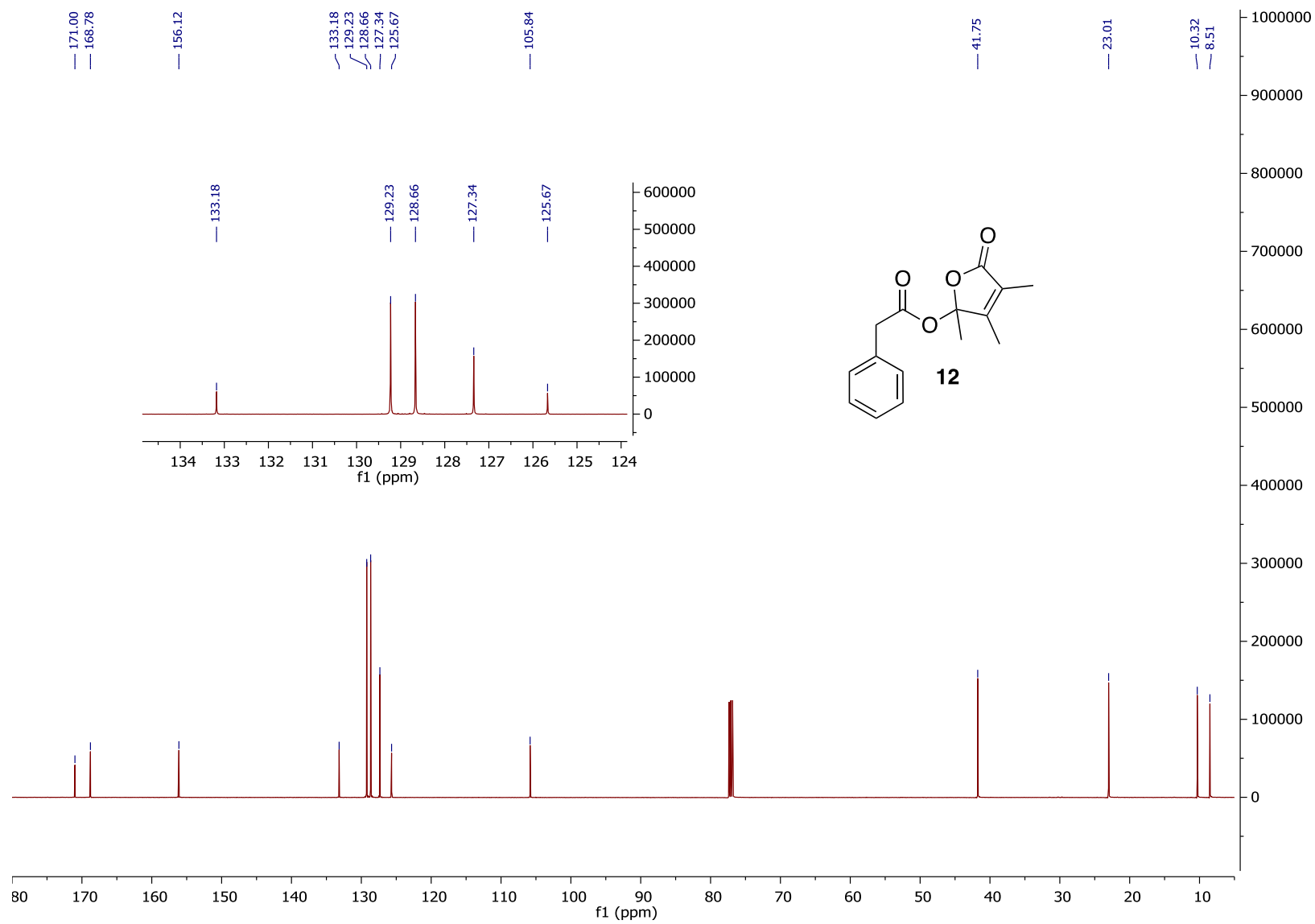












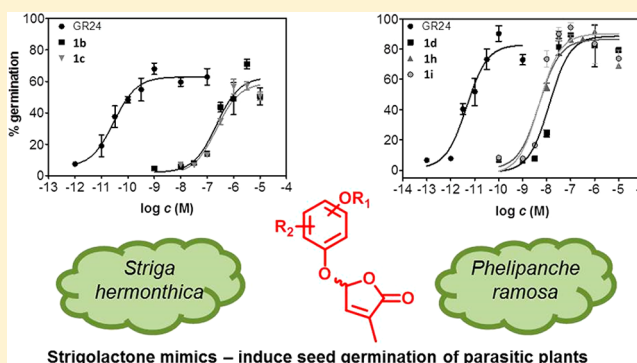
11.2. DVOŘÁKOVÁ, M., HÝLOVÁ, A., SOUDEK, P., RETZER, K., SPÍCHAL, L., AND VANĚK, T. (2018). RESORCINOL-TYPE STRIGOLACTONE MIMICS AS POTENT GERMINATORS OF THE PARASITIC PLANTS *STRIGA HERMONTHICA* AND *PHELIPANCHE RAMOSA*. *J. NAT. PROD.* 81(11):2321-2328.

DVOŘÁKOVÁ, M., HÝLOVÁ, A., SOUDEK, P., RETZER, K., SPÍCHAL, L., AND VANĚK, T. (2019). CORRECTION TO RESORCINOL-TYPE STRIGOLACTONE MIMICS AS POTENT GERMINATORS OF THE PARASITIC PLANTS *STRIGA HERMONTHICA* AND *PHELIPANCHE RAMOSA*. *J. NAT. PROD.* 82:168–168.

Resorcinol-Type Strigolactone Mimics as Potent Germinators of the Parasitic Plants *Striga hermonthica* and *Phelipanche ramosa*Marcela Dvorakova,[†] Adela Hylova,[‡] Petr Soudek,[†] Katarzyna Retzer,[†] Lukas Spichal,[†] and Tomas Vanek^{*,†}[†]Institute of Experimental Botany, Czech Academy of Sciences, v.v.i., Rozvojova 263, 16502, Prague 6, Czech Republic[‡]Centre of the Region Hana for Biotechnological and Agricultural Research, Department of Chemical Biology and Genetics, Faculty of Science, Palacky University, Slechtitelu 241/27, 783 71, Olomouc, Czech Republic

Supporting Information

ABSTRACT: Strigolactones are a particular class of plant metabolites with diverse biological functions starting from the stimulation of parasitic seed germination to phytohormonal activity. The expansion of parasitic weeds in the fields of developing countries is threatening the food supply and calls for simple procedures to combat these weeds. Strigolactone analogues represent a promising approach for such control through suicidal germination, i.e., parasitic seed germination without the presence of the host causing parasite death. In the present work, the synthesis of resorcinol-type strigolactone mimics related to debranones is reported. These compounds were highly stable even at alkaline pH levels and able to induce seed germination of parasitic plants *Striga hermonthica* and *Phelipanche ramosa* at low concentrations, $EC_{50} \approx 2 \times 10^{-7}$ M (*Striga*) and $EC_{50} \approx 2 \times 10^{-9}$ M (*Phelipanche*). On the other hand, the mimics had no significant effect on root architecture of *Arabidopsis* plants, suggesting a selective activity for parasitic seed germination, making them a primary target as suicidal germinators.



With weeds (*Striga* spp.) and broomrapes (*Orobanchaceae* and *Phelipanche* spp.) are parasitic plants that infest various crops and cause severe yield losses around the world, especially in tropical and subtropical areas. Their control is difficult, primarily due to the production of thousands of tiny seeds that may persist in the soil for decades.^{1a–d} In addition, these seeds germinate only at specific conditions such as the right temperature and humidity and in the presence of a chemical signal exuded by a host that suggests nutrient accessibility.^{1a,2a,b} These parasitic plants are a real threat to food security, as they cause enormous crop losses, especially in developing countries with increasing populations. A recent study on the impact of *Orobanchaceae* family (*Striga* spp. and *Rhizophicarpa fistulosa*) infestations of rice in sub-Saharan Africa has revealed that almost 1.5 million hectares of rice are infested by at least one of these parasitic plants, and together they cause economic losses of U.S. \$200 million every year with a 15% increase annually.³ An older study estimated losses caused only by *Striga* spp. to all crops in Africa to be around U.S. \$7 billion every year.⁴

As early as in 1966, the first chemical compound recognized as a rhizosphere signal for *Striga* spp., strigol (Figure 1A), was isolated from the root exudates of cotton.⁵ Since then, around 20 naturally occurring rhizosphere chemicals, structurally related to strigol and collectively called strigolactones, have been isolated and characterized.^{6a–c} However, the identifica-

tion and characterization of natural strigolactones are challenging, as they are produced by plants in picogram levels.⁷ In addition, strigolactones are rather complex molecules consisting of a tricyclic lactone part (ABC part) connected to a furanone ring (D-ring) via an enol ether bond (depicted for strigol: Figure 1A). Furthermore, the enol ether bond makes this structure rather unstable, especially in alkaline environments.

The intricate, labile structure and the low abundance of strigolactones also thwart their potential for the control of parasitic weeds. Thus, there is a continuing interest in the synthesis of strigolactone analogues with simplified structures and maintained biological activity. Although there are also other methods to regulate parasitic plant emergence, such as the use of herbicides, ethylene injection, or *Fusarium* pathogens, none of these methods is infallible.^{2a,8} Ethylene injection is costly and limited only to *Striga* spp., and the use of *Fusarium* is strictly regulated. In addition, the utilization of chemical herbicides is often nonselective and environmentally unfriendly due to environmental persistence and the undesired impact on host plants.

The utilization of strigolactones for parasitic weed control dates as far back as 1976, when the first strigolactone

Received: February 21, 2018

Published: October 26, 2018

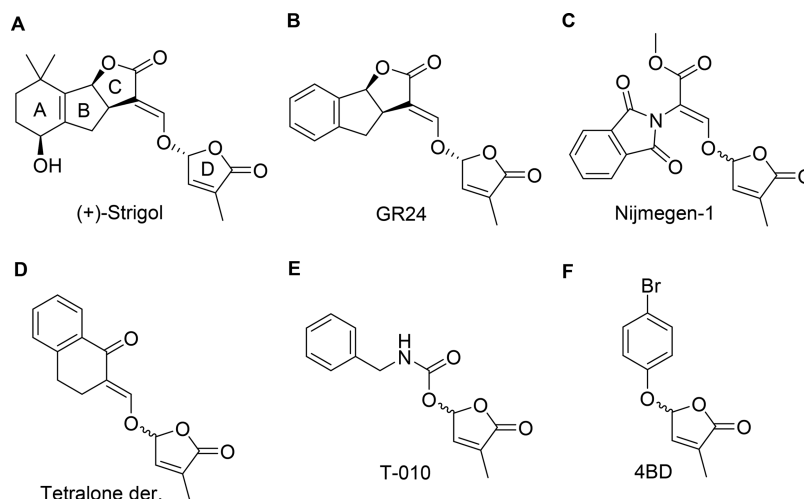


Figure 1. (A) Strigol; (B) GR24; (C) Nijmegen-1; (D) tetralone derivative; (E) T-010; (F) 4-bromodebranone (4BD).

derivatives (GR compounds) with high germination activity were synthesized.⁹ These derivatives showed promising results when applied as suicidal germinators, i.e., compounds that induce seed germination of parasitic plants without the presence of a host, thus causing parasite death. However, the commercial utilization of these compounds was later abandoned, probably due to their low stability in alkaline soil and limited commercial availability.^{2a,10a,b} In spite of this, one of these compounds, *rac*-GR24, herein referred to simply as GR24 (*rac*-GR24 is a racemic mixture of GR24^{SDS}, with natural conformation, and its enantiomer GR24^{ent-SDS}), is used as a reference compound in biological tests (Figure 1B).

Since 1976, many strigolactone analogues have been synthesized in order to combat parasitic plants.^{2b,9,11a–k} From these, Nijmegen-1 (Figure 1C) and a tetralone-based derivative (Figure 1D) exerted the most promising results, even in field trials (Nijmegen-1).^{2a,11c} It was established by SAR studies that for seed germination biological activity, the presence of a D-ring together with a conjugated enol ether bond is essential. These structural motifs facilitate the hydrolysis of a D-ring by a serine residue in an enzyme catalytic core (Ser-His-Asp catalytic triad).^{12a,b} A mechanism of this hydrolysis was also proposed.^{12b} However, like in the case of natural strigolactones, the presence of the enol ether bond renders these analogues unstable.

On the other hand, it has been shown that also other strigolactone analogues, missing the enol ether bond, exert biological activities corresponding to those of the strigolactones. These analogues are called strigolactone mimics, and structurally, they have aryloxy-, aroyloxy-, phthalimide-, urethane-, or triazolidine-substituted D-rings.^{2a,b,7,11d,h,13a–f} The strigolactone mimics are more stable and often easily synthesized. Their strigolactone-related activity was explained by a modified hydrolysis mechanism.^{12b} In the case of aryloxy mimics called debranones, the enzymatic hydrolysis releasing the D-ring was confirmed using a fluorescent ABC part of the molecule.^{13b} Moreover, the mechanism of hydrolysis for debranones (4-bromodebranone) was proposed based on the AtD14 enzyme crystal structure with a covalently bound D-ring molecule to H247 and the ability of these compounds to effectively induce AtD14-D3 complex formation necessary for the activation of strigolactone signaling.¹⁴ The potential of strigolactone mimics in suicidal germination was confirmed

even in field trials on *Striga* spp., using the urethane strigolactone mimic T-010 (Figure 1E).^{13c} Furthermore, these compounds are also able to exert phytohormonal activity as shown in the case of the debranones.^{13a,d}

Debranones are the most well-studied strigolactone mimics, from which it is possible to demonstrate how small alterations to the core structure may cause substantial changes to biological activity. The first-generation debranones exhibited phytohormonal activity in a rice tillering assay when they inhibited tiller bud outgrowth in rice strigolactone-biosynthesis mutant *d10*.^{13a} In this assay, from 11 4-substituted aryloxy analogues, 4-bromodebranone (4BD, Figure 1F) was the most active and even surpassed GR24 in efficacy. On the other hand, these compounds were inactive in a *Striga hermonthica* assay.^{13a} As the second generation of debranones, monochlorodebranones were prepared with chloro substituents at different positions on the phenyl ring (2-, 3- and 4-).^{13d} Also, bicyclic debranones were prepared. In these debranones, the bioactivity shifted partly from a phytohormonal effect to a germination-inducing effect.^{13d,15} The most active compound in both assays was 2-chlorodebranone, thus showing the importance of the position of the substituent on the phenyl ring for the bioactivity of the final compound.^{13d} Recently, also third-generation debranone analogues were prepared in order to improve their activity in a seed germination assay using *Striga* spp.^{13e} Various disubstituted chlorodebranones were evaluated. From these, 2,5- and 2,6-dichlorodebranones showed the most potent activities in the *Striga* assay. Thus, another series of 2,5- and 2,6-disubstituted debranones was prepared by introducing stronger electron-withdrawing substituents (CN, NO₂) instead of a chlorine atom. The authors speculated that such debranones (those with electron-withdrawing substituents) would readily be hydrolyzed by D14 hydrolase, as the corresponding phenols with low pK_a would make better leaving groups. Indeed, the activity of some of these debranone derivatives in a *Striga* assay improved significantly (EC₅₀ ca. 10^{−6} M). On the other hand, their activity in a rice assay (inhibition of second tiller growth) diminished. The authors assigned this inactivity to possible hydrolysis of these compounds in the culture medium due to the longer assessment period used.^{13e}

While the previous study on debranones was quite extensive, it did not include any debranones with electron-donating

substituents for the comparison of biological activity, except for three compounds from the first generation. Therefore, it was decided to synthesize alkyl-substituted resorcinol-type strigolactone mimics in the present work, which contain one additional OH substituent (free or alkyl substituted) when compared to the debranone structure in order to see what effect this may have on biological activity. These resorcinol-type strigolactone mimics would be formed by phenols with a higher pK_a and thus theoretically may not be as active in a *Striga* assay as the debranones. On the other hand, it may be speculated that their additional OH substituent may have an influence on the accommodation of these mimics in the catalytic site of the corresponding enzymes through additional H-bonding and consequently may increase their biological activity in a *Striga* assay when compared to the debranones.

RESULTS AND DISCUSSION

Chemistry. A series of resorcinol-type strigolactone mimics were synthesized following a slightly modified published procedure from commercially available starting materials by the reaction with 5-bromo-3-methyl-2(5H)-furanone under basic conditions using *t*-BuOK.^{13a} Purification by silica gel column chromatography afforded the pure final compounds (Table 1). Also, another published procedure using K_2CO_3 and tetra-*n*-butylammonium bromide reagents and avoiding an inert atmosphere was employed successfully with comparable yields.^{11a}

Table 1. Synthesis of Resorcinol-Type Strigolactone Mimics

entry	reagent	product (yield) ^a	entry	reagent	product (yield) ^a
1		 1a (39%)	6		 1g (49%)
2		 1b (42%)	7		 1h (52%)
3		 1c (38%)	8		 1i (53%)
4		 1d (23%)	9		 1j (54%)
5		 1e (34%)			 1f (10%)

^aYield after column chromatography.

The stability of the synthesized resorcinol mimics was evaluated using HPLC/UV with compound **1g** as their representative. The stability was examined under pH 5 and 8. At both pH levels, the hydrolysis of the compound was rather slow. Complete hydrolysis of **1g** at pH 8 occurred after 7 days. At the same time, about half the compound was hydrolyzed at pH 5.

Phytohormonal Activity. The synthesized resorcinol mimics were evaluated for their phytohormonal activity on *Arabidopsis thaliana*. As phytohormones, strigolactones are known to modulate shoot and root architecture of model plants (*Arabidopsis*, *Oryza*, *Pisum*, etc.). In *Arabidopsis*, strigolactones regulate various stages of root development, starting from root hair elongation to primary root elongation.¹⁶ In the present case, the ability of strigolactone mimics to influence the total root length of *A. thaliana* plants was examined. The compounds were tested at four concentrations (0.1, 1, 10, and 100 μ M) with GR24 as a reference compound.

Most of the tested compounds did not display any statistically significant variation from the control. At the highest concentration (10^{-4} M), the toxicity of this high concentration for the plants was obvious. At the lower concentrations, ranging from 10^{-5} to 10^{-7} M, only two compounds, **1a** and **1g**, stimulated very slightly root elongation (Figure 2). The effect of these two compounds was more profound than the effect of GR24; however, it was much weaker than the effect of triazolidone strigolactone mimics published earlier.^{13h}

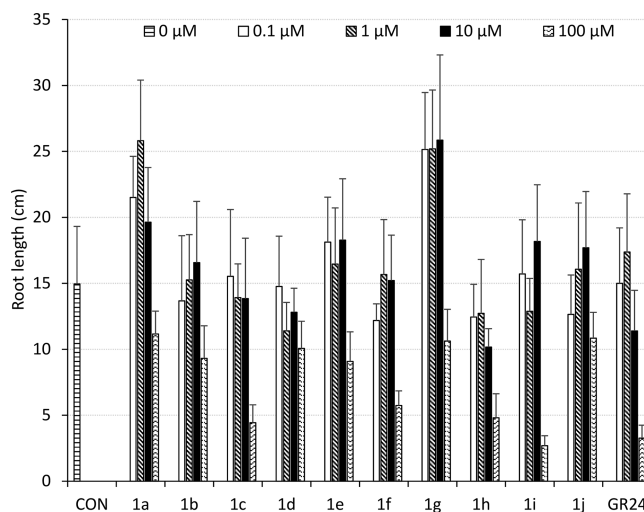


Figure 2. Root length of *A. thaliana* seedlings grown 7 days on nutrient medium in the presence of different strigolactone mimics. The error bars indicate the standard deviation of analyzed concentrations made in nine replicates.

Therefore, the eventuality that the second hydroxy group in resorcinol-type mimics would facilitate their accommodation within the AtD14 enzyme catalytic site was not confirmed. On the other hand, the results may have been slightly masked by the experimental conditions applied. The increase of primary root length in *Arabidopsis* was reported upon treatment with GR24 caused by the increase in cortical cells of the primary root meristem.¹⁷ However, it was reported that when media supplemented with sucrose were used (which was also the present case), a general high rate of primary root growth may obscure the specific root growth stimulating effect of GR24.¹⁷

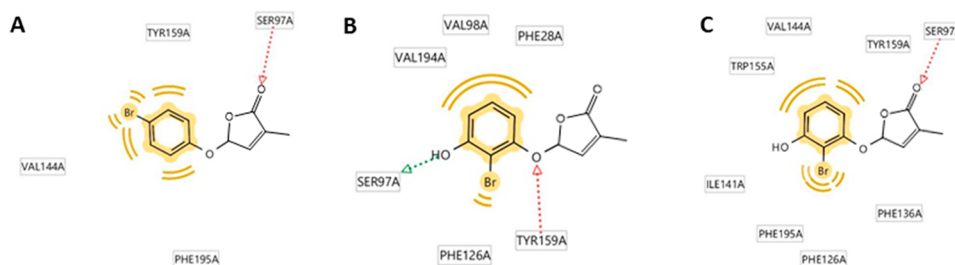


Figure 3. Interaction of the docked position of a ligand within the OsD14 catalytic site: (A) 4BD; (B) **1b**, position with the best scoring function; (C) **1b**, position with the right orientation for hydrolysis.

Table 2. EC₅₀ Values for Strigolactone Mimics Able to Stimulate Seed Germination of the Parasitic Plants *S. hermonthica* and *P. ramosa* (host: Bn = *B. napus*, Cs = *C. sativa*)

compound/EC ₅₀ (mol/L)	pK _a values ^a	CLogP	<i>Striga hermonthica</i>	<i>Phelipanche ramosa</i> (Bn)	<i>Phelipanche ramosa</i> (Cs)
1a	9.80	1.31	$>1.00 \times 10^{-5}$	1.27×10^{-7}	5.95×10^{-8}
1b		1.44	2.25×10^{-7}	1.16×10^{-8}	4.06×10^{-9}
1c		1.24	2.26×10^{-7}	2.52×10^{-8}	7.39×10^{-9}
1d	9.42	0.40	2.19×10^{-6}	1.30×10^{-8}	2.07×10^{-9}
1e	9.44	0.86	$>1.00 \times 10^{-5}$	7.39×10^{-8}	2.33×10^{-8}
1f	9.44	0.73	1.73×10^{-7}	7.19×10^{-9}	4.73×10^{-9}
1g	9.56	1.36	$>1.00 \times 10^{-5}$	1.51×10^{-7}	7.30×10^{-8}
1h	9.35	1.43	4.25×10^{-7}	4.83×10^{-9}	8.31×10^{-9}
1i		1.94	2.88×10^{-7}	4.90×10^{-9}	9.38×10^{-9}
1j	10.28	1.59	5.29×10^{-7}	1.97×10^{-8}	1.24×10^{-9}
GR24		0.61	1.30×10^{-10}	5.54×10^{-12}	6.09×10^{-11}

^aKnown pK_a values of the corresponding phenols are provided.

In spite of this possible masking, the results obtained suggest only negligible phytohormonal activity of these compounds. Still, the evaluation of phytohormonal activity in another assay, for example, in an *Arabidopsis* shoot branching assay, may be necessary to confirm the results.

Docking. The experimental results on *Arabidopsis* were found to be in accordance with the results obtained from in silico modeling. A simulation of the binding of the proposed structures to the catalytic site of OsD14 (PDB: 5DJS) was carried out. The OsD14 enzyme was chosen as an alternative to AtD14, as there is no crystal structure of AtD14 with a cocrystallized active compound. The compounds **1a–1k** and 4BD were docked into the OsD14 catalytic site using AutoDock Vina 4.2.6 software. According to the obtained scoring function values, compounds **1a–1k** may be expected to bind to the OsD14 receptor comparatively well to the 4BD molecule. However, for the successful hydrolysis of the ligand, it is necessary that the carbonyl group of the D-ring forms a polar contact with S97 in the catalytic site, as may be seen on the 4BD docking position (Figure 3A). Therefore, from the docked position of compound **1b** (Figure 3B) it may be concluded that the resorcinol-type strigolactone mimics interact with the catalytic site preferentially in a conformation unfavorable for their hydrolysis. It can be seen that the additional OH group on the phenyl ring forms the hydrogen bond with S97 preferentially to the carbonyl group, thus forestalling the hydrolysis (Figure 3B). The right orientation of **1b** is less favorable, and it does not provide polar interactions of the additional oxygen with any amino acid in the catalytic site (Figure 3C). Thus, these simulations did not confirm the assumption that the second oxygen in the strigolactone mimic molecule would provide better interaction with the amino acids in the catalytic site of the AtD14 enzyme. In addition,

despite the high similarity, the catalytic pockets of the two enzymes vary slightly in size (357 Å³ for AtD14 vs 432 Å³ for OsD14); thus the extra substituent in resorcinol mimics may further restrict its interaction within the smaller AtD14 pocket.

Seed Germination of Parasitic Plants *Striga hermonthica* and *Phelipanche ramosa*. The synthesized compounds were also evaluated for their ability to stimulate seed germination of the parasitic plants *S. hermonthica* and *P. ramosa*. In the case of *P. ramosa*, seeds from two different hosts (*Cannabis sativa* and *Brassica napus*) were employed. The seed germination was tested in the concentration range from 10^{−13} to 10^{−5} M with GR24 as a reference compound. The ability of resorcinol-type mimics to induce seed germination was determined as the half-maximal effective concentration (EC₅₀; Table 2). From the results, it was clear that in the case of *S. hermonthica* the two compounds showing slight phytohormonal activity in the *Arabidopsis* assay (**1a** and **1g**) were inactive in the terms of the stimulation of seed germination. On the other hand, all other compounds (except for **1e**) were able to induce seed germination of *S. hermonthica*, with varying potency. The lowest EC₅₀ concentrations were very similar for four compounds, namely, **1b**, **1c**, **1f**, and **1i**, with EC₅₀ values around 2 × 10^{−7} M. Almost the same EC₅₀ values were obtained for the two compounds with a weak electron-withdrawing substituent at position C-2 on the phenyl ring (Br, **1b**; Cl, **1c**). A slightly higher EC₅₀ value was recorded for the resorcinol mimic **1i** derived from 3-methoxy-5-methylphenol. The best activity was observed for the disubstituted resorcinol mimic **1f**. Structurally very alike to compound **1i**, were compounds **1h** and **1j**, which exerted only slightly less potent activity for *S. hermonthica* (EC₅₀ ≈ 5 × 10^{−7} M). In the case of *P. ramosa*, all compounds were able to induce seed germination at even lower concentrations. There

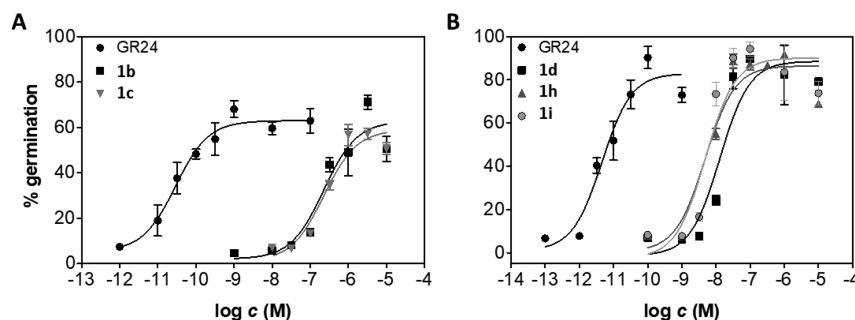


Figure 4. Stimulation of seed germination caused by strigolactone mimics in comparison with GR24 on (A) *S. hermonthica* (compounds 1b and 1c) and (B) *P. ramosa* (host *Brassica napus*, compounds 1d, 1h, and 1i).

were differences in their activity between the *P. ramosa* seeds from a different host. Thus, generally, compounds were about 1 order of magnitude more active for *P. ramosa* from a *C. sativa* host where seven out of 11 compounds reached a nanomolar EC_{50} value. The most active were compounds 1f, 1h, and 1i, which exhibited EC_{50} values at the nanomolar level for *P. ramosa* from both hosts.

The synthesized compounds were able to induce germination of parasitic plant seeds to the same extent as GR24 (ca. 65% for *S. hermonthica*, Figure 4A, and ca. 90% for *P. ramosa*, Figure 4B).

The resorcinol-type mimics exerted potent activities in inducing seed germination of both *S. hermonthica* and *P. ramosa*. Even though their general activity was still about 2 to 3 orders of magnitude weaker than that of GR24, these values are still of significance. In the case of the debranones, only one compound with strong electron-withdrawing substituents was able to induce *S. hermonthica* seed germination at 10^{-7} M,^{13e} whereas six of the resorcinol-type mimics stimulated *S. hermonthica* seed germination at this level. However, it must be pointed out that the EC_{50} values could not be compared precisely, as they were not determined for the debranone compounds. Thus, the approximate EC_{50} values of the debranones were estimated from published graphics.^{13a,d,e}

As reported, the biological activity of the debranones shifted from a phytohormonal effect to parasitic seed germination-inducing activity by the introduction of strong electron-withdrawing substituents to the phenyl ring.^{13a,d,e} The rationale of this shift may be attributed to the higher hydrolysis rate of the debranones to the corresponding phenols (with low pK_a) and the D-ring, causing inactivity in the phytohormonal assay due to the longer assessment period.^{13e} However pragmatic this explanation may be, the results of this study show that also other factors may play an important role in the biological activity of strigolactone mimics. The resorcinol-type strigolactone mimics synthesized herein were formed from phenols of much higher pK_a values (around 9) than those of the debranones, and yet they exhibited potent activities in the seed germination assays using parasitic plants. Moreover, the potential influence of polarity and membrane permeability on the activity was evaluated by the comparison of the partition coefficient (CLogP) of the resorcinol-type mimics and GR24 (Table 2) and 4BD (2.35) and of the eight most active debranone molecules with electron-withdrawing substituents (1.11–2.81). However, this comparison did not reveal any pattern suggesting that polarity and membrane permeability play any role in the germination-inducing ability of these molecules. Therefore, it may be suggested that the substitution pattern on the phenyl ring may in some cases be more

important than the electronic properties of individual substituents.

In the case of parasitic plants, the enzymes for strigolactone recognition in *Striga* spp. were identified recently. These enzymes include 11 α/β -hydrolases (ShHTL1–11) encoded by the HYPOSENSITIVE TO LIGHT/KARRIKIN INSENSITIVE2 (HTL/KAI2) gene. These proteins are homologues of the KAI2 enzyme in *Arabidopsis*. For ShHTL5 it has been shown that its catalytic site is about twice the size of the KAI2 catalytic site (998 vs 403 Å³) and that about half of the amino acid residues in the enzyme catalytic site are different. Particularly, the changes in amino acid residues at positions 124 and 196 deepened the catalytic pocket of ShHTL5 to better accommodate the D-ring of strigolactones.¹⁸ Therefore, the excellent activity of resorcinol-type mimics in the seed germination assay may be due to better accommodation of their structure in the ShHTL enzyme catalytic site than in the much smaller OsD14 or AtD14 catalytic pockets. Also, it may be possible that, in contrast to AtD14, the additional hydroxy group in resorcinol-type mimics would indeed play a role in their accommodation within the catalytic site of the ShHTL enzyme and thus facilitate their hydrolysis, potentially through an extra H-bond interaction with amino acids in the close vicinity.

Hydrolytic Stability. The stability of strigolactone analogues may be another key factor in determining their success rate as potential suicidal germinators. Even though there are possibilities to enhance the stability of these compounds in the soil, for example, by their formulation as emulsions,^{2a} there are several factors with potential high impact on their hydrolysis rate, especially the pH of the soil, its humidity, or the presence of microorganisms. The stability of the resorcinol-type mimics synthesized herein was excellent at either pH 5 or 8, with it taking 7 days for the compounds to be completely hydrolyzed at alkaline pH. Under acidic pH, the hydrolysis was even slower (not completed after 12 days). These results indicate that the compounds will completely decompose in the soil, thus avoiding their accumulation and possible negative effect on the environment. Accordingly, the resorcinol mimics described herein are therefore suitable to be further studied as suicidal germinators.

EXPERIMENTAL SECTION

General Experimental Procedures. All reactions requiring anhydrous or inert conditions were carried out under a positive atmosphere of argon in oven-dried glassware. Solutions or liquids were introduced in round-bottomed flasks using oven-dried syringes through rubber septa. All reactions were stirred magnetically using Teflon-coated stirring bars. If needed, reactions were warmed using an

electrically heated silicon oil bath, and the stated temperature corresponds to the temperature of the bath. Organic solutions obtained after aqueous workup were dried over MgSO_4 . The removal of solvents was accomplished using a rotary evaporator at water aspirator pressure. GR24 represents *rac*-GR24, which was purchased from Stichting Chemiefonds Paddepoel, Malden, The Netherlands. Chemicals for the syntheses were purchased from Sigma-Aldrich (Prague, Czech Republic). Solvents for extractions and chromatography were of technical grade and purchased from Penta Chemicals s.r.o. (Prague, Czech Republic) or from VWR (Stribrna Skalice, Czech Republic). Solvents used in the reactions were distilled from appropriate drying agents and stored under argon over activated Linde 4 Å molecular sieves. Column and flash chromatography was carried out using Merck silica gel (60–200 μm). Analytical TLC was performed with Merck silica gel 60 F254 plates. Visualization was accomplished by UV light (254 nm) and staining with a vanillin solution, followed by heating. ^1H , ^{13}C , and 2D (^1H -COSY, HMQC) NMR spectra were recorded on a Bruker Avance III HD 400 MHz spectrometer equipped with a Prodigy cryo-probe. TMS (0 ppm, ^1H NMR), CDCl_3 (77 ppm, ^{13}C NMR), and CD_3OD (49 ppm, ^{13}C NMR) were used as internal references. The chemical shifts (δ) are reported in ppm, and the coupling constants are recorded in Hz. The hydrogen and carbon assignments were done according to ^1H - ^1H COSY and ^1H - ^{13}C HMQC experiments. Mass spectra were recorded on an LTQ Orbitrap XL spectrometer. The stability of the compounds was evaluated using a Delta Chrom Q-Grad/Lab Alliance Thermo Finnigan UV6000LP-HPLC/UV system.

Plant Material. Seeds of *Arabidopsis thaliana* var. Col-0 (Columbia) were purchased from NASC (The European *Arabidopsis* Stock Centre, NASC ID: N1092 and N9565, Col-0). Seeds were washed in 70% (v/v) EtOH for 10 min, then surface sterilized in 10% (v/v) NaOCl for 15 min, and soaked in sterile water three times for 10 min.

Seeds of parasitic plants were collected at different sites: *Striga hermonthica* (Sudan, 2007), *Phelipanche ramosa* (Poitou-Charentes, France, host *Cannabis sativa*, 2012), and *Phelipanche ramosa* (St. Jean d'Angely, France, host *Brassica napus*, 2015). Seeds were surface sterilized in 2% (v/v) NaOCl and 1% Triton X 100 (v/v) for 6 min, then washed with 200 mL of Milli-Q water. Seeds were incubated in 1 mM HEPES buffer (pH 7.5) with 0.1% PPM (Plant Preservative Mixture) for 4 days at 27 °C (*S. hermonthica*) or 7 days at 21 °C (*P. ramosa*).

5-Bromo-3-methyl-2(5H)-furanone. 5-Bromo-3-methyl-2(5H)-furanone was synthesized according to a reported procedure.¹⁹ To a solution of 3-methyl-2(5H)-furanone (90% technical grade, 339 mg, 3.11 mmol) in CCl_4 (4 mL) were added *N*-bromosuccinimide (NBS, 677 mg, 3.80 mmol) and a catalytic amount of benzoyl peroxide (167 mg, 0.69 mmol) as a radical initiator. The reaction mixture was heated under reflux at 78 °C for 1.5 h, cooled to 0 °C, and filtered, and the solvent evaporated. The 5-bromo-3-methyl-2(5H)-furanone produced was used directly in the next step.

General Synthetic Procedures for Resorcinol-Type Mimics (1a–1j). Dihydroxybenzene (2.86 mmol) was dissolved in dry THF (15 mL), and the solution was cooled to 0 °C. Then, potassium *tert*-butoxide (2.86 mmol, 579 mg) was added to the solution, and the reaction mixture was stirred for 15 min. Next, a solution of 5-bromo-3-methyl-2(5H)-furanone (3.14 mmol, 556 mg) in 5 mL of dry THF was added to the reaction mixture, which was then stirred overnight. The reaction mixture was filtered through Celite, and the filtrate was evaporated. The residue was purified by column chromatography. Also, another published procedure avoiding an inert atmosphere was applied successfully with comparable yields.^{11a}

5-(3-Hydroxy-2-methylphenoxy)-3-methylfuran-2(5H)-one (1a). For the reaction, 641 mg of 2,6-dihydroxytoluene was used. Column chromatography in petroleum ether/ethyl acetate (8/2, v/v) afforded a pure product, **1a**, in 39% yield (488 mg): ^1H NMR (CDCl_3 , 400 MHz) δ 7.05 (1H, dt, J = 0.5, 8.2 Hz, Ar), 7.00 (1H, quin., J = 1.6 Hz, H-4), 6.82 (1H, d, J = 8.3 Hz, Ar), 6.58 (1H, dd, J = 0.4, 8.1 Hz, Ar), 6.27 (1H, quin., J = 1.4 Hz, H-5), 4.94 (1H, s, OH), 2.13 (3H, s, CH_3), 2.02 (3H, t, J = 1.6 Hz, CH_3); ^{13}C NMR (CDCl_3 , 100 MHz) δ

171.5 (CO), 155.7 (C, Ar), 154.7 (C, Ar), 142.4 (CH, C-4), 134.4 (CH, C-3), 126.8 (CH, Ar), 114.1 (C, Ar), 110.6 (CH, Ar), 108.1 (CH, Ar), 99.6 (CH, C-5), 10.6 (CH_3), 8.4 (CH_3 , Ar); HRMS m/z 221.08086 [$\text{M} + \text{H}$]⁺ (calcd for $\text{C}_{12}\text{H}_{14}\text{O}_4$, 221.08084).

5-(2-Bromo-3-hydroxyphenoxy)-3-methylfuran-2(5H)-one (1b). For the reaction, 976 mg of 2-bromo-1,3-dihydroxybenzene was used. Column chromatography in petroleum ether/ethyl acetate (9/1–3/1, v/v) afforded a pure product, **1b**, in 42% yield (679 mg): ^1H NMR (CDCl_3 , 400 MHz) δ 7.21 (1H, t, J = 8.2 Hz, Ar), 7.05 (1H, quin., J = 1.6 Hz, H-4), 6.90 (1H, dd, J = 1.3, 8.2 Hz, Ar), 6.82 (1H, dd, J = 1.3, 8.2 Hz, Ar), 6.27 (1H, quin., J = 1.4 Hz, H-5), 5.70 (1H, s, OH), 2.03 (3H, t, J = 1.5 Hz, CH_3); ^{13}C NMR (CDCl_3 , 100 MHz) δ 171.1 (CO), 153.6 (C, Ar), 153.6 (C, Ar), 141.9 (CH, C-4), 134.8 (CH, C-3), 129.0 (CH, Ar), 111.4 (CH, Ar), 109.2 (CH, Ar), 101.7 (C, Ar), 99.5 (CH, C-5), 10.7 (CH_3); HRMS m/z 284.97582 [$\text{M} + \text{H}$]⁺ (calcd for $\text{C}_{11}\text{H}_{10}\text{O}_4\text{Br}$, 284.97570).

5-(2-Chloro-3-hydroxyphenoxy)-3-methylfuran-2(5H)-one (1c). For the reaction, 746 mg of 2-chloro-1,3-dihydroxybenzene was used. Column chromatography in petroleum ether/ethyl acetate (9/1–8/2, v/v) afforded a pure product, **1c**, in 38% yield (518 mg): ^1H NMR (CDCl_3 , 400 MHz) δ 7.16 (1H, t, J = 8.3 Hz, Ar), 7.05 (1H, quin., J = 1.6 Hz, H-4), 6.92 (1H, dd, J = 1.4, 8.4 Hz, Ar), 6.82 (1H, dd, J = 1.4, 8.3 Hz, Ar), 6.27 (1H, quin., J = 1.4, H-5), 5.68 (1H, s, OH), 2.03 (3H, t, J = 1.6 Hz, CH_3); ^{13}C NMR (CDCl_3 , 100 MHz) δ 171.0 (CO), 152.7 (C, Ar), 152.5 (C, Ar), 141.9 (CH, C-4), 134.9 (CH, C-3), 128.0 (CH, Ar), 111.5 (CH, Ar), 110.4 (C, Ar), 109.4 (CH, Ar), 99.4 (CH, C-5), 10.7 (CH_3); HRMS m/z 263.00819 [$\text{M} + \text{Na}$]⁺ (calcd for $\text{C}_{11}\text{H}_9\text{O}_4\text{ClNa}$, 263.00816).

5-(2-Hydroxy-3-methoxyphenoxy)-3-methylfuran-2(5H)-one (1d). For the reaction, 704 mg of 1,2-dihydroxy-3-methoxybenzene was used. Column chromatography in petroleum ether/ethyl acetate (8/2–3/1, v/v) afforded a pure product, **1d**, in 23% yield (308 mg): ^1H NMR (CDCl_3 , 400 MHz) δ 7.10 (1H, quin., J = 1.6 Hz, H-4), 7.01 (1H, t, J = 8.3 Hz, Ar), 6.63 (1H, dd, J = 1.4, 8.3 Hz, Ar), 6.49 (1H, dd, J = 1.4, 8.3 Hz, Ar), 6.23 (1H, quin., J = 1.4 Hz, H-5), 5.79 (1H, s, OH), 3.87 (3H, s, CH_3O), 1.99 (3H, t, J = 1.5 Hz, CH_3); ^{13}C NMR (CDCl_3 , 100 MHz) δ 170.9 (CO), 151.9 (C, Ar), 150.0 (C, Ar), 142.6 (CH, C-4), 134.3 (CH, C-3), 132.1 (C, Ar), 126.0 (CH, Ar), 109.2 (CH, Ar), 103.7 (CH, Ar), 102.8 (CH, C-5), 56.0 (CH_3O), 10.6 (CH_3); HRMS m/z 259.05760 [$\text{M} + \text{Na}$]⁺ (calcd for $\text{C}_{12}\text{H}_{12}\text{O}_5\text{Na}$, 259.05769).

5-(3-Hydroxyphenoxy)-3-methylfuran-2(5H)-one (1e). For the reaction, 625 mg of 1,3-dihydroxybenzene was used. Column chromatography in petroleum ether/ethyl acetate (8/2, v/v) afforded two pure products, **1e**, in 34% yield (398 mg), and 5,5'-(1,3-phenylenbis(oxy))bis(3-methylfuran-2(5H)-one), **1f**, in 10% yield (171 mg). **1e**: ^1H NMR (CD_3OD , 400 MHz) δ 7.14–7.10 (2H, m, H-4, Ar), 6.59 (1H, ddd, J = 0.9, 2.3, 8.2 Hz, Ar), 6.56 (1H, t, J = 2.3 Hz, Ar), 6.53 (1H, ddd, J = 0.9, 2.3, 8.1 Hz, Ar), 6.41 (1H, quin., J = 1.4 Hz, H-5), 1.95 (3H, t, J = 1.5 Hz, CH_3); ^{13}C NMR (CD_3OD , 100 MHz) δ 173.4 (CO), 159.9 (C, Ar), 159.1 (C, Ar), 144.8 (CH, C-4), 144.8 (C, Ar), 134.8 (CH, C-3), 131.8 (CH, Ar), 111.5 (CH, Ar), 108.7 (CH, Ar), 105.3 (CH, Ar), 100.7 (CH, C-5), 10.4 (CH_3); HRMS m/z 229.04712 [$\text{M} + \text{Na}$]⁺ (calcd for $\text{C}_{11}\text{H}_{10}\text{O}_4\text{Na}$, 229.04713). **1f**: ^1H NMR (CDCl_3 , 400 MHz) δ 7.31–7.26 (1H, m, Ar), 6.99 (2H, quin., J = 1.4 Hz, H-4a, H-4b), 6.92–6.87 (3H, m, Ar), 6.31 (1H, quin., J = 1.4 Hz, H-5a), 6.28 (1H, quin., J = 1.4 Hz, H-5b), 2.02 (3H, d, J = 1.4 Hz, CH_3a), 2.01 (3H, d, J = 1.4 Hz, CH_3b); ^{13}C NMR (CDCl_3 , 100 MHz) δ 171.2 (CO), 171.2 (CO), 157.3 (2 \times C, Ar), 157.2 (2 \times C, Ar), 142.2 (CH, C-4a), 142.2 (CH, C-4b), 134.3 (CH, C-3a), 134.3 (CH, C-3b), 130.4 (CH, Ar), 130.4 (CH, Ar), 111.7 (CH, Ar), 111.5 (CH, Ar), 106.1 (CH, Ar), 106.0 (CH, Ar), 98.8 (CH, C-5a), 98.7 (CH, C-5b), 10.5 (2 \times CH_3); HRMS m/z 325.06827 [$\text{M} + \text{Na}$]⁺ (calcd for $\text{C}_{16}\text{H}_{14}\text{O}_6\text{Na}$, 325.06826).

5-(3-Hydroxy-5-methylphenoxy)-3-methylfuran-2(5H)-one (1g). For the reaction, 641 mg of 3,5-dihydroxytoluene (orcinol) was used. Column chromatography in petroleum ether/ethyl acetate (9/1–8/2, v/v) afforded a pure product, **1g**, in 49% yield (613 mg): ^1H NMR (CDCl_3 , 400 MHz) δ 6.96 (1H, quin., J = 1.6 Hz, H-4), 6.54 (1H, brs, Ar), 6.45 (1H, t, J = 2.1 Hz, Ar), 6.41 (1H, brs, Ar), 6.26 (1H, quin., J

= 1.4 Hz, H-5), 6.22 (1H, t, J = 2.2 Hz, Ar), 4.97 (1H, s, OH), 2.28 (3H, d, J = 0.3 Hz, CH₃), 2.01 (3H, t, J = 1.5 Hz, CH₃); ¹³C NMR (CDCl₃, 100 MHz) δ 171.5 (CO), 157.4 (C, Ar), 156.5 (C, Ar), 142.3 (CH, C-4), 141.1 (C, Ar), 134.4 (CH, C-3), 111.5 (CH, Ar), 109.9 (CH, Ar), 101.7 (CH, Ar), 99.1 (CH, C-5), 21.5 (CH₃, Ar), 10.6 (CH₃); HRMS m/z 221.08080 [M + H]⁺ (calcd for C₁₂H₁₃O₄, 221.08084).

5-(3,5-Dimethoxyphenoxy)-3-methylfuran-2(5H)-one (1h). For the reaction, 796 mg of 3,5-dimethoxyphenol was used. Column chromatography in petroleum ether/ethyl acetate (9/1–8/2, v/v) afforded a pure product, 1h, in 52% yield (738 mg): ¹H NMR (CDCl₃, 400 MHz) δ 6.96 (1H, quin., J = 1.6 Hz, H-4), 6.31 (2H, d, J = 2.2 Hz, Ar), 6.28 (1H, quin., J = 1.4 Hz, H-5), 6.22 (1H, t, J = 2.2 Hz, Ar), 3.78 (6H, s, CH₃O), 2.03 (3H, t, J = 1.5 Hz, CH₃); ¹³C NMR (CDCl₃, 100 MHz) δ 171.3 (CO), 161.5 (C, Ar), 161.5 (C, Ar), 158.2 (C, Ar), 142.2 (CH, C-4), 134.5 (CH, C-3), 98.9 (CH, C-5), 95.8 (CH, Ar), 95.6 (2 × CH, Ar), 55.5 (2 × CH₃O, Ar), 10.6 (CH₃); HRMS m/z 273.07335 [M + H]⁺ (calcd for C₁₃H₁₄O₅Na, 273.07334).

5-(3-Methoxy-5-methylphenoxy)-3-methylfuran-2(5H)-one (1i). For the reaction, 713 mg of 3-methoxy-5-methylphenol was used. Column chromatography in petroleum ether/ethyl acetate (9/1–8/2, v/v) afforded a pure product, 1i, in 53% yield (704 mg): ¹H NMR (CDCl₃, 400 MHz) δ 6.96 (1H, quin., J = 1.6 Hz, H-4), 6.57 (1H, br.d, J = 0.4 Hz, Ar), 6.49–6.47 (2H, m, Ar), 6.27 (1H, quin., J = 1.4 Hz, H-5), 3.78 (3H, s, CH₃O), 2.31 (3H, d, J = 0.5 Hz, CH₃), 2.01 (3H, t, J = 1.6 Hz, CH₃); ¹³C NMR (CDCl₃, 100 MHz) δ 171.4 (CO), 160.6 (C, Ar), 157.4 (C, Ar), 142.3 (CH, C-4), 140.7 (C, Ar), 134.4 (CH, C-3), 110.2 (CH, Ar), 109.6 (CH, Ar), 100.3 (CH, Ar), 99.1 (CH, C-5), 55.3 (CH₃O, Ar), 21.7 (CH₃, Ar), 10.6 (CH₃); HRMS m/z 235.09642 [M + H]⁺ (calcd for C₁₃H₁₅O₄, 235.09649).

5-(2-Methoxy-4-methylphenoxy)-3-methylfuran-2(5H)-one (1j). For the reaction, 713 mg of 2-methoxy-4-methylphenol was used. Column chromatography in petroleum ether/ethyl acetate (9/1–8/2, v/v) afforded a pure product, 1j, in 54% yield (718 mg): ¹H NMR (CDCl₃, 400 MHz) 7.10 (1H, d, J = 8.0 Hz, Ar), 7.04 (1H, quin., J = 1.6 Hz, H-4), 6.74 (1H, s, Ar), 6.71 (1H, d, J = 8.1 Hz, Ar), 6.23 (1H, quin., J = 1.4 Hz, H-5), 3.86 (3H, s, CH₃O), 2.32 (3H, s, CH₃), 1.97 (3H, t, J = 1.5 Hz, CH₃); ¹³C NMR (CDCl₃, 100 MHz) δ 171.6 (CO), 149.9 (C, Ar), 142.9 (C, Ar), 142.6 (CH, C-4), 134.8 (CH, C-3), 134.4 (C, Ar), 121.2 (CH, Ar), 119.5 (CH, Ar), 113.1 (CH, Ar), 100.5 (CH, C-5), 55.8 (CH₃O, Ar), 21.23 (CH₃, Ar), 10.6 (CH₃); HRMS m/z 257.08745 [M + Na]⁺ (calcd for C₁₃H₁₄O₄Na, 257.07843).

Stability Testing. A 100 mM stock solution of compound 1g in methanol was prepared. Then, both phosphate-citrate buffer of pH 5 and Sørensen phosphate buffer of pH 8 were prepared. In a vial, 10 μ L of a stock solution was dissolved in 990 μ L of buffer, and the vial was kept at 25 °C. The stability of the compound was measured by HPLC/UV after 60, 160, and 270 min and 1, 2, 3, 5, 6, 7, 8, and 12 days.

Docking Experiments. The in silico docking experiments were performed using AutoDock Vina 4.2.6 on the OsD14 protein (PDB: 5DJ5) with cocrystallized GR24.²⁰ The protein and the compounds for the docking were adjusted using The PyMOL Molecular Graphics System, Version 4.4.0, Schrödinger, LLC (DeLano, W.L., www.pymol.com), and the results were processed with the LigandScout 4.2 program.²¹ The position of GR24 was set as the center of the grid box (coordinates: x = −30.80, y = 14.65, z = −21.05). The grid box was defined as a 20 × 20 × 20 Å cube. The redocking was performed with the original ligand, GR24, to evaluate the suitability of the crystal structure and the docking workflow. The results showed that GR24 docks into the catalytic pocket with the same orientation as the cocrystallized GR24.

CLogP Estimation. The CLogP numbers were obtained using ChemDraw Professional 16.0 software and compared to CLogP numbers obtained with the Bio-Loom program from BioByte Corp., Claremont, CA, USA. Both programs provided the same results.

Biological Activity Assays. *Arabidopsis* Assay. Seeds of *A. thaliana* (Col-0) were germinated on hormone-free Murashige and

Skoog (MS) medium, supplied with sucrose, at 25 °C, with a 16 h photoperiod (irradiance of 115 μ mol m^{−2} s^{−1}). After emergence of the first pair of leaves (approximately 7 days) the seedlings were used for the test. Nine seedlings of *A. thaliana* were placed in three plastic dishes (three seedlings per dish) of 10 × 10 cm dimension with 40 mL of hormone-free MS medium, supplemented with agar and sucrose, with 100 μ L of tested strigolactone mimics in solutions at concentrations of 1, 10, and 100 μ M. Each treatment had three replicates. The exposure took 7 days under a 16 h photoperiod (irradiance of 115 μ mol m^{−2} s^{−1}) at 25 °C with vertical positioning of dishes. The roots of each plant were then scanned on an Epson Perfection V700 photo scanner. The root images were processed by the software WinRHIZO (Regent Instruments, Inc., Ville de Quebec, Canada), which calculated the total root length. The differences among treatments were tested by one-way ANOVA with the Fisher LSD post hoc test. A significance level of p = 0.05 was used for both analyses. Each strigolactone treatment (each concentration) was represented by nine biological replicates. Statistica 7 (StatSoft, Tulsa, OK, USA) software was used for all the computations.

Parasitic Plants. The assay was carried out by a slightly modified published procedure.²² Thus, 50 μ L of incubated seeds was transferred into each well of a 96-well plate. Seed germination was induced by the addition of 10 μ L of each test compound in a concentration range from 10^{−13} to 10^{−5} M, and the volume in each well was adjusted to 100 μ L using sterilized water. As a negative control, a 0.1% solution of acetone was used. Seed germination was carried out in the dark for 4 days in an incubator at either 27 °C (*S. hermonthica*) or 21 °C (*P. ramosa*). Then, 10 μ L of MTT (3-[4,5-dimethylthiazol-2-yl]-2,5-diphenyltetrazolium bromide) of 5 g/L concentration was added to each well. After 24 h, a lysis solution was added (10% Triton X-100 and 0.04% HCl in isopropanol) to dissolve the formed formazan. After the next 24 h, the difference in absorbance between 570 and 690 nm was measured for each well. Data were evaluated by nonlinear regression using the GraphPad Prism 5.0 program, and EC₅₀ values were determined. The test was carried out twice for each compound.

■ ASSOCIATED CONTENT

● Supporting Information

The Supporting Information is available free of charge on the ACS Publications website at DOI: [10.1021/acs.jnatprod.8b00160](https://doi.org/10.1021/acs.jnatprod.8b00160).

¹H and ¹³C NMR spectroscopic data for compounds 1a–j (PDF)

■ AUTHOR INFORMATION

Corresponding Author

*Tel: +420225106832. Fax: +420225106832. E-mail: vanek@ueb.cas.cz.

ORCID

Marcela Dvorakova: [0000-0002-6664-6870](https://orcid.org/0000-0002-6664-6870)

Petr Soudek: [0000-0002-5298-5978](https://orcid.org/0000-0002-5298-5978)

Katarzyna Retzer: [0000-0001-6074-7999](https://orcid.org/0000-0001-6074-7999)

Lukas Spichal: [0000-0001-6483-8628](https://orcid.org/0000-0001-6483-8628)

Notes

The authors declare no competing financial interest.

■ ACKNOWLEDGMENTS

The authors gratefully acknowledge financial support from grant DP072017 from Gama Project from Technology Agency of the Czech Republic and from grants LD14127 from INTER-COST program, LO1204 from the National Program of Sustainability I, and CZ.02.1.01/0.0/0.0/16_019/0000738 from European Regional Development Fund-Project “Centre for Experimental Plant Biology”, all from the Ministry of

Education, Youth and Sports of the Czech Republic. A.H. was supported by the Internal Grant Agency of Palacký University (IGA_PrF_2018_023). The authors also would like to express their thanks to Prof. P. Delavault (Laboratory of Plant Biology and Pathology, University of Nantes, France), who kindly donated the *P. ramosa* seeds, and to Prof. B. Zwanenburg (Department of Organic Chemistry, Institute for Molecules and Materials, Radboud Universiteit, Nijmegen, The Netherlands) for the donation of *S. hermonthica* seeds.

REFERENCES

- (1) (a) Musselman, L. J. *Annu. Rev. Phytopathol.* **1980**, *18*, 463–489. (b) Parker, C. *Crop Prot.* **1991**, *10*, 6–22. (c) Parker, C. *Pest Manage. Sci.* **2009**, *65*, 453–459. (d) Parker, C. *Weed Sci.* **2012**, *60*, 269–276.
- (2) (a) Zwanenburg, B.; Mwakaboko, A. S.; Kannan, C. *Pest Manage. Sci.* **2016**, *72*, 2016–2025. (b) Cala, A.; Ghooray, K.; Fernández-Aparicio, M.; Molinillo, J. M. G.; Galindo, J. C. G.; Rubiales, D.; Macías, F. A. *Pest Manage. Sci.* **2016**, *72*, 2069–2081.
- (3) Rodenburg, J.; Demont, M.; Zwart, S. J.; Bastiaans, L. *Agric. Ecosyst. Environ.* **2016**, *235*, 306–317.
- (4) Ejeta, G. In *Integrating New Technologies for Striga Control, Towards Ending the Witch-Hunt*; Ejeta, G.; Gressel, J., Eds.; World Scientific Publishing Co.: Hackensack, NJ, 2007; pp 3–16.
- (5) Cook, C. E.; Whichard, L. P.; Turner, B.; Wall, M. E.; Egle, G. H. *Science* **1966**, *154*, 1189–1190.
- (6) (a) Kim, H. I.; Kisugi, T.; Khetkam, P.; Xie, X.; Yoneyama, K.; Uchida, K.; Yokota, T.; Nomura, T.; McErlean, C. S. P.; Yoneyama, K. *Phytochemistry* **2014**, *103*, 85–88. (b) Ueno, K.; Furumoto, T.; Umeda, S.; Mizutani, M.; Takikawa, H.; Batchvarova, R.; Sugimoto, Y. *Phytochemistry* **2014**, *108*, 122–128. (c) Dvorakova, M.; Vanek, T. *Chem. Listy* **2015**, *109*, 762–769.
- (7) Boyer, F. D.; de Saint Germain, A.; Pillot, J.-P.; Pouvreau, J.-B.; Chen, V. X.; Ramos, S.; Stevenin, A.; Simier, P.; Delavault, P.; Beau, J.-M.; Rameau, C. *Plant Physiol.* **2012**, *159*, 1524–1544.
- (8) Tasker, A. V.; Westwood, J. H. *Weed Sci.* **2012**, *60*, 267–268.
- (9) Johnson, A. W.; Rosebery, G.; Parker, C. *Weed Res.* **1976**, *16*, 223–227.
- (10) (a) Babiker, A. G. T.; Hamdoun, A. M. *Weed Res.* **1982**, *22*, 111–115. (b) Babiker, A. G. T.; Hamdoun, A. M.; Rudwan, A.; Mansi, N. G.; Faki, H. H. *Weed Res.* **1987**, *27*, 173–178.
- (11) (a) Mangnus, E. M.; Zwanenburg, B. *J. Agric. Food Chem.* **1992**, *40*, 1066–1070. (b) Mangnus, E. M.; van Vliet, L. A.; Vandenput, D. A. L.; Zwanenburg, B. *J. Agric. Food Chem.* **1992**, *40*, 1222–1229. (c) Nefkens, G. H. L.; Thuring, J. W. J. F.; Beenakkers, M. F. M.; Zwanenburg, B. *J. Agric. Food Chem.* **1997**, *45*, 2273–2277. (d) Kondo, Y.; Tadokoro, E.; Matsuura, M.; Iwasaki, K.; Sugimoto, Y.; Miyake, H.; Takikawa, H.; Sasaki, M. *Biosci., Biotechnol., Biochem.* **2007**, *71*, 2781–2786. (e) Zwanenburg, B.; Mwakaboko, A. S.; Reizelman, A.; Anilkumar, G.; Sethumadhavan, D. *Pest Manage. Sci.* **2009**, *65*, 478–491. (f) Mwakaboko, A. S.; Zwanenburg, B. *Plant Cell Physiol.* **2011**, *52*, 699–715. (g) Mwakaboko, A. S.; Zwanenburg, B. *Bioorg. Med. Chem.* **2011**, *19*, 5006–5011. (h) Zwanenburg, B.; Mwakaboko, A. S. *Bioorg. Med. Chem.* **2011**, *19*, 7394–7400. (i) Kgosi, R. L.; Zwanenburg, B.; Mwakaboko, A. S.; Murdoch, A. J. *Weed Res.* **2012**, *52*, 197–203. (j) Boyer, F. D.; de Saint Germain, A.; Pouvreau, J.-B.; Clavé, G.; Pillot, J.-P.; Roux, A.; Rasmussen, A.; Depuydt, S.; Laressergues, D.; Frei Dit Frey, N.; Heugebaert, T. S. A.; Stevens, C. V.; Geelen, D.; Goormachtig, S.; Rameau, C. *Mol. Plant* **2014**, *7*, 675–690. (k) Screpanti, C.; Fonné-Pfister, R.; Lumbroso, A.; Rendine, S.; Lachia, M.; de Mesmaeke, A. *Bioorg. Med. Chem. Lett.* **2016**, *26*, 2392–2400.
- (12) (a) Hamiaux, C.; Drummond, R. S.; Janssen, B. J.; Ledger, S. E.; Cooney, J. M.; Newcomb, R. D.; Snowden, K. C. *Curr. Biol.* **2012**, *22*, 2032–2036. (b) Zwanenburg, B.; Pospisil, T.; Zeljovic, S. C. *Planta* **2016**, *243*, 1311–1326.
- (13) (a) Fukui, K.; Ito, S.; Ueno, K.; Yamaguchi, S.; Kyojuka, J.; Asami, T. *Bioorg. Med. Chem. Lett.* **2011**, *21*, 4905–4908. (b) Tsuchiya, Y.; Yoshimura, M.; Sato, Y.; Kuwata, K.; Toh, S.; Holbrook-Smith, D.; Zhang, H.; McCourt, P.; Itami, K.; Kinoshita, T.; Hagiwara, S. *Science* **2015**, *349*, 864–868. (c) Samejima, H.; Babiker, A. G.; Takikawa, H.; Sasaki, M.; Sugimoto, Y. *Pest Manage. Sci.* **2016**, *72*, 2035–2042. (d) Takahashi, I.; Fukui, K.; Asami, T. *Pest Manage. Sci.* **2016**, *72*, 2048–2053. (e) Fukui, K.; Yamagami, D.; Ito, S.; Asami, T. *Front. Plant Sci.* **2017**, *8*, 936, DOI: [10.3389/fpls.2017.00936](https://doi.org/10.3389/fpls.2017.00936). (f) Dvorakova, M.; Soudek, P.; Vanek, T. *J. Nat. Prod.* **2017**, *80*, 1318–1327.
- (14) Yao, R.; Ming, Z.; Yan, L.; Li, S.; Wang, F.; Ma, S.; Yu, C.; Yang, M.; Chen, L.; Chen, L.; Li, Y.; Yan, C.; Miao, D.; Sun, Z.; Yan, J.; Sun, Y.; Wang, L.; Chu, J.; Fan, S.; He, W.; Deng, H.; Nan, F.; Li, J.; Rao, Z.; Lou, Z.; Xie, D. *Nature* **2016**, *536*, 469–473.
- (15) Fukui, K.; Ito, S.; Asami, T. *Mol. Plant* **2013**, *6*, 88–99.
- (16) Matthys, C.; Walton, A.; Struk, S.; Stes, E.; Boyer, F.-D.; Gevaert, K.; Goormachtig, S. *Planta* **2016**, *243*, 1327–1337.
- (17) Ruyter-Spira, C.; Kohlen, W.; Charnikhova, T.; van Zeijl, A.; van Bezouwen, L.; de Ruijter, N.; Cardoso, C.; Lopez-Raez, J. A.; Matusova, R.; Bours, R.; Verstappen, F.; Bouwmeester, H. *Plant Physiol.* **2011**, *155*, 721–734.
- (18) Toh, S.; Holbrook-Smith, D.; Stogios, P. J.; Onopriyenko, O.; Lumba, S.; Tsuchiya, Y.; Savchenko, A.; McCourt, P. *Science* **2015**, *350*, 203–207.
- (19) Macias, F. A.; Garcia-Diaz, M. D.; Perez-de-Luque, A.; Rubiales, D.; Galindo, A. C. G. *J. Agric. Food Chem.* **2009**, *57*, 5853–5864.
- (20) Trott, O.; Olson, A. J. *J. Comput. Chem.* **2010**, *31*, 455–461.
- (21) Wolber, G.; Langer, T. *J. Chem. Inf. Model.* **2005**, *45*, 160–169.
- (22) Pouvreau, J. B.; Gaudin, Z.; Auger, B.; Lechat, M.-M.; Gauthier, M.; Delavault, P.; Simier, P. *Plant Methods* **2013**, *9*, 32.32.

Correction to Resorcinol-Type Strigolactone Mimics as Potent Germinators of the Parasitic Plants *Striga hermonthica* and *Phelipanche ramosa*

Marcela Dvorakova,¹ Adela Hylova, Petr Soudek,² Katarzyna Retzer,³ Lukas Spichal,⁴ and Tomas Vanek*

J. Nat. Prod. 2018, 81 (11), 2321–2328, [10.1021/acs.jnatprod.8b00160](https://doi.org/10.1021/acs.jnatprod.8b00160)

Page 2326: The seeds of the parasitic plant *Phelipanche ramosa* from *Cannabis sativa* host were in fact collected at St. Martin de Bossenay, France, in 2012, not at Poitou-Charentes, France. The authors apologize for any inconvenience this error may have caused.

Resorcinol-Type Strigolactone Mimics as Potent Germinators of the Parasitic Plants *Striga* *hermonthica* and *Phelipanche ramosa*.

Marcela Dvorakova,[†] Adela Hylova,[‡] Petr Soudek,[†] Katarzyna Retzer,[†] Lukas Spichal,[‡]
Tomas Vanek^{*,†}

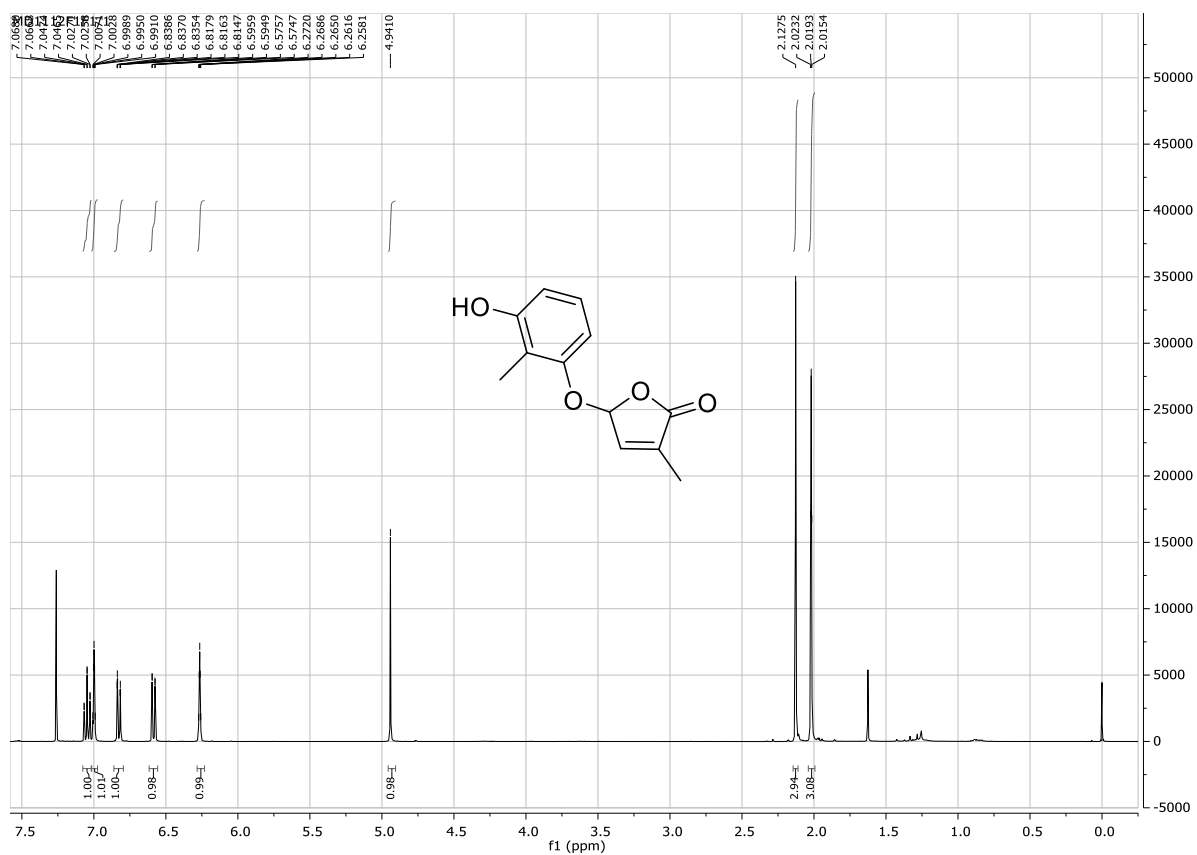
[†]Institute of Experimental Botany, Czech Academy of Sciences, v.v.i., Rozvojova 263, 16502,
Prague 6, Czech Republic

[‡] Centre of the Region Hana for Biotechnological and Agricultural Research, Department of
Chemical Biology and Genetics, Faculty of Science, Palacky University, Slechtitelu 241/27,
783 71 Olomouc, Czech Republic

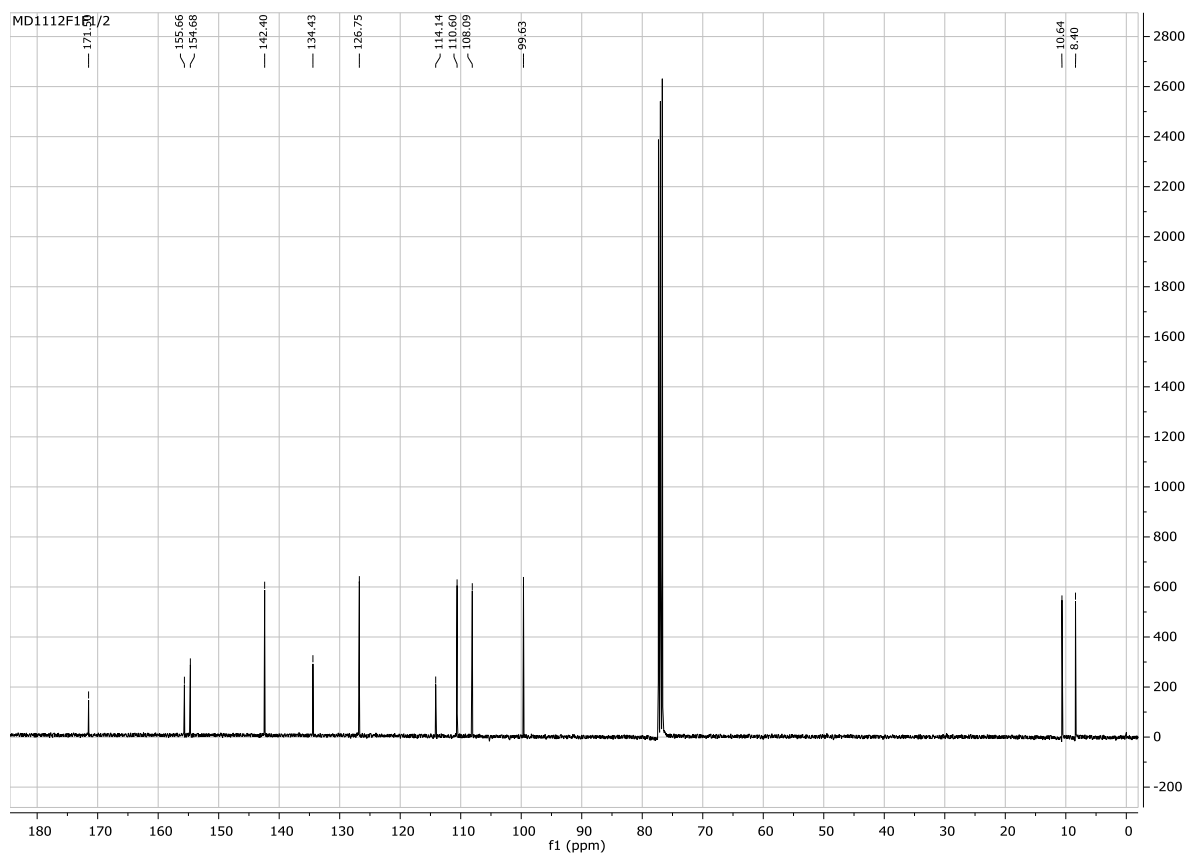
Supporting Information

Table of Contents

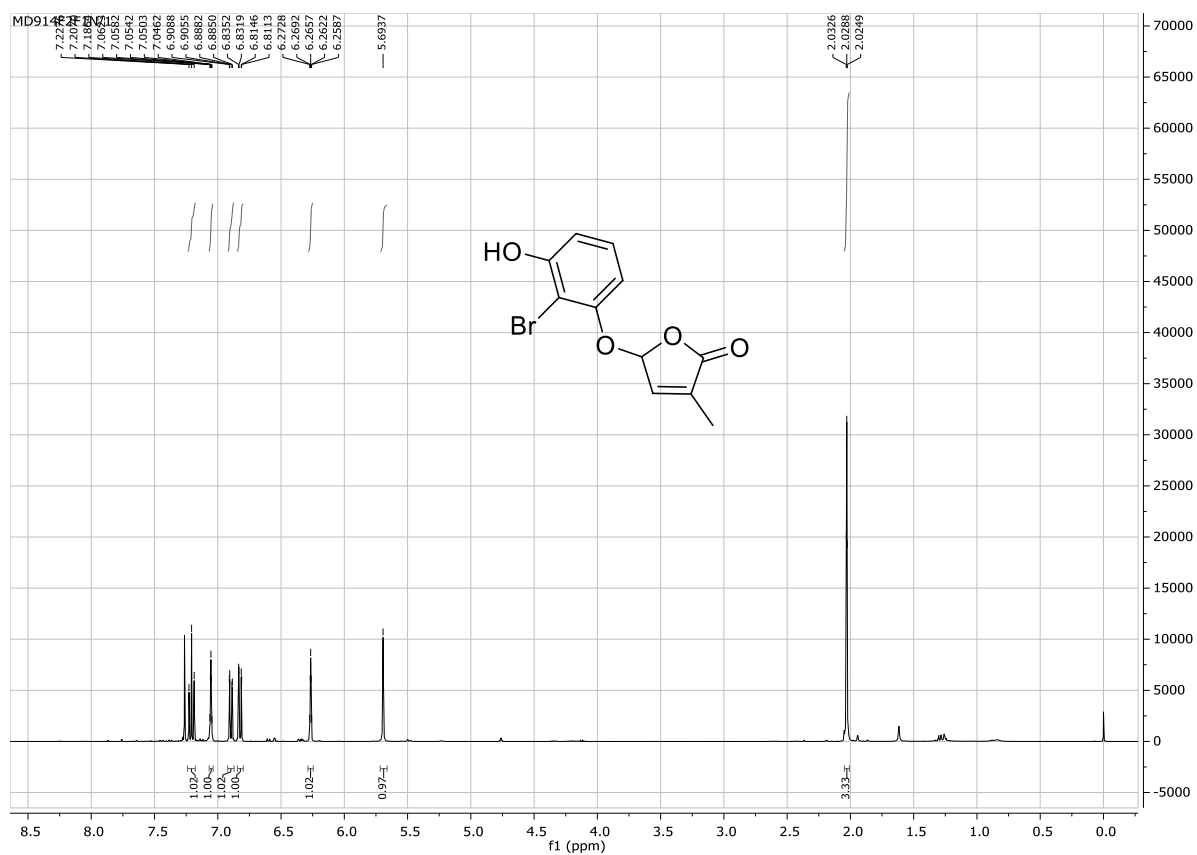
¹ H NMR and ¹³ C NMR spectra of compounds 1a-j	S3-12
---	-------



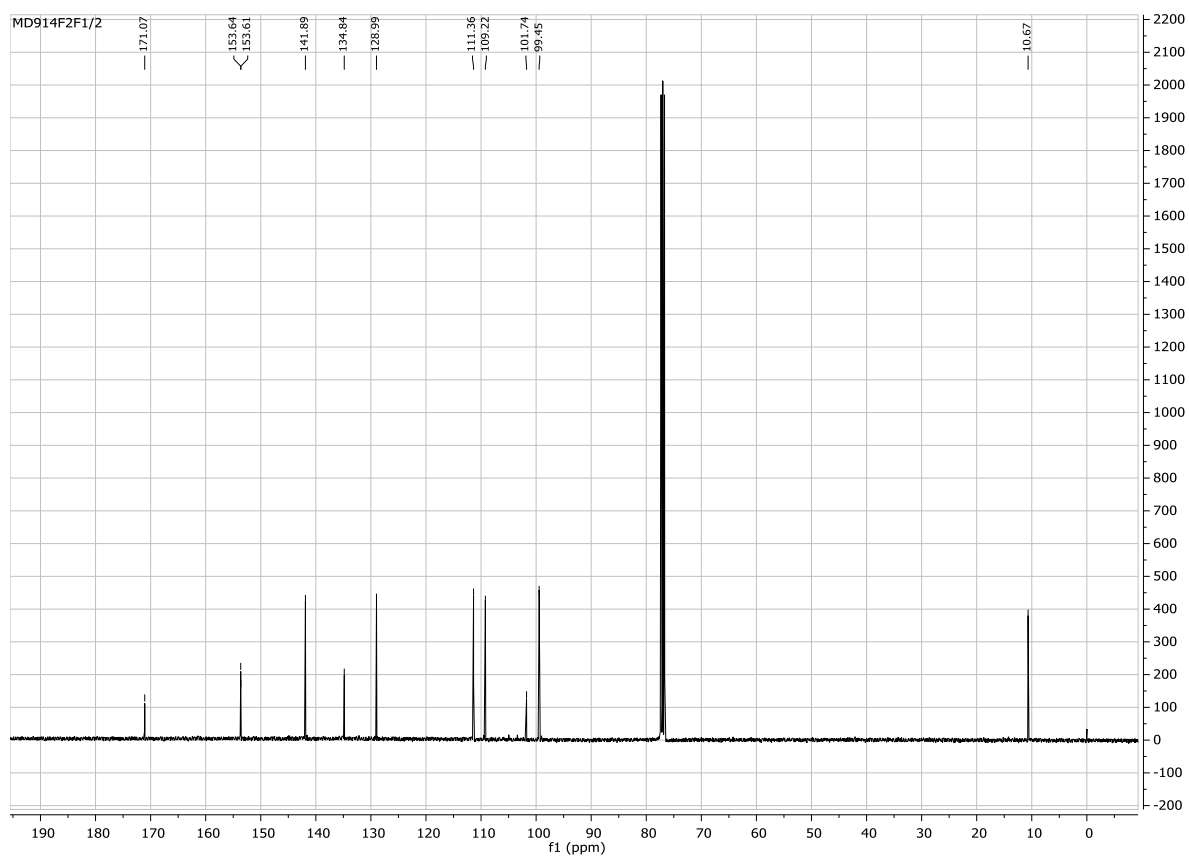
S1. ¹H NMR (400 MHz, CDCl₃) spectrum of compound **1a**



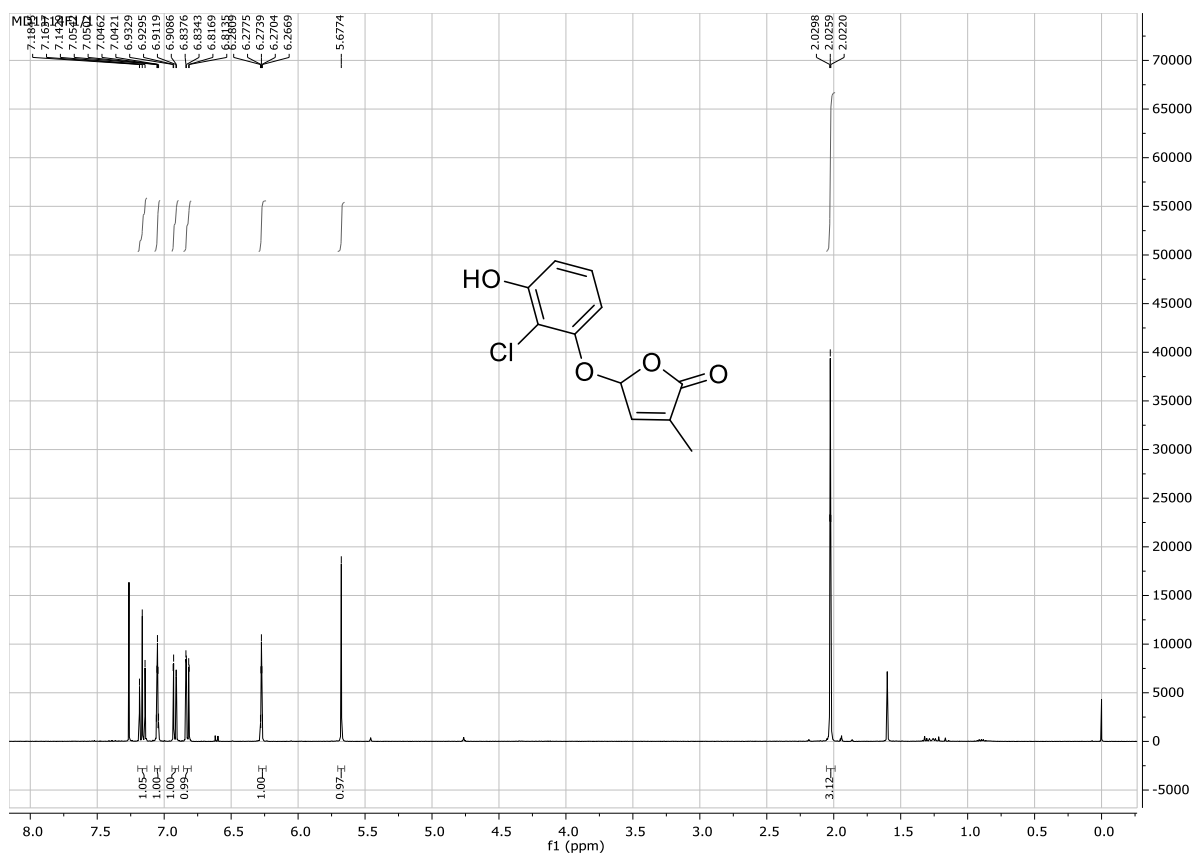
S2. ¹³C NMR (100 MHz, CDCl₃) spectrum of compound **1a**



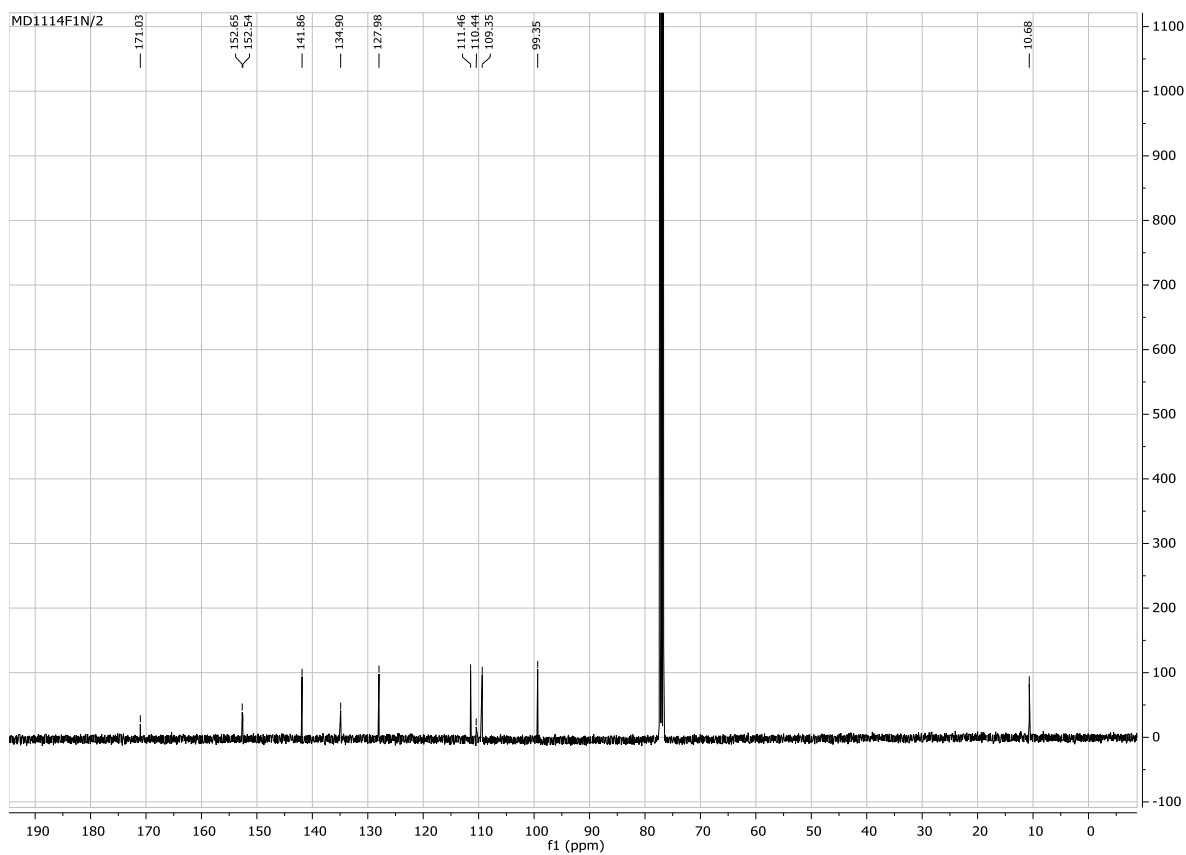
S3. ¹H NMR (400 MHz, CDCl₃) spectrum of compound **1b**



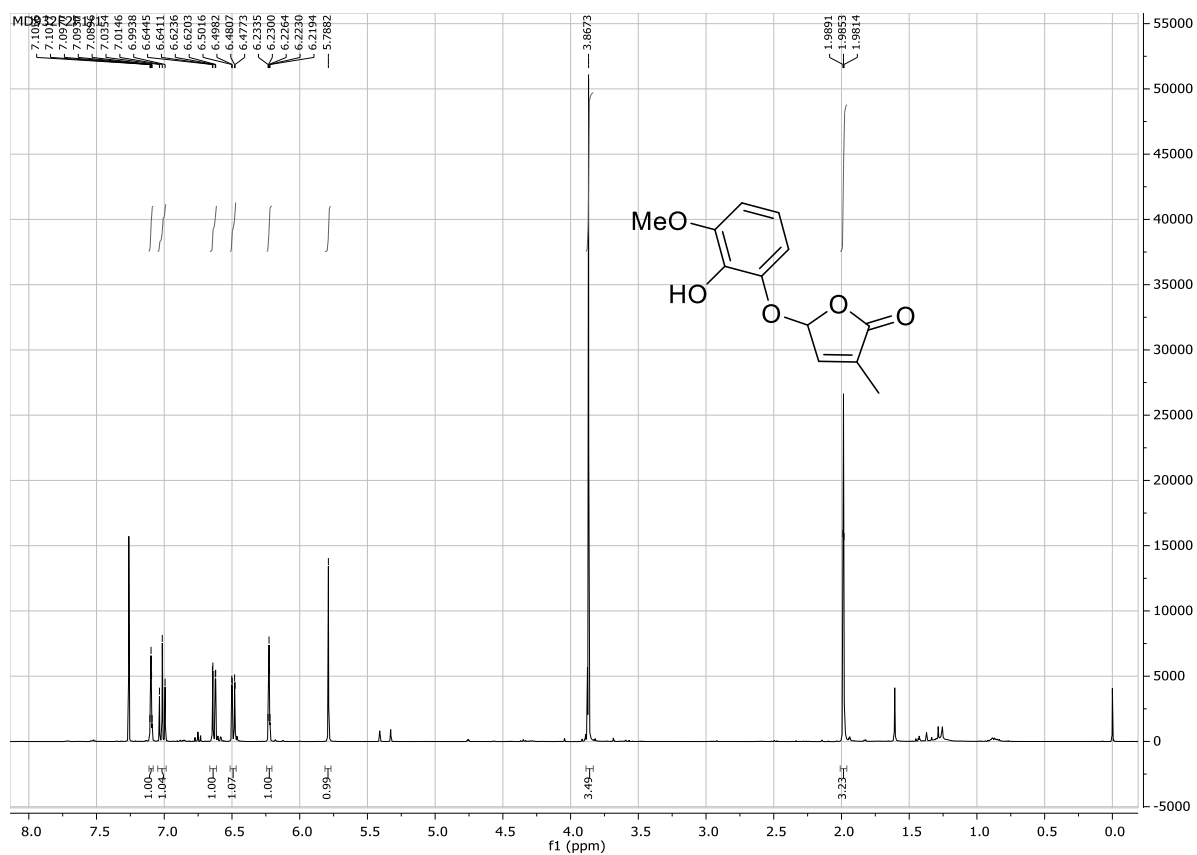
S4. ¹³C NMR (400 MHz, CDCl₃) spectrum of compound **1b**



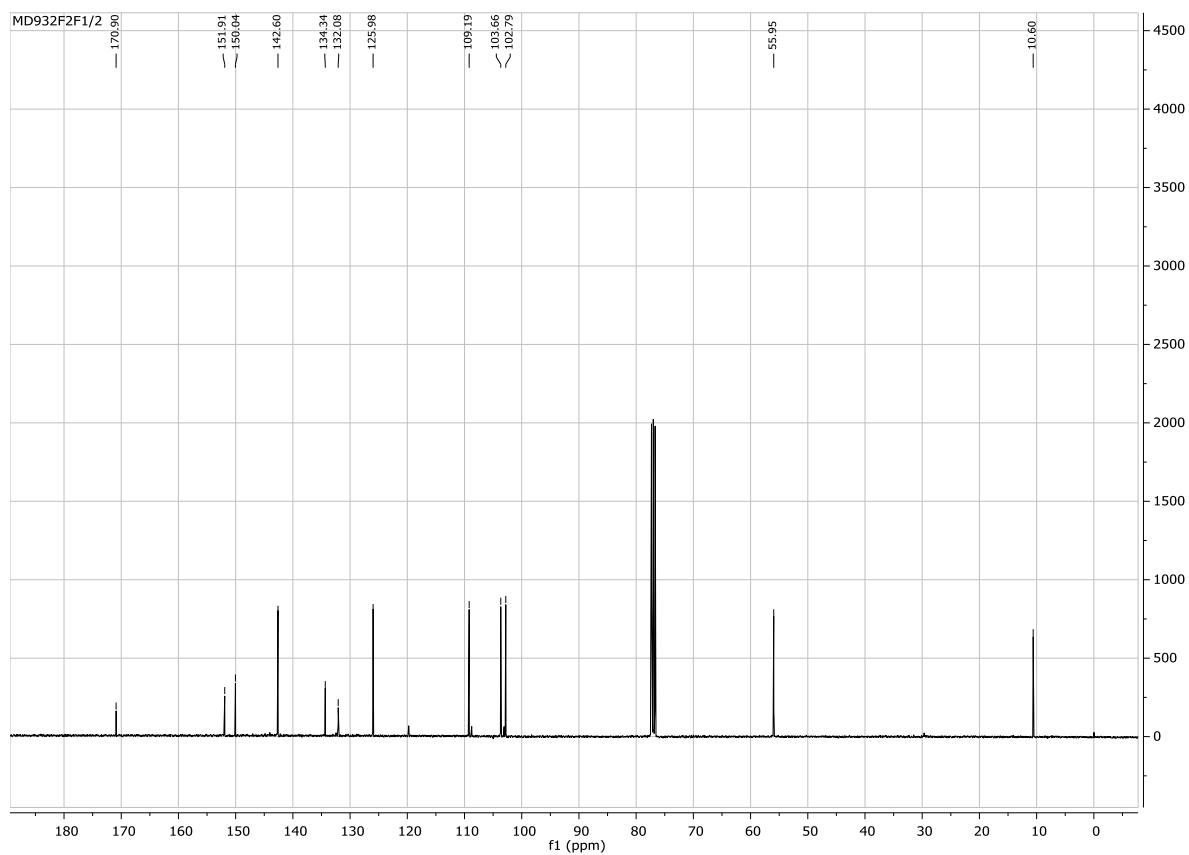
S5. ^1H NMR (400 MHz, CDCl_3) spectrum of compound **1c**



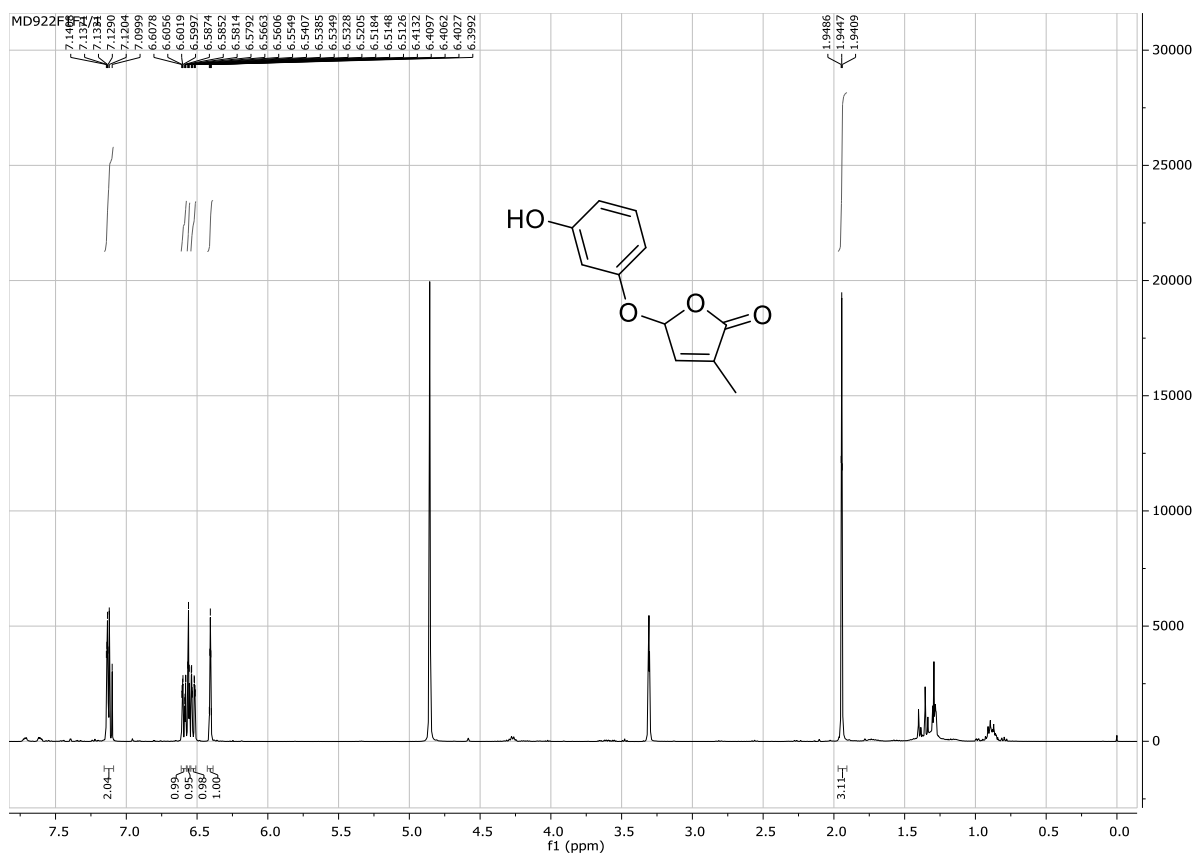
S6. ^{13}C NMR (400 MHz, CDCl_3) spectrum of compound **1c**



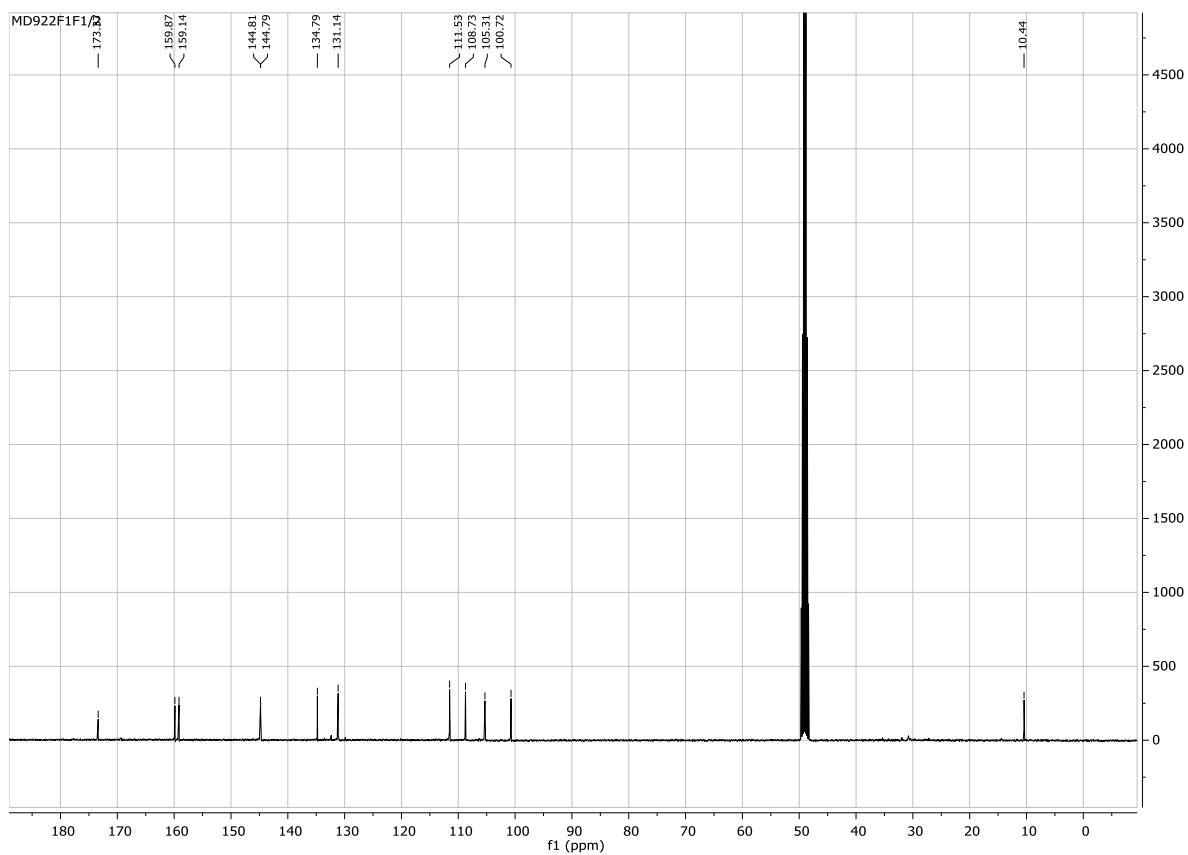
S7. ^1H NMR (400 MHz, CDCl_3) spectrum of compound **1d**



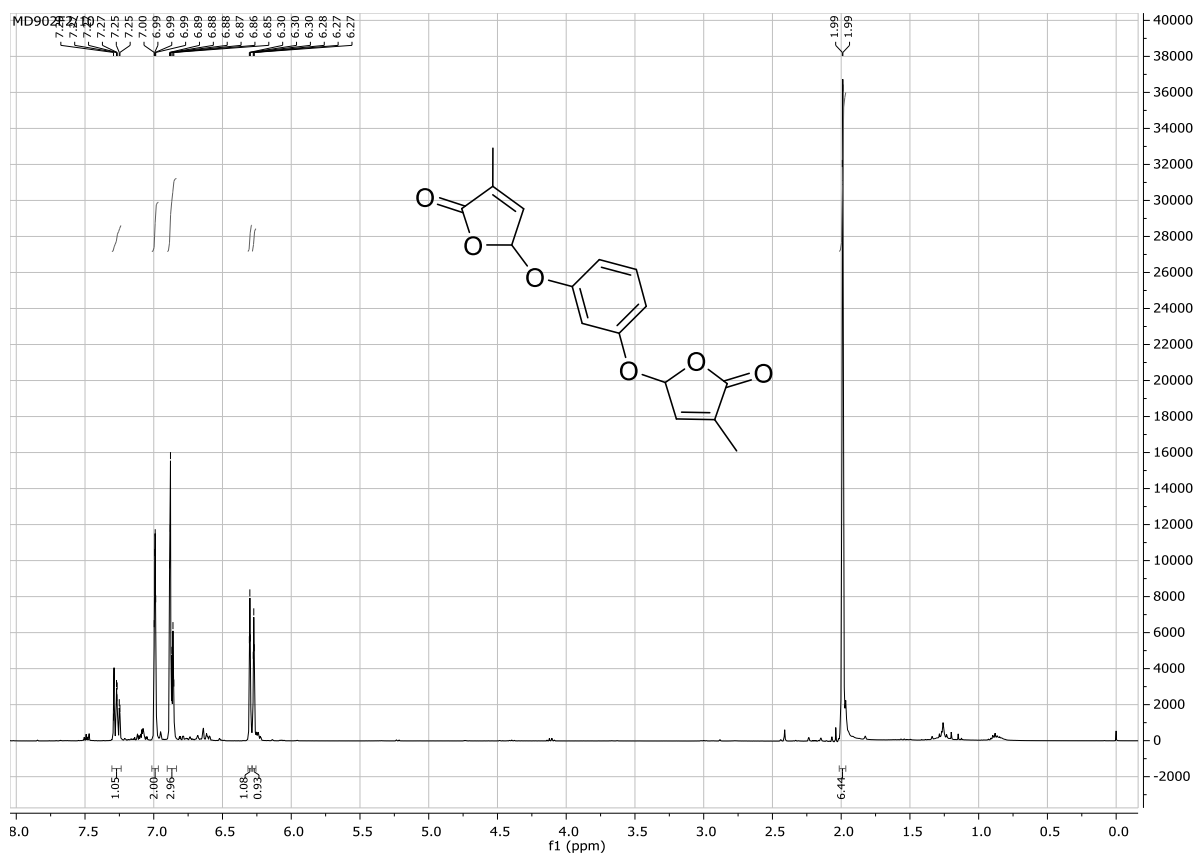
S8. ^{13}C NMR (400 MHz, CDCl_3) spectrum of compound **1d**



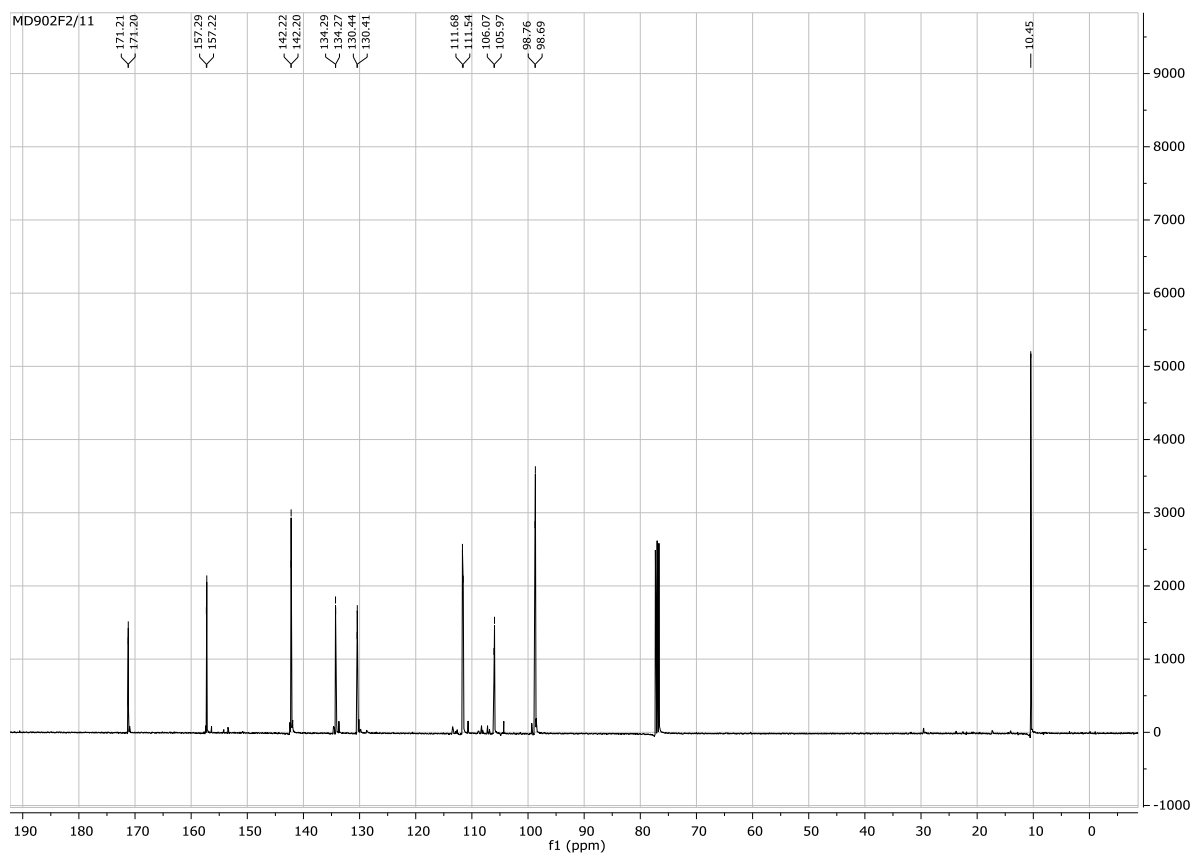
S9. ¹H NMR (400 MHz, CD₃OD) spectrum of compound **1e**



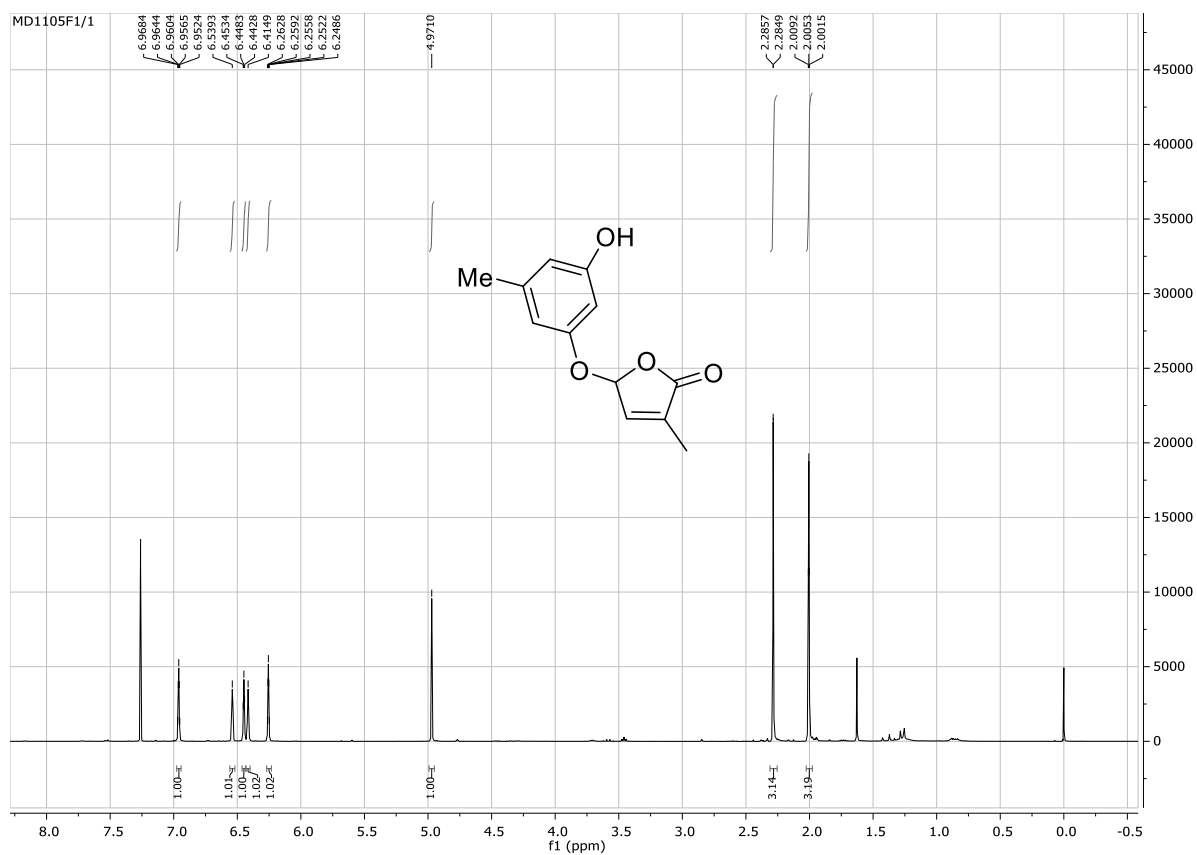
S10. ¹³C NMR (400 MHz, CD₃OD) spectrum of compound **1e**



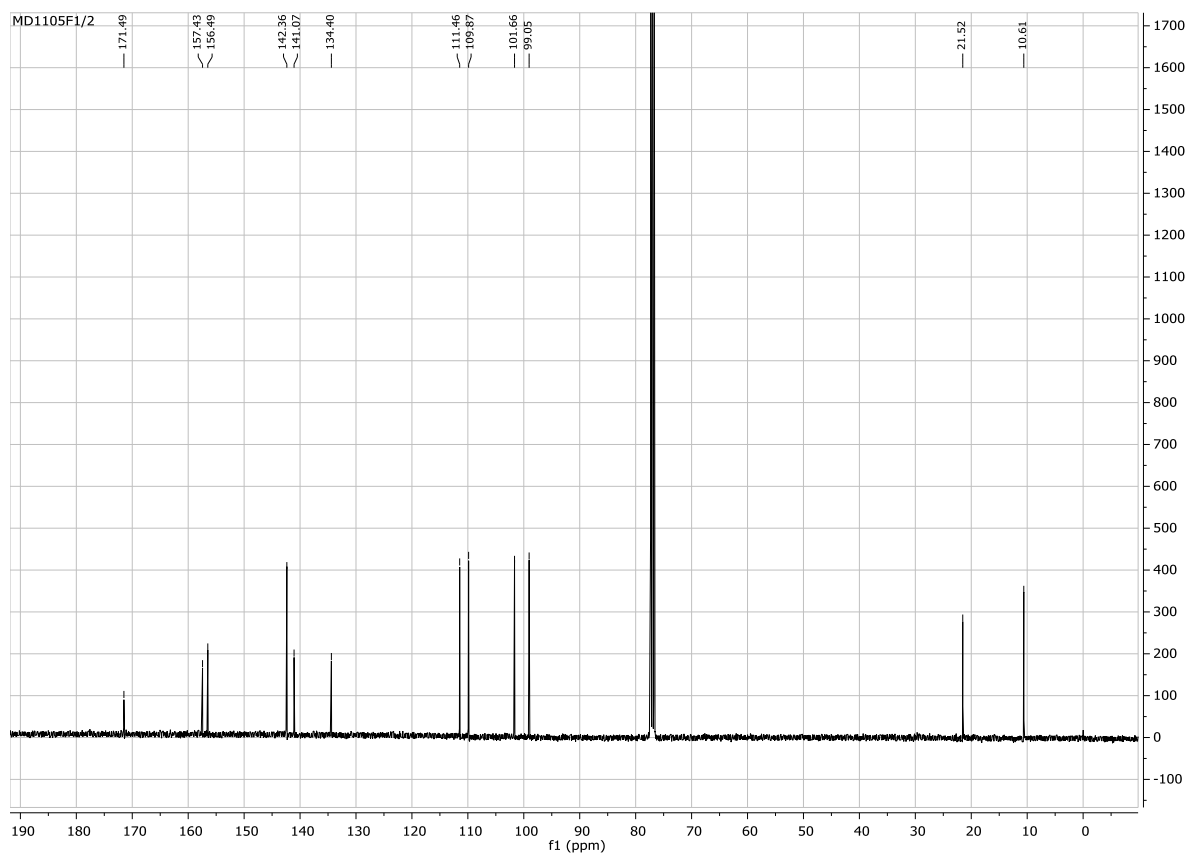
S11. ¹H NMR (400 MHz, CDCl₃) spectrum of compound **1f**



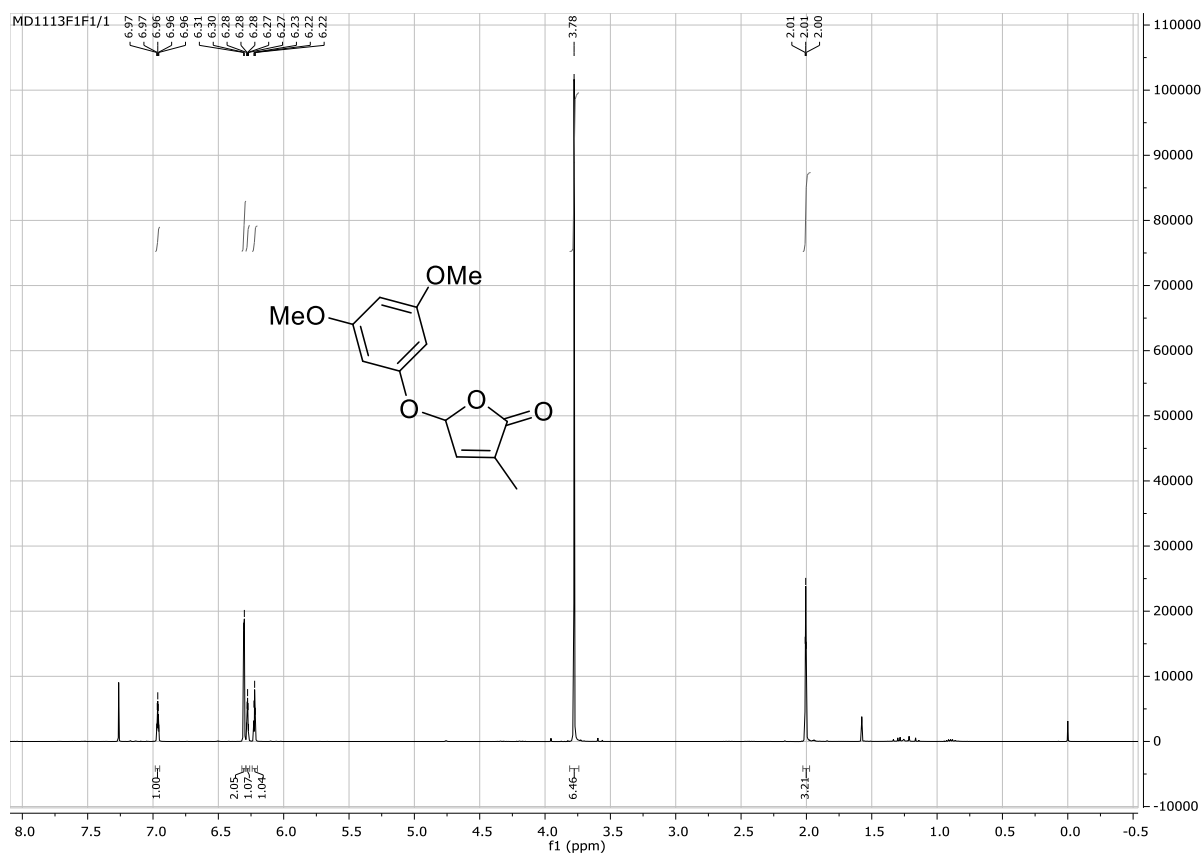
S12. ¹³C NMR (400 MHz, CDCl₃) spectrum of compound **1f**



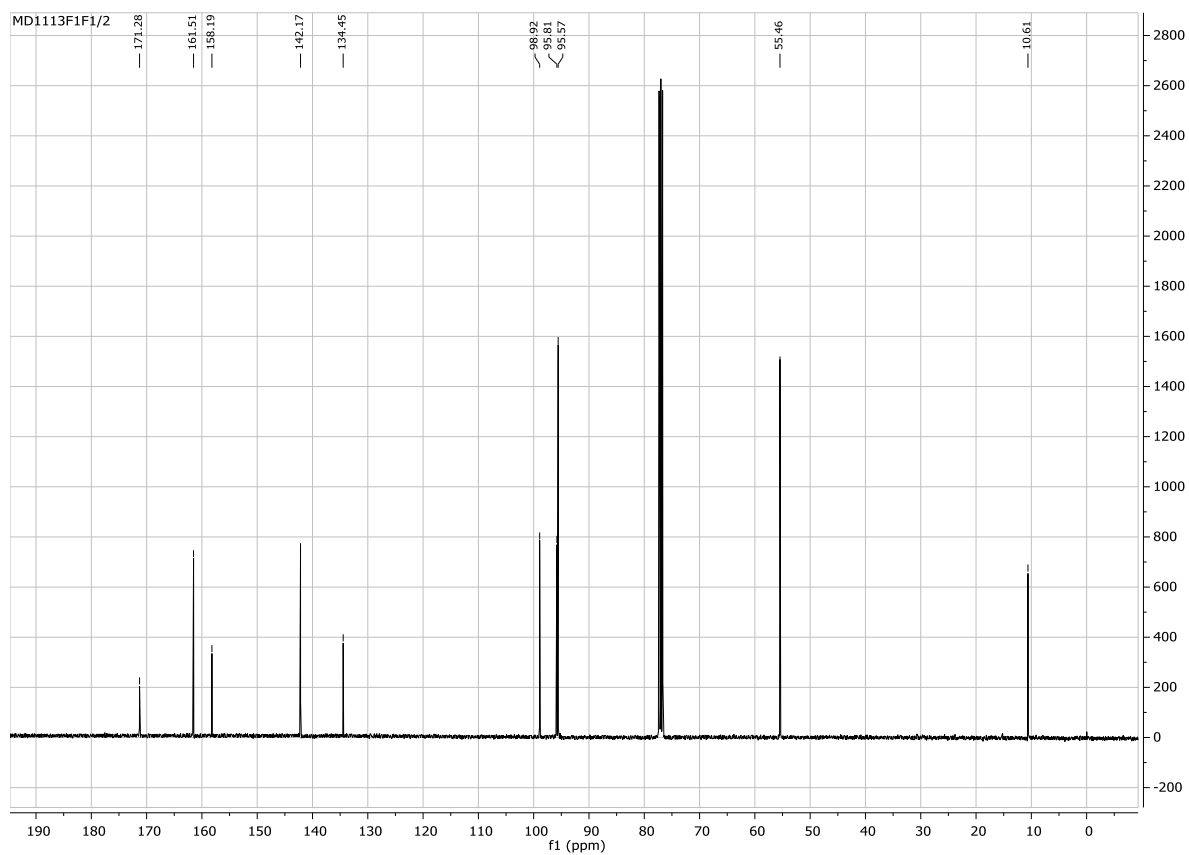
S13. ^1H NMR (400 MHz, CDCl_3) spectrum of compound **1g**



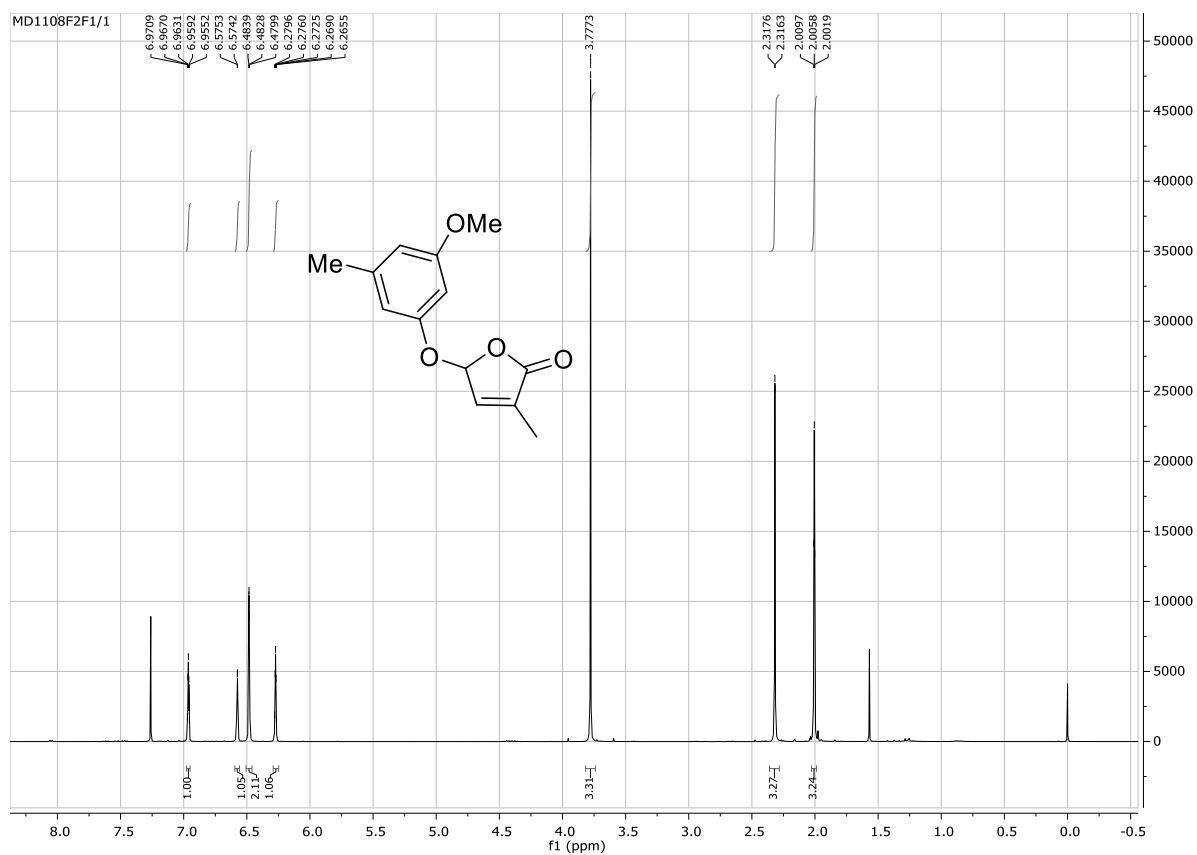
S14. ^{13}C NMR (400 MHz, CDCl_3) spectrum of compound **1g**

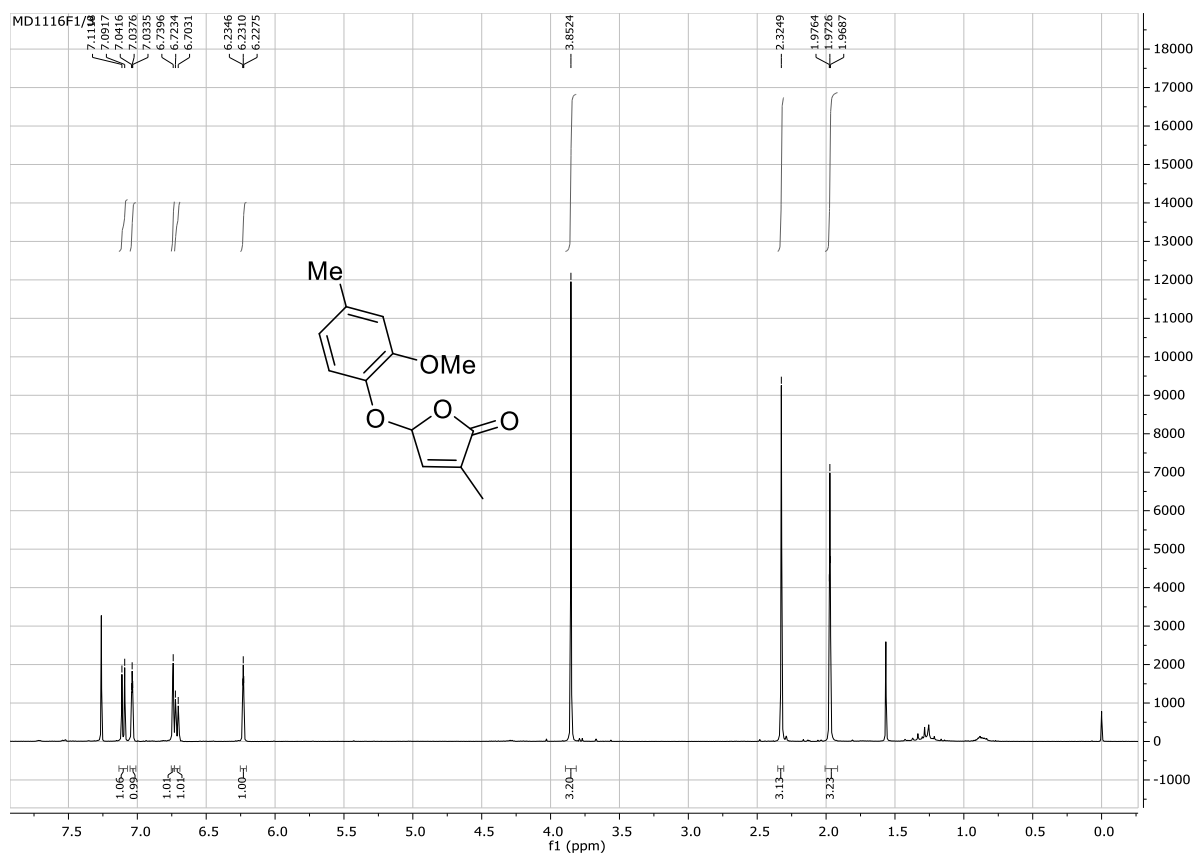


S15. ¹H NMR (400 MHz, CDCl₃) spectrum of compound **1h**

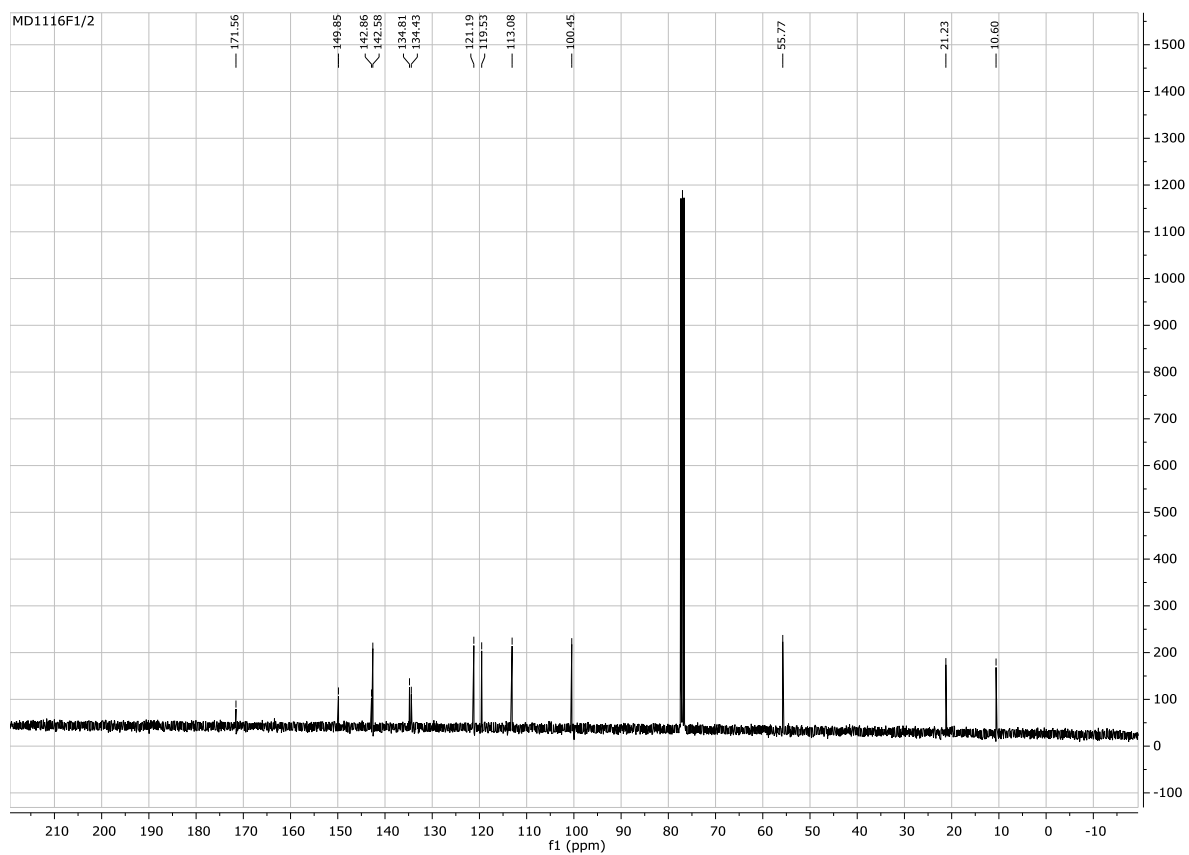


S16. ¹³C NMR (400 MHz, CDCl₃) spectrum of compound **1h**





S19. ¹H NMR (400 MHz, CDCl₃) spectrum of compound **1j**



S20. ¹³C NMR (400 MHz, CDCl₃) spectrum of compound **1j**

- 11.3. DVOŘÁKOVÁ, M., HÝLOVÁ, A., SOUDEK, P., PETROVÁ, Š., SPÍCHAL, L., AND VANĚK, T. (2019). TRIAZOLIDE STRIGOLACTONE MIMICS AS POTENT SELECTIVE GERMINATORS OF PARASITIC PLANT *PHELIPANCHE RAMOSA*. *PEST MANAG. SCI.* 75:2049–2056.

Triazolid strigolactone mimics as potent selective germinators of parasitic plant *Phelipanche ramosa*

Marcela Dvorakova,^{a*} Adela Hylova,^b Petr Soudek,^a Sarka Petrova,^a Lukas Spichal^b and Tomas Vanek^a



Abstract

BACKGROUND: Strigolactones are a unique class of plant metabolites which serve as a rhizosphere signal for parasitic plants and evocate their seed germination. The expansion of these parasitic weeds in the food crop fields urgently calls for their increased control and depletion. Simple strigolactone analogues able to stimulate seed germination of these parasitic plants may represent an efficient control measure through the induction of suicidal germination.

RESULTS: Triazolid-type strigolactone mimics were easily synthesized in three steps from commercially available materials. These derivatives induced effectively seed germination of *Phelipanche ramosa* with EC₅₀ as low as 5.2×10^{-10} M. These mimics did not induce seed germination of *Striga hermonthica* even at high concentration ($\geq 1 \times 10^{-5}$ M).

CONCLUSIONS: Simple and stable strigolactone mimics with selective activity against *Phelipanche ramosa* were synthesized.

© 2019 Society of Chemical Industry

Supporting information may be found in the online version of this article.

Keywords: strigolactones; *Arabidopsis*; *Phelipanche*; *Striga*; seed germination

1 INTRODUCTION

Witchweeds (*Striga* spp.) and broomrapes (*Phelipanche* and *Orobanche* spp.) are parasitic plants highly infesting food crops around the world thus causing a real threat to food security.^{1–5} While successful eradication of *Striga* has been achieved in the USA using ethylene injection technique together with strict quarantine measures, such an approach is too expensive and arduous to be used in developing countries and is ineffective when broomrapes come to play.⁶

Parasitic plants produce hundreds of thousands of tiny seeds, which may persist in soil for more than a decade waiting for the right germination conditions. Such an extensive seed bank is hard to deplete. To germinate, these seeds require the right temperature and humidity and the recognition of a rhizosphere signal suggesting the host presence. Unlike *Striga* seeds, which require high preconditioning temperatures and thus they are active especially in Sub-Saharan regions of Africa, broomrapes germinate at lower temperatures thus affecting vast areas in Asia, Australia, Central America, Northern Africa and Mediterranean regions in Europe, also spreading to Central and Eastern Europe.⁷ Several types of rhizosphere signals triggering seed germination of parasitic plants and belonging to plant secondary metabolites or fungal metabolites, such as strigolactones, isothiocyanates, sesquiterpene lactones, dehydrocostus lactone, fusicoccins and ophiobolin A, have been recognized, with natural strigolactones being the most potent.^{8–11} Very recently, a strigolactone mimic called sphynolactone-7 was found to induce *Striga hermonthica*

seed germination at femtomolar level, thus resembling the potency of natural strigolactones, namely of 5-deoxystrigol.¹² The germination inducing capacity of these signals depends on parasitic weed species. While some species respond to various signals (*P. ramosa*, *P. aegyptiaca*), some respond only to those exuded by their host (*O. cumana*, *O. densiflora*).⁸ Hosts are generally important crop species. Witchweeds affect mainly cereal crops whereas broomrapes thrive on legumes, tomato, tobacco and oilseed rape.^{7,8} The isolated rhizosphere signals or their synthetic derivatives may be used in parasite management using so called 'suicidal germination'. This approach uses chemical entities that are able to induce germination of parasitic seeds without the presence of a host thus causing parasite's death.^{13,14}

While a lot of attention is paid to *Striga* management strategies due to its presence in areas already seriously threatened with starvation due to crops affected by severe droughts and soil barrenness, broomrape species stay a bit in the background.

* Correspondence to: M Dvorakova, Laboratory of Plant Biotechnologies, The Czech Academy of Sciences, Institute of Experimental Botany, Rozvojova 263, 16502 Prague 6, Czech Republic. E-mail: dvorakova@ueb.cas.cz

a Laboratory of Plant Biotechnologies, The Czech Academy of Sciences, Institute of Experimental Botany, Prague, Czech Republic

b Department of Chemical Biology and Genetics, Palacky University, Faculty of Science, Centre of the Region Hana for Biotechnological and Agricultural Research, Olomouc, Czech Republic

Broomrape control relies mainly on the use of resistant cultivars and few herbicides.¹⁵ Thus, there is an urgent demand for more effective and environmentally friendly alternatives, which would stop broomrapes to spread further to new regions with the unwelcomed help of global warming causing worldwide increase in average temperature.¹⁶

From broomrapes, *P. ramosa* is the most widespread.⁹ It germinates upon a recognition of a range of chemical signals, but the effectivity of these signals varies. The most active germination stimulants for *P. ramosa* are strigolactones and their synthetic derivative GR24, which are able to induce *P. ramosa* seed germination at picomolar level.⁹ Though as effective, complicated structure and synthesis forestall strigolactones' commercial utilization as control agents. In here, we report a series of simple triazolidine strigolactone mimics which exhibit nanomolar germination activity on *P. ramosa* seeds.

2 MATERIALS AND METHODS

2.1 General experimental procedure

All reactions requiring anhydrous or inert conditions were carried out under a positive atmosphere of argon in oven-dried glassware. Solutions or liquids were introduced in round-bottomed flasks using oven-dried syringes through rubber septa. All reactions were stirred magnetically using Teflon-coated stirring bars. If needed, reactions were warmed using an electrically-heated silicon oil bath, and the stated temperature corresponds to the temperature of the bath. Organic solutions obtained after aqueous work-up were dried over MgSO_4 . The removal of solvents was accomplished using a rotary evaporator at water aspirator pressure. GR24 stands for *rac*-GR24, which was purchased from Stichting Chemiefonds Paddepoel, Malden, The Netherlands. Chemicals for the syntheses were purchased from Sigma-Aldrich (Prague, Czech Republic). Solvents for extractions and chromatography were of technical grade and purchased from Penta Chemicals s.r.o. (Prague, Czech Republic) or from VWR (Stribrna Skalice, Czech Republic). Solvents used in reactions were distilled from appropriate drying agents and stored under argon over activated Linde 4 Å molecular sieves. Column and flash chromatography was carried out using Merck silica gel (60–200 µm). Analytical TLC was performed with Merck silica gel 60 F254 plates. Visualization was accomplished by UV-light (254 nm) and staining with a vanillin solution, followed by heating. ^1H , ^{13}C , and 2D (^1H -COSY, HMQC) NMR spectra were recorded on a Bruker Avance III[™] HD 400 MHz spectrometer equipped with a Prodigy cryo-probe. TMS (0 ppm, ^1H NMR) and CDCl_3 (77 ppm, ^{13}C NMR) or CD_3OD (49 ppm, ^{13}C NMR) were used as internal references. The chemical shifts (δ) are reported in ppm and the coupling constants (J) are recorded in Hz. The hydrogen and carbon assignments were done according to ^1H - ^1H COSY and ^1H - ^{13}C HMQC experiments. Mass spectra were recorded on a LTQ Orbitrap XL spectrometer. The stability of the compounds was evaluated using Waters Alliance e2695 HPLC system with Waters 2998 Photodiode Array (PDA) Detector.

2.2 Plant material

Seeds of parasitic plants were collected at different sites – *Striga hermonthica* (Sudan, 2007), *Phelipanche ramosa* (St. Martin de Bossenay, France, host *Cannabis sativa*, 2012) and *Phelipanche ramosa* (St. Jean d'Angely, France, host *Brassica napus*, 2015). Seeds were surface sterilized in 2% (v/v) NaOCl and 1% Triton X 100 (v/v) for 6 min, then washed with 200 mL of Milli-Q water. Seeds

were incubated in 1 mM HEPES buffer (pH = 7.5) with 0.1% PPM (Plant Preservative Mixture) for 4 days at 27 °C (*S. hermonthica*) or 7 days at 21 °C (*P. ramosa*).

2.3 Biological activity assays

The assay was carried out using slightly modified published procedure.¹⁷ Fifty microliters of incubated seeds were transferred into each well of 96-well plate. Seed germination was induced by the addition of 10 µL of tested compounds in concentrations ranging from 10^{-13} to 10^{-5} M and the volume in each well was adjusted to 100 µL using sterilized water. As a negative control, 0.1% solution of acetone was used. Seed germination was carried out in the dark for 4 days in an incubator at either 27 °C (*S. hermonthica*) or 21 °C (*P. ramosa*). Then, 10 µL of MTT (3-[4,5-dimethylthiazol-2-yl]-2,5-diphenyltetrazolium bromide) of 5 g/L concentration were added to each well. After 24 h, a lysis solution was added (10% Triton X-100 and 0.04% HCl in isopropanol) to dissolve the formed formazan. After next 24 h, the difference in absorbance between 570 nm and 690 nm was measured for each well. Data were evaluated by nonlinear regression using GraphPad Prism 5.0 program and EC_{50} values were determined. The test was carried out twice for each compound.

2.4 Chemistry

2.4.1 5-Bromo-3-methyl-2(5H)-furanone

5-Bromo-3-methyl-2(5H)-furanone was synthesized according to a reported procedure.¹⁸ To a solution of 3-methyl-2(5H)-furanone (90% technical grade, 339 mg, 3.11 mmol) in CCl_4 (4 mL) was added *N*-bromosuccinimide (NBS, 677 mg, 3.80 mmol) and a catalytic amount of benzoyl peroxide (167 mg, 0.69 mmol) as a radical initiator. The reaction mixture was heated under reflux at 78 °C for 1.5 h, cooled to 0 °C, filtered, and the solvent evaporated. The 5-bromo-3-methyl-2(5H)-furanone was used directly in the next step.

2.4.2 5-Azido-3-methyl-2(5H)-furanone

5-Azido-3-methyl-2(5H)-furanone was synthesized according to a reported procedure.¹⁹ Sodium azide (292 mg, 4.49 mmol) was suspended in dry DMF (3 mL) under an argon atmosphere and 5-bromo-3-methyl-2(5H)-furanone dissolved in dry DMF (3 mL) was added dropwise *via* syringe. The reaction mixture was stirred for 1.5 h at room temperature and the solvent was evaporated. The residue was dissolved in MeOH and adsorbed on silica gel. Purification by column chromatography (85/15, v/v, petroleum ether/ethyl acetate) gave 5-azido-3-methyl-2(5H)-furanone (258 mg, 60%) as a yellow oil. The spectroscopic data corresponded to the reported ones.¹⁹

2.4.3 General procedure for the synthesis of triazolidine strigolactone mimics (1a–y)

To a solution of 5-azido-3-methyl-2(5H)-furanone (1.85 mmol, 258 mg) in 15 mL of *t*-BuOH/ H_2O (1/1, v/v) was added the appropriate ethynyl compound (2.23 mmol), and successively solutions of $\text{CuSO}_4 \times 5\text{H}_2\text{O}$ (0.37 mmol, 93 mg) in 0.5 mL H_2O and sodium ascorbate (0.74 mmol, 147 mg) in 0.5 mL H_2O .¹⁹ The reaction mixture was stirred overnight at 40 °C and the solvent evaporated. The residue was dissolved in ethyl acetate, washed with water, and the water phase was extracted with ethyl acetate (4 × 20 mL). The products were racemic mixtures.

The following compounds were prepared using this method:

3-Methyl-5-(4-phenyl-1H-1,2,3-triazol-1-yl)furan-2(5H)-one (**1a**). The procedure and the spectroscopic data corresponded to the reported ones.¹⁹

5-(4-Mesityl-1H-1,2,3-triazol-1-yl)-3-methylfuran-2(5H)-one (**1b**). The procedure and the spectroscopic data corresponded to the reported ones.¹⁹

3-Methyl-5-[4-(4-pentylphenyl)-1H-1,2,3-triazol-1-yl]furan-2(5H)-one (**1c**). The procedure and the spectroscopic data corresponded to the reported ones.¹⁹

5-[4-(4-Fluorophenyl)-1H-1,2,3-triazol-1-yl]-3-methylfuran-2(5H)-one (**1d**). The procedure and the spectroscopic data corresponded to the reported ones.¹⁹

3-Methyl-5-[4-(4-(trifluoromethyl)phenyl)-1H-1,2,3-triazol-1-yl]furan-2(5H)-one (**1e**). The procedure and the spectroscopic data corresponded to the reported ones.¹⁹

5-[4-(3,5-Difluorophenyl)-1H-1,2,3-triazol-1-yl]-3-methylfuran-2(5H)-one (**1f**). The procedure and the spectroscopic data corresponded to the reported ones.¹⁹

5-[4-(4-(Dimethylamino)phenyl)-1H-1,2,3-triazol-1-yl]-3-methylfuran-2(5H)-one (**1g**). The procedure and the spectroscopic data corresponded to the reported ones.¹⁹

5-[4-(1-Hydroxycyclohexyl)-1H-1,2,3-triazol-1-yl]-3-methylfuran-2(5H)-one (**1h**). The procedure and the spectroscopic data corresponded to the reported ones.¹⁹

5-(4-Cyclopropyl-1H-1,2,3-triazol-1-yl)-3-methylfuran-2(5H)-one (**1i**). For the reaction 400 mg (2.88 mmol) of 5-azido-3-methyl-2(5H)-furanone was used. Purification by column chromatography (gradient 7/3 to 6/4, v/v, petroleum ether/ethyl acetate) afforded pure product, **1i** in 90% yield (533 mg). **1i**: ¹H NMR (CDCl₃, 400 MHz): δ 7.34 (1H, s, H-5'), 7.19 (1H, quin., J 1.7 Hz, H-4), 6.97 (1H, quin., J 1.7 Hz, H-5), 2.09 (3H, t, J 1.7 Hz, CH₃), 1.98–1.92 (1H, m, CH), 1.00–0.95 (2H, m, CH₂), 0.87–0.83 (2H, m, CH₂); ¹³C NMR (CDCl₃, 100 MHz): δ 170.6 (CO), 151.4 (C), 141.1 (CH, C-4), 134.7 (C), 118.1 (CH, C-5'), 84.8 (CH, C-5), 10.8 (CH₃), 7.8 (CH), 7.8 (CH₂), 6.54 (CH₂); HRMS *m/z* ([M + Na]⁺) calcd for C₁₀H₁₁O₂N₃Na 228.07435, found 228.07431.

5-(4-Cyclopentyl-1H-1,2,3-triazol-1-yl)-3-methylfuran-2(5H)-one (**1j**). For the reaction 248 mg (1.78 mmol) of 5-azido-3-methyl-2(5H)-furanone was used. Purification by column chromatography (gradient 7/3 to 6/4, v/v, petroleum ether/ethyl acetate) afforded pure product, **1j** in 92% yield (382 mg). **1j**: ¹H NMR (CDCl₃, 400 MHz): δ 7.34 (1H, d, J 0.72 Hz, H-5'), 7.21 (1H, quin., J 1.7 Hz, H-4), 6.99 (1H, quin., J 1.7 Hz, H-5), 3.23–3.15 (1H, m, CH), 2.14–2.07 (4H, m, CH₃, CH₂), 1.81–1.61 (7H, m, CH₂); ¹³C NMR (CDCl₃, 100 MHz): δ 170.6 (CO), 153.9 (C), 141.2 (CH, C-4), 134.7 (C), 118.0 (CH, C-5'), 84.9 (CH, C-5), 36.6 (CH), 33.1 (2 × CH₂), 25.1 (2 × CH₂), 10.8 (CH₃); HRMS *m/z* ([M + H]⁺) calcd for C₁₂H₁₆O₂N₃ 234.12370, found 234.12372.

5-(4-Cyclohexyl-1H-1,2,3-triazol-1-yl)-3-methylfuran-2(5H)-one (**1k**). For the reaction 393 mg (2.83 mmol) of 5-azido-3-methyl-2(5H)-furanone was used. Purification by column chromatography (gradient 3/1 to 2/1, v/v, petroleum ether/ethyl acetate) afforded pure product, **1k** in 88% yield (615 mg). **1k**: ¹H NMR (CDCl₃, 400 MHz): δ 7.32 (1H, d, J 0.80 Hz, H-5'), 7.21 (1H, quin., J 1.7 Hz, H-4), 6.99 (1H, quin., J 1.7 Hz, H-5), 2.81–2.74 (1H, m, CH), 2.10 (3H, t, J 1.7 Hz, CH₃), 2.07–2.02 (2H, m, CH₂), 1.84–1.71 (3H, m, CH₂), 1.43–1.36 (4H, m, CH₂), 1.29–1.21 (1H, m, CH₂); ¹³C NMR (CDCl₃, 100 MHz): δ 170.6 (CO), 154.8 (C), 141.2 (CH, C-4), 134.7 (C), 117.8 (CH, C-5'), 84.9 (CH, C-5), 35.2 (CH), 32.8 (2 × CH₂), 26.0 (CH₂), 25.9 (CH₂), 10.8 (CH₃); HRMS *m/z* ([M + H]⁺) calcd for C₁₃H₁₈O₂N₃ 248.13935, found 248.13941.

5-[4-(Cyclohex-1-en-1-yl)-1H-1,2,3-triazol-1-yl]-3-methylfuran-2(5H)-one (**1l**). For the reaction 200 mg (1.44 mmol) of 5-azido-3-methyl-2(5H)-furanone was used. Purification by column chromatography (3/1, v/v, petroleum ether/ethyl acetate) afforded pure product, **1l** in 94% yield (330 mg). **1l**: ¹H NMR (CDCl₃, 400 MHz): δ 7.46 (1H, s, H-5'), 7.21 (1H, quin., J 1.7 Hz, H-4), 7.01 (1H, quin., J 1.7 Hz, H-5), 6.59–6.56 (1H, m, CH), 2.36–2.32 (2H, m, CH₂), 2.23–2.18 (2H, m, CH₂), 2.10 (3H, t, J 1.7 Hz, CH₃), 1.79–1.73 (2H, m, CH₂), 1.70–1.64 (2H, m, CH₂); ¹³C NMR (CDCl₃, 100 MHz): δ 170.6 (CO), 150.4 (C), 141.1 (CH, C-4), 134.8 (C), 126.5 (CH), 126.4 (C), 116.5 (CH, C-5'), 84.9 (CH, C-5), 26.3 (CH₂), 25.2 (CH₂), 22.3 (CH₂), 22.0 (CH₂), 10.8 (CH₃); HRMS *m/z* ([M + H]⁺) calcd for C₁₃H₁₆O₂N₃ 246.12370, found 246.12372.

3-Methyl-5-(4-propyl-1H-1,2,3-triazol-1-yl)furan-2(5H)-one (**1m**). For the reaction 170 mg (1.22 mmol) of 5-azido-3-methyl-2(5H)-furanone was used. Purification by column chromatography (7/3, v/v, petroleum ether/ethyl acetate) afforded pure product, **1m** in 95% yield (240 mg). **1m**: ¹H NMR (CDCl₃, 400 MHz): δ 7.38 (1H, s, H-5'), 7.22 (1H, quin., J 1.7 Hz, H-4), 6.99 (1H, quin., J 1.7 Hz, H-5), 2.71 (2H, dt, J 0.8, 7.6 Hz, CH₂), 2.10 (3H, t, J 1.7 Hz, CH₃), 1.74–1.65 (2H, m, CH₂), 0.97 (3H, t, J 7.4 Hz, CH₃); ¹³C NMR (CDCl₃, 100 MHz): δ 170.6 (CO), 149.4 (C), 141.1 (CH, C-4), 134.8 (C), 119.1 (CH, C-5'), 84.8 (CH, C-5), 27.5 (CH₂), 22.5 (CH₂), 13.7 (CH₃), 10.8 (CH₃); HRMS *m/z* ([M + H]⁺) calcd for C₁₀H₁₄O₂N₃ 208.10805, found 208.10809.

5-[4-(3-Hydroxypropyl)-1H-1,2,3-triazol-1-yl]-3-methylfuran-2(5H)-one (**1n**). For the reaction 244 mg (1.75 mmol) of 5-azido-3-methyl-2(5H)-furanone was used. Purification by column chromatography (gradient 98/2 to 90/10, v/v, CHCl₃/methanol) afforded pure product, **1n** in 84% yield (330 mg). **1n**: ¹H NMR (CD₃OD, 400 MHz): δ 7.91 (1H, t, J 0.7 Hz, H-5'), 7.37 (1H, quin., J 1.7 Hz, H-4), 7.17 (1H, quin., J 1.7 Hz, H-5), 3.59 (2H, t, J 6.4 Hz, CH₂), 2.79 (2H, dt, J 0.7, 7.6 Hz, CH₂), 2.05 (3H, t, J 1.7 Hz, CH₃), 1.92–1.85 (2H, m, CH₂); ¹³C NMR (CD₃OD, 100 MHz): δ 172.7 (CO), 149.7 (C), 143.2 (CH, C-4), 122.3 (CH, C-5'), 86.5 (CH, C-5), 61.9 (CH₂), 33.1 (CH₂), 22.7 (CH₂), 10.6 (CH₃); HRMS *m/z* ([M + H]⁺) calcd for C₁₀H₁₄O₃N₃ 224.10297, found 224.10293.

5-[4-(3-Chloropropyl)-1H-1,2,3-triazol-1-yl]-3-methylfuran-2(5H)-one (**1o**). For the reaction 229 mg (1.65 mmol) of 5-azido-3-methyl-2(5H)-furanone was used. Purification by column chromatography (gradient 3/2 to 1/1, v/v, petroleum ether/ethyl acetate) afforded pure product, **1o** in 98% yield (391 mg). **1o**: ¹H NMR (CDCl₃, 400 MHz): δ 7.46 (1H, t, J 0.8 Hz, H-5'), 7.22 (1H, quin., J 1.7 Hz, H-4), 7.00 (1H, quin., J 1.7 Hz, H-5), 3.58 (2H, t, J 6.3 Hz, CH₂), 2.91 (2H, dt, J 0.7, 7.2 Hz, CH₂), 2.20–2.14 (2H, m, CH₂), 2.10 (3H, t, J 1.7 Hz, CH₃); ¹³C NMR (CDCl₃, 100 MHz): δ 170.5 (CO), 147.5 (C), 140.9 (CH, C-4), 134.9 (C), 119.7 (CH, C-5'), 84.8 (CH, C-5), 44.0 (CH₂), 31.5 (CH₂), 22.5 (CH₂), 10.8 (CH₃); HRMS *m/z* ([M + Na]⁺) calcd for C₁₀H₁₂O₂N₃ClNa 264.05103, found 264.05081.

3-[1-(4-Methyl-5-oxo-2,5-dihydrofuran-2-yl)-1H-1,2,3-triazol-4-yl]propanoic acid (**1p**). For the reaction 374 mg (2.69 mmol) of 5-azido-3-methyl-2(5H)-furanone was used. Purification by column chromatography (gradient 100/0 to 96/4, v/v, CHCl₃/methanol) afforded pure product, **1p** in 73% yield (468 mg). **1p**: ¹H NMR (CD₃OD, 400 MHz): δ 7.92 (1H, t, J 0.8 Hz, H-5'), 7.37 (1H, quin., J 1.7 Hz, H-4), 7.17 (1H, quin., J 1.7 Hz, H-5), 3.00 (2H, t, J 7.4 Hz, CH₂), 2.69 (2H, t, J 7.4 Hz, CH₂), 2.05 (3H, t, J 1.7 Hz, CH₃); ¹³C NMR (CD₃OD, 100 MHz): δ 175.9 (CO), 172.7 (CO), 148.7 (C), 143.1 (CH, C-4), 135.5 (C), 122.6 (CH, C-5'), 86.5 (CH, C-5), 34.0 (CH₂), 31.5 (CH₂), 21.8 (CH₂), 10.6 (CH₃); HRMS *m/z* ([M + H]⁺) calcd for C₁₀H₁₂O₄N₃ 238.08223, found 238.08211.

3-Methyl-5-[4-(prop-1-en-2-yl)-1H-1,2,3-triazol-1-yl]furan-2(5H)-one (**1r**). For the reaction 186 mg (1.34 mmol) of 5-azido-3-methyl-2(5H)-furanone was used. Purification by column chromatography (gradient 3/1 to 3/2, v/v, petroleum ether/ethyl acetate) afforded pure product, **1r** in 96% yield (263 mg). **1r**: ^1H NMR (CDCl_3 , 400 MHz): δ 7.55 (1H, s, H-5'), 7.22 (1H, quin., J 1.7 Hz, H-4), 7.02 (1H, quin., J 1.7 Hz, H-5), 5.79 (1H, t, J 1.2 Hz, CH_2a), 5.17 (1H, q, J 1.6 Hz, CH_2b), 2.12–2.11 (6H, m, $2 \times \text{CH}_3$); ^{13}C NMR (CDCl_3 , 100 MHz): δ 170.5 (CO), 149.7 (C), 141.0 (CH, C-4), 134.9 (C), 132.6 (C), 117.8 (CH, C-5'), 113.9 (CH_2), 84.9 (CH, C-5), 20.5 (CH_2), 20.5 (CH_2), 10.9 (CH_3), 10.9 (CH_3); HRMS m/z ($[\text{M} + \text{H}]^+$) calcd for $\text{C}_{10}\text{H}_{12}\text{O}_2\text{N}_3$ 206.09240, found 206.09241.

5-[4-(3-Hydroxypentan-3-yl)-1H-1,2,3-triazol-1-yl]-3-methylfuran-2(5H)-one (**1s**). For the reaction 411 mg (2.95 mmol) of 5-azido-3-methyl-2(5H)-furanone was used. Purification by column chromatography (gradient 7/3 to 1/1, v/v, petroleum ether/ethyl acetate) afforded pure product, **1s** in 85% yield (631 mg). **1s**: ^1H NMR (CDCl_3 , 400 MHz): δ 7.53 (1H, s, H-5'), 7.22 (1H, quin., J 1.7 Hz, H-4), 7.02 (1H, quin., J 1.7 Hz, H-5), 2.11 (3H, t, J 1.7 Hz, CH_3), 2.00–1.80 (4H, m, $2 \times \text{CH}_2$), 0.82 (6H, t, J 7.4 Hz, $2 \times \text{CH}_3$); ^{13}C NMR (CDCl_3 , 100 MHz): δ 170.5 (CO), 154.4 (C), 141.0 (CH, C-4), 134.9 (C), 132.6 (C), 119.3 (CH, C-5'), 84.9 (CH, C-5), 74.2 (C), 33.7 (CH_2), 33.6 (CH_2), 10.8 (CH_3), 7.7 (CH_3), 7.7 (CH_3); HRMS m/z ($[\text{M} + \text{Na}]^+$) calcd for $\text{C}_{12}\text{H}_{17}\text{O}_3\text{N}_3\text{Na}$ 274.11621, found 274.11629.

2-[1-(4-Methyl-5-oxo-2,5-dihydrofuran-2-yl)-1H-1,2,3-triazol-4-yl]ethyl 2-bromo-2-methylpropanoate (**1t**). For the reaction 270 mg (1.94 mmol) of 5-azido-3-methyl-2(5H)-furanone was used. Purification by column chromatography (gradient 2/1 to 1/1, v/v, petroleum ether/ethyl acetate) afforded pure product, **1t** in 87% yield (605 mg). **1t**: ^1H NMR (CDCl_3 , 400 MHz): δ 7.63 (1H, t, J 0.7 Hz, H-5'), 7.20 (1H, quin., J 1.7 Hz, H-4), 7.01 (1H, quin., J 1.7 Hz, H-5), 4.44 (2H, t, J 6.3 Hz, CH_2), 3.16 (2H, dt, J 0.8, 6.3 Hz, CH_2), 2.09 (3H, t, J 1.7 Hz, CH_3), 0.91 (6H, s, $2 \times \text{CH}_3$); ^{13}C NMR (CDCl_3 , 100 MHz): δ 171.3 (CO), 170.4 (CO), 145.0 (C), 140.9 (CH, C-4), 134.9 (C), 120.6 (CH, C-5'), 84.8 (CH, C-5), 64.3 (CH_2), 56.0 (C), 30.7 (CH_3), 30.7 (CH_3), 25.1 (CH_2), 10.8 (CH_3); HRMS m/z ($[\text{M} + \text{H}]^+$) calcd for $\text{C}_{13}\text{H}_{17}\text{O}_4\text{N}_3\text{Br}$ 358.03970, found 358.03978.

5-[4-(Cyclohexylmethyl)-1H-1,2,3-triazol-1-yl]-3-methylfuran-2(5H)-one (**1u**). For the reaction 370 mg (2.66 mmol) of 5-azido-3-methyl-2(5H)-furanone was used. Purification by column chromatography (gradient 3/1 to 2/1, v/v, petroleum ether/ethyl acetate) afforded pure product, **1u** in 92% yield (637 mg). **1u**: ^1H NMR (CDCl_3 , 400 MHz): δ 7.36 (1H, t, J 0.7 Hz, H-5'), 7.22 (1H, quin., J 1.7 Hz, H-4), 6.99 (1H, quin., J 1.7 Hz, H-5), 2.59 (2H, d, J 6.8 Hz, CH_2), 2.10 (3H, t, J 1.7 Hz, CH_3), 1.71–1.65 (5H, m, CH_2), 1.64–1.57 (1H, m, CH), 1.29–1.12 (3H, m, CH_2), 0.99–0.88 (2H, m, CH_2); ^{13}C NMR (CDCl_3 , 100 MHz): δ 170.6 (CO), 148.1 (C), 141.1 (CH, C-4), 134.7 (C), 119.7 (CH, C-5'), 84.8 (CH, C-5), 37.9 (CH), 33.2 (CH_2), 32.9 (CH_2), 26.2 (CH_2), 26.1 (CH_2), 10.8 (CH_3); HRMS m/z ($[\text{M} + \text{H}]^+$) calcd for $\text{C}_{14}\text{H}_{20}\text{O}_2\text{N}_3$ 262.15500, found 262.15503.

3-Methyl-5-(4-phenethyl-1H-1,2,3-triazol-1-yl)furan-2(5H)-one (**1v**). For the reaction 160 mg (1.15 mmol) of 5-azido-3-methyl-2(5H)-furanone was used. Purification by column chromatography (gradient 7/3 to 6/4, v/v, petroleum ether/ethyl acetate) afforded pure product, **1v** in 87% yield (270 mg). **1v**: ^1H NMR (CDCl_3 , 400 MHz): δ 7.30–7.27 (2H, m, Ar + H-5'), 7.23–7.19 (2H, m, Ar), 7.19–7.15 (3H, m, Ar + H-4), 6.95 (1H, quin., J 1.7 Hz, H-5), 3.08–2.97 (4H, m, CH_2), 2.09 (3H, t, J 1.7 Hz, CH_3); ^{13}C NMR (CDCl_3 , 100 MHz): δ 170.5 (CO), 148.4 (C), 141.0 (CH, C-4), 140.7 (Ar), 134.8 (C), 128.4 (Ar), 128.4 (Ar), 126.2 (Ar), 119.5 (CH, C-5'), 84.8 (CH, C-5), 35.3 (CH_2), 27.4 (CH_2), 10.8 (CH_3); HRMS m/z ($[\text{M} + \text{H}]^+$) calcd for $\text{C}_{15}\text{H}_{16}\text{O}_2\text{N}_3$ 270.12370, found 270.12381.

5-[4-(3-Ethynylphenyl)-1H-1,2,3-triazol-1-yl]-3-methylfuran-2(5H)-one (**1w**). For the reaction 300 mg (2.16 mmol) of 5-azido-3-methyl-2(5H)-furanone was used. Purification by column chromatography (gradient 3/1 to 3/2, v/v, petroleum ether/ethyl acetate) afforded pure product, **1w** in 85% yield (486 mg). **1w**: ^1H NMR (CDCl_3 , 400 MHz): δ 7.93 (1H, dt, J 0.5, 1.7 Hz, Ar), 7.88 (1H, s, H-5'), 7.84 (1H, ddd, J 1.4, 1.6, 7.8 Hz, Ar), 7.48 (1H, td, J 1.4, 7.8, Ar), 7.40 (1H, dt, J 0.6, 7.8 Hz, Ar), 7.28–7.26 (1H, m, H-4), 7.07 (1H, quin., J 1.7 Hz, H-5), 3.12 (1H, s, CH), 2.13 (3H, t, J 1.7 Hz, CH_3); ^{13}C NMR (CDCl_3 , 100 MHz): δ 170.4 (CO), 147.9 (C), 140.9 (CH, C-4), 135.1 (C), 132.3 (Ar), 129.9 (C), 129.5 (Ar), 129.0 (Ar), 126.2 (Ar), 122.9 (C), 118.2 (CH, C-5'), 85.0 (CH, C-5), 83.0 (C), 77.8 (CH), 10.9 (CH_3); HRMS m/z ($[\text{M} + \text{H}]^+$) calcd for $\text{C}_{15}\text{H}_{12}\text{O}_2\text{N}_3$ 266.09240, found 266.09247.

5,5'-[1,3-Phenylenebis(1H-1,2,3-triazole-4,1-diyl)]bis(3-methylfuran-2(5H)-one) (**1x**). For the reaction 55.0 mg (0.40 mmol) of 5-azido-3-methyl-2(5H)-furanone and 126 mg (0.47 mmol) of **1w** was used. Purification by column chromatography (gradient 1/1 to 1/3, v/v, petroleum ether/ethyl acetate) afforded pure product, **1x** in 97% yield (155 mg). **1x**: ^1H NMR (CDCl_3 , 400 MHz): δ 8.23–8.21 (1H, m, Ar), 7.96 (2H, s, $2 \times \text{H-5'}$), 7.81 (1H, ddd, J 1.2, 1.7, 7.7 Hz, Ar), 7.48 (1H, t, J 7.7, Ar), 7.29–7.26 (2H, m, $2 \times \text{H-4}$), 7.10–7.08 (2H, m, $2 \times \text{H-5}$), 2.14–2.13 (6H, m, $2 \times \text{CH}_3$); ^{13}C NMR (CDCl_3 , 100 MHz): δ 170.5 (CO), 148.2 (C), 141.0 (CH, C-4), 135.2 (C), 130.3 (Ar), 129.7 (Ar), 126.0 (Ar), 123.2 (Ar), 118.5 ($2 \times \text{CH, C-5'}$), 85.0 (CH, C-5), 10.9 (CH_3); HRMS m/z ($[\text{M} + \text{H}]^+$) calcd for $\text{C}_{20}\text{H}_{16}\text{O}_4\text{N}_6\text{Na}$ 427.11252, found 427.11254.

3-Methyl-5-[4-(pyridin-2-yl)-1H-1,2,3-triazol-1-yl]furan-2(5H)-one (**1y**). For the reaction 294 mg (2.11 mmol) of 5-azido-3-methyl-2(5H)-furanone was used. Purification by column chromatography (gradient 1/1 to 3/4, v/v, petroleum ether/ethyl acetate) afforded pure product, **1y** in 98% yield (502 mg). **1y**: ^1H NMR (CDCl_3 , 400 MHz): δ 8.58 (1H, qd, J 0.9, 4.9 Hz, Ar), 8.24 (1H, s, H-5'), 8.18 (1H, td, J 1.1, 7.9 Hz, Ar), 7.80 (1H, dt, J 1.8, 7.7 Hz, Ar), 7.29–7.25 (1H, m, Ar), 7.23 (1H, quin., J 1.7 Hz, H-4), 7.10 (1H, quin., J 1.7 Hz, H-5), 2.12 (3H, t, J 1.7 Hz, CH_3); ^{13}C NMR (CDCl_3 , 100 MHz): δ 170.3 (CO), 149.5 (Ar), 149.3 (Ar), 149.2 (Ar), 140.7 (CH, C-4), 137.1 (Ar), 135.3 (C), 123.4 (Ar), 120.5 (Ar), 120.4 (CH, C-5'), 84.9 (CH, C-5), 10.9 (CH_3); HRMS m/z ($[\text{M} + \text{H}]^+$) calcd for $\text{C}_{12}\text{H}_{11}\text{O}_2\text{N}_4$ 243.08765, found 243.08772.

2.5 Hydrolytic stability

A 100 mM stock solution of compound **1b** in methanol was prepared. Then, both phosphate–citrate buffer of pH 5 and Sørensen phosphate buffer of pH 8 were prepared. In a vial, 10 μL of a stock solution were dissolved in 990 μL of buffer and the vial was kept at 25 °C. The stability of the compound was measured by HPLC/UV after 1, 2, 3, 5, 7 and 10 h and 1, 2, 3, 5, 7, 10 and 14 days on C18 column (Phenomenex Luna 5 μm , 250 \times 4.6 mm) at 230 nm with 40 min gradient of 25–100% AcCN in water.

3 RESULTS

Triazolidine strigolactone mimics (**1a–1h**) were prepared previously¹⁹ as potent activators of *Arabidopsis* root growth. This first series was later tested for its ability to induce seed germination of parasitic plants *Striga hermonthica* and *Phelipanche ramosa*. Both species showed great viability in the germination assay with maximal germination rate of 70% and 90%, respectively. On *S. hermonthica*, except for one compound, **1e**, which induced seed germination with $\text{EC}_{50} = 7.4 \times 10^{-7} \text{ M}$, all the other compounds were inactive at concentrations below micromolar

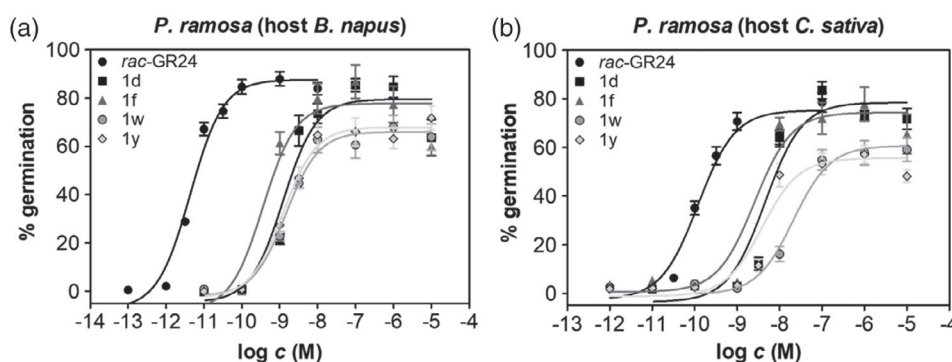


Figure 1. Stimulation of seed germination showing the ability of triazole mimics to stimulate seed germination almost to the same extent as GR24 on: (a) *P. ramosa* (host *B. napus*); and (b) *P. ramosa* (host *C. sativa*).

level (10^{-6} M). On the contrary, most of the compounds were excellently active in *P. ramosa* assay, with two compounds (**1d** and **1f**) exerting the highest activity. These two compounds were able to induce *P. ramosa* seed germination at nanomolar level, which was only two orders of magnitude lower than that of GR24 (Table 1).

In order to further explore the influence of triazole substitution on the activity of strigolactone mimics and possibly increase their activity in seed germination, two new series of triazole strigolactone mimics were synthesized. In the first series, the phenyl substituent was replaced by cycloalkane rings with different number of atoms. In the second series, aliphatic chain substituents were used instead. Also, three compounds (**1w**–**1y**) not belonging to any of these series were synthesized additionally. These three compounds carried an aromatic substituent. All the newly synthesized compounds were evaluated for their effect on the growth of *Arabidopsis thaliana* roots and for their ability to induce seed germination of parasitic weeds *S. hermonthica* and *P. ramosa*.

On *A. thaliana*, the compounds were tested at 1, 10 and 100 μ M concentration as previously described for the aromatic triazole mimics,¹⁹ however, none of the compounds induced root growth at the two lowest concentration. Only the toxic effect of high concentration could be observed (data not shown).

In the case of effect on seed germination, the activity of newly synthesized triazole mimics corresponded to the activity of the previously synthesized aromatic triazoles. Thus, the new compounds were found inactive on *S. hermonthica* below micromolar concentration and their activity on *P. ramosa* varied with their substitution pattern. Two polar compounds with free primary hydroxyl or carboxylic acid substituent were found inactive ($EC_{50} = >1.00 \times 10^{-5}$ M). Most of the other compounds exerted EC_{50} activity around 10^{-7} – 10^{-8} M (Table 1). Therefore, the activity of the compounds was dependent on the structure and polarity of the triazole substituent. The EC_{50} values were increasing with the size of the aliphatic chain or ring, whereas they were decreasing with its polarity. Thus, the most active compounds found were **1w** and **1y** carrying an aromatic substituent (Table 1). The triazole mimics stimulated seed germination of *P. ramosa* almost to the same extent as GR24 (cca 60–80% Fig. 1).

The hydrolytic stability of strigolactone analogues is another key factor in determining their success rate as potential suicidal germinators. The stability of herein synthesized triazole mimics was tested at pH 5 and 8 with compound **1b** as their representative. Compound **1b** was very stable at pH 5, when 22% of the compound was hydrolyzed after 14 days. On the other hand, in alkaline environment (pH 8), the compound was completely hydrolyzed after 10 h.

4 DISCUSSION

The hereby synthesized triazole mimics were found inactive in *A. thaliana* root growth assay. It may be possible that aromatic triazoles are better accommodated within the catalytic site of the enzyme than triazoles with other substituents. The inactivity of the three newly synthesized aromatic triazoles may be explained by either their size forestalling their entrance to the catalytic site (**1x**) or by their electronic properties (**1w** and **1y**) when compared to the most active aromatic triazoles **1b** and **1c**.¹⁹

The simple triazole strigolactone mimics significantly stimulated the germination of *P. ramosa* seeds at nanomolar levels. This bioactivity was found specific for *P. ramosa* as the compounds were not able to induce seed germination of *S. hermonthica*. From the first series, the compounds exerting the highest activity in seed germination assay carried fluorinated substituents on the phenyl ring. This was not very surprising as fluorinated compounds are more lipophilic and thus show increased membrane permeability. In addition, in medicinal chemistry, fluorinated compounds have exerted increased binding affinity to proteins.²⁰ In that case, the electronegativity of fluorine atoms may play a role.

From the other series, the triazoles possessing an aromatic substituent (**1w** and **1y**) exerted again the highest activity towards *P. ramosa* germination. The activity of compound with pyridyl substituent (**1y**) may be explained by increased electron-deficiency of the ring due to presence of nitrogen atom. Such effect is similar to the effect caused by the electronegativity of fluorine substituents. Therefore, the electronic properties of phenyl substituents seem to be important determinants for the ability of compounds to induce *P. ramosa* seed germination.

There are other compounds, especially plant secondary metabolites, which have been studied and exerted activity in inducing broomrape seed germination (isothiocyanates, sesquiterpene lactones, dehydrocostus lactone).^{11,16,21,22} However, most of these compounds caused a response at concentrations well above nanomolar. In addition, plant secondary metabolites are often of complex structure that may forestall their utilization due to complicated synthesis. From these compounds, dehydrocostus lactone was found moderately active in inducing seed germination (EC_{50} cca 1×10^{-5} M) of *P. ramosa*. However, it was more effective on *P. aegyptiaca* and excellently active on *O. cumana* seeds.^{23,24} From synthetic compounds, phthalimide strigolactone mimics have been reported to be efficient in inducing seed germination of broomrapes.²⁵ The mimics were tested on four broomrape species – *O. cumana*, *O. minor*, *P. aegyptiaca* and *P. ramosa*. Much higher concentrations of the mimics were needed to induce seed germination in *Orobanch* species (EC_{50} values around

Table 1. The activity of triazole strigolactone mimics with various substituents in germination assays. ('Bn' stands for *Brassica napus*, 'Cs' for *Cannabis sativa*).

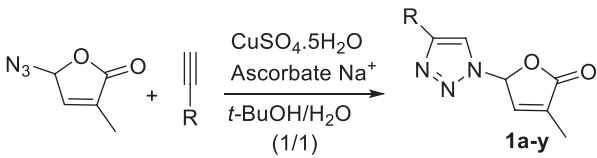
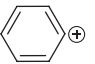
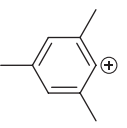
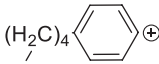
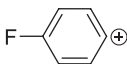
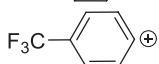
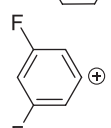
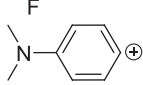


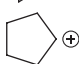
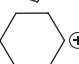
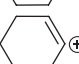
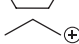
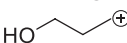
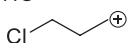
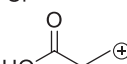
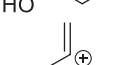
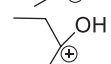
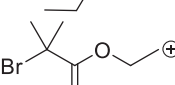
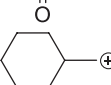
							
Compound	Substituent (R)	<i>Phelipanche ramosa</i> (Bn)		<i>Phelipanche ramosa</i> (Cs)		<i>Striga hermonthica</i>	
		EC ₅₀ (M)	SE (M)	EC ₅₀ (M)	SE (M)	EC ₅₀ (M)	SE (M)
1a		6.50×10^{-9}	2.50×10^{-9}	2.40×10^{-8}	5.80×10^{-9}	$>1.00 \times 10^{-5}$	$>1.00 \times 10^{-5}$
1b		2.40×10^{-8}	5.30×10^{-9}	3.00×10^{-8}	1.90×10^{-8}	$>1.00 \times 10^{-5}$	$>1.00 \times 10^{-5}$
1c		$>1.00 \times 10^{-5}$	$>1.00 \times 10^{-5}$	$>1.00 \times 10^{-5}$	$>1.00 \times 10^{-5}$	$>1.00 \times 10^{-5}$	$>1.00 \times 10^{-5}$
1d		1.60×10^{-9}	1.90×10^{-10}	5.60×10^{-9}	5.20×10^{-10}	1.40×10^{-6}	4.60×10^{-7}
1e		5.10×10^{-9}	7.10×10^{-10}	8.20×10^{-8}	1.70×10^{-8}	7.40×10^{-7}	3.70×10^{-7}
1f		5.20×10^{-10}	8.00×10^{-11}	4.50×10^{-9}	4.10×10^{-9}	3.00×10^{-6}	2.60×10^{-7}
1g		3.10×10^{-8}	1.80×10^{-8}	3.80×10^{-7}	1.30×10^{-7}	$>1.00 \times 10^{-5}$	$>1.00 \times 10^{-5}$
1h		1.00×10^{-6}	1.30×10^{-7}	4.90×10^{-7}	1.90×10^{-8}	3.00×10^{-6}	2.90×10^{-6}
1i		1.50×10^{-7}	4.40×10^{-8}	1.30×10^{-7}	2.80×10^{-8}	$>1.00 \times 10^{-5}$	$>1.00 \times 10^{-5}$
1j		2.10×10^{-8}	5.20×10^{-9}	7.10×10^{-8}	1.80×10^{-8}	$>1.00 \times 10^{-5}$	$>1.00 \times 10^{-5}$
1k		1.70×10^{-8}	1.10×10^{-8}	6.40×10^{-8}	2.50×10^{-8}	$>1.00 \times 10^{-5}$	$>1.00 \times 10^{-5}$
1l		4.50×10^{-9}	4.10×10^{-9}	3.00×10^{-8}	6.10×10^{-10}	$>1.00 \times 10^{-5}$	$>1.00 \times 10^{-5}$
1m		9.80×10^{-8}	2.80×10^{-8}	1.20×10^{-7}	6.80×10^{-9}	$>1.00 \times 10^{-5}$	$>1.00 \times 10^{-5}$
1n		$>1.00 \times 10^{-5}$	$>1.00 \times 10^{-5}$	2.80×10^{-5}	1.20×10^{-5}	$>1.00 \times 10^{-5}$	$>1.00 \times 10^{-5}$
1o		6.90×10^{-8}	1.50×10^{-8}	7.40×10^{-8}	6.50×10^{-9}	$>1.00 \times 10^{-5}$	$>1.00 \times 10^{-5}$
1p		$>1.00 \times 10^{-5}$	$>1.00 \times 10^{-5}$	$>1.00 \times 10^{-5}$	$>1.00 \times 10^{-5}$	$>1.00 \times 10^{-5}$	$>1.00 \times 10^{-5}$
1r		2.60×10^{-8}	3.20×10^{-9}	2.40×10^{-8}	2.20×10^{-9}	$>1.00 \times 10^{-5}$	$>1.00 \times 10^{-5}$
1s		2.40×10^{-7}	3.20×10^{-8}	4.40×10^{-7}	3.20×10^{-8}	$>1.00 \times 10^{-5}$	$>1.00 \times 10^{-5}$
1t		3.00×10^{-7}	1.60×10^{-9}	1.40×10^{-8}	4.00×10^{-9}	$>1.00 \times 10^{-5}$	$>1.00 \times 10^{-5}$
1u		1.10×10^{-8}	5.40×10^{-9}	7.90×10^{-8}	2.80×10^{-8}	$>1.00 \times 10^{-5}$	$>1.00 \times 10^{-5}$

Table 1. continued

Compound	Substituent (R)	<i>Phelipanche ramosa</i> (Bn)		<i>Phelipanche ramosa</i> (Cs)		<i>Striga hermonthica</i>	
		EC ₅₀ (M)	SE (M)	EC ₅₀ (M)	SE (M)	EC ₅₀ (M)	SE (M)
1v		1.40 × 10 ⁻⁸	4.20 × 10 ⁻⁹	3.20 × 10 ⁻⁸	1.20 × 10 ⁻⁸	>1.00 × 10 ⁻⁵	>1.00 × 10 ⁻⁵
1w		7.70 × 10 ⁻¹⁰	3.80 × 10 ⁻¹⁰	2.00 × 10 ⁻⁸	1.00 × 10 ⁻⁸	2.00 × 10 ⁻⁶	3.80 × 10 ⁻⁷
1x		5.30 × 10 ⁻⁸	1.30 × 10 ⁻⁸	2.60 × 10 ⁻⁸	1.10 × 10 ⁻⁸	>1.00 × 10 ⁻⁵	>1.00 × 10 ⁻⁵
1y		7.40 × 10 ⁻¹⁰	1.80 × 10 ⁻¹⁰	4.60 × 10 ⁻⁹	1.10 × 10 ⁻⁹	>1.00 × 10 ⁻⁵	>1.00 × 10 ⁻⁵
rac-GR24		4.40 × 10 ⁻¹²	1.90 × 10 ⁻¹³	8.70 × 10 ⁻¹¹	5.20 × 10 ⁻¹²	7.50 × 10 ⁻¹¹	8.60 × 10 ⁻¹²
SE, standard error.							

mM levels) than in *Phelipanche* species (EC₅₀ values around μM level), suggesting the responsible *Orobanchae* receptor(s) are more structure-specific, thus may efficiently discriminate the signals for germination. Another type of simple strigolactone mimics, aryloxy butenolides significantly stimulated *P. ramosa* (collected in France) seed germination reaching EC₅₀ around 5 × 10⁻⁸ M. However, the precise evaluation of EC₅₀ is difficult as the results are expressed graphically.²⁶ The activity of these mimics seemed even better towards *P. ramosa* seeds collected in Italy, unfortunately, the response of the seeds within the tested concentration range was relatively inconsistent rendering EC₅₀ estimation impossible.²⁶ On the other hand, similarly to our results, these mimics are easily synthesized and in terms of their activity, it could have been observed that even small changes of structure through its substitution had significant impact on their activity.

The degradation products of glucosinolates exuded by *P. ramosa* host, *Brassica napus*, were recognized as very good germination inducers.⁹ From these, two degradation products, 4-pentenyl isothiocyanate and 2-phenylethyl isothiocyanate were the most active with EC₅₀ around 1.5 × 10⁻⁹ M and 1.5 × 10⁻⁸ M, respectively. Moreover, 2-phenylethyl isothiocyanate did not stimulate seed germination of other tested broomrape species, thus its activity seems selective towards *P. ramosa*. When compared to our triazole mimics, these compounds are also very simple to synthesize though they are slightly less active. On the other hand, the selectivity or broad activity of our triazole mimics within the *Orobanchaceae* family still needs to be established. In spite of that, it is obvious that our triazole strigolactone mimics have their potential to be used as suicidal germinators as their synthesis is high-yielding and very simple and their potency to induce *P. ramosa* seed germination is also excellent with the best compounds reaching EC₅₀ between 5 × 10⁻⁹ M and 5 × 10⁻¹⁰ M.

The hydrolytic stability of triazole strigolactone mimics was very good at pH 5, whereas at pH 8, the compound **1b**, which

was chosen as their representative, was completely hydrolyzed within 10 h. Such stability is a bit lower than the stability of GR24, which is also rapidly hydrolyzed in alkaline environment (1 to 3 days in alkaline soil).^{13,27,28} Thus, the stability of triazole strigolactone mimics may need to be enhanced by their formulation as emulsions in order to be used in alkaline soils. Even though the hydrolysis of the compound under acidic pH was rather slow (22% after 14 days), the results indicate that the triazole mimics will decompose in the soil thus avoiding their accumulation and possible negative effect on the environment. This may be supported by the comparison with the hydrolysis of GR24, which takes about 6 to 8 days in acidic soil, whereas only about 50% of GR24 was hydrolyzed in ethanol: water (1/4) mixture of pH 6.7.²⁷ All in all, the triazole strigolactone mimics have potential to be further studied as suicidal germinators.

5 CONCLUSION

Triazole strigolactone mimics with a variety of substituents were tested for their germination inducing activity on *Striga hermonthica* and *Phelipanche ramosa*. The hereby synthesized compounds were also tested for their potential phytohormonal activity on the root growth of *Arabidopsis thaliana* plants, however, none of these compounds exerted such activity. In addition, except for one compound, the triazole mimics did not induce *Striga* seed germination below micromolar level. On the other hand, most of the compounds induced seed germination of *P. ramosa*. From these, the most active compounds were the ones carrying an electronegative substituent/atom on aromatic ring. Such compounds were able to induce *P. ramosa* seed germination at EC₅₀ concentration as low as 5.2 × 10⁻¹⁰ M. These results, together with simple synthesis, make these compounds an exciting target for their potential utilization as broomrape suicidal germinators. Still, their other

properties, such as stability in soil and toxicology, need to be established.

ACKNOWLEDGEMENTS

The authors gratefully acknowledge the financial support by the grant No. DP072017 from the GAMA program from Technology Agency of the Czech Republic and by the grant LO1204 from the National Program of Sustainability I from the Ministry of Education, Youth and Sports of the Czech Republic. A.H. was supported by the Internal Grant Agency of Palacký University Olomouc (IGA_PrF_2018_023). The authors also would like to express their thanks to Professor Philippe Delavault (Laboratory of Plant Biology and Pathology, University of Nantes, France) who kindly donated the *P. ramosa* seeds, and to Professor Binne Zwanenburg (Department of Organic Chemistry, Institute for Molecules and Materials, Radboud Universiteit, Nijmegen, Netherlands) for the donation of *S. hermonthica* seeds.

SUPPORTING INFORMATION

Supporting information may be found in the online version of this article.

REFERENCES

- 1 Cook CE, Whichard LP, Turner B, Wall ME and Egle GH, Germination of witchweed (*Striga lutea* Lour.): isolation and properties of a potent stimulant. *Science* **154**:1189–1190 (1966).
- 2 Zwanenburg B, Mwakaboko AS, Reizelman A, Anilkumar G and Sethumadhavan D, Structure and function of natural and synthetic signalling molecules in parasitic weed germination. *Pest Manag Sci* **65**:478–491 (2009).
- 3 Midega CAO, Bruce TJA, Pittchar JO, Murage A and Khan ZR, Climate-adapted companion cropping increases agricultural productivity in East Africa. *Field Crop Res* **180**:118–125 (2015).
- 4 Runo S and Kuria EK, Habits of a highly successful cereal killer, *Striga*. *PLoS Pathog* **14**:e1006731 (2018).
- 5 Ejeta G, The *Striga* scourge in Africa: a growing problem in integrating new technologies for *Striga* control, in *Toward Ending the Witch-Hunt*, ed. by Ejeta G and Gressel J. World Scientific Publishing Co., Hackensack, NJ, pp. 3–16 (2007).
- 6 Tasker AV and Westwood JH, The U.S. Witchweed eradication effort turns 50: a retrospective and look-ahead on parasitic weed management. *Weed Sci* **60**:267–268 (2012).
- 7 Parker C, Observations on the current status of *Orobanche* and *Striga* problems worldwide. *Pest Manag Sci* **65**:453–459 (2009).
- 8 Brun G, Braem L, Thoirion S, Gevaert K, Goormachtig S and Delavault P, Seed germination in parasitic plants: what insights can we expect from strigolactone research? *J Exp Bot* **69**:2265–2280 (2018).
- 9 Auger B, Pouvreau J-B, Pouponneau K, Yoneyama K, Montiel G, Le Bizec B et al., Germination stimulants of *Phelipanche ramosa* in the rhizosphere of *Brassica napus* are derived from glucosinolate pathway. *Mol Plant Microbe Interact* **25**:993–1004 (2012).
- 10 Bao YZ, Yao ZQ, Cao XL, Peng JF, Xu Y, Chen MX et al., Transcriptome analysis of *Phelipanche aegyptiaca* seed germination mechanisms stimulated by fluoridone, TIS108, and GR24. *PLoS ONE* **12**:e0187539 (2017).
- 11 Evidente A, Cimmino A, Fernandez-Aparicio M, Rubiales D, Andolfi A and Melck D, Soysapogenol B and trans-22-dehydrocampesterol from common vetch (*Vicia sativa* L.) root exudates stimulate broomrape seed germination. *Pest Manag Sci* **67**:1015–1022 (2011).
- 12 Uraguchi D, Kuwata K, Hijikata Y, Yamaguchi R, Imaizumi H, Sathiyarayanan AM et al., A femtomolar-range suicide germination stimulant for the parasitic plant *Striga hermonthica*. *Science* **362**:1301–1305 (2018).
- 13 Kgosi RL, Zwanenburg B, Mwakaboko AS and Murdoch AJ, Strigolactone analogues induce suicidal seed germination of *Striga* spp. in soil. *Weed Res* **52**:197–203 (2012).
- 14 Samejima H, Babiker AG, Takikawa H, Sasaki M and Sugimoto Y, Practicality of the suicidal germination approach for controlling *Striga hermonthica*. *Pest Manag Sci* **72**:2035–2042 (2016).
- 15 Perez-de-Luque A, Eizenberg H, Grenz JH, Sillero JC, Avila C, Sauerborn J et al., Broomrape management in faba bean. *Field Crop Res* **115**:319–328 (2010).
- 16 Cimmino A, Fernandez-Aparicio M, Avolio F, Yoneyama K, Rubiales D and Evidente A, Ryecyanatines a and B and rye-carbonitrilines a and B, substituted cyanatophenol, cyanatobenzo[1,3]dioxolecarbonitriles from rye (*Secale cereale* L.) root exudates: novel metabolites with allelopathic activity on *Orobanche* seed germination and radicle growth. *Phytochemistry* **109**:57–65 (2015).
- 17 Pouvreau JB, Gaudin Z, Auger B, Lechat M-M, Gauthier M, Delavault P et al., A high-throughput seed germination assay for root parasitic plants. *Plant Methods* **9**:32 (2013).
- 18 Macias FA, Garcia-Diaz MD, Perez-de-Luque A, Rubiales D and Galindo ACG, New chemical clues for broomrape-sunflower host–parasite interactions: synthesis of guaianestrigolactones. *J Agric Food Chem* **57**:5853–5864 (2009).
- 19 Dvorakova M, Soudek P and Vanek T, Triazolide strigolactone mimics influence root development in *Arabidopsis*. *J Nat Prod* **80**:1318–1327 (2017).
- 20 Shah P and Westwell AD, The role of fluorine in medicinal chemistry. *J Enzyme Inhib Med Chem* **22**:527–540 (2007).
- 21 Evidente A, Fernandez-Aparicio M, Cimmino A, Rubiales D, Andolfi A and Motta A, Peagol and peagoldione, two new strigolactone-like metabolites isolated from pea root exudates. *Tetrahedron Lett* **50**:6955–6958 (2009).
- 22 Evidente A, Cimmino A, Fernandez-Aparicio M, Andolfi A, Rubiales D and Motta A, Polyphenols, including the new peapolyphenols A-C, from pea root exudates stimulate *Orobanche fleotida* seed germination. *J Agric Food Chem* **58**:2902–2907 (2010).
- 23 Joel DM, Chaudhuri SK, Plakhine D, Ziadna H and Steffens JC, Dehydrocoster lactone is exuded from sunflower roots and stimulates germination of the root parasite *Orobanche cumana*. *Phytochemistry* **72**:624–634 (2011).
- 24 Cala A, Molinillo JMG, Fernandez-Aparicio M, Ayuso J, Alvarez JA, Rubiales D et al., Complexation of sesquiterpene lactones with cyclodextrins: synthesis and effects on their activities on parasitic weeds. *Org Biomol Chem* **15**:6500–6510 (2017).
- 25 Cala A, Ghooray K, Fernández-Aparicio M, Molinillo JMG, Galindo JCG, Rubiales D et al., Phthalimide-derived strigolactone mimics as germinating agents for seeds of parasitic weeds. *Pest Manag Sci* **72**:2069–2081 (2016).
- 26 Zwanenburg B, Nayak SK, Charnikhova TV and Bouwmeester HJ, New strigolactone mimics: structure-activity relationship and mode of action as germinating stimulants for parasitic weeds. *Bioorg Med Chem Lett* **23**:5182–5186 (2013).
- 27 Zwanenburg B and Pospisil T, Structure and activity of strigolactones: new plant hormones with a rich future. *Mol Plant* **6**:38–62 (2013).
- 28 Babiker AGT, Hamdoun AM, Rudwan A, Mansi NG and Faki HH, Influence of soil moisture on activity and persistence of the strigol analogue GR24. *Weed Res* **27**:173–178 (1987).

Triazolide strigolactone mimics as potent selective germinators of parasitic plant *Phelipanche ramosa*.

Marcela Dvorakova,^{a,*} Adela Hylova,^b Petr Soudek,^a Sarka Petrova,^a Lukas Spichal,^b Tomas Vanek^a

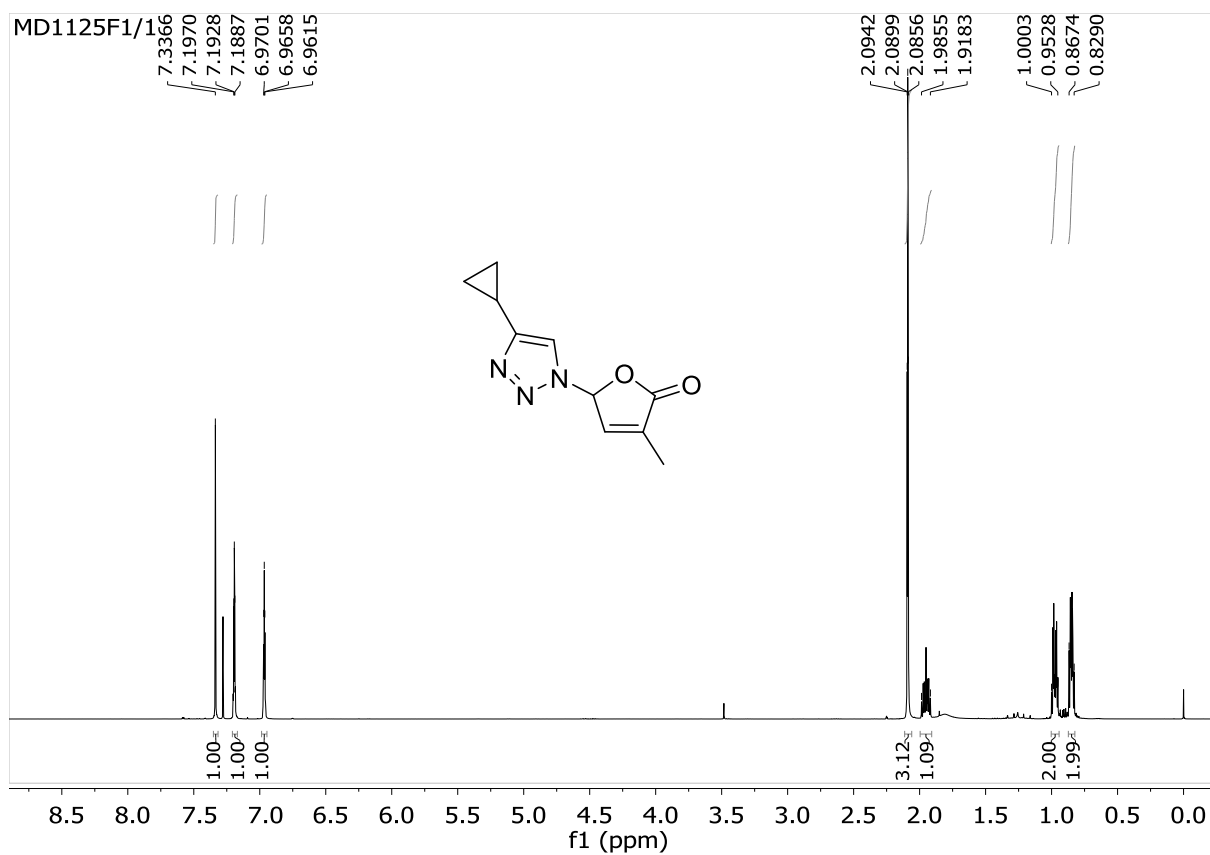
^aLaboratory of Plant Biotechnologies, The Czech Academy of Sciences, Institute of Experimental Botany, Rozvojova 263, 16502, Prague 6, Czech Republic

^bPalacky University, Faculty of Science, Centre of the Region Hana for Biotechnological and Agricultural Research, Department of Chemical Biology and Genetics, Slechtitelu 241/27, 783 71 Olomouc, Czech Republic

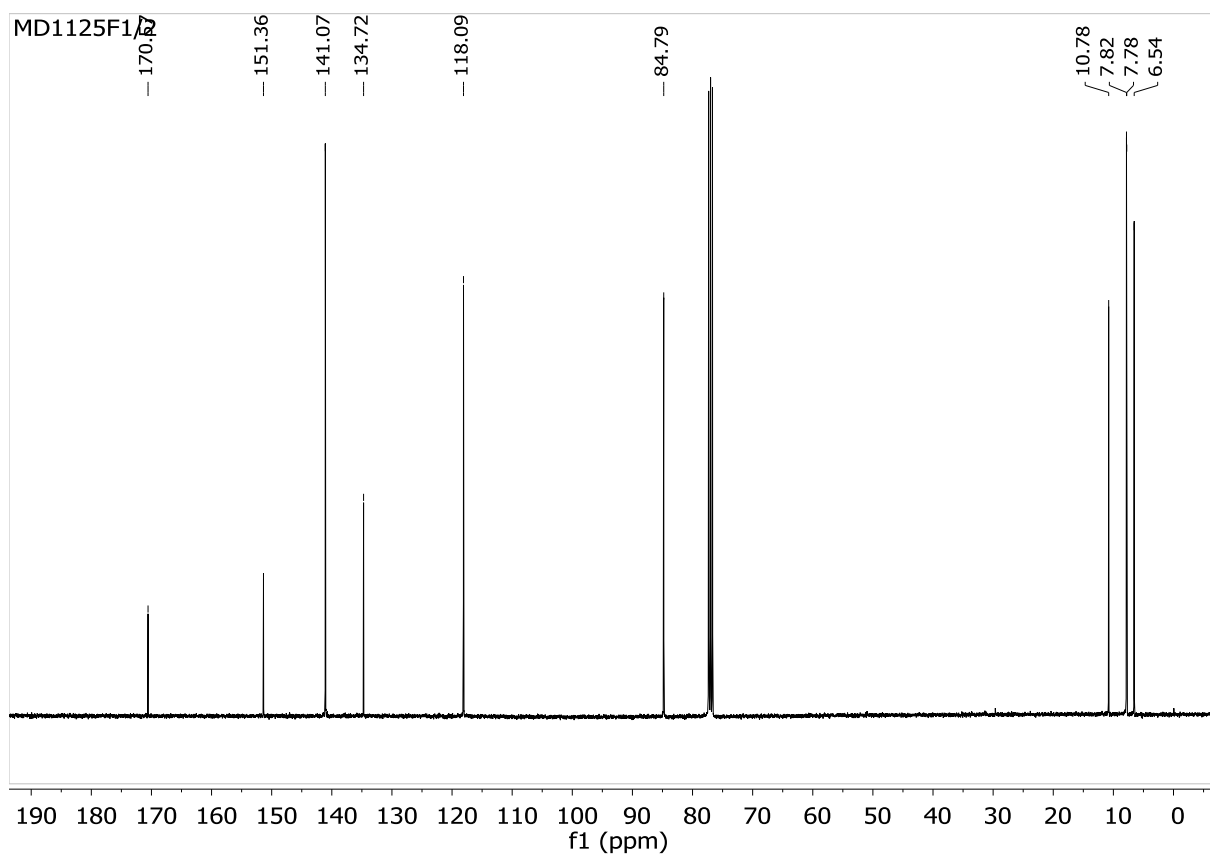
Supporting Information

Table of Contents

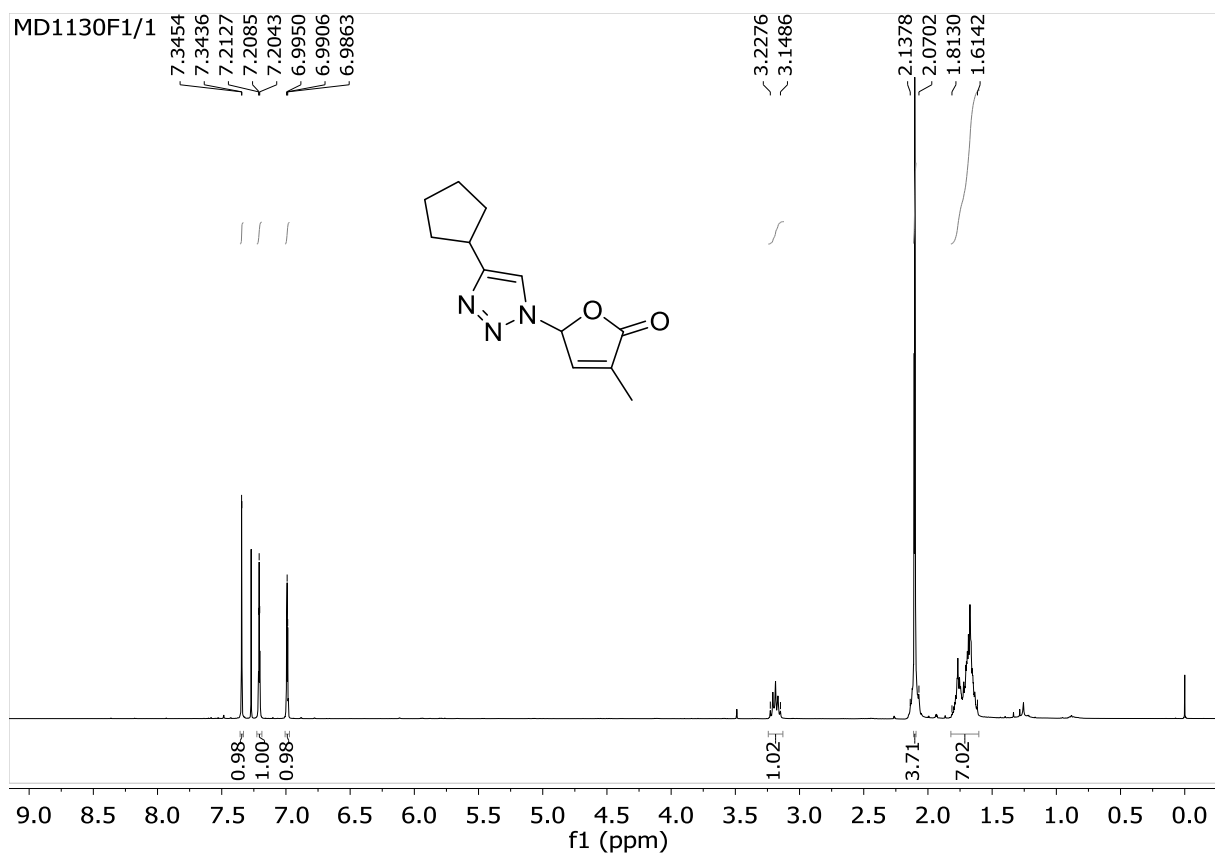
¹ H-NMR and ¹³ C-NMR spectras of compounds 1i-y	S2-17
--	-------



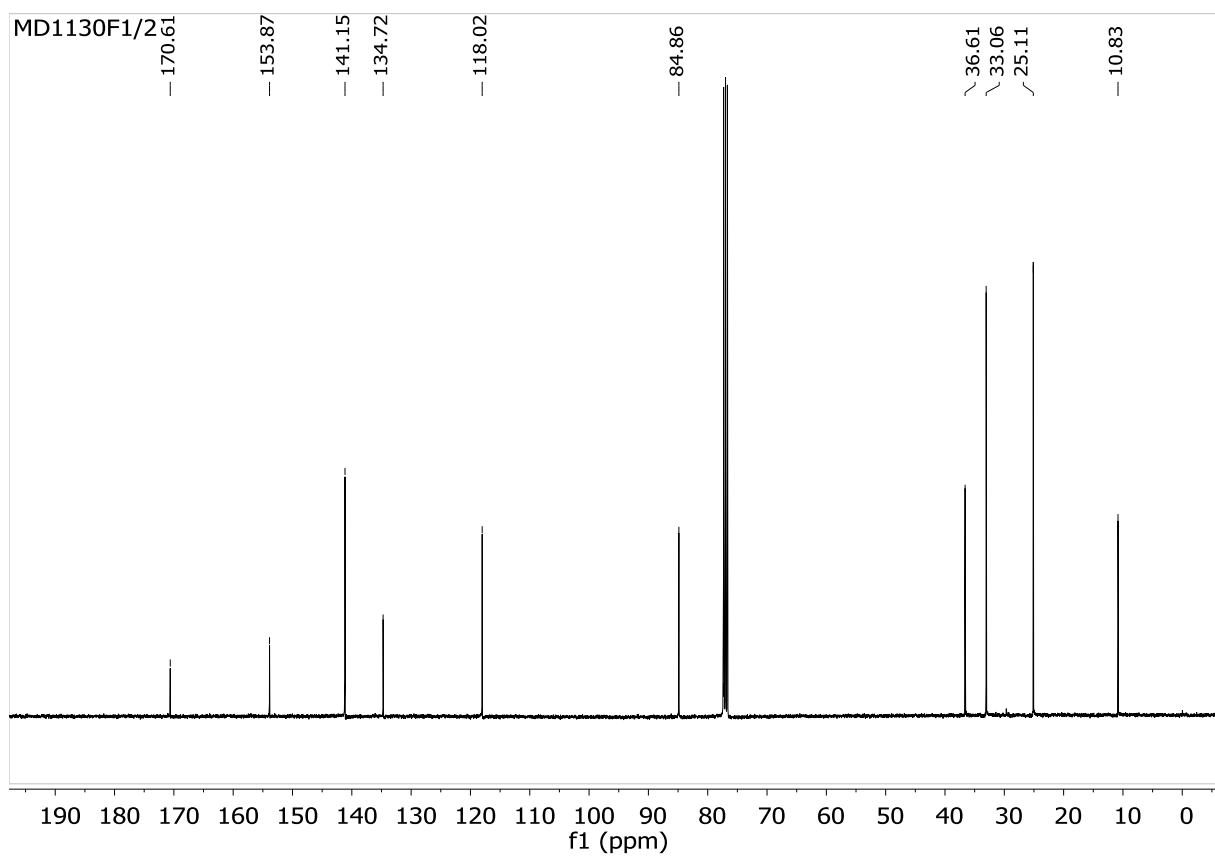
S1. ^1H -NMR (400 MHz, CDCl_3) of compound **1i**



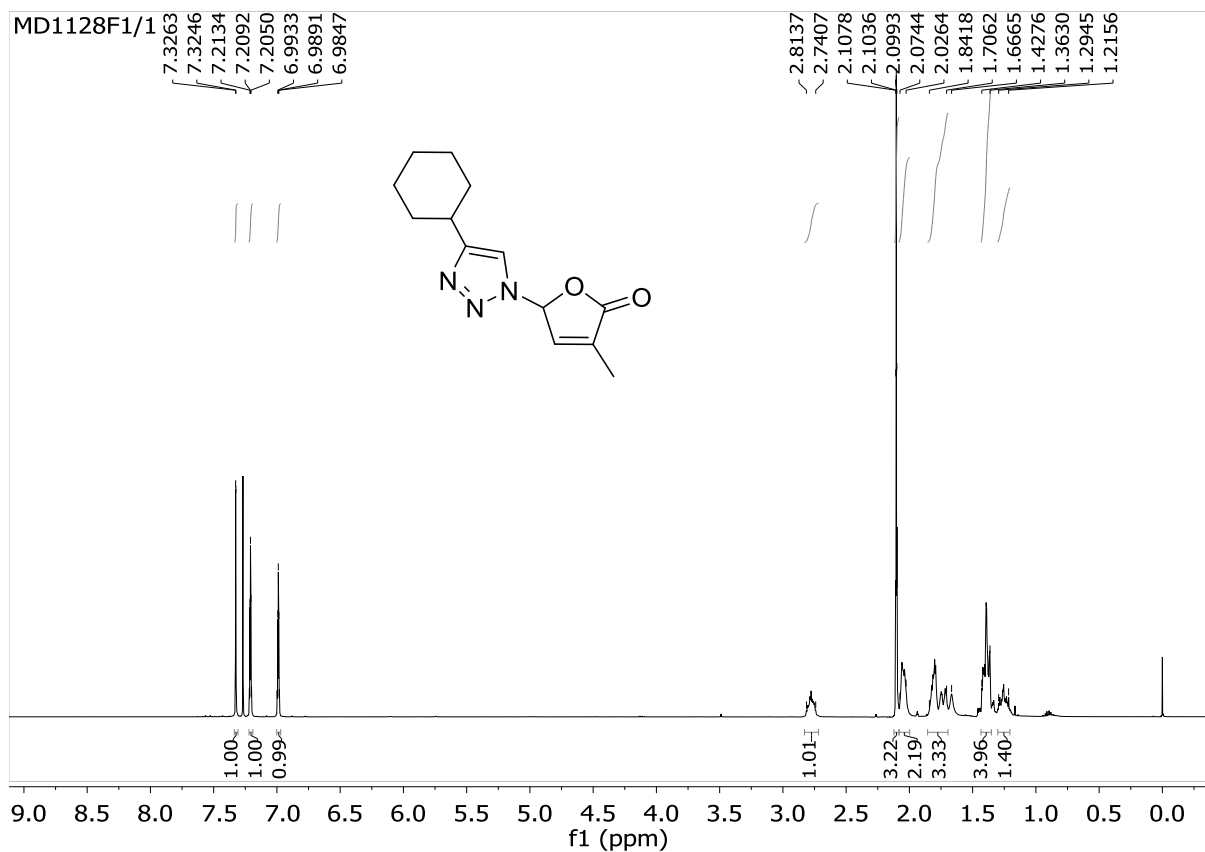
S2. ^{13}C -NMR (100 MHz, CDCl_3) of compound **1i**



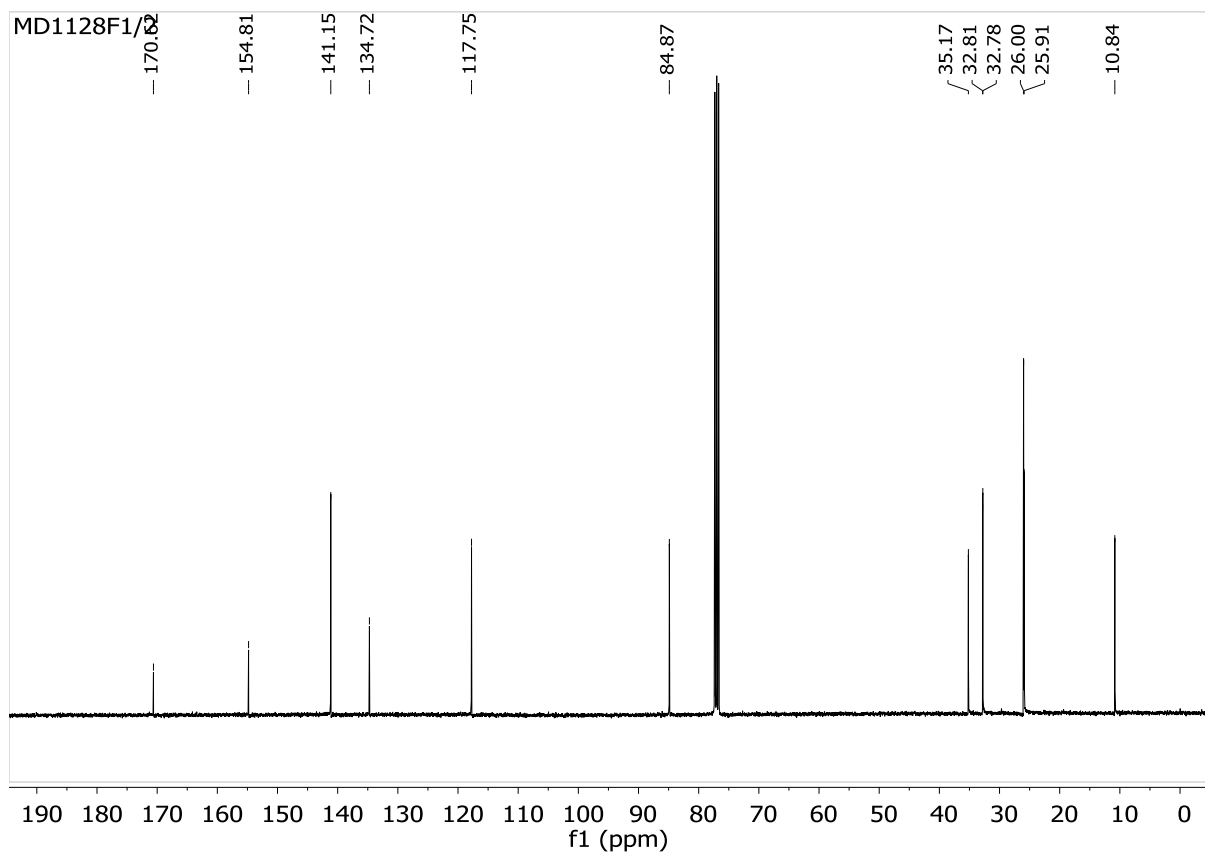
S3. ¹H-NMR (400 MHz, CDCl₃) of compound **1j**



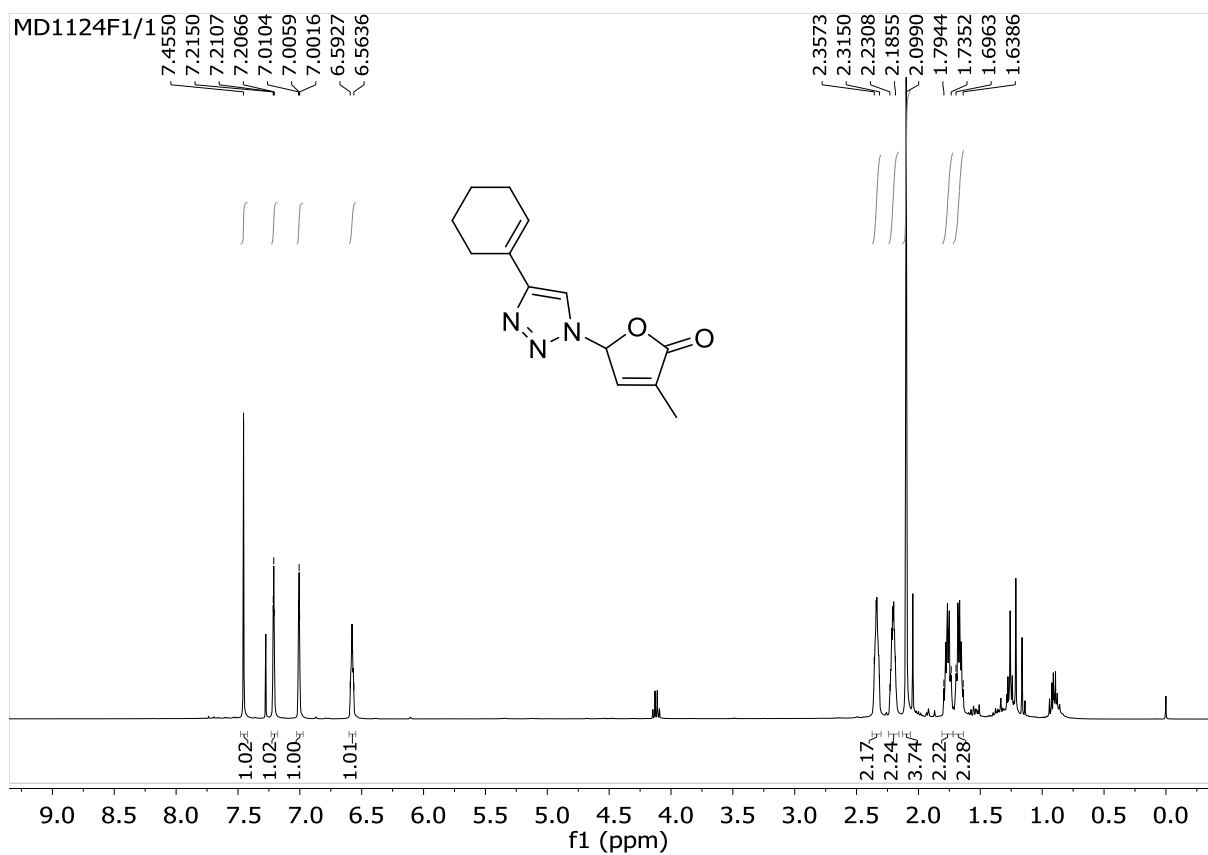
S4. ¹³C-NMR (400 MHz, CDCl₃) of compound **1j**



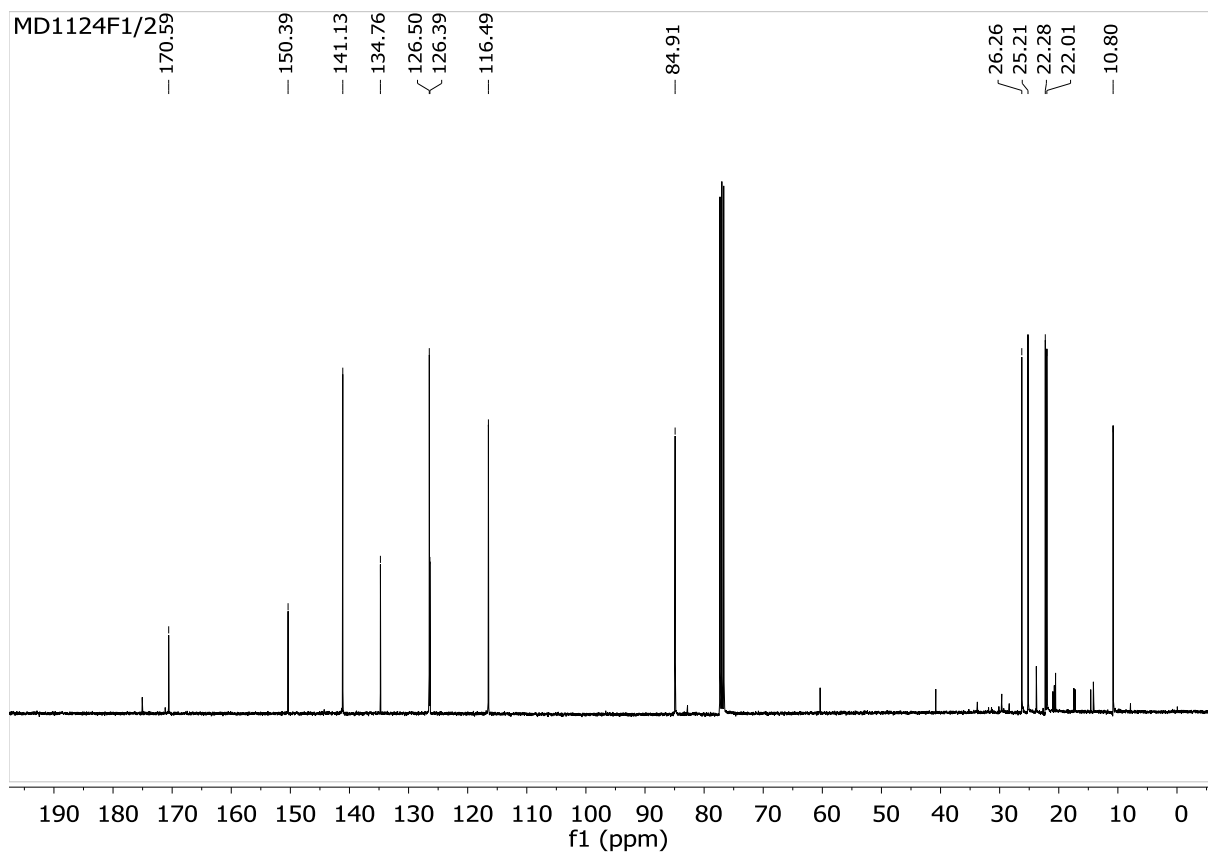
S5. ^1H -NMR (400 MHz, CDCl_3) of compound **1k**



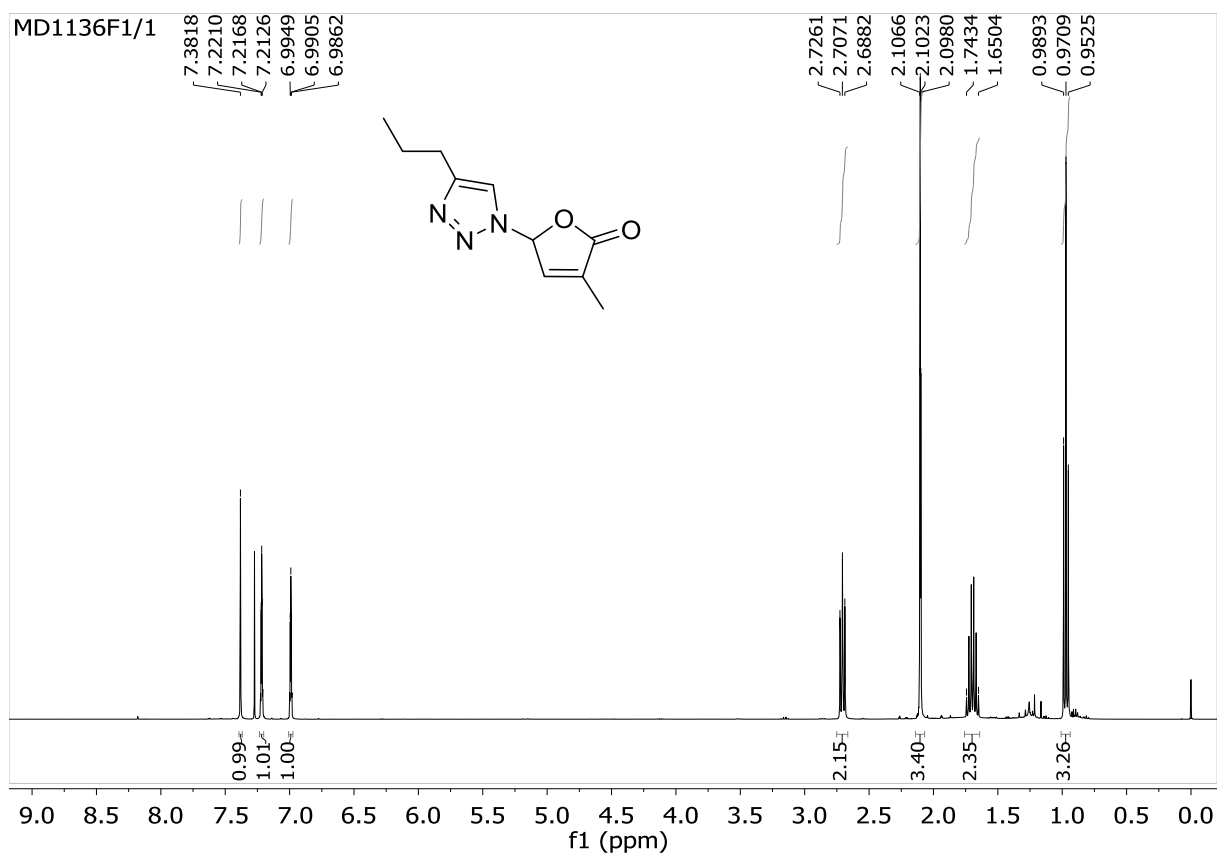
S6. ^{13}C -NMR (400 MHz, CDCl_3) of compound **1k**



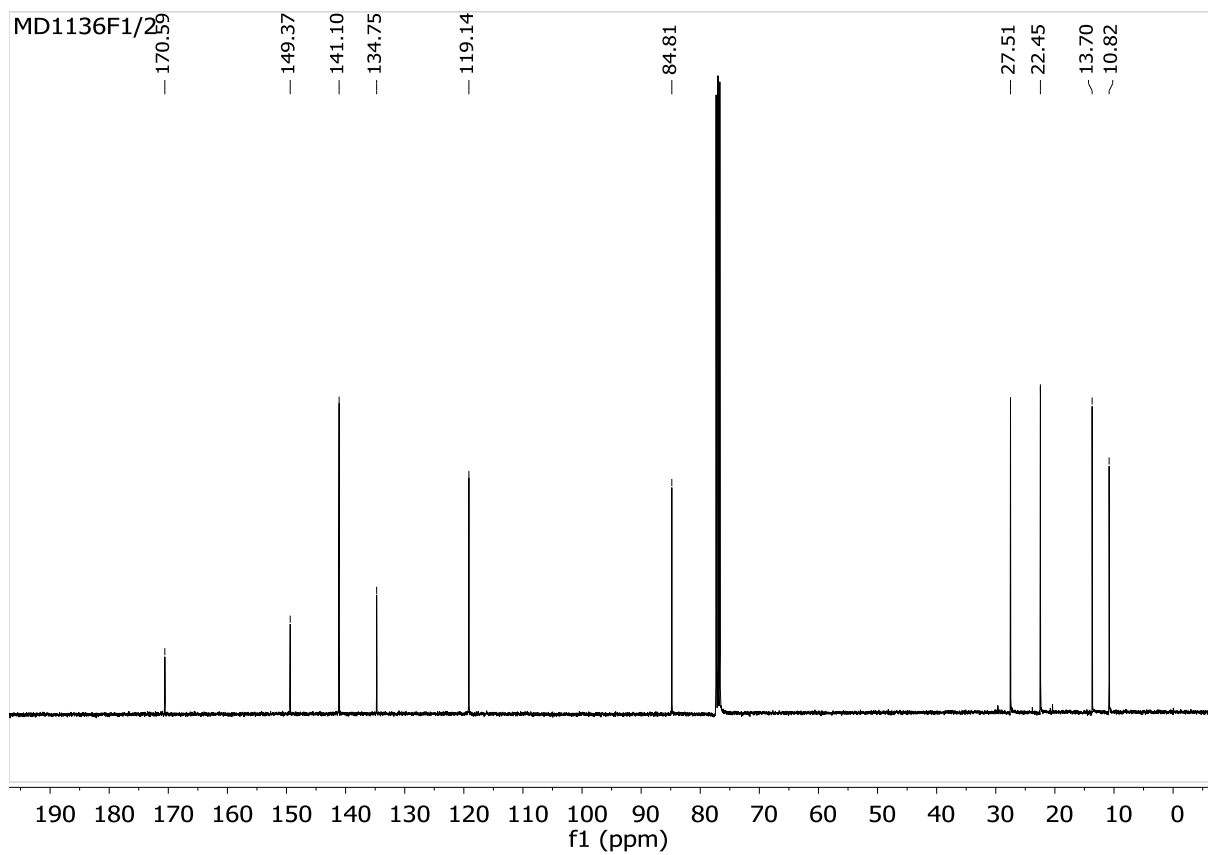
S7. ^1H -NMR (400 MHz, CDCl_3) of compound **11**



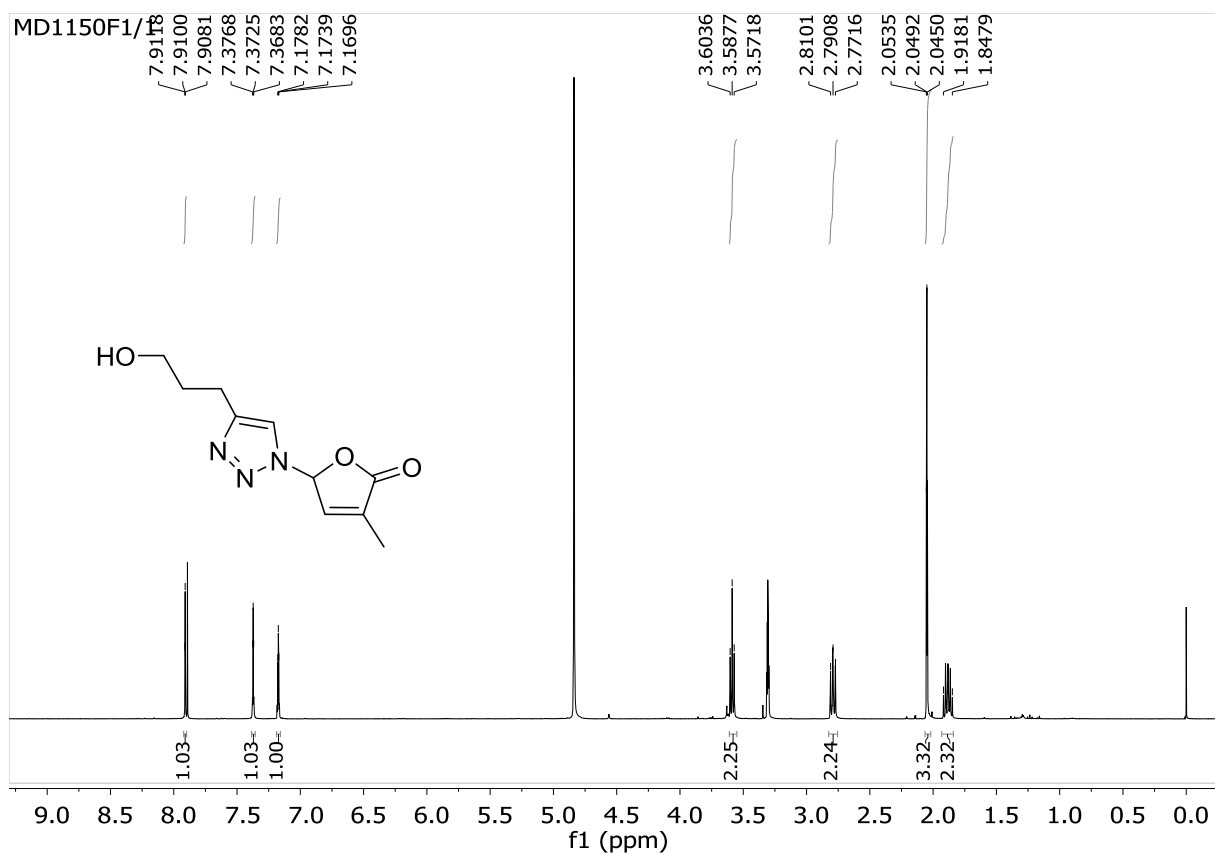
S8. ^{13}C -NMR (400 MHz, CDCl_3) of compound **11**



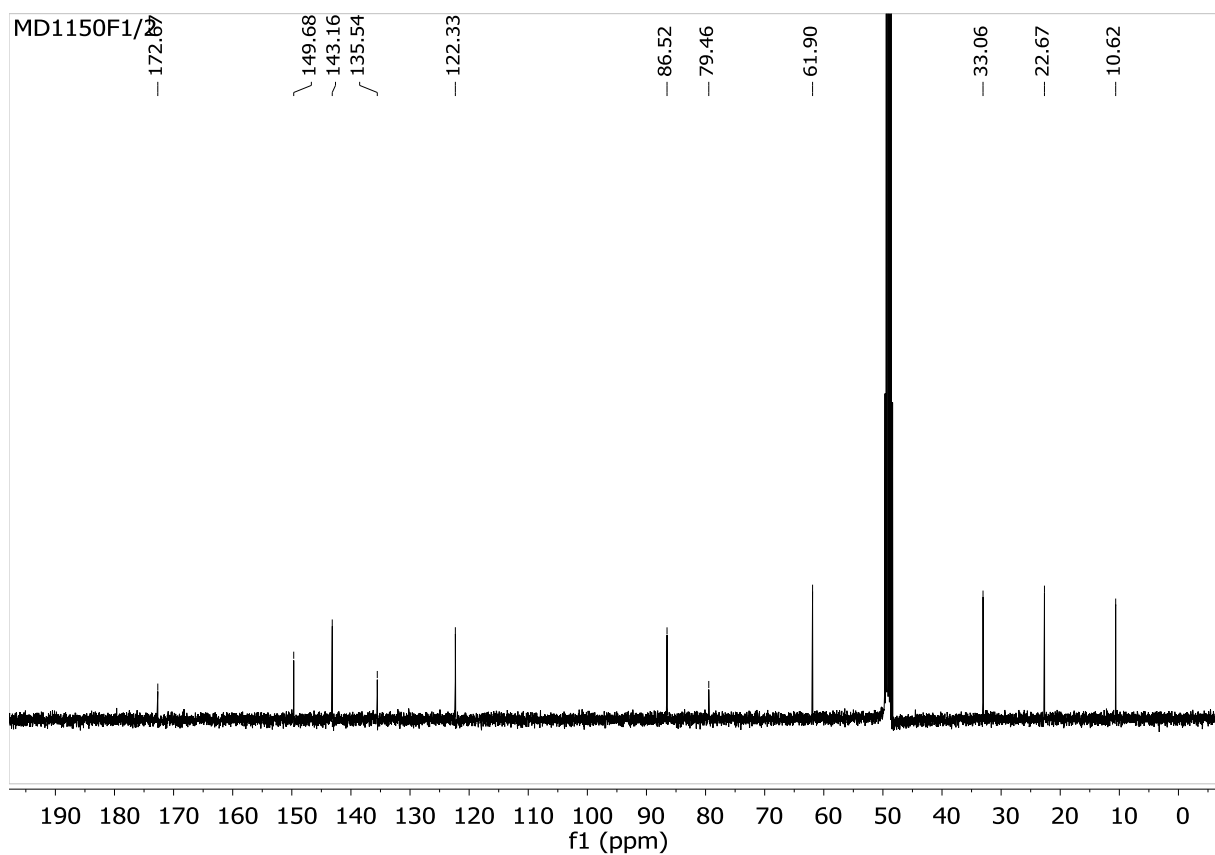
S9. ^1H -NMR (400 MHz, CDCl_3) of compound **1m**



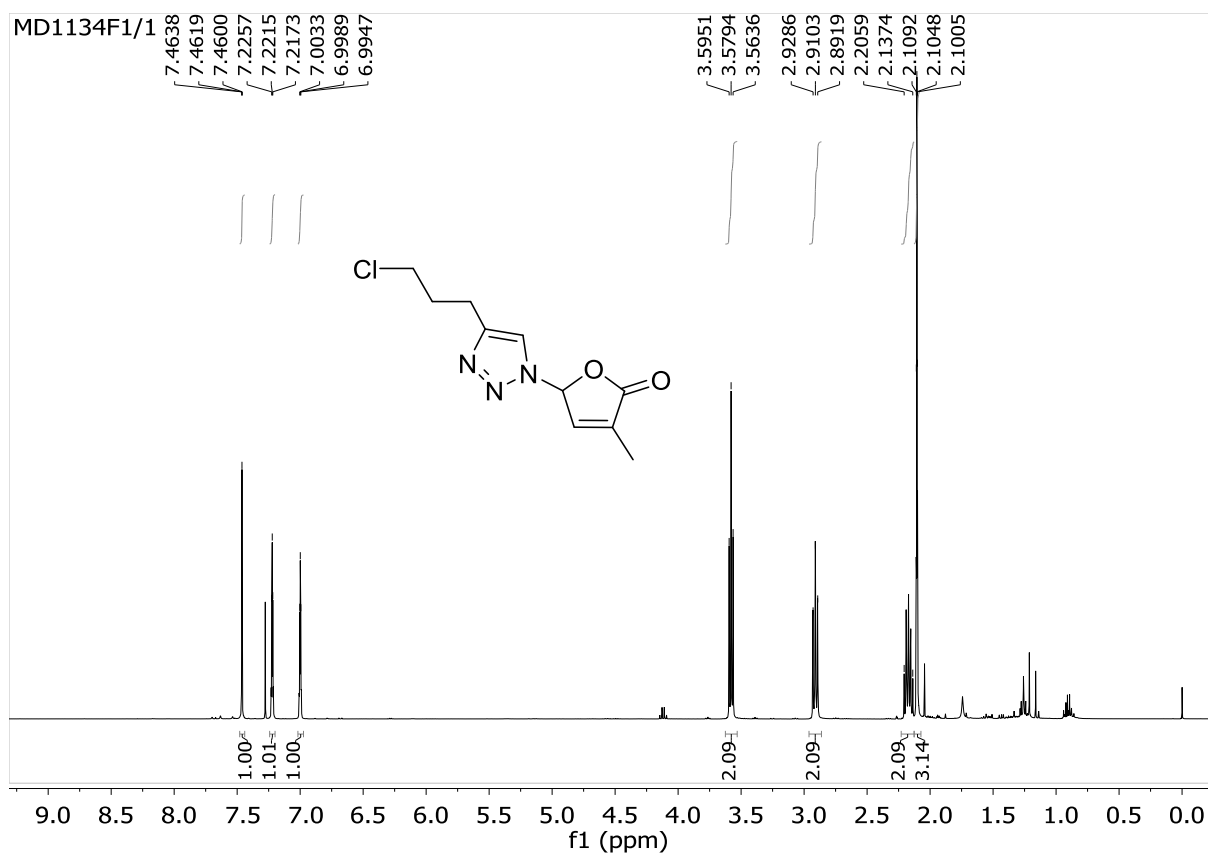
S10. ^{13}C -NMR (400 MHz, CDCl_3) of compound **1m**



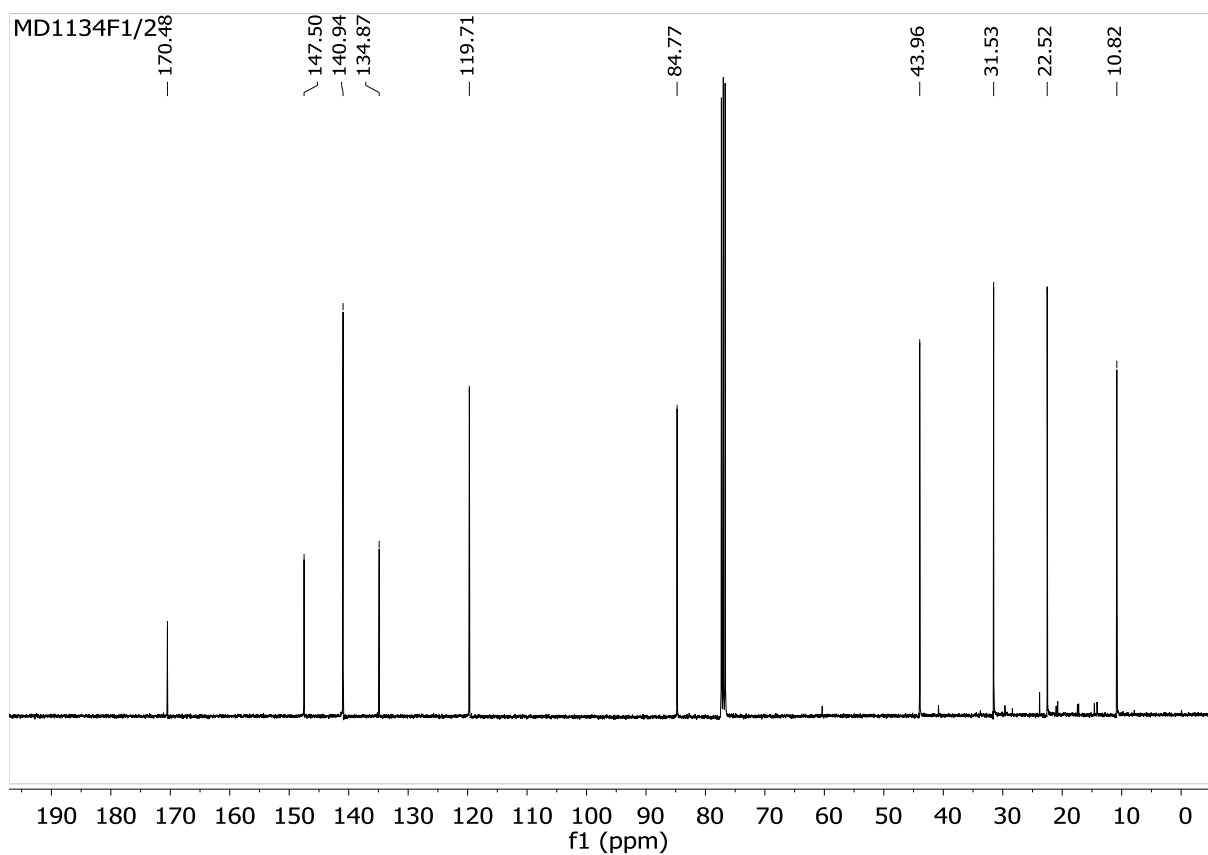
S11. ^1H -NMR (400 MHz, CD_3OD) of compound **1n**



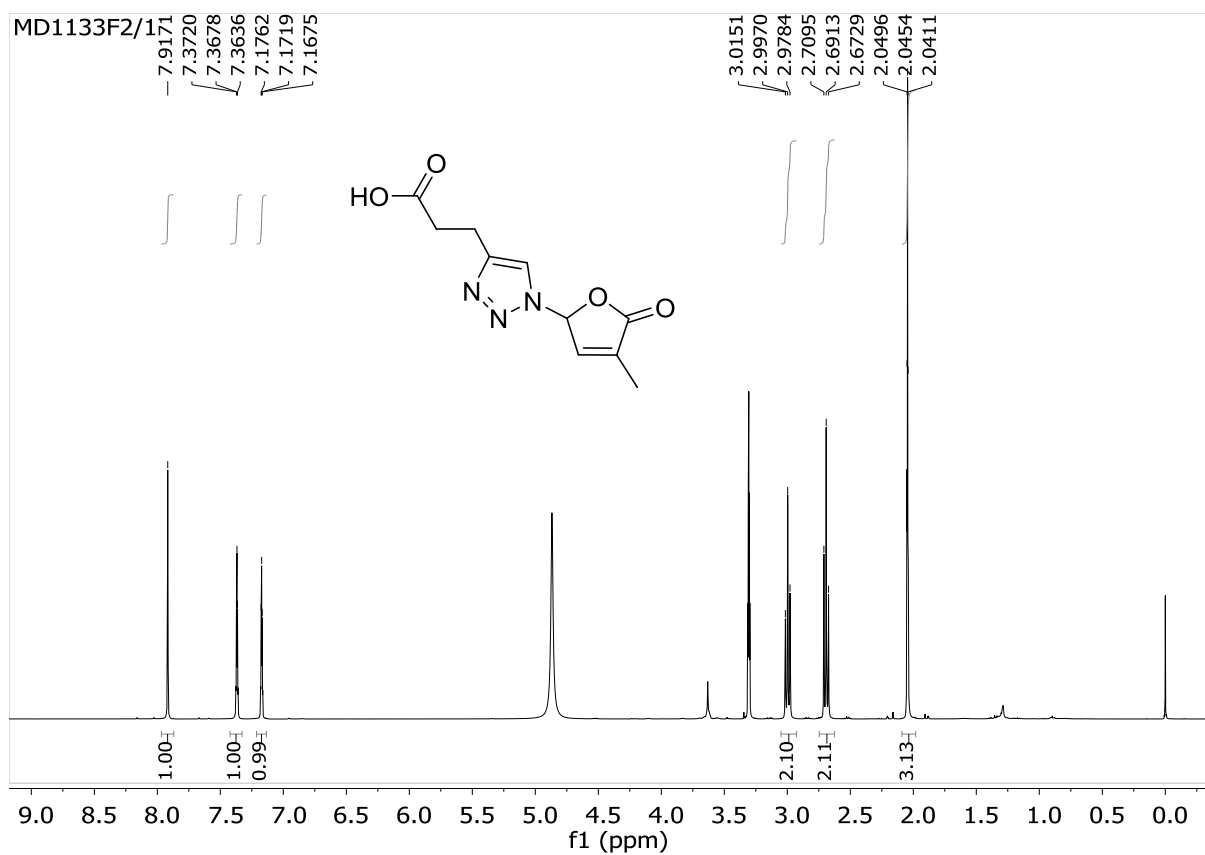
S12. ^{13}C -NMR (400 MHz, CD_3OD) of compound **1n**



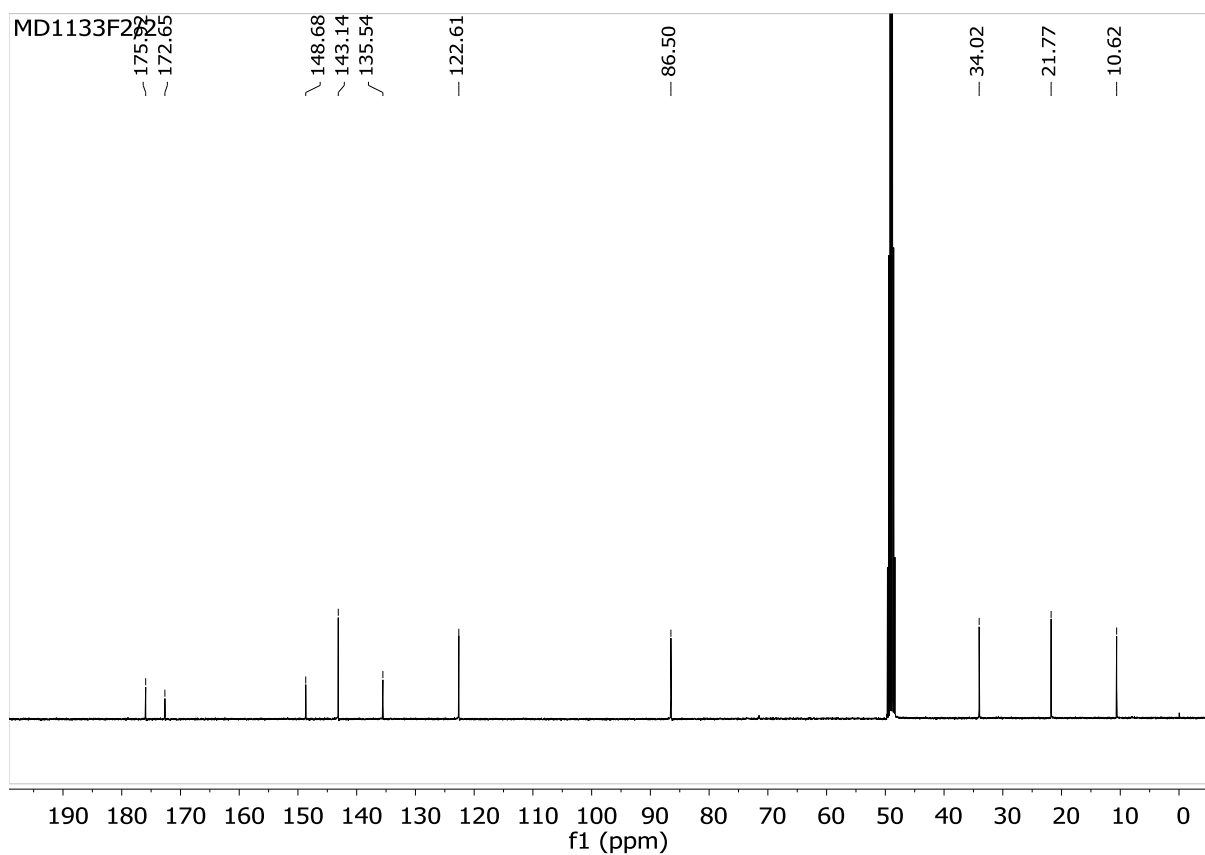
S13. ^1H -NMR (400 MHz, CDCl_3) of compound **1o**



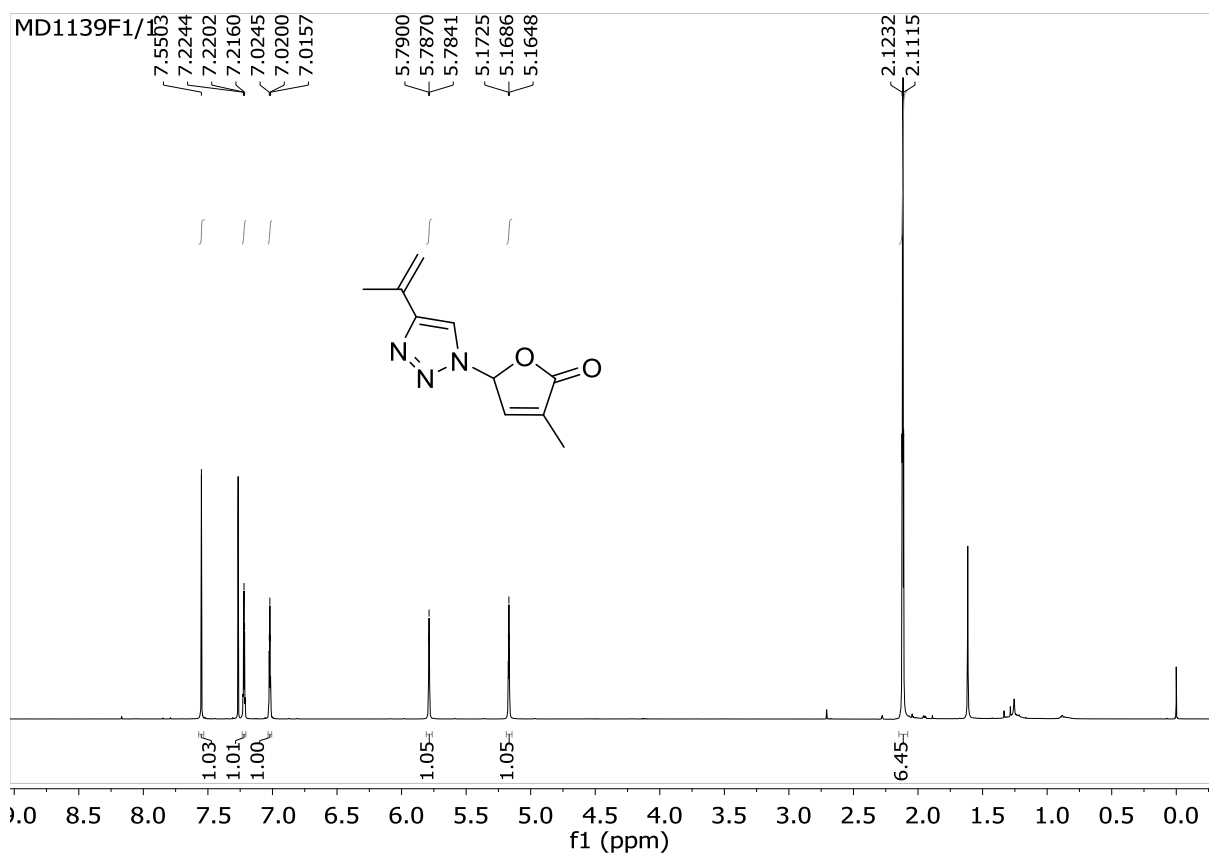
S14. ^{13}C -NMR (400 MHz, CDCl_3) of compound **1o**



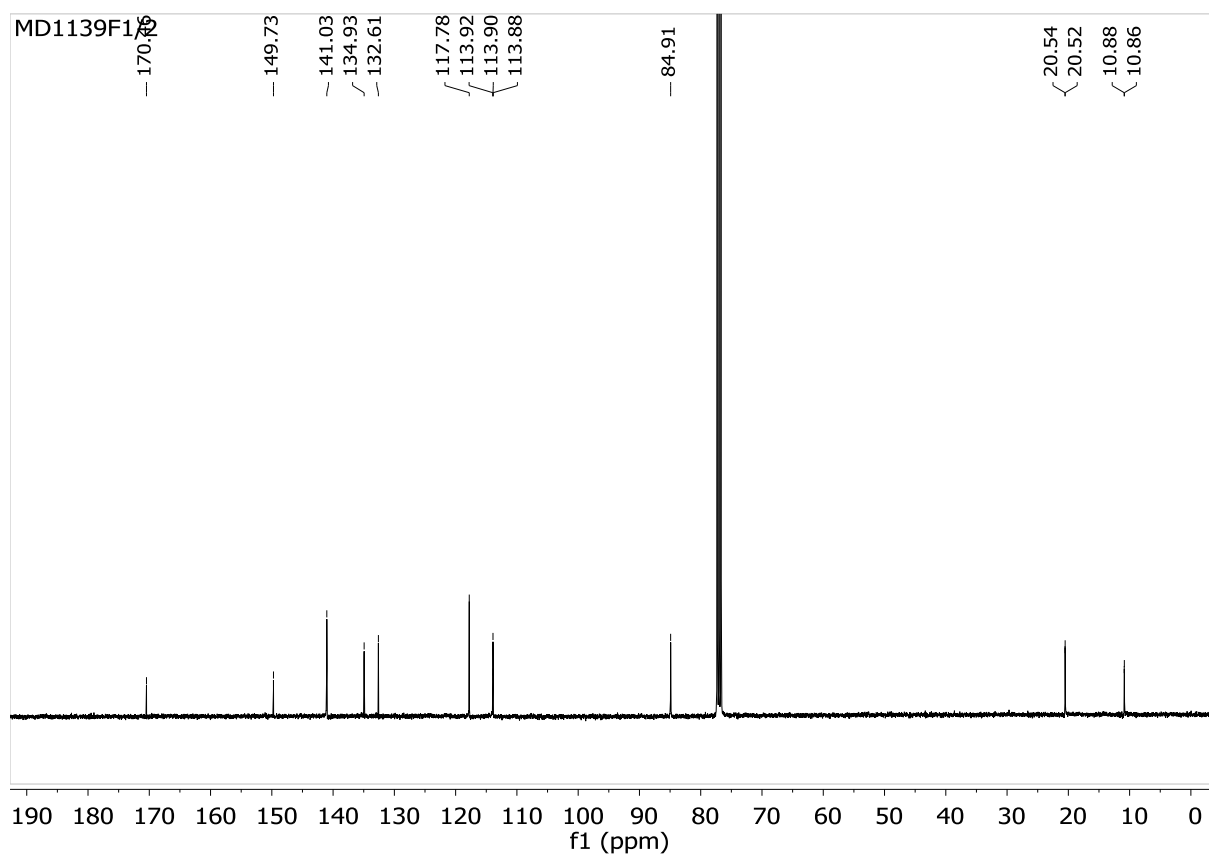
S15. ^1H -NMR (400 MHz, CD_3OD) of compound **1p**



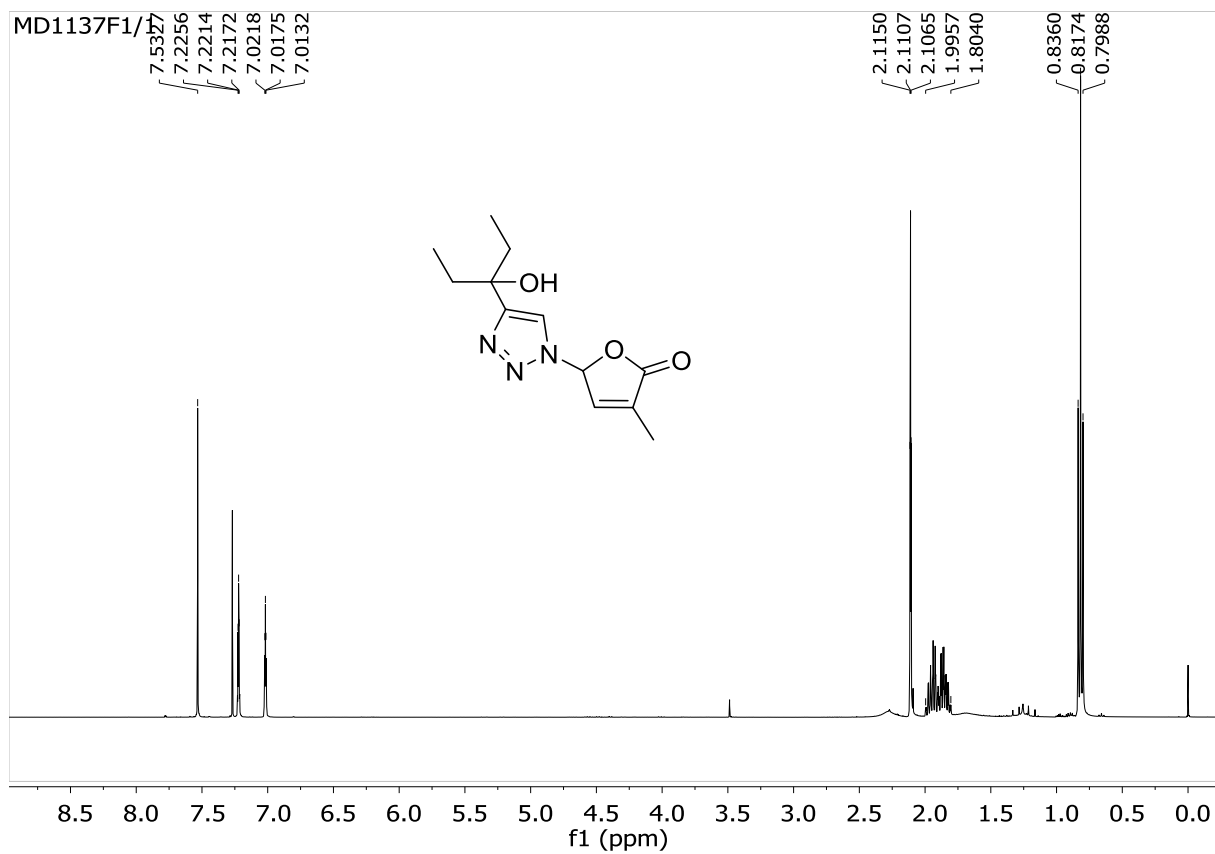
S16. ^{13}C -NMR (400 MHz, CD_3OD) of compound **1p**



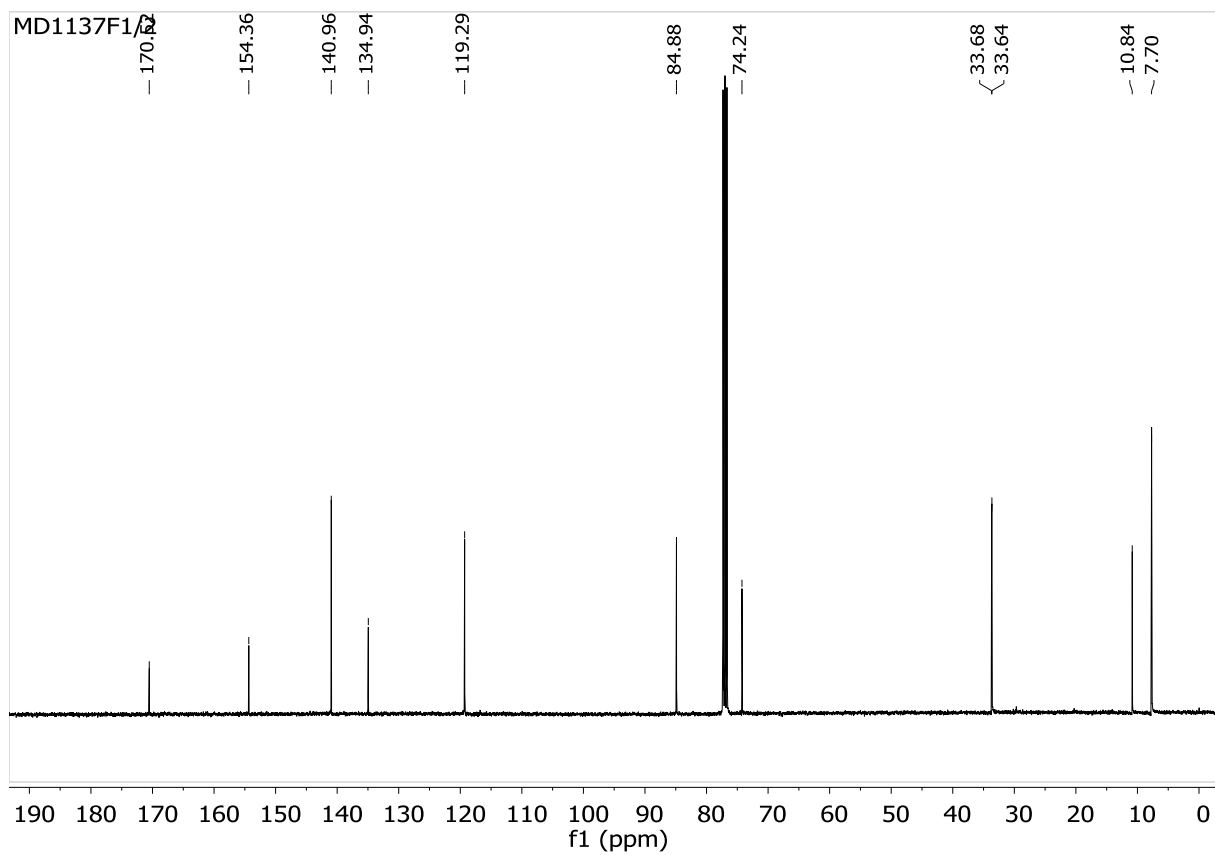
S17. ^1H -NMR (400 MHz, CDCl_3) of compound **1r**



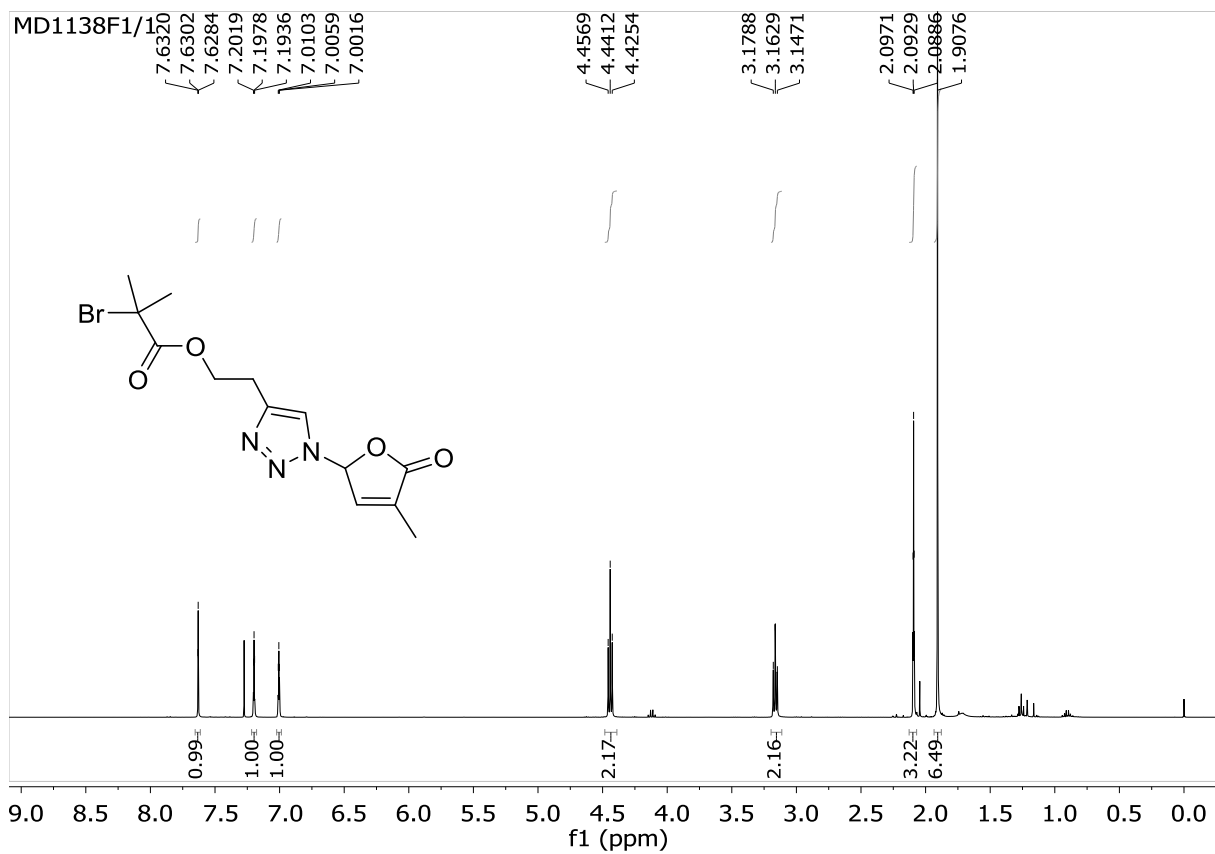
S18. ^{13}C -NMR (400 MHz, CDCl_3) of compound **1r**



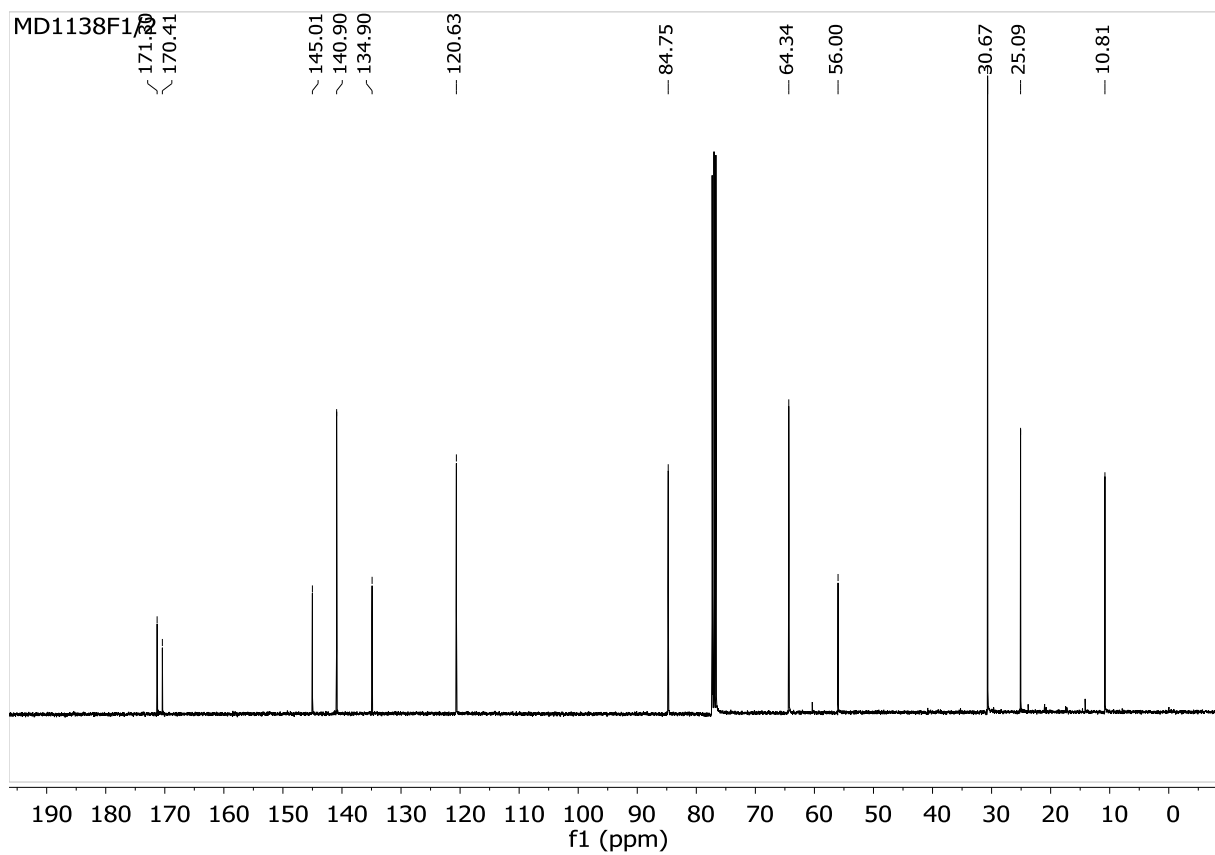
S19. ^1H -NMR (400 MHz, CDCl_3) of compound **1s**



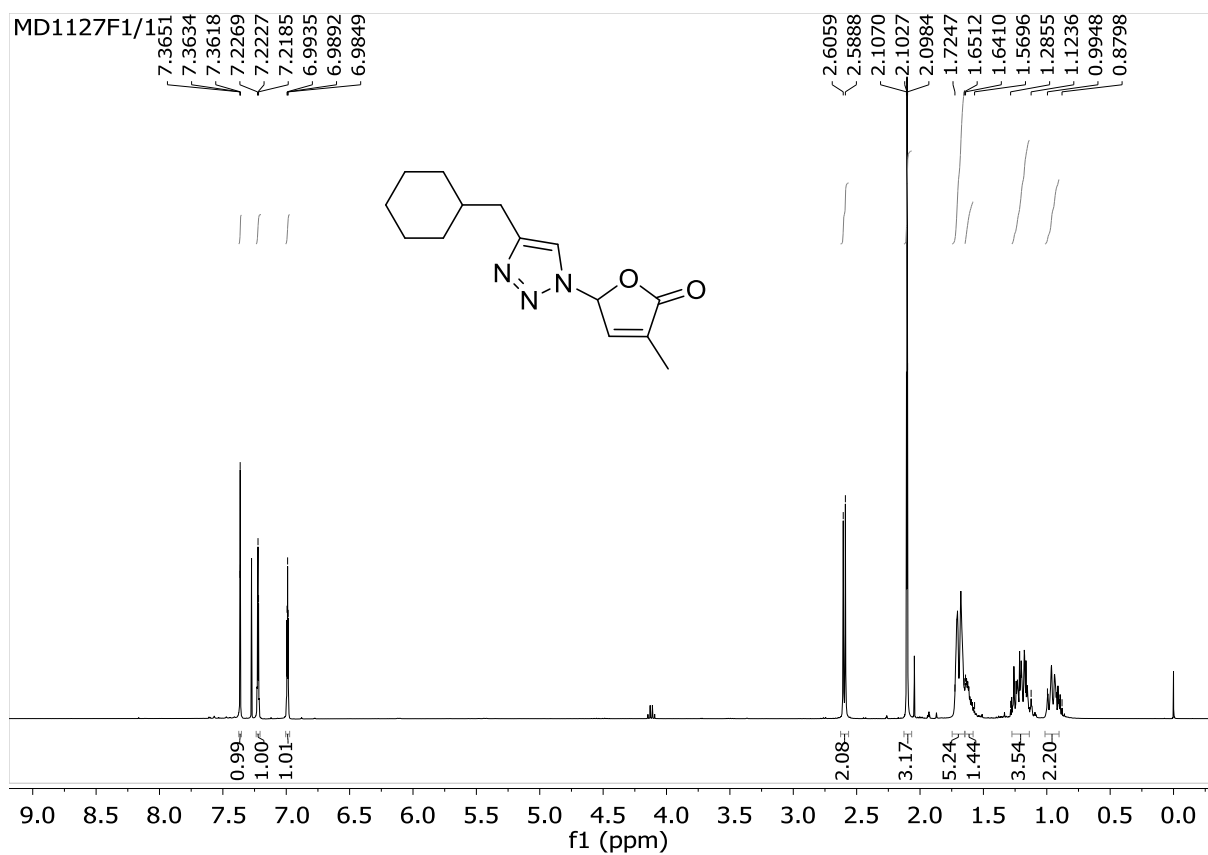
S20. ^{13}C -NMR (400 MHz, CDCl_3) of compound **1s**



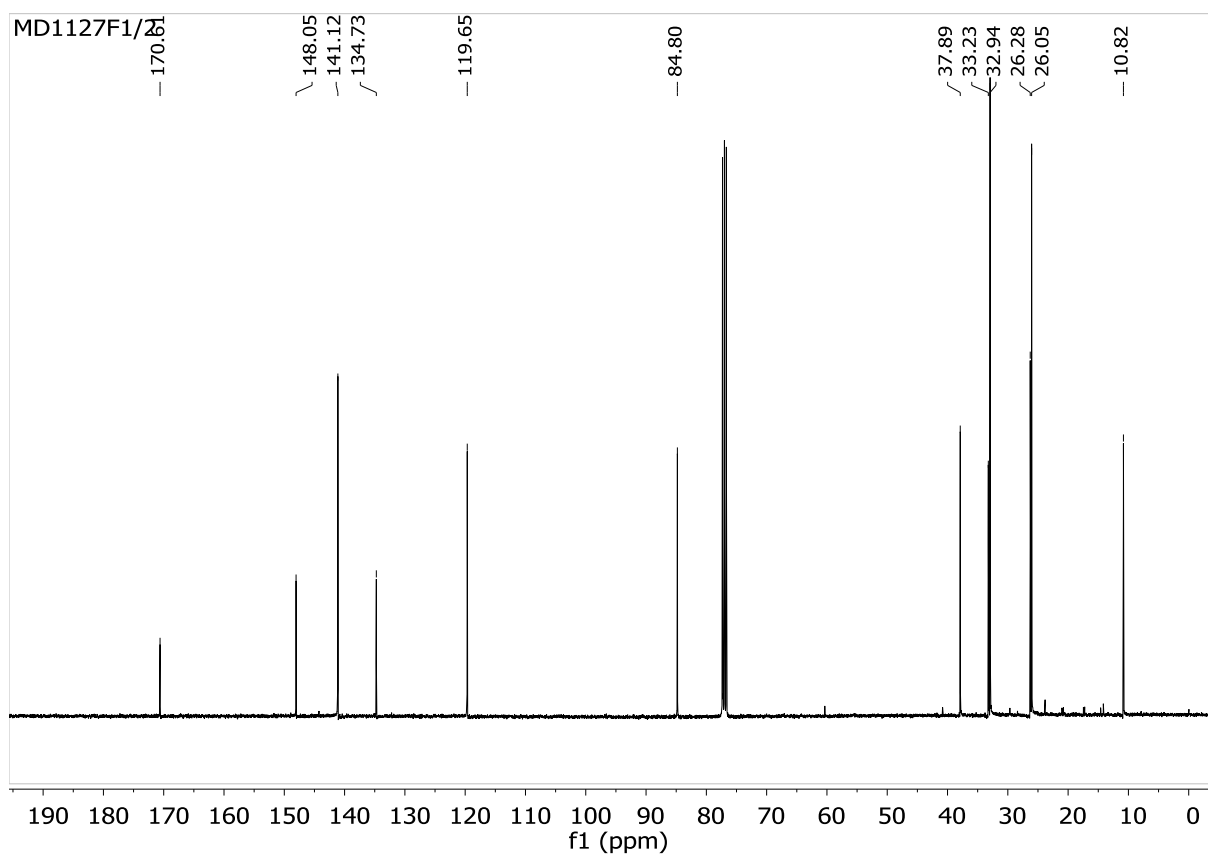
S21. ¹H-NMR (400 MHz, CDCl₃) of compound **1t**



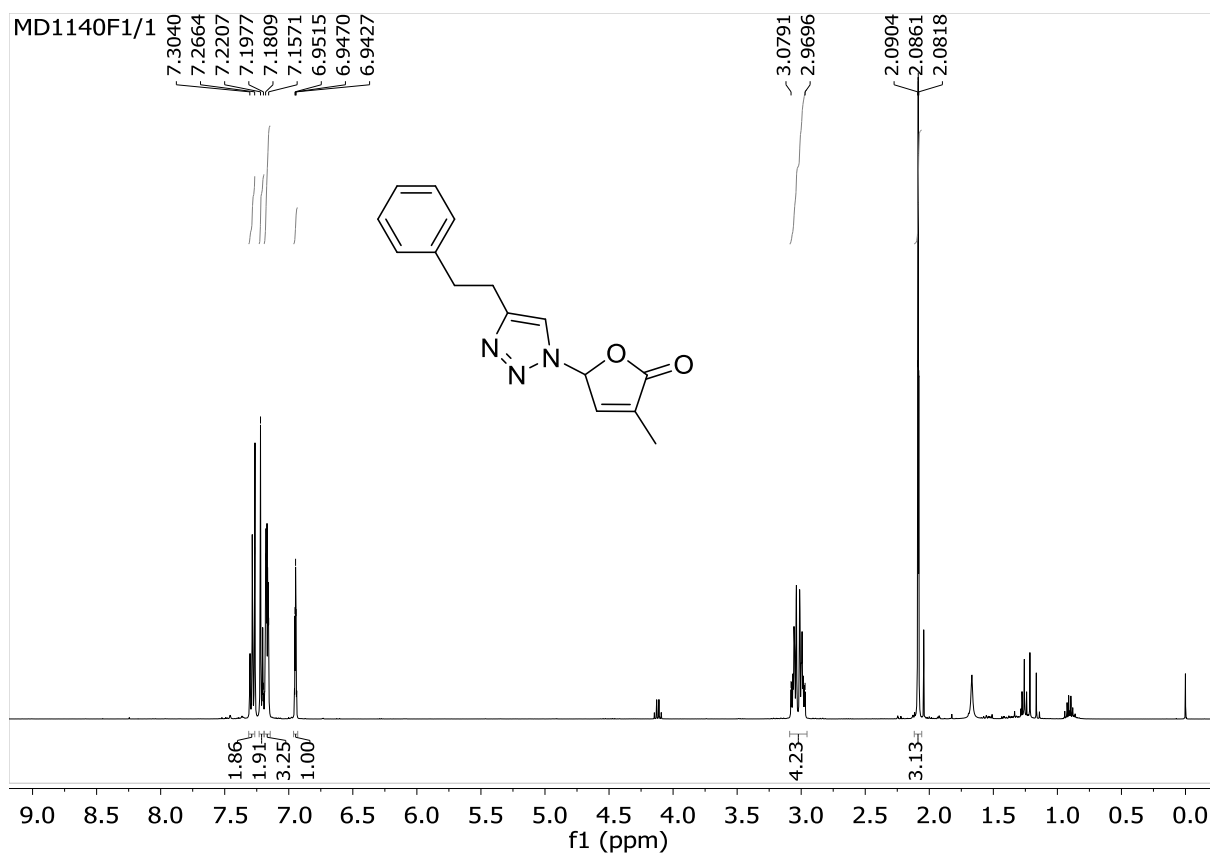
S22. ¹³C-NMR (400 MHz, CDCl₃) of compound **1t**



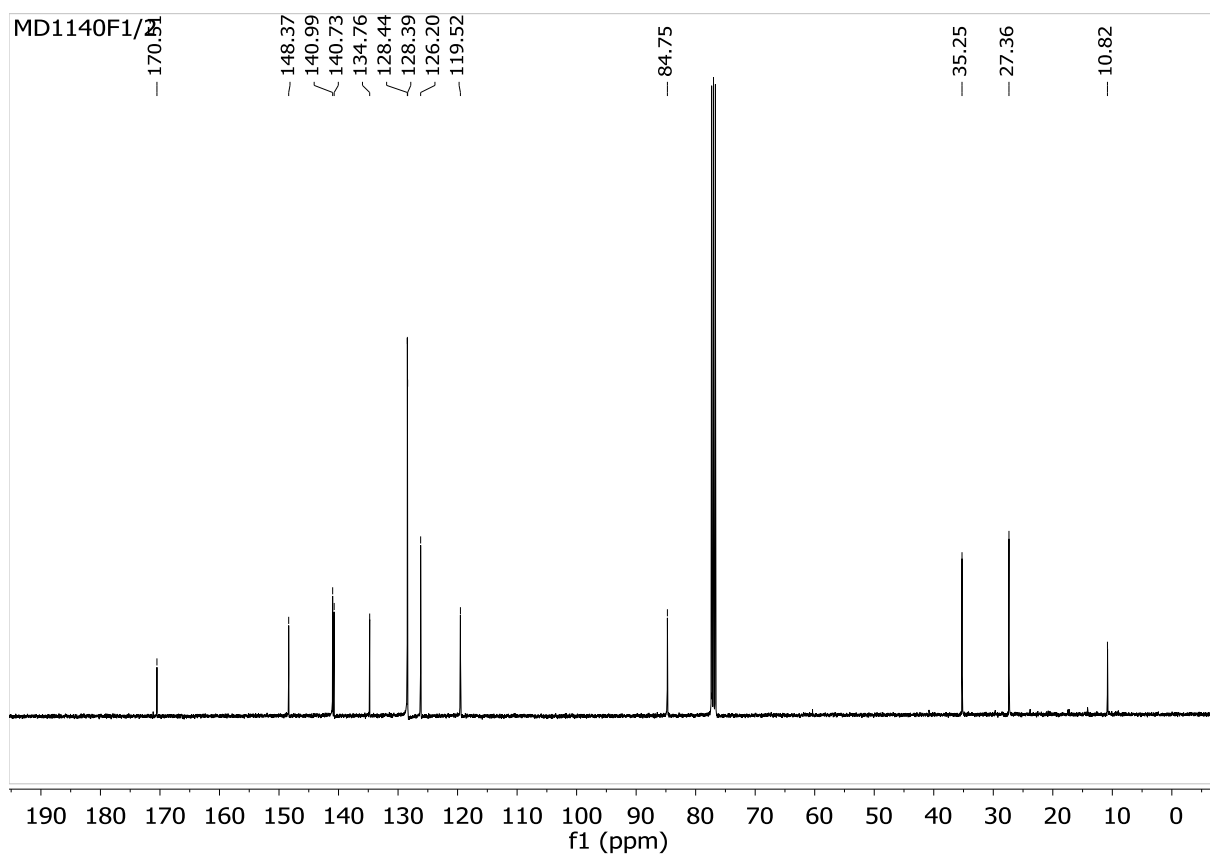
S23. ^1H -NMR (400 MHz, CDCl_3) of compound **1u**



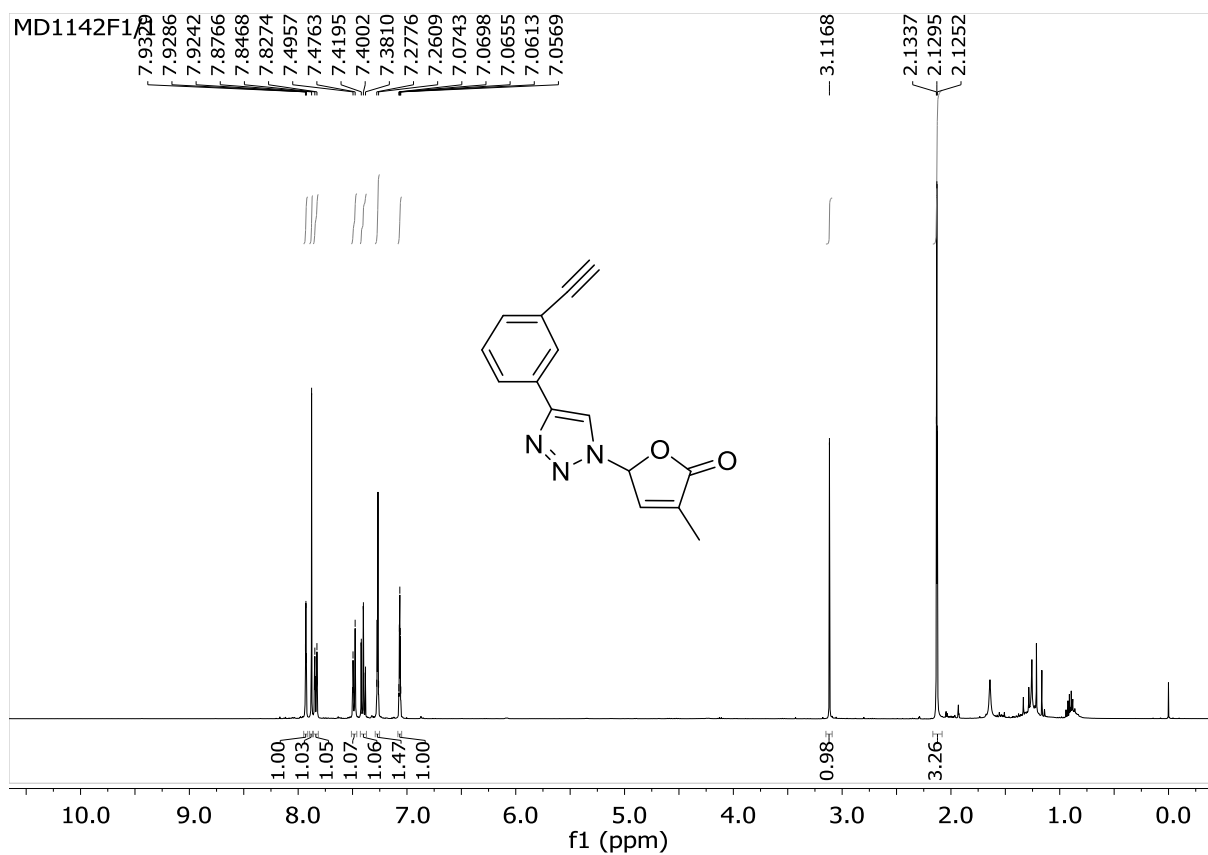
S24. ^{13}C -NMR (400 MHz, CDCl_3) of compound **1u**



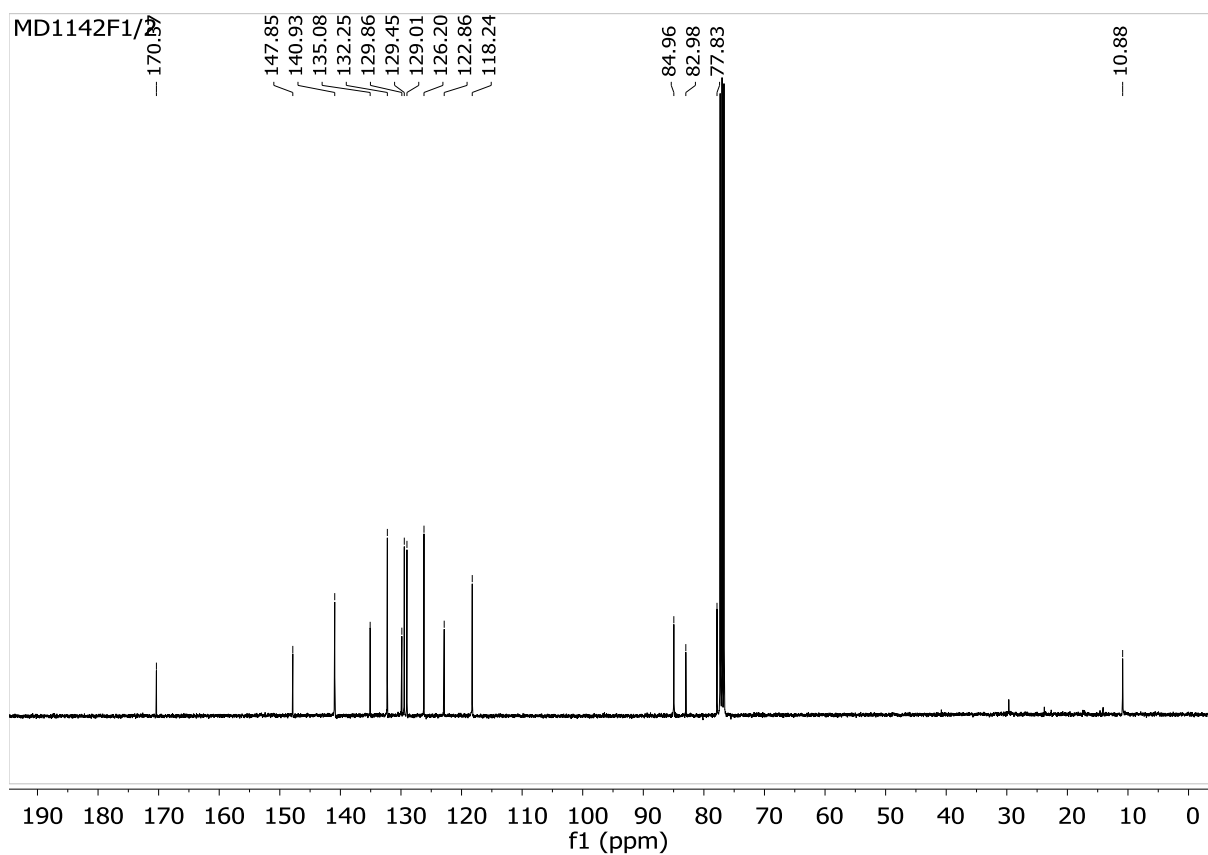
S25. ^1H -NMR (400 MHz, CDCl_3) of compound **1v**



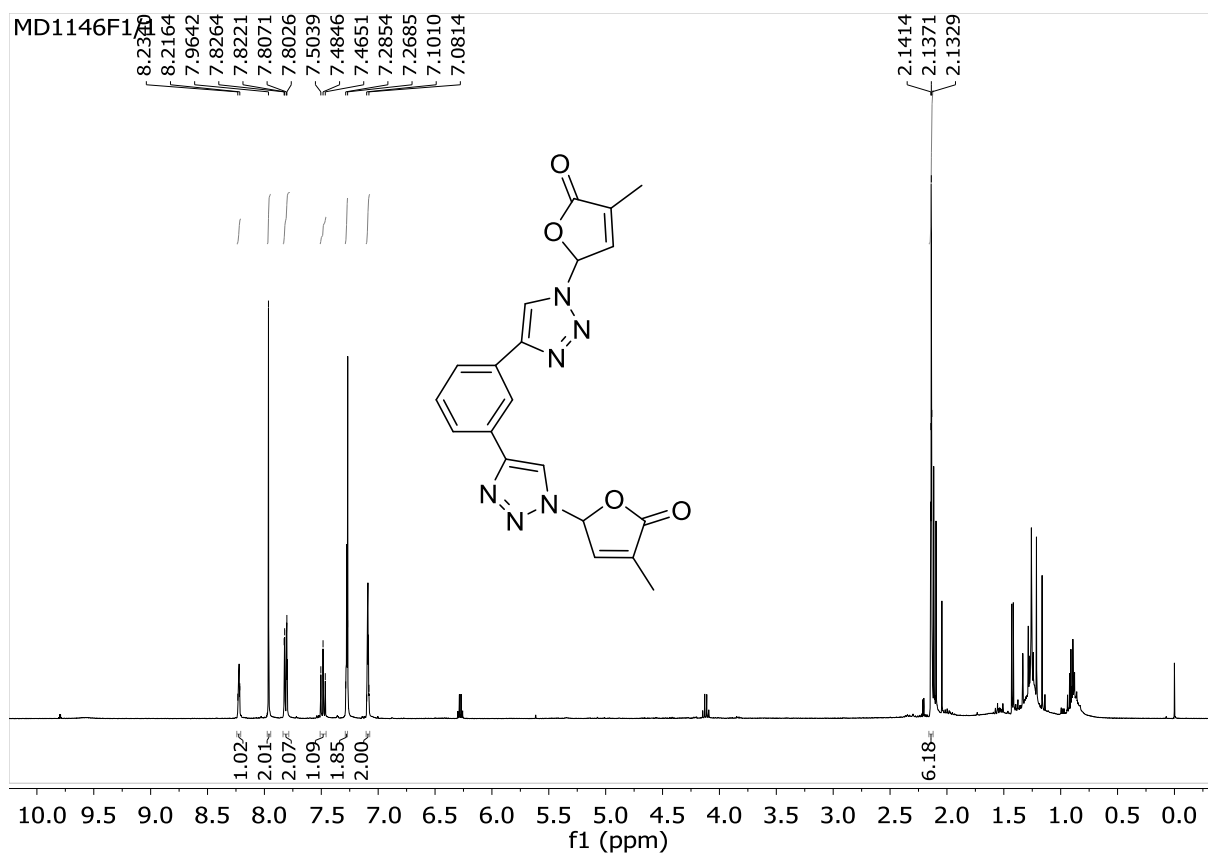
S26. ^{13}C -NMR (400 MHz, CDCl_3) of compound **1v**



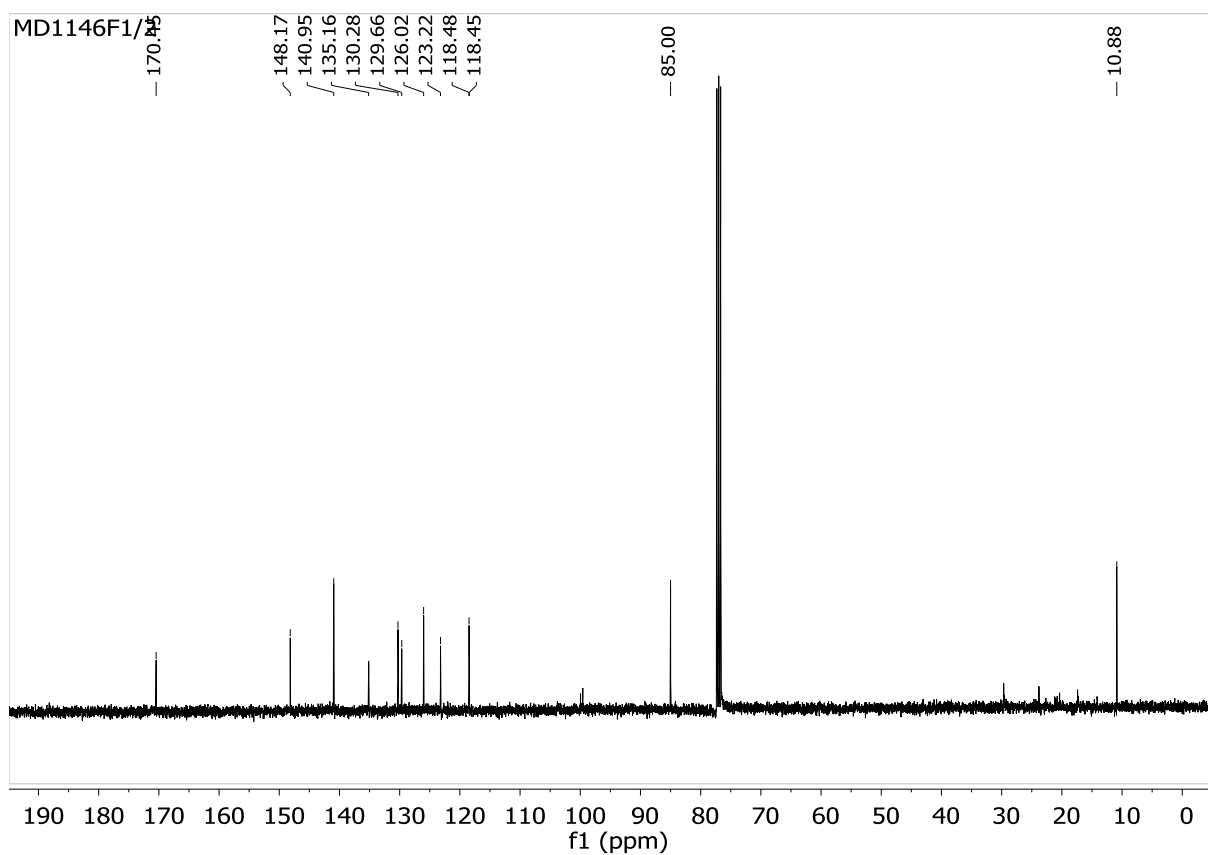
S27. ¹H-NMR (400 MHz, CDCl₃) of compound **1w**



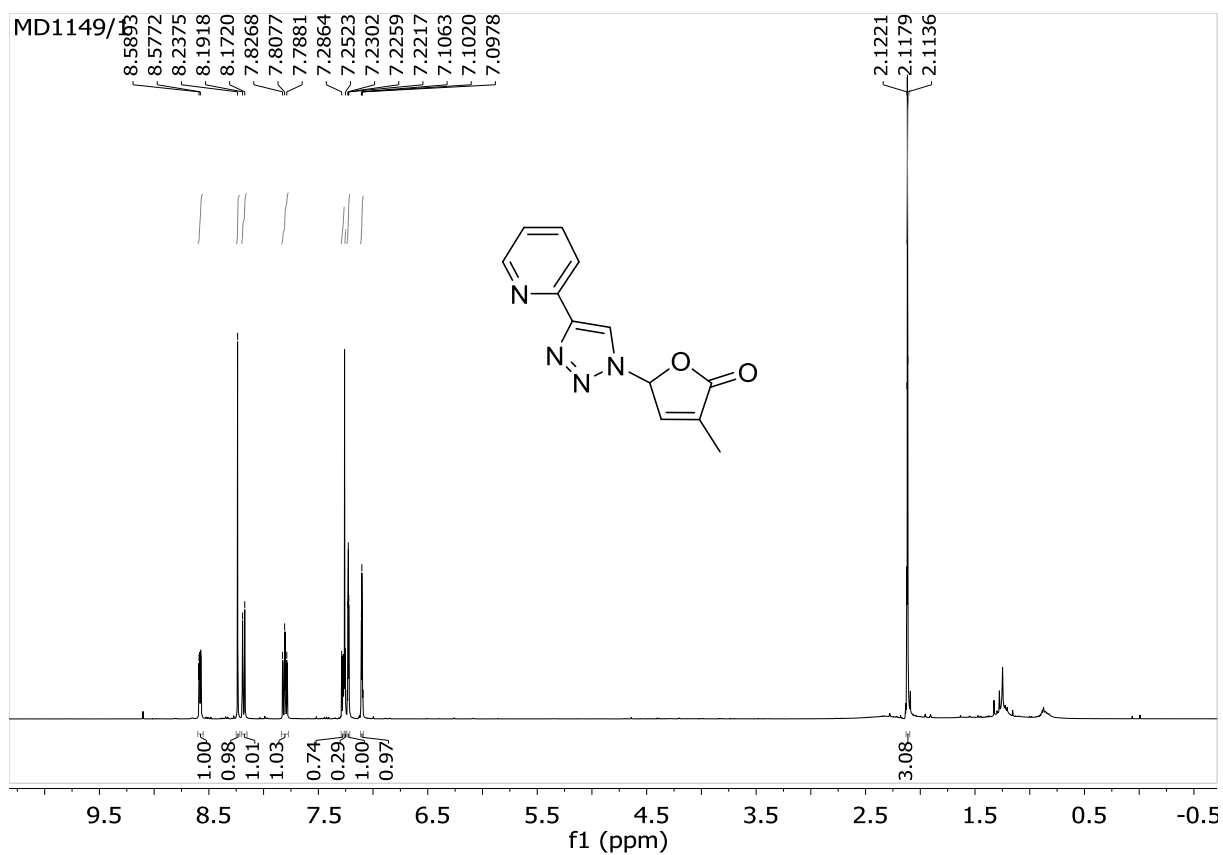
S28. ¹³C-NMR (400 MHz, CDCl₃) of compound **1w**



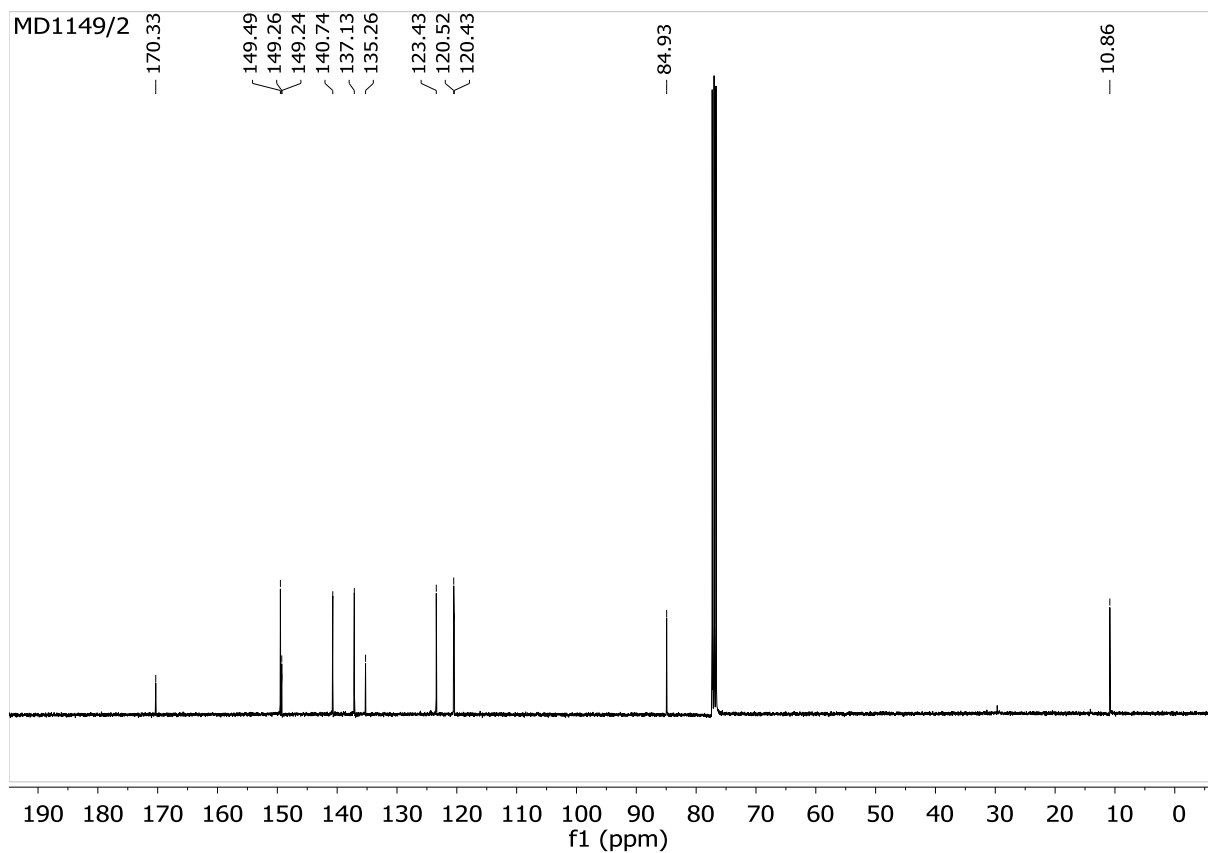
S29. ^1H -NMR (400 MHz, CDCl_3) of compound **1x**



S30. ^{13}C -NMR (400 MHz, CDCl_3) of compound **1x**



S31. ^1H -NMR (400 MHz, CDCl_3) of compound **1y**



S32. ^{13}C -NMR (400 MHz, CDCl_3) of compound **1y**

- 11.4. UGENA, L., HÝLOVÁ, A., PODLEŠÁKOVÁ, K., HUMPLÍK, J. F., DOLEŽAL, K., DE DIEGO, N., AND SPÍCHAL, L. (2018). CHARACTERIZATION OF BIOSTIMULANT MODE OF ACTION USING NOVEL MULTI-TRAIT HIGH-THROUGHPUT SCREENING OF *ARABIDOPSIS* GERMINATION AND ROSETTE GROWTH. *FRONT. PLANT SCI.* 9:1327.



Characterization of Biostimulant Mode of Action Using Novel Multi-Trait High-Throughput Screening of *Arabidopsis* Germination and Rosette Growth

Lydia Ugena^{1†}, Adéla Hýlová^{1†}, Kateřina Podlešáková¹, Jan F. Humplík^{1,2}, Karel Doležal¹, Nuria De Diego^{1*} and Lukáš Spíchal¹

¹ Department of Chemical Biology and Genetics, Centre of the Region Haná for Biotechnological and Agricultural Research, Faculty of Science, Palacký University, Olomouc, Czechia, ² Laboratory of Growth Regulators, Centre of the Region Haná for Biotechnological and Agricultural Research, Institute of Experimental Botany, Czech Academy of Sciences, Olomouc, Czechia

OPEN ACCESS

Edited by:

Giuseppe Colla,
Università degli Studi della Tuscia, Italy

Reviewed by:

Magdalena Maria Julkowska,
King Abdullah University of Science
and Technology, Saudi Arabia
Antonio Ferrante,
Università degli Studi di Milano, Italy
Barbara De Lucia,
Università degli Studi di Bari Aldo
Moro, Italy

*Correspondence:

Nuria De Diego
nuria.de@upol.cz

[†] These authors have contributed
equally to this work

Specialty section:

This article was submitted to
Crop and Product Physiology,
a section of the journal
Frontiers in Plant Science

Received: 31 May 2018

Accepted: 23 August 2018

Published: 13 September 2018

Citation:

Ugena L, Hýlová A, Podlešáková K,
Humplík JF, Doležal K, De Diego N
and Spíchal L (2018) Characterization
of Biostimulant Mode of Action Using
Novel Multi-Trait High-Throughput
Screening of *Arabidopsis* Germination
and Rosette Growth.
Front. Plant Sci. 9:1327.
doi: 10.3389/fpls.2018.01327

Environmental stresses have a significant effect on agricultural crop productivity worldwide. Exposure of seeds to abiotic stresses, such as salinity among others, results in lower seed viability, reduced germination, and poor seedling establishment. Alternative agronomic practices, e.g., the use of plant biostimulants, have attracted considerable interest from the scientific community and commercial enterprises. Biostimulants, i.e., products of biological origin (including bacteria, fungi, seaweeds, higher plants, or animals) have significant potential for (i) improving physiological processes in plants and (ii) stimulating germination, growth and stress tolerance. However, biostimulants are diverse, and can range from single compounds to complex matrices with different groups of bioactive components that have only been partly characterized. Due to the complex mixtures of biologically active compounds present in biostimulants, efficient methods for characterizing their potential mode of action are needed. In this study, we report the development of a novel complex approach to biological activity testing, based on multi-trait high-throughput screening (MTHTS) of *Arabidopsis* characteristics. These include the *in vitro* germination rate, early seedling establishment capacity, growth capacity under stress and stress response. The method is suitable for identifying new biostimulants and characterizing their mode of action. Representatives of compatible solutes such as amino acids and polyamines known to be present in many of the biostimulant irrespective of their origin, i.e., well-established biostimulants that enhance stress tolerance and crop productivity, were used for the assay optimization and validation. The selected compounds were applied through seed priming over a broad concentration range and the effect was investigated simultaneously under control, moderate stress and severe salt stress conditions. The new MTHTS approach represents a powerful tool in the field of biostimulant research and development and offers direct classification of the biostimulants mode of action into three categories: (1) plant growth promoters/inhibitors, (2) stress alleviators, and (3) combined action.

Keywords: biostimulants, multi-trait high-throughput screening assay, proline, polyamines, plant biostimulant characterization index, salinity

INTRODUCTION

Agricultural crop production will be extremely challenging in the coming decades. Due to the increase in population, a 50% (maximum) increase in the demand for food is expected by 2030. During the growing season, crops around the world are subjected to environmental stresses that affect plant germination, metabolism, growth and yield. Breeders worldwide have therefore focused on quantitative analyses of plant traits in order to accelerate the development of appropriate strategies for improving lines or varieties which are adaptable to resource-limited environments (Rahaman et al., 2017). Soil salinity is an important environmental factor that results in decreased crop productivity on a global scale. In fact, owing to this factor, an estimated 1.5 million hectares of land is taken out of production each year and by 2050 a 50% loss of cultivable lands is expected (Ibrahim, 2016).

The application of biostimulants represents one of the most innovative and promising strategies for minimizing stress impact, including salinity. A plant biostimulant is defined as a material of biological origin which includes bacteria, fungi, seaweeds, higher plants, animals and humate-containing raw materials (Sharma et al., 2014; Yakhin et al., 2016; Cristiano et al., 2018). This material induces beneficial plant processes (including nutrient uptake, nutrient use efficiency, tolerance to abiotic stress and crop quality), independently of its nutrient content (Calvo et al., 2014; Yakhin et al., 2016). Exposure of seeds to abiotic stresses, such as salinity among others, results in lower seed viability, reduced germination, and poor seedling establishment (Savvides et al., 2016). Increasing the salt concentration of the soil leads to a decrease in the germination percentage and delays the germination starting point (Kaveh et al., 2011; Thiam et al., 2013; Ibrahim, 2016). Seed-priming might improve seed stress-tolerance through 'priming memory,' which is established during priming and can be recruited later when seeds are exposed to stresses during germination (Chen and Arora, 2013). Seeds primed with biostimulants from varied origins trigger fast seed germination (Zeng et al., 2012; Colla et al., 2014; Garcia-Gonzalez and Sommerfeld, 2016). Besides, priming seeds with certain biostimulants can promote tolerance to adverse environmental conditions during the imbibition and germination stages (Mahdavi, 2013; Sharma et al., 2014; Pichyangkura and Chadchawan, 2015; Van Oosten et al., 2017).

Recently, the global biostimulant market has grown rapidly and, to satisfy crop requirements, many companies are actively introducing various innovative products and ingredients (Calvo et al., 2014; Sharma et al., 2014). However, in general, the raw materials used by the biostimulant manufacturers exhibit considerable compositional variations which may impact on the composition and concentration of major components (Povero et al., 2016; Sharma et al., 2016). The origin of biostimulants is diverse, and can range from single compounds to complex matrices with different groups of bioactive components that have

only been partly characterized (du Jardin, 2015). Irrespective of their complexity, biostimulants are known to contain different groups of plant signaling compounds such as plant hormones, amino acids, and polyamines among others (Craigie, 2011; du Jardin, 2015). The exogenous application of these signaling molecules has been reported to ameliorate the adverse effect of stress through a sophisticated crosstalk among them leading to the activation of conserved pathways [reviewed in Podlešáková et al. (2018)].

In this work we present a novel approach for biostimulant mode of action characterization based on multi-trait high-throughput screening (MTHTS) of *Arabidopsis* germination and rosette growth under salinity. The analyzed traits included the germination rate, rosette growth rate and color. The potential of the approach was demonstrated by applying (via seed priming) representatives of the most common compounds present in biostimulants (i.e., polyamines and amino acids). In addition, we optimized the principles of two previously described protocols for implementation into the MTHTS approach. These included (i) the fast scoring of the germination rate based on a standardized 96-well plate test coupled with spectrophotometric reading of tetrazolium salt reduction (Pouvreau et al., 2013) and (ii) an automated method for high-throughput screening of *Arabidopsis* rosette growth in multi-well plates (De Diego et al., 2017). A highly efficient and reliable method for characterizing biostimulant efficacy at various salt stress levels was realized by developing and combining a high-throughput seed germination assay in *Arabidopsis* with the improved *Arabidopsis* rosette growth assay.

MATERIALS AND METHODS

HTS of *Arabidopsis in vitro* Seed Germination

Arabidopsis thaliana (L.) Heynh seeds (accession Col-0) were surface-sterilized by soaking in 70% Ethanol plus 0.01% Triton X-100 for 10 min. After that, the seeds were washed with sterilized water and then resuspended at a density of 10 g L⁻¹ in 1 mM HEPES [4-(2-hydroxyethyl)-1-piperazineethanesulfonic acid] buffer (Carl Roth GmbH + Co. KG., Germany) (pH 7.5). Seeds were stratified at 4°C in the dark for 72 h. To investigate the effect of biostimulants on *Arabidopsis in vitro* seed germination, four single active compounds commonly present in many commercial biostimulant products were selected for seed priming; three polyamines: putrescine (Put) (1,4-butanediamine dihydrochloride), spermidine (Spd) (N-(3-aminopropyl)-1,4-butanediamine trihydrochloride), spermine (Spm) [N-(3-Aminopropyl)-1,4-butanediamine trihydrochloride] and the amino acid L-proline (Pro) [(S)-Pyrrolidine-2-carboxylic acid], all purchased from Sigma-Aldrich, Inc., (Germany). These compounds were added before the stratification, reaching final concentrations of 0.001, 0.01, 0.1, or 1 mM. After the cold stratification, seed suspension was washed three times with 20 mL sterile water to remove the biostimulants. In the last wash half of the water volume was removed and an additional 10 mL solution of sterilized 0.1% agarose with 1 mM of HEPES

Abbreviations: GLI, green leaf index; MTHTS, multi-trait high-throughput screening; NGRDI, normalized green red difference index; Pro, L-proline; Put, putrescine; Spd, spermidine; Spm, Spermine; VARI, visible atmospherically resistant index.

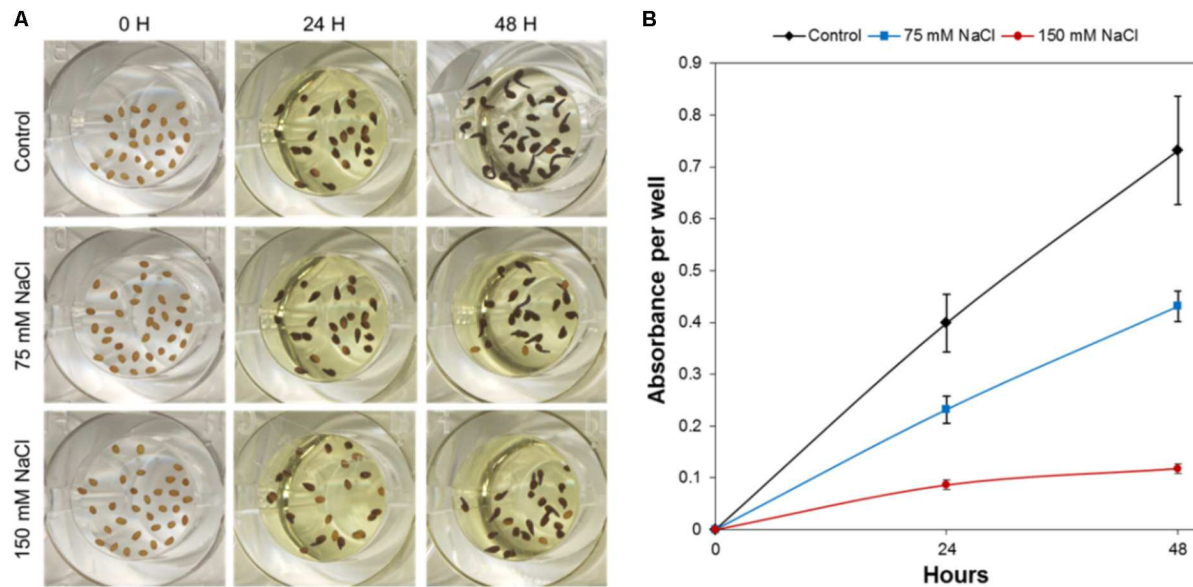


FIGURE 1 | HTS of *Arabidopsis* germination under control, moderate (75 mM NaCl), and severe (150 mM NaCl) stress conditions. **(A)** Characteristics of *Arabidopsis* seeds in one well of the 96-well plate before germination (0 h), and after 24 and 48 h, respectively, of germination with subsequent MTT treatment. **(B)** Absorbance of MTT after solubilization of formazan from *Arabidopsis* seeds germinated under control, moderate (75 mM NaCl), and severe (150 mM NaCl) stress conditions. The values represent Mean \pm SE.

buffer was added. This is because seeds do not sediment in 0.05% agarose and are suspended in an adequate homogeneous solution for pipetting. The 96-well plate was filled with the seed suspension, 50 μ L per well, representing \sim 20–30 seeds per well. The final volume was adjusted to 100 μ L per well with demineralized water or, in the case of the salt stress treatments, a NaCl solution that yields a final concentration of 75 or 150 mM NaCl in the well. Plates were sealed and incubated for seed germination at 21°C in darkness.

For the quantification of the *Arabidopsis* germination rate, the methylthiazolyldiphenyl-tetrazolium bromide (MTT; Sigma-Aldrich, Inc.) assay was performed in accordance with Pouvreau et al. (2013). In this process, 10 μ L of 0.5% MTT solution per well was added after 24 or 48 h under germination conditions. Plates were placed in the culture chamber for an additional 24 h in darkness and a redox reaction, which is a reduction of MTT to formazan, lasted for 24 h (Figure 1). After MTT addition, the formazan salt deposit was solubilized by adding 100 μ L of lysis buffer (10% Triton X-100, 0.04 mol L⁻¹ HCl in isopropanol) to each well, and holding at 21°C in darkness for another 24 h. Subsequently, the absorbance was read with a BioTekTM SynergyTM H4 Hybrid Microplate Reader (BioTek Instruments, Inc., United States). For each well, the final absorbance was calculated by subtracting the absorbance at a reference wavelength of 690 nm from a test absorbance of 570 nm (A570–690 nm).

Image Acquisition and Data Analysis

Images were acquired by scanning each plate twice (HP ScanJet 5300c; resolution 1200 DPI; HP Development Company,

L.P., United States), immediately after placing the seeds in the 96 multi-well plates (0 h) and after 24 or 48 h under seed-germination conditions with the subsequent 24 h MTT treatment. The images were saved as TIFF format. For seed counting, the images of *Arabidopsis* seeds at 0 h (immediately after cold stratification) were used and the number of seeds per well was estimated using an in-house software routine implemented in MATLAB R2015. The free of charge access to the software application for academical purposes is described in the next section.

HTS of *Arabidopsis* Rosette Growth

Experimental Setup and Assay Conditions

The protocol for analysis of *Arabidopsis* rosette growth described by De Diego et al. (2017) was modified as follows. Seeds of *A. thaliana* (ecotype Col-0) were surface-sterilized and sown on 12 cm \times 12 cm square plates containing a 0.5 \times MS medium (Murashige and Skoog, 1962) (pH 5.7) supplemented with a gelling agent (0.6% Phytagel; Sigma-Aldrich, Germany). The seeds were kept for 4 days at 4°C in the dark (in the case of primed variants, the growth medium contained the tested biostimulant described below). The plates were then positioned vertically in a growth chamber under controlled conditions (22°C, 16/8 h light/dark cycle with the light cycle starting at 5 a.m., photon irradiance: 120 μ mol photons of PAR m⁻² s⁻¹). Three days after germination, seedlings of similar size were transferred under sterile conditions into 48-well plates (Jetbiofil, Guangzhou, China). One seedling was transferred to each well filled with 850 μ L 1 \times MS medium (pH 5.7; supplemented with 0.6% Phytagel), with NaCl added for different salt stress

intensities (75 and 150 mM NaCl) and the plates were sealed with perforated transparent foil allowing gas and water exchange. The 48-well plates containing the transferred *Arabidopsis* seedlings were placed the OloPhen platform¹ that uses the PlantScreenTM XYZ system installed in a growth chamber with a controlled environment and cool-white LED and far-red LED lighting (Photon Systems Instruments, Brno, Czechia). The conditions were set to simulate a long day with a regime of at 22°C/20°C in a 16/8 h light/dark cycle, an irradiance of 120 mmol photons of PAR m⁻² s⁻¹ and a relative humidity of 60%. The PlantScreenTM XYZ system consists of a robotically driven arm holding an RGB camera with customized lighting panel and growing tables with a total area of approximately 7 m². To increase the throughput of the assay, the capacity of the growing area was improved to accommodate in total 572 multi-well. The XYZ robotic arm was automatically moved above the plates to take RGB images of single plates from the top. The imaging of each 48 well plate was performed twice per day (at 10 a.m. and 4 p.m.) for 7 days. RGB images (resolution 2500 × 2000 pixels) of a single plate with a file size of approximately 10 MB in the PNG compression format were stored in a database on a server, using a filename containing information about the acquisition time and the (x, y) coordinates of the camera. The data were automatically stored in PlantScreen XYZ database, exported by PlantScreen Data Analyzer software and analyzed using an in-house software routine implemented in MATLAB R2015.

The software application for *Arabidopsis* rosette growth analysis (same as for above described *Arabidopsis* seed counting) can be used without any charge upon obtaining a license from the author. The license can be obtained by e-mail to Palacky University upon agreeing not to use the application for commercial purpose. After obtaining the license, the enduser will be provided (free of charge) with the MCRInstaller.exe. MCRInstaller simulates the MATLAB environment on computers where MATLAB is not installed and enables to execute the applications. To obtain the application executable files, please contact the author Tomas Furst by email tomas.furst@upol.cz. The email must contain the following statement: “Neither the application nor the MCRInstaller will be used for any commercial purpose.”

Seed Priming With Biostimulants

The biostimulant effect was determined using Put, Spd, Spm, and Pro for seed priming. After sterilization, the aforementioned seeds were placed on 12 cm × 12 cm square plates containing a 0.5 × MS medium (pH 5.7) supplemented with the tested compounds at four concentrations (0.001, 0.01, 0.1, or 1 mM). After 4 days in the dark and 3 days of germination, seedlings were transferred into 48 multi-well plates filled with a 1 × MS with/without salt (75 or 150 mM NaCl solution) addition. Two plates per growth condition, compound and concentration (96 seedlings) were used as replicates for the control and 75 mM NaCl. Due to the high mortality of seedlings under severe salt stress conditions, three plates for the seedling in 150 mM NaCl

were used to obtain sufficient reproducible data and an adequate number of measurable individuals.

Biometrical Parameters

The changes in green area (Pixels) were measured twice per day in each *Arabidopsis* seedling using the aforementioned automatic system. From the obtained data, the relative growth rate (RGR) per hour or day was estimated for each replicate and variant as follows:

$$\text{RGR} = [\ln(\text{green area})_{t_i} - \ln(\text{green area})_{t_{i-1}}] / (t_i - t_{i-1}) \quad (1)$$

Where t_i is the i time (h or days).

Determination of the Leaf Color in *Arabidopsis*

Rosette Under Control and Salt Stress Conditions

For non-invasive estimation of the changes in leaf color, we calculated three vegetative indices (NGRDI, GLI, and VARI) which have exhibited correlation with the plant biomass, nutrient status or tolerance to abiotic stress (Gitelson et al., 2002; Perry and Roberts, 2008; Hunt et al., 2013). The images captured on the seventh day of an *Arabidopsis* rosette growth assay subjected to HTS were segmented for the extraction of leaf rosettes using software described in our previous report (De Diego et al., 2017). Afterward, the values corresponding to particular color channels (red = R, green = G, and blue = B) were extracted for each pixel within the plant mask, and the vegetative indices were calculated as follows:

Normalized green red difference index

$$\text{NGRDI} = (G - R) / (G + R) \quad (2)$$

Green leaf index

$$\text{GLI} = (2G - R - B) / (2G + R + B) \quad (3)$$

Visible atmospherically resistant index

$$\text{VARI} = (G - R) / (G + R - B) \quad (4)$$

Subsequently, indices representing particular seedlings were determined by calculating the mean values for each plant mask. The mean value for each 48-well plate was then calculated.

Statistical Analysis

The one-way analysis of variance (ANOVA) was used to assess the differences between the projected areas (Pixels) or seed germination (absorbance) of two or more plant groups at a particular time-point. The test compares the variance (or variation) between the data samples to variation within each particular sample. When ANOVA was significant the differences among groups was determined using Dunn & Sidák's approach.

The relationship among traits was analyzed via Pearson's correlation. Furthermore, the significance of the regression was determined by applying a Student's t -test to the linear curves and after linearization of non-linear curves.

¹http://www.plant-phenotyping.org/db_infrastructure#/tool/57

RESULTS

Development of HTS of *Arabidopsis* Seed Germination Under Control and Salt Stress Conditions

To efficiently determine the effect of biostimulant priming on the seed germination rate, we developed a HTS assay for seed germination using the MTT method proposed by Pouvreau et al. (2013). In this method, the MTT is used as a marker of metabolic activity in the embryo and its reduction to purple formazan can be quantified spectrophotometrically in a microtiter plate. We optimized this assay for *Arabidopsis* seeds and validated the assay for determining the effect of salinity at two time points (i.e., 24 and 48 h; see **Figure 1**). The severity of the salinity was expected to exert a dose-dependent negative effect on seed germination (seed staining and radicle length decrease; **Figure 1A**), leading to a decrease in the absorbance values measured (**Figure 1B**). During optimization of the assay, we observed a strong correlation between the absorbance values and the number of seeds per well under all three growth conditions (**Figure 2A**). Thus, a stable number of seeds per well was critical to reducing the variability in the experiment. This is, however, technically difficult under HTS conditions when a high number of wells/plates must be rapidly filled. To solve this problem we used 0.05% agarose solution allowing homogeneous suspension of seeds through vortexing. This way using multi-step pipette the average number of 21 ± 5.4 (mean \pm SD) seeds per well was achieved. Besides, we handled the relatively high variability ($\sim 25\%$) by developing an automatic simple software that counts the exact number of seeds per well (rather than finding a technical solution that allows precise and repeated filling of the plate wells with the same number of seeds). Using this software routine, the measured absorbance per well can be recounted to the absorbance per seed. In the first step of this process, the software identifies the wells in the plate. The seeds are then identified via simple thresholding in the R, G, and B channels and single seeds or clusters of seeds are subsequently separated from the background. Afterward, single seeds are distinguished from clusters by computing the solidity (i.e., the ratio of the area of the convex hull of an object to the area of an object) of each object. Single seeds have a high solidity (usually >0.9), whereas clusters of seeds are larger and have lower solidity. The number of seeds in a cluster is estimated by dividing the area of the cluster by the average seed area which is determined from previous runs of the software. The accuracy of the software was determined by manually counting the seeds on several plates, and a high correlation was obtained between the real number and the software-estimated number of seeds (**Figure 2B**). As shown in **Table 1**, the counting of the seeds allowed us to reduce the dispersion of the absorbance per variant, with an at least three times lower standard deviation (28 vs. 9%) in the two analyzed points at 24 and 48 h. Thus, we observed a significant correlation ($p < 0.001$) between the absorbance per seed and the percentage of *Arabidopsis* seeds germinated under control and salt stress conditions (**Figure 2C**).

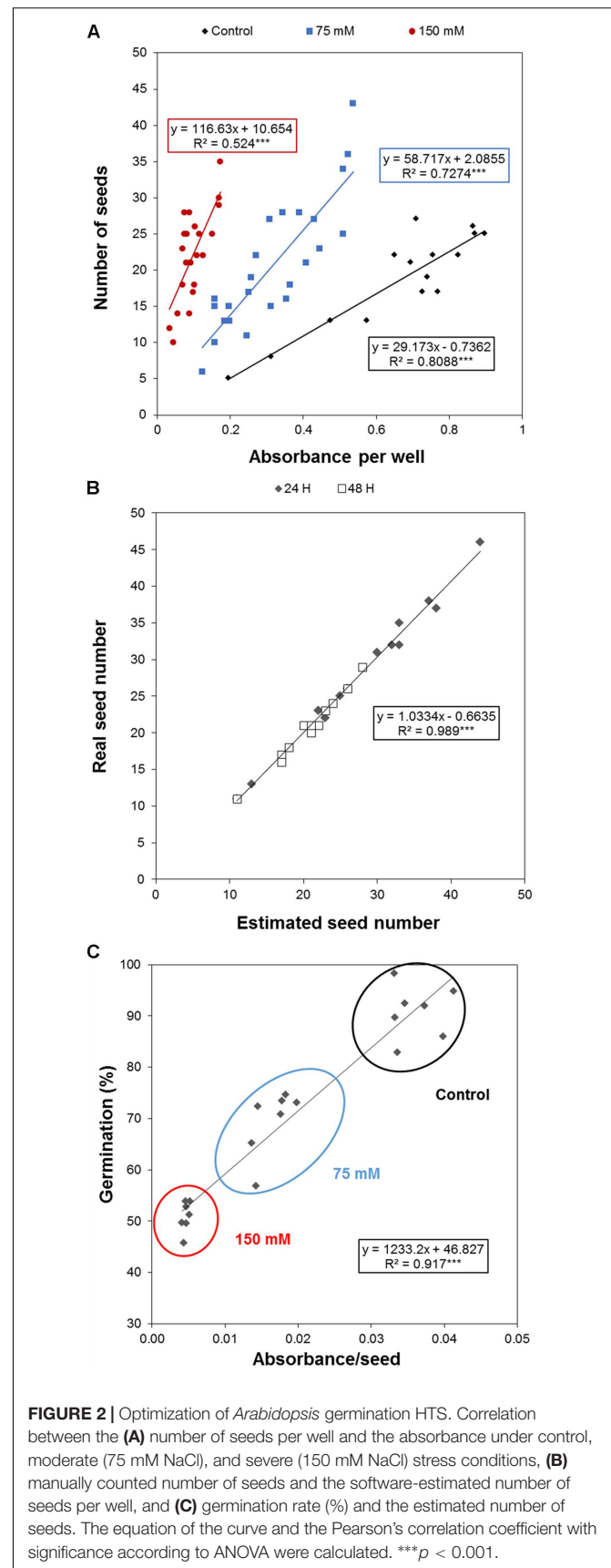


FIGURE 2 | Optimization of *Arabidopsis* germination HTS. Correlation between the (A) number of seeds per well and the absorbance under control, moderate (75 mM NaCl), and severe (150 mM NaCl) stress conditions, (B) manually counted number of seeds and the software-estimated number of seeds per well, and (C) germination rate (%) and the estimated number of seeds. The equation of the curve and the Pearson's correlation coefficient with significance according to ANOVA were calculated. $^{***}p < 0.001$.

TABLE 1 | Comparison of measured overall formazan absorbance and the absorbance recounted per seed after 24 or 48 h of germination.

	24 h		48 h	
	Absorbance	Absorbance/seed	Absorbance	Absorbance/seed
Mean	0.399	0.019	0.73	0.041
SD	0.112	0.002	0.21	0.003
%	28.08	9.14	28.52	8.28

Mean \pm SD and contribution of the SD to each mean.

Effect of Biostimulant Seed Priming on *Arabidopsis* Seed Germination

We used the above-described optimized protocol to evaluate the effect of biostimulant (Put, Spd, Spm, and Pro) seed priming on seed germination under salt stress conditions. After 24 h, the tested variants differed only slightly (**Figure 3**). However, 1 mM Spd inhibited seed germination under control conditions and after 48 h of exposure to 75 mM NaCl, but exerted no effect under severe salt conditions (**Figure 3**). The same holds true for 1 mM Spm which also inhibited seed germination in 75 mM NaCl. The most visible effect was obtained for seeds primed with 0.01 and 0.1 mM Put and (to a lesser extent) 1 mM Pro, which yielded a significant increase in the germination in 150 mM NaCl (**Figure 3**).

Seed Size Conditions Associated With *Arabidopsis* Rosette Growth

To determine the effect of biostimulants on the early seedling development of *Arabidopsis* plants under salt stress conditions, we further optimized our previously published protocol (De Diego et al., 2017) for HTS of the rosette growth. For rapid characterization of the plant biostimulants, the protocol was improved as follows: the response of 4-day-old *Arabidopsis* seedlings grown in 1 \times MS was evaluated using 48 well plates with four biological replicates randomly distributed in the platform. Due to the rapid image acquisition of our system (\sim 250 plates per hour) the seedlings were imaged twice per day (at 10:00 and at 16:00) for seven consecutive days (**Supplementary Figure S1**). The time-dependent increase in the rosette area (represented by the green region) and RGR were determined for each replicate. The green area differed negligibly among the replicates according to ANOVA (**Figure 4A**), which also exhibited similar RGR. Using this approach, we could record fluctuations in the RGR (per hour) between the 2 days sessions, thereby increasing the sensitivity and applicability of the assay to analysis of circadian rhythms. Higher RGR occurred in the period from 10:00 a.m. to 4:00 p.m. (**Figure 1B**) than in other sessions.

The effect of seed size on the variability of early seedling development via rosette growth was evaluated to further increase the technical precision of the assay. Using sieves, the seed batch was separated into three different size categories: 250–280, 280–300, and >300 μ m. Seeds larger than 280 μ m produced seedlings with similar rosette area (see **Figure 4C**), whereas seeds with sizes of 250–280 μ m yielded significantly smaller rosettes (**Supplementary Table S1**). Although seeds with sizes of 280–300 μ m were quite abundant, seeds larger than 300 μ m

were rare. Thus, due to their abundance and good growth performance, we selected the 280–300 μ m seeds as the standard for subsequent experiments.

HTS of *Arabidopsis* Rosette Growth as a Suitable Assay for the Characterization of Biostimulants Under Control and Salt Stress Conditions

Our OloPhen platform has sufficient capacity for the simultaneous testing of numerous variants (De Diego et al., 2017). To demonstrate the capacity for large-scale stress-response studies, we performed an experiment analogous to the germination assay using a 1 \times MS medium supplemented with two concentrations of NaCl (75 or 150 mM). The seeds were primed with Put, Spd, Spm, and Pro over the same concentration range (0.001, 0.01, 0.1, and 1 mM) described in the Methods section. The 4-day old seedlings were transferred for continued growth under three different conditions: control, moderate salt (75 mM NaCl) and severe salt (150 mM NaCl). In this experimental design, 119 units of 48 well plates containing a total of 5,712 plants were analyzed in a single run. As shown in **Figure 5**, seed priming with biostimulants induced significant differences in the rosette growth of individual variants (**Supplementary Table S2**). All concentrations of Put and Spd improved rosette growth and RGR, in both control and salt stress conditions, acting as plant growth promoters and stress alleviators (**Figure 5**). The best results were obtained with Put and Spd (**Figures 5, 6**), especially under the severe salt condition (150 mM NaCl). In this case, exponential growth of the plants was maintained (**Figure 5**) through more efficient RGR per day (**Figure 7**) than that associated with other conditions. Spm priming promoted concentration-dependent growth under control and moderate salt stress conditions, although this growth stimulation was less than that induced by Put or Spd (**Figure 5**). Although Spm application improved rosette growth under severe stress conditions, maximum growth of the Spm-primed seedlings occurred earlier than that of seedlings grown only with 150 mM NaCl (**Figure 5**). Spm can therefore be classified as a plant growth promotor rather than a stress alleviator. In the case of stress-related amino acid Pro, we observed that low concentrations of Pro inhibited plant growth, whereas the highest concentrations stimulated growth in control and 75 mM NaCl conditions (**Figure 5** and **Supplementary Table S2**). Under the moderate stress induced by 75 mM NaCl, high concentrations of Pro exerted a stress-alleviating effect, but had

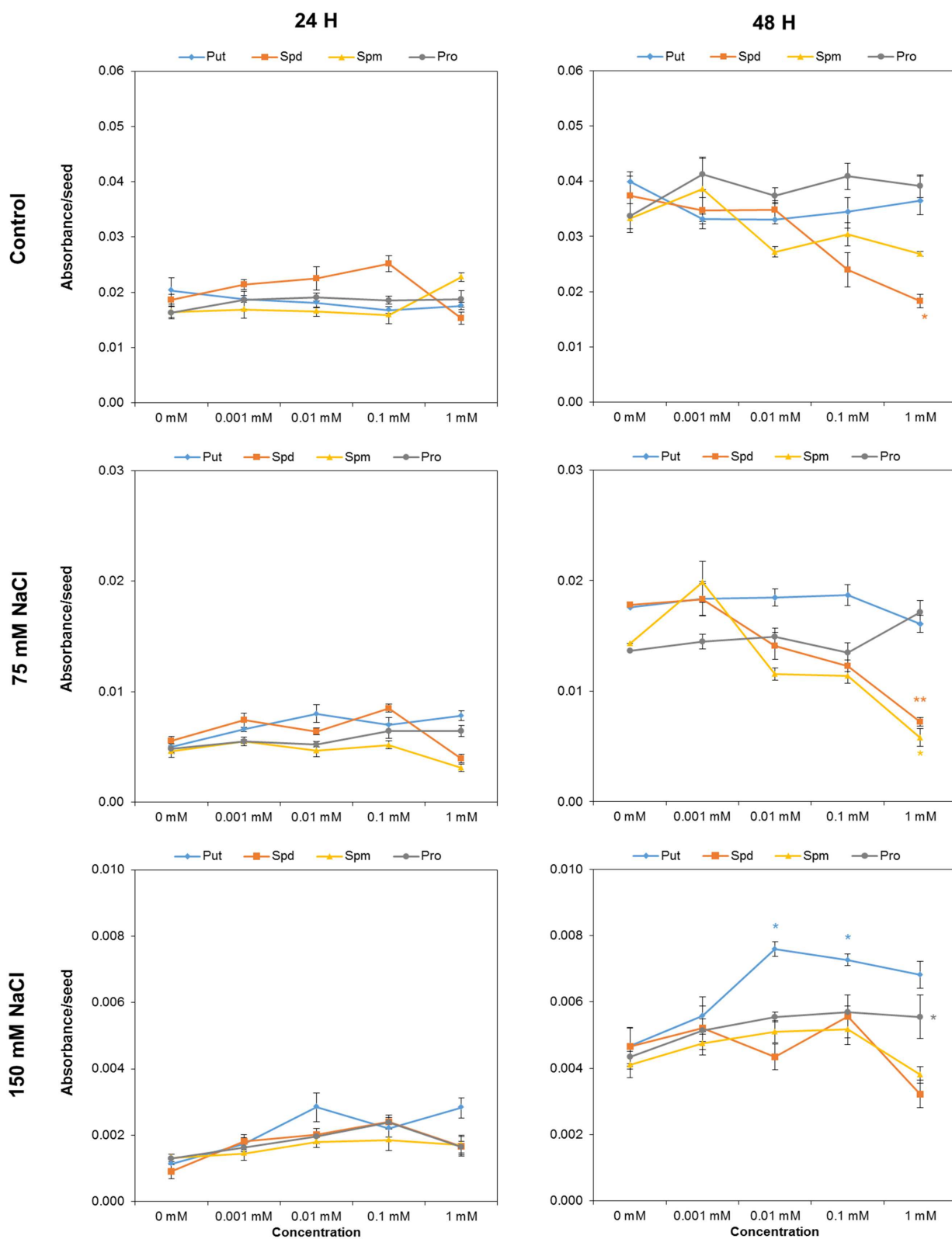


FIGURE 3 | Absorbance per seed of *Arabidopsis* seeds primed with Put, Spd, Spm, and Pro at four concentrations (0.001, 0.01, 0.1, and 1 mM), after 24 or 48 h of germination. Mean \pm SE. Statistical analysis was performed via the Kruskal-Wallis test. Asterisks indicate differences relative to the non-treated variant ** $p < 0.01$; * $p < 0.05$.

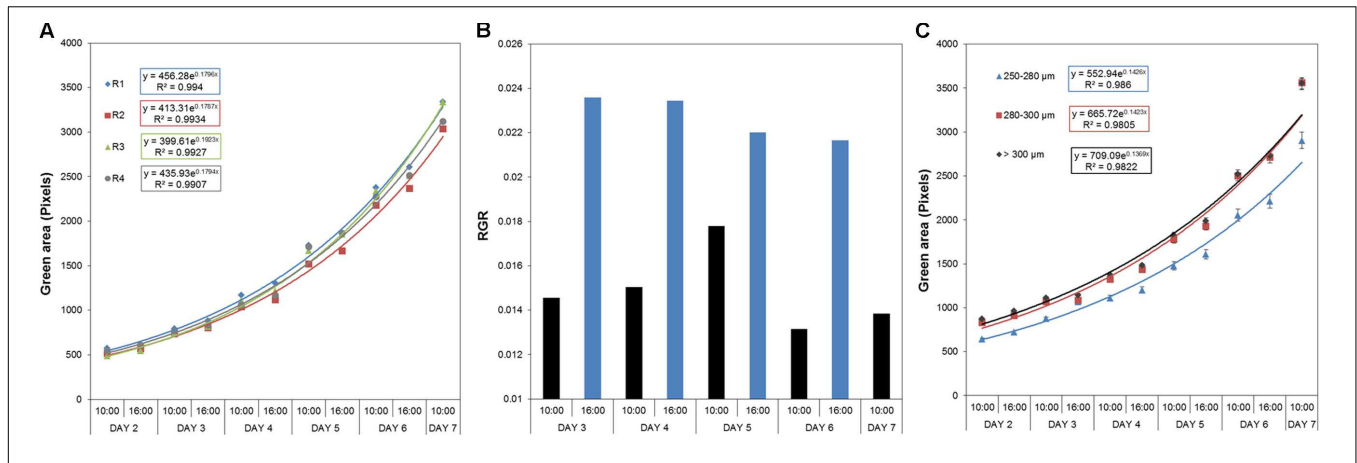


FIGURE 4 | Natural variation in *Arabidopsis* rosette growth in 48 multi-well plates under control conditions. **(A)** Green area (pixels) associated with the growth of four DAG *Arabidopsis* seedlings in independent 48-well plates (replicates; R1–R4) for 7 days. *Mean* \pm *SE*. **(B)** Relative growth ratio (RGR, pixel pixel⁻¹ hour⁻¹) of four DAG *Arabidopsis* seedlings grown in 48-well plates (*n* = 192). **(C)** Effect of the seed size on the green area (pixels) associated with the growth of four DAG *Arabidopsis* seedlings in independent 48-well plates. Three different size categories of seeds were considered: 250–280, 280–300, and >300 μm . The equation of the curve and the Pearson's correlation coefficient were calculated. 250–280 μm seeds were significantly smaller than 280–300 and >300 μm ones, according to the multiple comparisons after ANOVA.

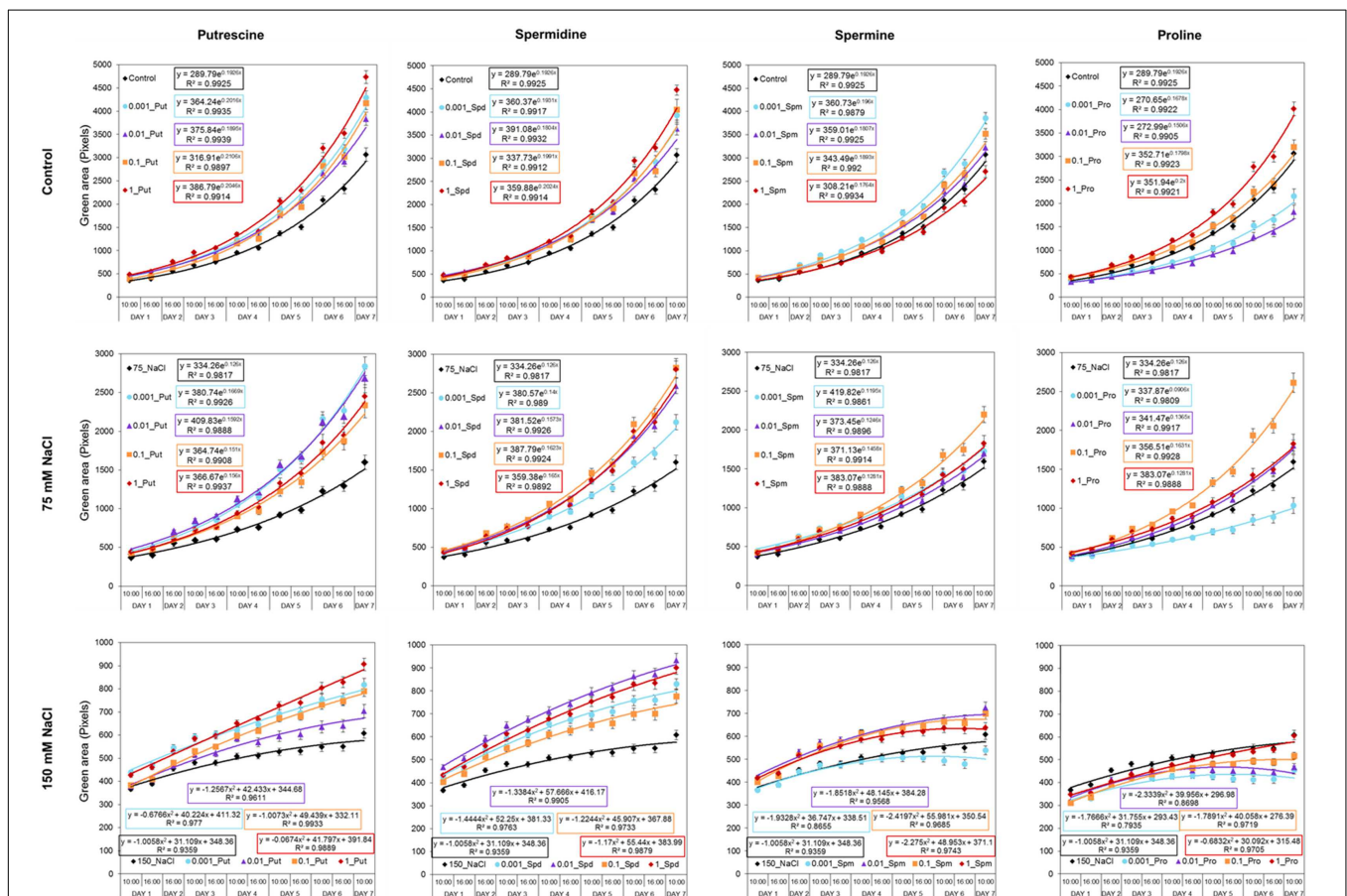


FIGURE 5 | Variation in *Arabidopsis* rosette growth from primed seeds with moderate and severe salt stress. Green area (pixels) of four DAG *Arabidopsis* seedlings primed with Put, Spd, Spm, and Pro at four concentrations (0.001, 0.01, 0.1, and 1 mM) and grown for 7 days in 48-well plates under control, moderate (75 mM NaCl), and severe (150 mM NaCl) salt stress conditions. *Mean* \pm *SE*. The equation of the curve and the Pearson's correlation coefficient were calculated.

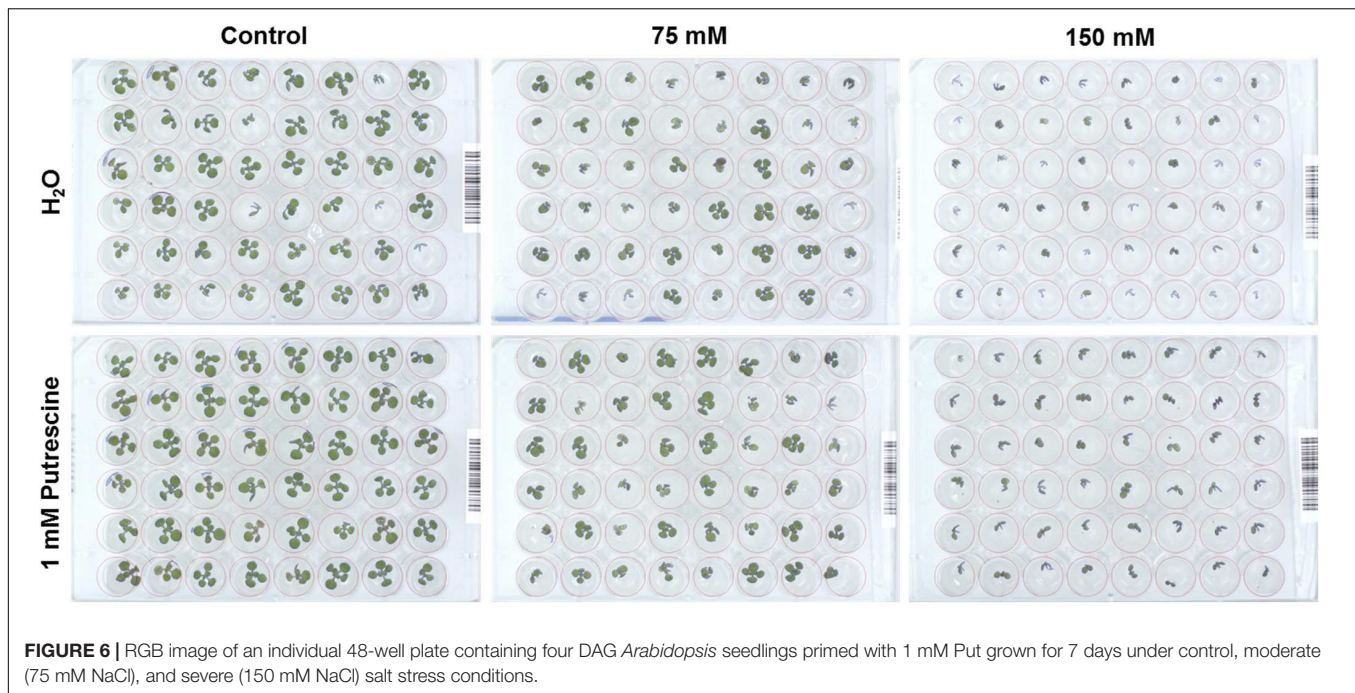


FIGURE 6 | RGB image of an individual 48-well plate containing four DAG *Arabidopsis* seedlings primed with 1 mM Put grown for 7 days under control, moderate (75 mM NaCl), and severe (150 mM NaCl) salt stress conditions.

a rather negative effect under the severe salt stress condition (Figure 5 and Supplementary Table S2).

Effect of Biostimulant on *Arabidopsis* Seedling Establishment

Analysis of the dataset recorded from the above-described HTS of rosette growth revealed the effect of seed priming on early-seedling establishment. In this case, we analyzed the green area of the *Arabidopsis* seedlings immediately after the transfer to 48 well plates, corresponding to time zero of the HTS focused on *Arabidopsis* rosette growth as a suitable assay. Without salt stress, the sizes of seedlings established from primed seeds differed significantly from the sizes of seedlings resulting from non-primed seeds (Figure 8). For the entire range of concentrations, the priming by Put and Spd resulted in significantly larger rosettes compared to those seedlings from non-primed seeds. Except for the highest (1 mM) concentration, all Spm concentrations lead to a significant increase in the green area of the seedlings, whereas for Pro a considerable increase was observed only at the highest concentration (Figure 8). These results showed that our method can record traits in a complex manner that describes the effect of priming on all important stages of early development (e.g., germination, early seedling establishment and rosette growth).

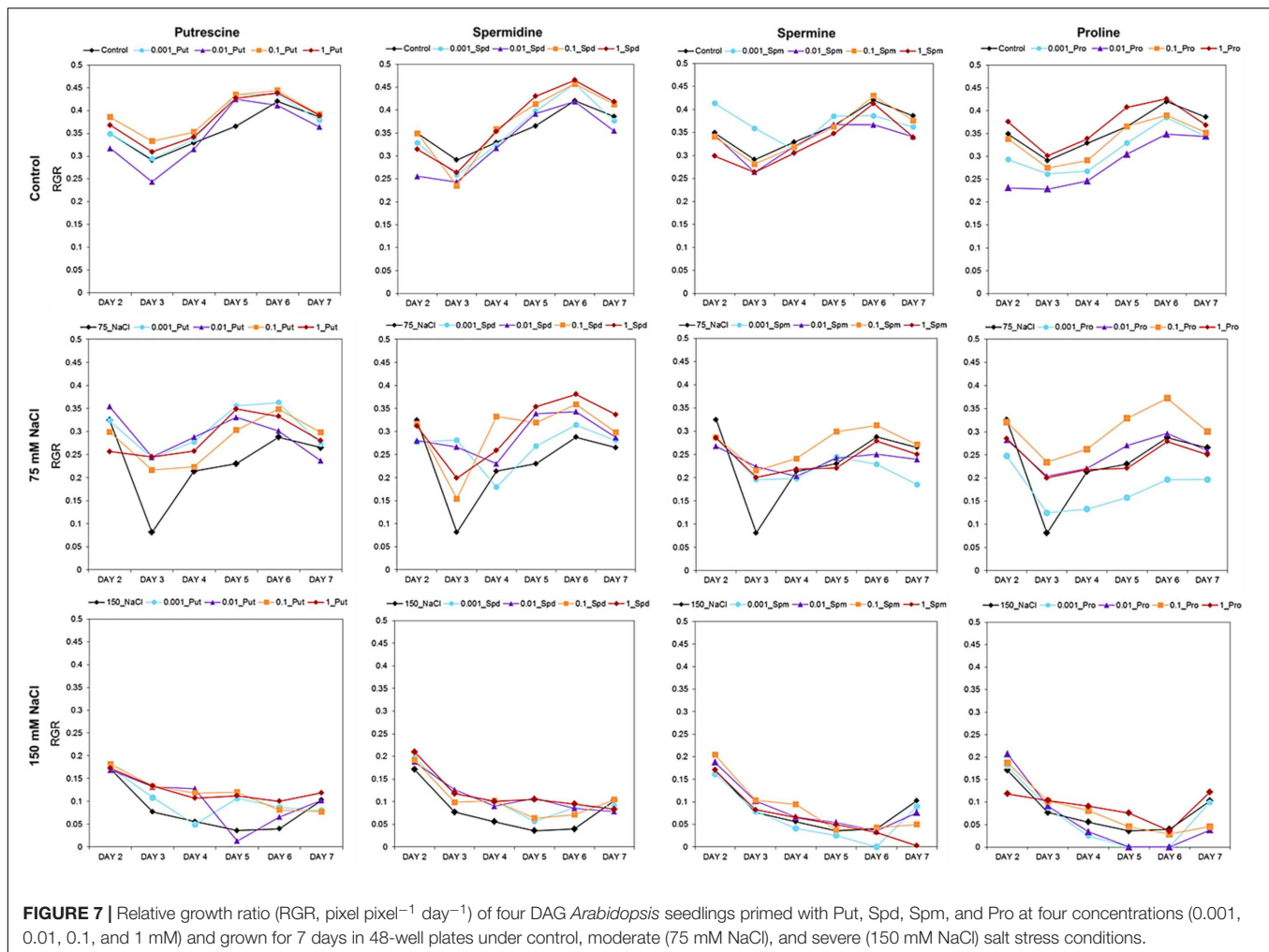
Effect of Biostimulants on the Leaf Color of *Arabidopsis* Rosettes Under Control and Salt Stress Conditions

The degradation of chlorophyll, manifested as a change in leaf color, represents one of the most important symptoms of stresses in plants. This change in color may serve as an important marker in stress-related plant studies, especially in those employing

salinity. To obtain this information, we introduced another trait into our method describing the effect of seed priming on the plant stress response. As described in the Methods section, the leaf color of the *Arabidopsis* rosettes was determined. We also evaluated the potential of three vegetation indices (VI) calculated using all three mixed visible bands (i.e., R, G, and B bands) which included the NGRDI, GLI, and VARI as indicators of leaf color change. These indices were strongly correlated with changes in the rosette area of the *Arabidopsis* seedlings and the values thereof depended on the seed priming treatment and salt intensity (Figures 9A,B). Of the three indices, GLI exhibited the highest sensitivity to salt stress (R^2 : 0.97; R^2 for NGRDI and VARI: 0.95). However, when the three VI were separately evaluated for the seedling with 150 mM NaCl, a significant positive correlation with the green area of the *Arabidopsis* rosette (Figures 9D–F) was obtained only for GLI. The seed priming with Put and Spd generated *Arabidopsis* rosettes with the highest greenness under control and salt stress conditions. The highest values were observed for GLI where 1 mM Put and Spd yielded 22 and 31%, respectively, higher levels of greenness than that of the non-treated seeds (Figure 9E).

PBC Index for Estimating the Biostimulant Mode of Action

We developed a Plant Biostimulant Characterization (PBC) index aimed at integrating both HTS methods into a pipeline that yields straight-forward information allowing simple selection of the best treatment under each condition. The index can represent up to four analyzed traits: seed germination rate (%), seedling establishment (green pixels after transfer to 48 well plates), growth capacity (Pixels) and the leaf color



index (GLI) for the primed and non-primed seeds. For the index calculation first the differences between the controls of the different growth conditions and variants (compound and concentration) under the same conditions were calculated as the log₂ of the ratio. The number represented by the independent traits and treatment constituting the PBC index can be then represented in a parallel coordinate plot (Figures 10, 11). This type of representation allows a better visualization (than that provided by other representations) of the variant-induced changes in each trait. In addition, the connection between the traits can be quickly identified. For example, under control conditions, it is easier to visualize that the seed priming with Put and Spd mainly improved *Arabidopsis* growth capacity, and to less extend the early seedling establishment and leaf color index, whereas the germination remained unchanged or was even inhibited by these agents (Figure 10). Under salt stress condition, seed priming with polyamines improved *Arabidopsis* growth capacity and leaf color index under both intensities tested (75 and 150 mM) (Figures 11A,B). Nevertheless, only under severe conditions, the priming with polyamines improved seed germination in almost all cases compared with their respective control (Figure 11A).

The concentration effect of the tested compound under three different growth conditions (control, 75 mM NaCl or 150 mM NaCl) was then determined by summing the relative changes (log₂) obtained for the parallel coordinate plot ending with a single number as shown in Figure 12. This sum yielded a total that can reach a positive (biostimulant- blue) or negative (inhibitor-red) value. The resulting numbers were then plotted in a multidimensional graphic “radar chart” using the concentrations as quantitative variables (Figure 12). From these results we confirmed that Put was the most efficient plant growth promotor and stress alleviator with higher values in each concentration and growth condition, compared with the controls. The remaining compounds exhibited a concentration- and growth-condition-dependent response. For example, Spd and Spm yielded the highest index values at low concentrations, whereas Pro acted as plant biostimulants at high concentrations only, and its effectiveness increased with increasing salt stress intensity (Figures 12B,C). These results confirm that the presented MHTS approach is an adequate tool for a fast and simultaneous analysis of various concentrations and growth conditions for identification and, especially, characterization of the operation mode associated with new biostimulants.

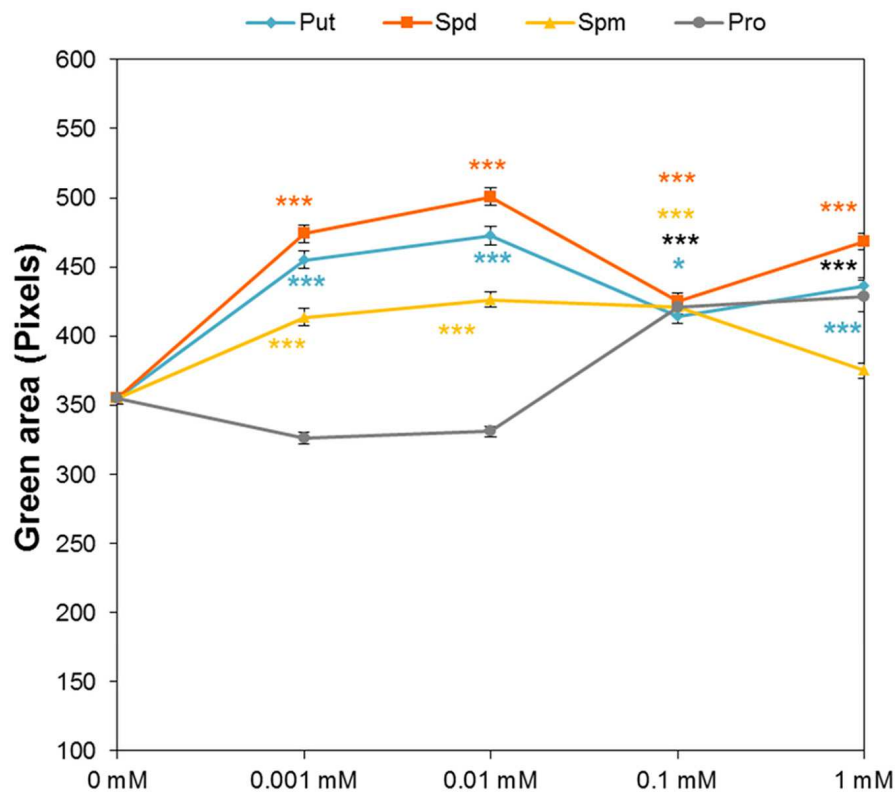


FIGURE 8 | Effect of biostimulant seed priming on the seedling establishment of *Arabidopsis*. Green area (pixels) of four DAG *Arabidopsis* seedlings primed with Put, Spd, Spm, and Pro at four concentrations (0.001, 0.01, 0.1, and 1 mM) and grown under control conditions after the transfer to 48-well plates. Statistical analysis was performed via the Kruskal-Wallis test. Asterisks indicate differences relative to the non-treated variant. *** $p < 0.001$; * $p < 0.05$.

DISCUSSION

Uniform and efficient seed germination and establishment of early seedlings are crucial for agricultural crop production under stress conditions, especially drought and/or salinity (Savvides et al., 2016). Seed priming, where seeds are pre-sown with certain compounds with the aim of increasing the uniformity and vigor of seedlings, represents an innovative alternative to coping with the negative stress effects. In addition, the use of natural compounds or biostimulants as priming agents can improve the efficiency of crop production and yield under suboptimal conditions. The use of these substances is more sustainable and environmentally friendly compared with the use of other materials. The priming with single compounds such as polyamines and amino acids can be a good technology against different abiotic stresses (Savvides et al., 2016). However, despite the fact that most of the complex biostimulants of several origins (i.e., protein hydrolysis from agroindustrial by-product from both plant sources and animal waste, and seaweed extracts) contain these types of compounds (du Jardin, 2015), their biostimulant activity potential hasn't been fully evaluated. For this reason, we used in this study the stress related amino acid Pro and polyamines' representatives as priming agents to bring additional information about their possible biostimulant mode of action. Therefore, biostimulant manufacturers require tools

for identifying new biostimulants, characterizing and quantifying their biological effects and describing the corresponding mode of action. Moreover, during biostimulant preparation, the tools for rapid control of the quality during the extraction processes and production of different batches are needed. Taking into account the mentioned facts, we suggest that Put, Spd, Spm, and Pro have potential to be used as positive controls in the biostimulant research and manufacturing.

Screening platforms based on the semi-automated or automated bioassaying of simple traits based on *in vitro Arabidopsis* assays might be useful to accelerate the process for preliminary screening of stability, composition and effect of raw material. This testing allows for a rapid first-step screening on plants, eliminating the influence of soil and other environmental parameters (Povero et al., 2016). The testing of biostimulants using bioassays has been traditionally performed with Petri dishes, thus having low-throughput requiring posterior manual quantification (Durand et al., 2003; Colla et al., 2014; Povero et al., 2016). Recently, Rodríguez-Furlán et al. (2016) published an *in vitro* bioassay using *Arabidopsis* for the testing of several compounds. However, the use of scanners for image analysis yields an analysis rate of 20 min per plate and the analysis is performed only at one time-point (Rodríguez-Furlán et al., 2016). Several other manual and semi-automated HTS protocols using RGB imaging for phenotyping of *Arabidopsis*

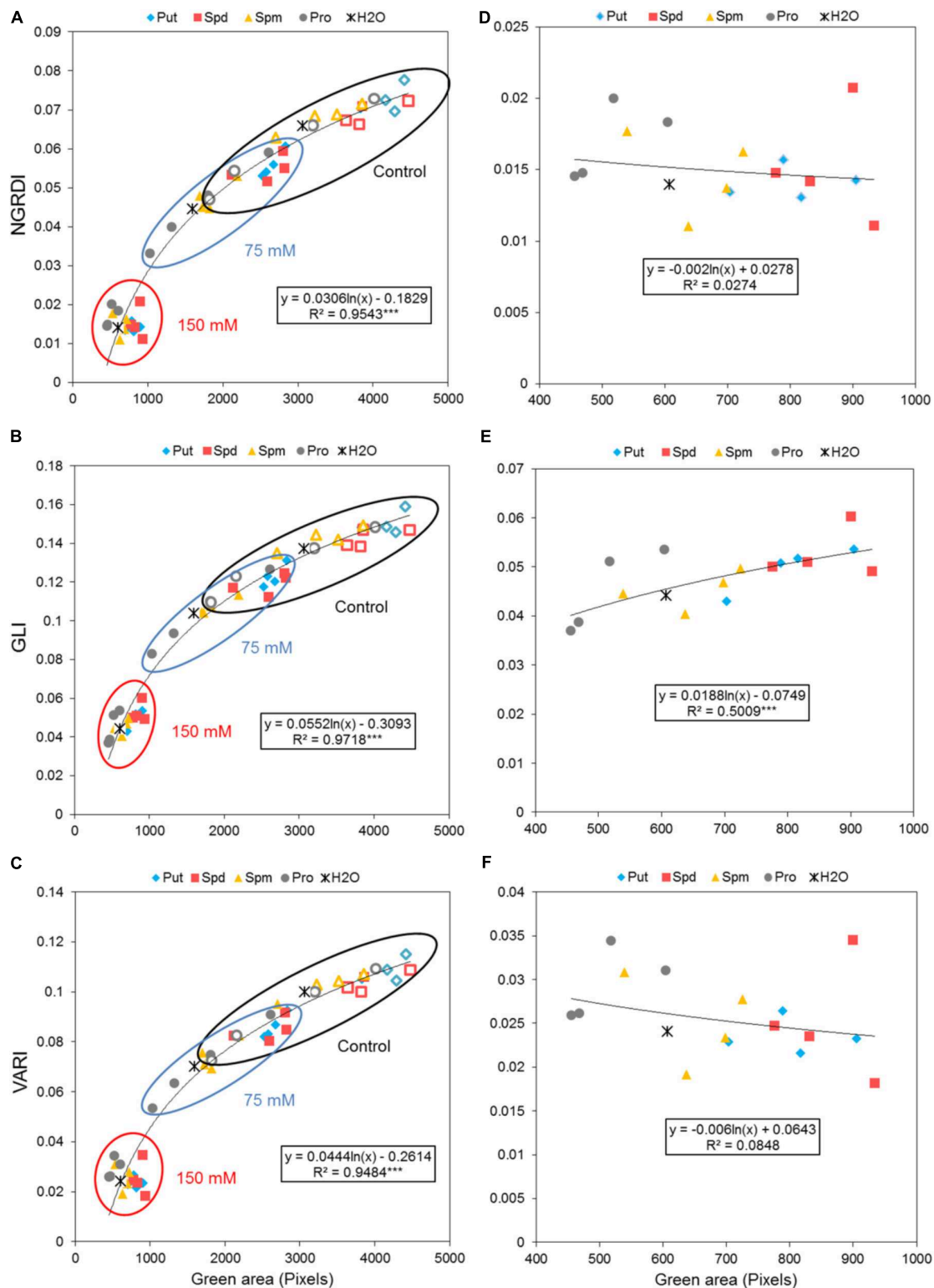
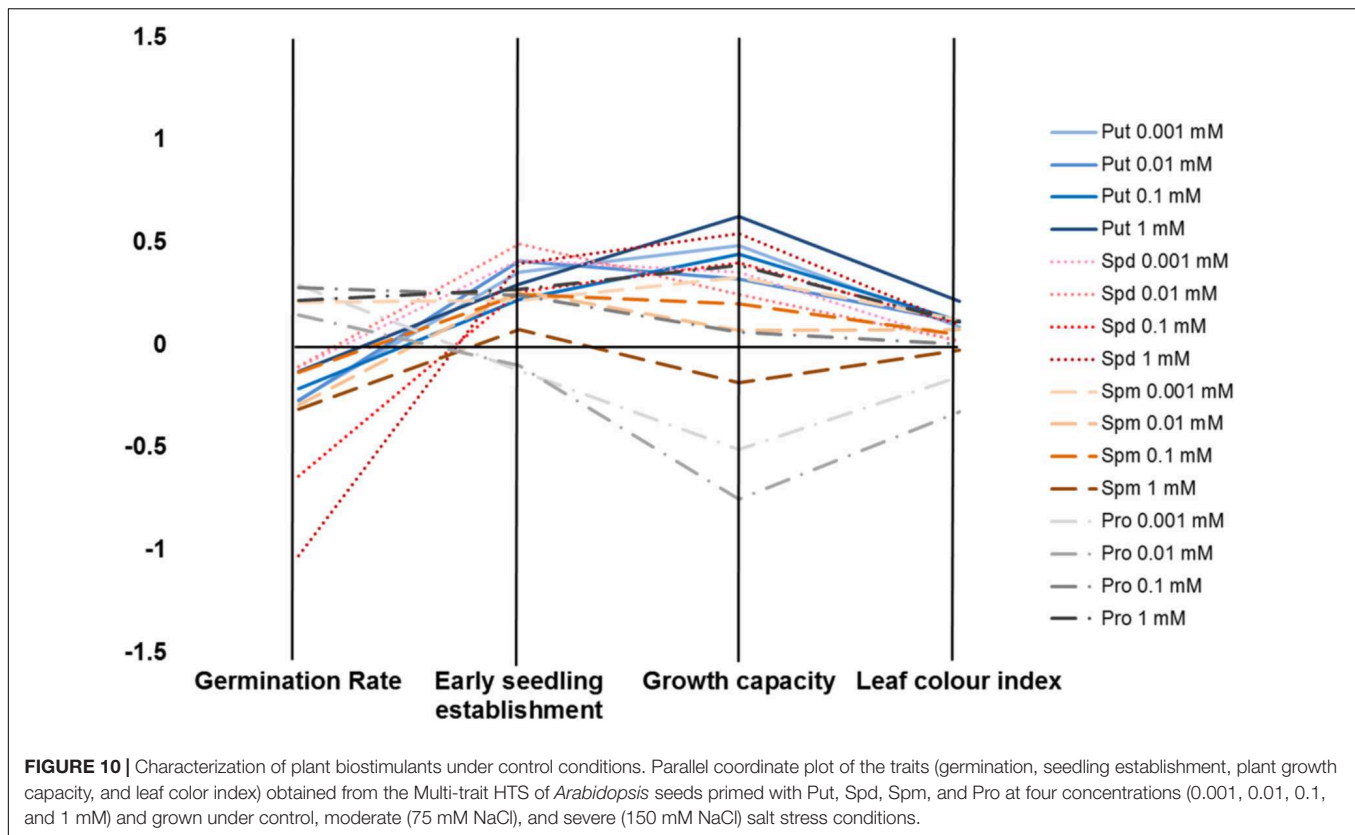


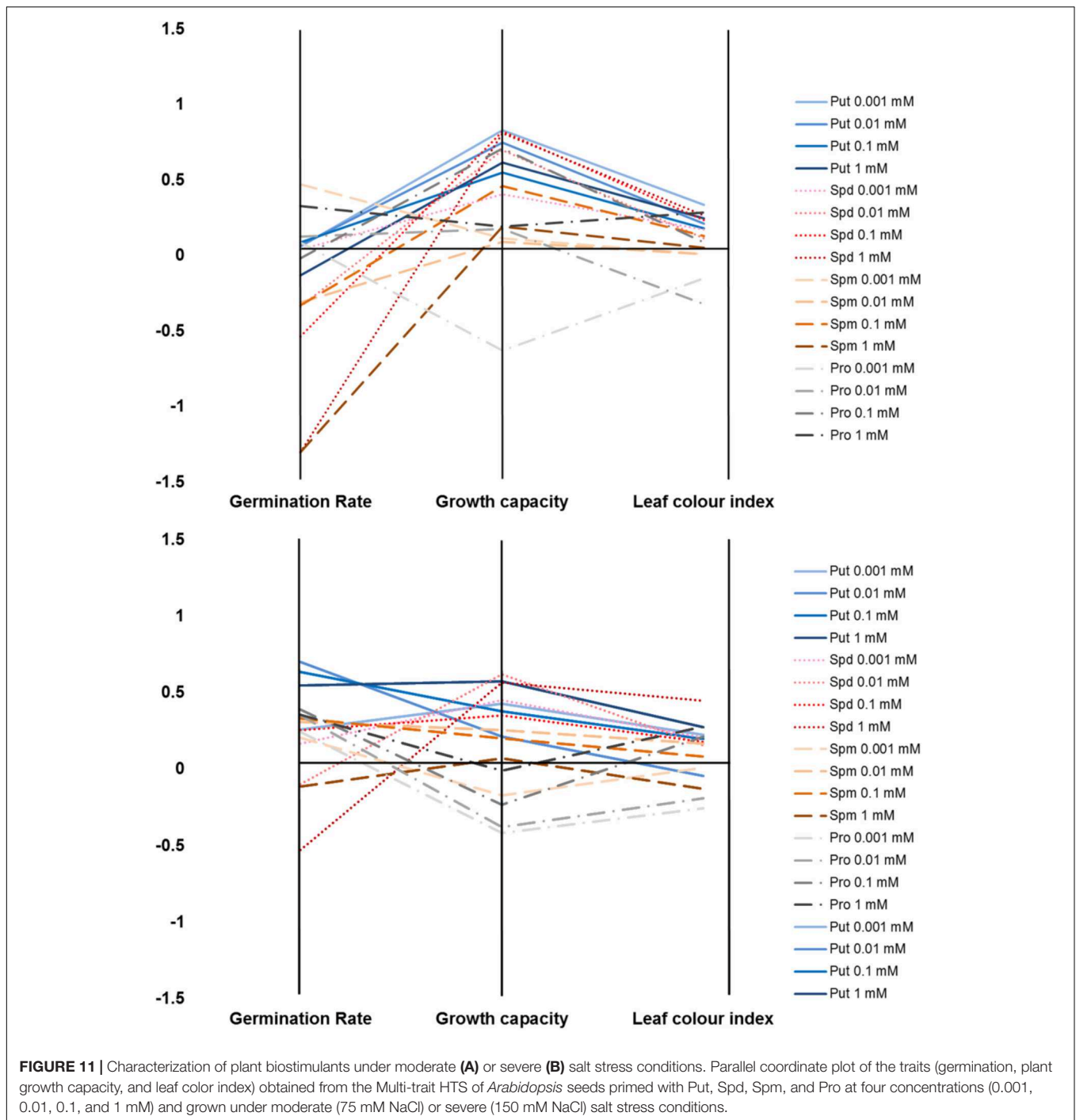
FIGURE 9 | Effect of biostimulant seed priming on the stress response of *Arabidopsis*. **(A)** Correlation between the color index; NGRDI **(A)**, GLI **(B)**, or VARI **(C)** and the green area (Pixels) of four DAG *Arabidopsis* seedlings primed with Put, Spd, Spm, and Pro at four concentrations (0.001, 0.01, 0.1, and 1 mM) and grown under control (empty symbols), moderate (75 mM NaCl), and severe (150 mM NaCl) salt stress conditions for 7 days. **(B)** Correlation between NGRDI **(D)**, GLI **(E)**, or VARI **(F)** and the green area of the *Arabidopsis* seedlings grown only under severe stress conditions. The equation of the curve and the Pearson's correlation coefficient with significance, according to ANOVA, were calculated after linearization. $***p < 0.001$.



in the controlled conditions have been published with different throughputs and (dis)advantages. The method of Granier et al. (2006) showed possibilities solving potential complications and methodological difficulties with the spatial and temporal variability of micrometeorological conditions within a growth chamber, reaching throughput of 500 plants per hour. Recently, simple HTS protocol based on *in vitro* growth of *Arabidopsis* using square plates with 16 seedlings and manual image acquisition followed by analysis of plant size and color was published by Faragó et al. (2018). The protocol presented by us is based on our previous report of an automated method for HTS of *Arabidopsis* rosette growth in multi-well plates accessible at OloPhen facility (De Diego et al., 2017). The potential of this method was in our recent protocol improved in several ways through (1) increase of the number of plates per run from 480 to 572; (2) significant increase of the total number of plants analyzed by use of 48-well plates, instead of 24-well plates that increased the number of analyzed plants to more than 27,000 in less than 3 h; and (3) through increase of the resolution of the growth analysis by automated measurement twice a day within 1 week. As presented here, our new method allows a simultaneous study of different growth conditions without compromising the number of variants, replicates and plants per treatment. Moreover, compared to Faragó et al. (2018), the growth analysis of each plant is done for the whole cycle by imaging of the same plant individual. Further, the use of independent wells per plant permits an easier detection of the single plant so they are located in a concrete XY position. Thus, there is no requirement

of any manual adjustment to separate individual plants. As clear example illustrating the potential of our method, in this work we automatically recorded the rosette growth of 5,712 *Arabidopsis* (119 plates \times 48 seedling). The imaging of each well-plate was performed twice per day (at 10 a.m. and 4 p.m.) for 7 days, ending with 14 data points per plant in very short time. Altogether, we developed a very fast *in vitro* bioassay to analyze simultaneously a huge amount of treatments and plants.

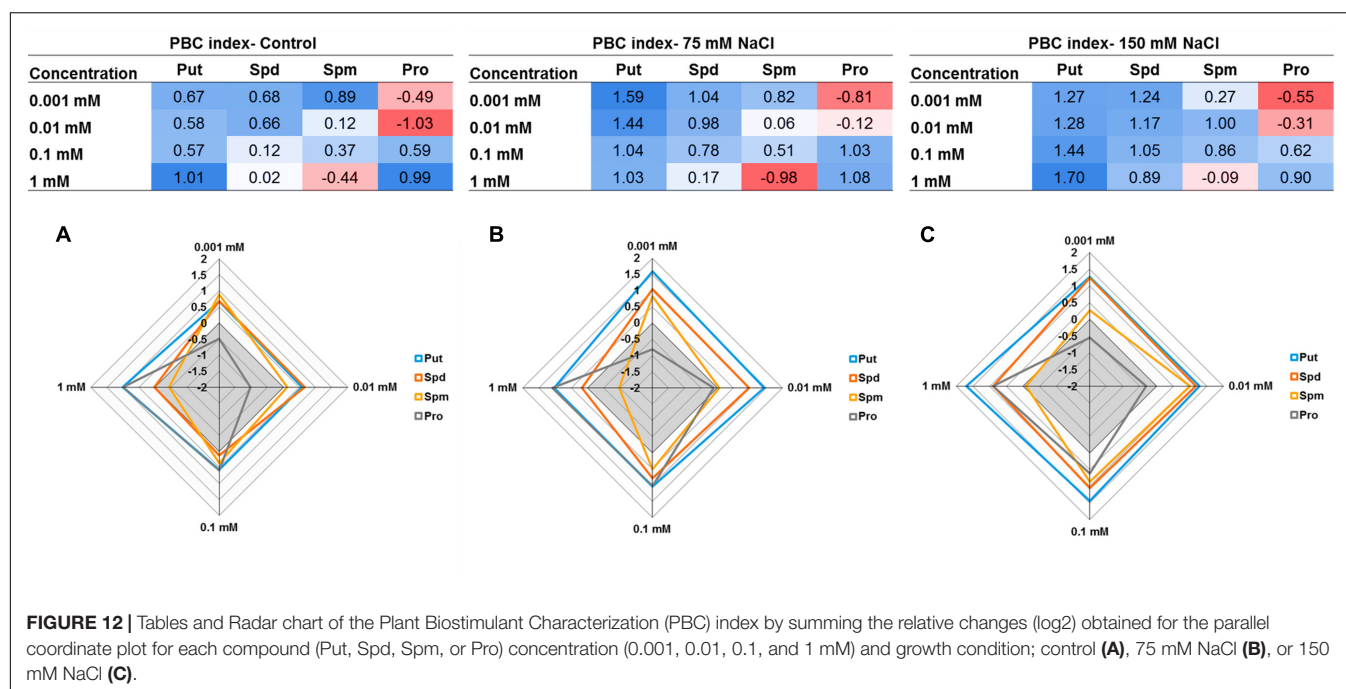
The improved HTS of rosette growth under control and stress salinity was integrated in a pipe-line for the screening of biostimulants together with the HTS of *Arabidopsis* seed germination. For that, we developed a simple and fast bioassay for *Arabidopsis* seed germination based on (Pouvreau et al., 2013) using spectrophotometric analysis of MTT reduction in microtiter plates. With the classical method using a microscope, the distinction between non-germinated seeds and germinated seeds with a very short protruded radicle is very difficult, increasing the risk of germination rate underestimation (Pouvreau et al., 2013). However, the MTT method is simple and accurate and can be easily adapted for high-throughput germination bioassays. The HTS method is performed in 96 well plates. These plates allow many variants per plate (compounds, concentrations, and/or germination conditions) using a spectrophotometric MTT method with a simple read out of the germination rate per variant (Figure 1). In addition, we developed a simple in-house software routine to automatically count the seed number per well. This reduced the time consuming counting of the seed number per well necessary



for increasing the accuracy of the method by reducing the variability within treatments (Figure 2A). Although free software applications exist for image-based analysis of seeds allowing automated definition of the seed shape and size (Tanabata et al., 2012), for our purpose we created a very simple software routine in MATLAB suitable for detecting and counting objects (seeds) in multi-well plates at 0 h (immediately after cold stratification and before seed germination). The obtained number is then used to recalculate the total absorbance of

the well recorded by spectrophotometer to the absorbance per seed that represents the germination rate. This trait together with those obtained from the HTS of *Arabidopsis* rosette growth (plant establishment, plant growth capacity under different conditions and leaf color index), constitute the MTHTS for biostimulant characterization achievable within 1 week.

Many biostimulants contain various groups of components including complex mixtures of biologically active compounds



and, hence, the testing should be performed over a broad concentration range allowing evaluation of concentration-dependent effects. We selected individual molecules as a first step in optimizing our bioassays for biostimulant characterization. The polyamines Put, Spd, and Spm, and the amino acid Pro, which also have been identified in the raw material of complex formulations from different natural origins, were selected (Colla et al., 2014; du Jardin, 2015). Moreover, we selected salinity as a stressor, owing to its negative impact on seed germination and plant growth. Using our approach, each compound can be simultaneously tested at different concentrations and plant growth conditions in both HTS methods. The results revealed differences in the mode of action for the four compounds applied to *Arabidopsis* seed germination and rosette growth (Figures 3–9). Put and Spd were identified as plant growth promoters and stress alleviators, whereas Spm and Pro were less efficient and their positive effect was concentration dependent (Figures 5, 10, and 11). The exogenous application of polyamines yields improved salt tolerance in many crops via enhanced germination and/or plant productivity (Roychoudhury et al., 2011; Li et al., 2015; Shekari et al., 2015). For example, exogenous application of Spd in *Cucumis sativus* L. induces accumulation of endogenous polyamines that act as free radical scavengers, thereby stabilizing cellular membranes and maintaining cellular ionic balance under salinity (Shu et al., 2012). This was attributed to a relatively high Put/(Spd+Spd) ratio that rendered seed priming with Put the most efficient treatment. As confirmation, Shu et al. (2015) demonstrated that Put application regulates protein expression at transcriptional and translational levels by increasing endogenous polyamine levels in thylakoid membranes which may stabilize the photosynthetic apparatus under a

salt stress. In addition, changes in polyamines biosynthesis and catabolism influence plant tolerance and recovery capacity though a sophisticated crosstalk with plant hormones, which induces changes in primary metabolism such as the synthesis of amino acids, and improves photosynthesis and nutrient uptake under stress conditions (review in Podlešáková et al., 2018). Therefore, priming with polyamines could be a cheap, healthy, and easy solution for mitigating adverse salinity-induced stresses occurring during the initial developmental phases of crops.

The priming with Pro was less effective than with polyamines, and the most positive effect was in the germination rate under a severe salt stress. This may have resulted from the fact that enhanced Pro levels in plants occur in the first phases of seed germination and the seed-to-seedling transition (Silva et al., 2017). Similar results were obtained in rice, where the seeds pre-treated with Pro provided significant evidence for assessing the salt tolerance at the germination stage (Deivanai et al., 2011). However, the effect was variety dependent. In sugar cane grown *in vitro*, the anti-stress effect was also genotype dependent (Medeiros et al., 2015), but both dependences increased the stress tolerance by activating the plant antioxidative response. Other studies consider the Pro mode of action to be long-term, when the plant accumulated high levels of Pro, and attributed this action to plant recovery and hardening (De Diego et al., 2015; Sabagh et al., 2015). This could be explained by the fact that stress-tolerance improvement in many other crops required relatively high concentrations (Talat et al., 2013; Dawood et al., 2014). However, contradictory results regarding the Pro effect have been obtained for the same crop under the same stress conditions. For example, Teh et al. (2016) reported that 5 or 10 mM Pro improved salt stress tolerance of rice, but Deivanai et al. (2011) considered

the 10 mM concentration toxic. This contradiction resulted mainly from the different intensities of salinity considered. Therefore, integrating a wide range of concentrations in the same bioassay combined with different stress levels for the testing of biostimulants constitutes a viable strategy for biostimulant mode of action characterization.

CONCLUSION

In this work we present a complex pipe-line for a fast characterization of plant biostimulants suitable for seed-priming application giving straight-forward information for simple selection of the best treatments under control, moderate and severe salt stress conditions, using treatment evaluation through newly introduced index. The MTHTS approach based on the semi-automated analysis of *Arabidopsis* germination and rosette growth analyses four traits: *in vitro* germination rate, early seedling establishment capacity, growth capacity under stress and stress response based on plant greenness. The approach allows the acceleration of the biostimulant characterization through a simultaneous spanning of a broad number of biostimulants in a wide range of concentrations and stress conditions. Further, the method helps to define a biostimulant mode of action based on its contribution to the plant development and stress tolerance such as plant growth promotor/inhibitor and/or stress alleviator. The presented approach (i) represents a useful tool for biostimulant research and development, and (ii) when combined with chemical-composition analysis and biological-activity measurements can help to identify the specific mode of action characterizing the biostimulants and their main bioactive ingredients.

REFERENCES

- Calvo, P., Nelson, L., and Kloepper, J. W. (2014). Agricultural uses of plant biostimulants. *Plant Soil* 383, 3–41. doi: 10.1007/s11104-014-2131-8
- Chen, K., and Arora, R. (2013). Priming memory invokes seed stress-tolerance. *Environ. Exp. Bot.* 94, 33–45. doi: 10.1016/j.envexpbot.2012.03.005
- Colla, G., Rouphael, Y., Canaguier, R., Svecova, E., and Cardarelli, M. (2014). Biostimulant action of a plant-derived protein hydrolysate produced through enzymatic hydrolysis. *Front. Microbiol.* 5:448. doi: 10.3389/fpls.2014.00448
- Craigie, J. S. (2011). Seaweed extract stimuli in plant science and agriculture. *J. Appl. Phycol.* 23, 371–393. doi: 10.1007/s10811-010-9560-4
- Cristiano, G., Pallozzi, E., Conversa, G., Tufarelli, V., and De Lucia, B. (2018). Effects of an animal-derived biostimulant on the growth and physiological parameters of potted snapdragon (*Antirrhinum majus* L.). *Front. Plant Sci.* 9:861. doi: 10.3389/fpls.2018.00861
- Dawood, M. G., Taie, H. A. A., Nassar, R. M. A., Abdelhamid, M. T., and Schmidhalter, U. (2014). The changes induced in the physiological, biochemical and anatomical characteristics of *Vicia faba* by the exogenous application of proline under seawater stress. *South African J. Bot.* 93, 54–63. doi: 10.1016/j.sajb.2014.03.002
- De Diego, N., Fürst, T., Humplik, J. F., Ugena, L., Podlešáková, K., and Spíchal, L. (2017). An automated method for high-throughput screening of *Arabidopsis* rosette growth in multi-well plates and its validation in stress conditions. *Front. Plant Sci.* 8:1702. doi: 10.3389/fpls.2017.01702

AUTHOR CONTRIBUTIONS

LU, AH, JH, KD, LS, and NDD designed the experiments. LU, AH, JH, and KP performed the experiments. NDD and LS supervised the study and formulated the concept of the project. LU, AH, and NDD performed the data analysis. All authors discussed the results. LU, AH, JH, NDD, and LS wrote the manuscript.

FUNDING

This work was funded by the Ministry of Education, Youth and Sports of the Czechia (Grant LO1204 from the National Program of Sustainability).

SUPPLEMENTARY MATERIAL

The Supplementary Material for this article can be found online at: <https://www.frontiersin.org/articles/10.3389/fpls.2018.01327/full#supplementary-material>

FIGURE S1 | *Arabidopsis* rosette growth in 48 multi-well plates for 7 days under control conditions.

TABLE S1 | Statistical differences in the green area (pixels) of 4 DAG *Arabidopsis* seedlings from three different size categories of seeds (250–280, 280–300, and >300 μ m) grown in 48-well plates (three biological replicates per treatment) for 7 days. Different letters indicate significant differences according to multiple comparisons performed after ANOVA.

TABLE S2 | Statistical differences in the green area (pixels) of 4 DAG *Arabidopsis* seedlings primed with Put, Spd, Spm, and Pro at four concentrations (0.001, 0.01, 0.1, and 1 mM) and grown under control, moderate (75 mM NaCl) and severe (150 mM NaCl) salt stress conditions for 7 days. Different letters indicate significant differences according to multiple comparisons performed after ANOVA.

- De Diego, N., Saiz-Fernandez, I., Rodriguez, J. L., Perez-Alfocea, F., Sampedro, M. C., Barrio, R. J., et al. (2015). Metabolites and hormones are involved in the intraspecific variability of drought hardening in radiata pine. *J. Plant Physiol.* 188, 64–71. doi: 10.1016/j.jplph.2015.08.006
- Deivana, S., Xavier, R., Vinod, V., Timalata, K., and Lim, O. F. (2011). Role of exogenous proline in ameliorating salt stress at early stage in two rice cultivars. *J. Stress Physiol. Biochem.* 7, 157–174.
- du Jardin, P. (2015). Plant biostimulants: definition, concept, main categories and regulation. *Sci. Hortic.* 196, 3–14. doi: 10.1016/j.scienta.2015.09.021
- Durand, N., Briand, X., and Meyer, C. (2003). The effect of marine bioactive substances (N PRO) and exogenous cytokinins on nitrate reductase activity in *Arabidopsis thaliana*. *Physiol. Plant.* 119, 489–493. doi: 10.1046/j.1399-3054.2003.00207.x
- Farág, D., Sass, L., Valkai, I., András, N., and Szabados, L. (2018). PlantSize offers an affordable, non-destructive method to measure plant size and color in vitro. *Front. Plant Sci.* 9:219. doi: 10.3389/fpls.2018.00219
- Garcia-Gonzalez, J., and Sommerfeld, M. (2016). Biofertilizer and biostimulant properties of the microalga *Acutodesmus dimorphus*. *J. Appl. Phycol.* 28, 1051–1061. doi: 10.1007/s10811-015-0625-2
- Gitelson, A. A., Kaufman, Y. J., Stark, R., and Rundquist, D. (2002). Novel algorithms for remote estimation of vegetation fraction. *Remote Sens. Environ.* 80, 76–87. doi: 10.1016/S0034-4257(01)00289-9
- Granier, C., Granier, C., Aguirrezabal, L., Aguirrezabal, L., Chenu, K., Chenu, K., et al. (2006). PHENOPSIS, an automated platform for reproducible

- phenotyping of plant responses to soil water deficit in. *New Phytol.* 169, 623–635. doi: 10.1111/j.1469-8137.2005.01609.x
- Hunt, E. R., Doraiswamy, P. C., McMurtrey, J. E., Daughtry, C. S. T., Perry, E. M., and Akhmedov, B. (2013). A visible band index for remote sensing leaf chlorophyll content at the canopy scale. *Int. J. Appl. Earth Obs. Geoinf.* 21, 103–112. doi: 10.1016/j.jag.2012.07.020
- Ibrahim, E. A. (2016). Seed priming to alleviate salinity stress in germinating seeds. *J. Plant Physiol.* 192, 38–46. doi: 10.1016/j.jplph.2015.12.011
- Kaveh, H., Nemati, H., Farsi, I. M., and Vatandoost Jartoodeh, S. (2011). How salinity affect germination and emergence of tomato lines. *J. Biol. Environ. Sci.* 5, 159–163.
- Li, J., Hu, L., Zhang, L., Pan, X., and Hu, X. (2015). Exogenous spermidine is enhancing tomato tolerance to salinity-alkalinity stress by regulating chloroplast antioxidant system and chlorophyll metabolism. *BMC Plant Biol.* 15:303. doi: 10.1186/s12870-015-0699-7
- Mahdavi, B. (2013). Seed germination and growth responses of Isabgol (*Plantago ovata* Forsk) to chitosan and salinity. *Int. J. Agric. Crop Sci.* 5, 1084–1088.
- Medeiros M. J. L., Silva M. M. A., Granja, M. M. C., Souza e Silva Júnior, G., Camara, T. R., Willadino, L. et al. (2015). Effect of exogenous proline in two sugarcane genotypes grown *in vitro* under salt stress. *Acta biol. Colomb.* 20, 57–63. doi: 10.15446/abc.v20n2.42830
- Murashige, T., and Skoog, F. (1962). A revised medium for rapid growth and bioassays with tobacco tissue cultures. *Physiol. Plant.* 15, 473–497. doi: 10.1111/j.1399-3054.1962.tb08052.x
- Perry, E. M., and Roberts, D. A. (2008). Sensitivity of narrow-band and broad-band indices for assessing nitrogen availability and water stress in an annual crop. *Agron. J.* 100:1211. doi: 10.2134/agronj2007.0306
- Pichyangkura, R., and Chadchawan, S. (2015). Biostimulant activity of chitosan in horticulture. *Sci. Hortic.* 196, 49–65. doi: 10.1016/j.scienta.2015.09.031
- Podlešáková, K., Ugena, L., Spichal, L., Doležal, K., and De Diego, N. (2018). Phytohormones and polyamines regulate plant stress responses by altering GABA pathway. *N. Biotechnol.* doi: 10.1016/j.nbt.2018.07.003 [Epub ahead of print].
- Pouvreau, J.-B., Gaudin, Z., Auger, B., Lechat, M.-M., Gauthier, M., Delavault, P., et al. (2013). A high-throughput seed germination assay for root parasitic plants. *Plant Methods* 9:32. doi: 10.1186/1746-4811-9-32
- Povero, G., Mejia, J. F., Di Tommaso, D., Piaggese, A., and Warrior, P. (2016). A systematic approach to discover and characterize natural plant biostimulants. *Front. Plant Sci.* 7:435. doi: 10.3389/fpls.2016.00435
- Rahaman, M. M., Ahsan, M. A., Gillani, Z., and Chen, M. (2017). Digital biomass accumulation using high-throughput plant phenotype data analysis. *J. Integr. Bioinform.* 14, 1–13. doi: 10.1515/jib-2017-0028
- Rodríguez-Furlán, C., Miranda, G., Reggiardo, M., Hicks, G. R., and Norambuena, L. (2016). High throughput selection of novel plant growth regulators: assessing the translatability of small bioactive molecules from *Arabidopsis* to crops. *Plant Sci.* 245, 50–60. doi: 10.1016/j.plantsci.2016.01.001
- Roychoudhury, A., Basu, S., and Sengupta, D. N. (2011). Amelioration of salinity stress by exogenously applied spermidine or spermine in three varieties of indica rice differing in their level of salt tolerance. *J. Plant Physiol.* 168, 317–328. doi: 10.1016/j.jplph.2010.07.009
- Sabagh, A., El Islam, M. S., Ueda, A., Saneoka, H., and Barutçular, C. (2015). Increasing reproductive stage tolerance to salinity stress in soybean. *Int. J. Agric. Crop Sci.* 8, 738–745.
- Savvides, A., Ali, S., Tester, M., and Fotopoulos, V. (2016). Chemical priming of plants against multiple abiotic stresses: mission possible? *Trends Plant Sci.* 21, 329–340. doi: 10.1016/j.tplants.2015.11.003
- Sharma, H. S. S., Fleming, C., Selby, C., Rao, J. R., and Martin, T. (2014). Plant biostimulants: a review on the processing of macroalgae and use of extracts for crop management to reduce abiotic and biotic stresses. *J. Appl. Phycol.* 26, 465–490. doi: 10.1007/s10811-013-0101-9
- Sharma, H. S. S., Selby, C., Carmichael, E., McRoberts, C., Rao, J. R., Ambrosino, P., et al. (2016). Physicochemical analyses of plant biostimulant formulations and characterisation of commercial products by instrumental techniques. *Chem. Biol. Technol. Agric.* 3:13. doi: 10.1186/s40538-016-0064-6
- Shekari, F., Danalo, A. A., and Mustafavi, S. H. (2015). Exogenous polyamines improve seed germination of borage under salt stress via involvement in antioxidant defenses. *WALLA J.* 31, 57–63.
- Shu, S., Yuan, L. Y., Guo, S. R., Sun, J., and Liu, C. J. (2012). Effects of exogenous spermidine on photosynthesis, xanthophyll cycle and endogenous polyamines in cucumber seedlings exposed to salinity. *Afr. J. Biotechnol.* 11, 6064–6074. doi: 10.5897/AJB11.1354
- Shu, S., Yuan, Y., Chen, J., Sun, J., Zhang, W., Tang, Y., et al. (2015). The role of putrescine in the regulation of proteins and fatty acids of thylakoid membranes under salt stress. *Sci. Rep.* 5:14390. doi: 10.1038/srep14390
- Silva, A. T., Ligterink, W., and Hilhorst, H. W. M. (2017). Metabolite profiling and associated gene expression reveal two metabolic shifts during the seed-to-seedling transition in *Arabidopsis thaliana*. *Plant Mol. Biol.* 95, 481–496. doi: 10.1007/s11103-017-0665-x
- Talat, A., Nawaz, K., Hussian, K., Bhatti, K. H., Siddiqi, E. H., Khalid, A., et al. (2013). Foliar application of proline for salt tolerance of two wheat (*Triticum aestivum* L.) cultivars. *World Appl. Sci. J.* 22, 547–554. doi: 10.5829/idosi.wasj.2013.22.04.19570
- Tanabata, T., Shibaya, T., Hori, K., Ebana, K., and Yano, M. (2012). SmartGrain: high-throughput phenotyping software for measuring seed shape through image analysis. *Plant Physiol.* 160, 1871–1880. doi: 10.1104/pp.112.205120
- Teh, C. Y., Shaharuddin, N. A., Ho, C. L., and Mahmood, M. (2016). Exogenous proline significantly affects the plant growth and nitrogen assimilation enzymes activities in rice (*Oryza sativa*) under salt stress. *Acta Physiol. Plant* 38:151. doi: 10.1007/s11738-016-2163-1
- Thiam, M., Champion, A., Diouf, D., and Mame Ourèye, S. Y. (2013). NaCl effects on *in vitro* germination and growth of some senegalese cowpea (*Vigna unguiculata* (L.) Walp.) Cultivars. *ISRN Biotechnol.* 2013:382417. doi: 10.5402/2013/382417
- Van Oosten, M. J., Pepe, O., De Pascale, S., Silletti, S., and Maggio, A. (2017). The role of biostimulants and bioeffectors as alleviators of abiotic stress in crop plants. *Chem. Biol. Technol. Agric.* 4:5. doi: 10.1186/s40538-017-0089-5
- Yakhin, O. I., Lubyantsev, A. A., Yakhin, I. A., and Brown, P. H. (2016). Biostimulants in plant science: a global perspective. *Front. Plant Sci.* 7:2049. doi: 10.3389/fpls.2016.02049
- Zeng, D., Luo, X., and Tu, R. (2012). Application of bioactive coatings based on chitosan for soybean seed protection. *Int. J. Carbohydr. Chem.* 2012, 1–5. doi: 10.1155/2012/104565

Conflict of Interest Statement: The authors declare that the research was conducted in the absence of any commercial or financial relationships that could be construed as a potential conflict of interest.

Copyright © 2018 Ugena, Hýlová, Podlešáková, Humplík, Doležal, De Diego and Spichal. This is an open-access article distributed under the terms of the Creative Commons Attribution License (CC BY). The use, distribution or reproduction in other forums is permitted, provided the original author(s) and the copyright owner(s) are credited and that the original publication in this journal is cited, in accordance with accepted academic practice. No use, distribution or reproduction is permitted which does not comply with these terms.

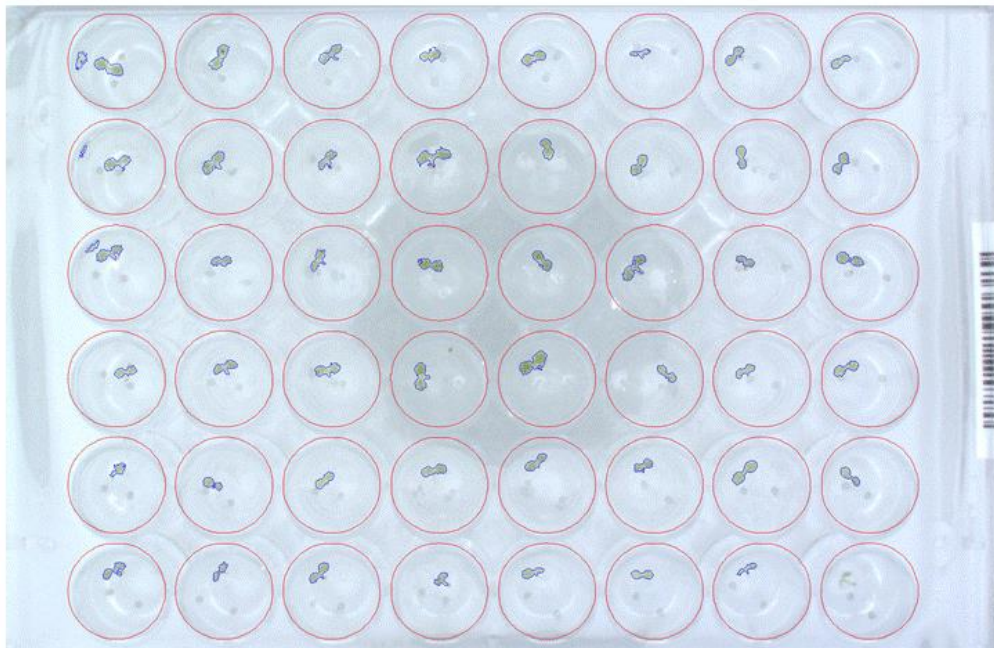


Figure S1. *Arabidopsis* rosette growth in 48 multi-well plates for 7 days under control conditions.

Table S1. Statistical differences in the green area (pixels) of 4 DAG *Arabidopsis* seedlings from three different size categories of seeds (250–280, 280–300, and >300 µm) grown in 48-well plates (three biological replicates per treatment) for 7 days. Different letters indicate significant differences according to multiple comparisons performed after ANOVA.

	Day 2		Day 3		Day 4		Day 5		Day 6		Day 7
	10:00 h	16:00 h	10:00 h	16:00 h	10:00 h	16:00 h	10:00 h	16:00 h	10:00 h	16:00 h	10:00 h
ANOVA	$p < 0.001$ ***	$p < 0.001$ ***	$p < 0.001$ ***	$p = 0.0301$ *	$p < 0.001$ ***	$p < 0.001$ ***	$p < 0.001$ ***	$p < 0.001$ ***	$p < 0.001$ ***	$p < 0.001$ ***	$p < 0.001$ ***
250-280 µm	b	b	b	b	b	b	b	b	b	b	b
280-300 µm	a	a	a	ab	a	a	a	a	a	a	a
>300 µm	a	a	a	a	a	a	a	a	a	a	a

Note: multiple comparison according Dunn & Sidák’s approach after ANOVA

Blue colour	Significantly higher size compared to 250-280 µm
-------------	--

Table S2. Statistical differences in the green area (pixels) of 4 DAG *Arabidopsis* seedlings primed with Put, Spd, Spm, and Pro at four concentrations (0.001, 0.01, 0.1, and 1 mM) and grown under control, moderate (75 mM NaCl) and severe (150 mM NaCl) salt stress conditions for 7 days. Different letters indicate significant differences according to multiple comparisons performed after ANOVA.

Control conditions

		Day 1		Day 2	Day 3		Day 4		Day 5		Day 6		Day 7
		10:00 h	16:00 h	16:00 h	10:00 h	16:00 h	10:00 h	16:00 h	10:00 h	16:00 h	10:00 h	16:00 h	10:00 h
Putrescine	ANOVA	$p < 0.001$ *** $p < 0.001$ ***		$p < 0.001$ ***	$p < 0.001$ ***	$p < 0.001$ ***	$p < 0.001$ ***	$p < 0.001$ ***	$p < 0.001$ ***	$p < 0.001$ ***	$p < 0.001$ ***	$p < 0.001$ ***	$p < 0.001$ ***
	H ₂ O	b	b	b	b	b	b	b	b	b	b	b	b
	0.001 mM	a	a	a	a	a	a	a	a	a	a	a	a
	0.01 mM	a	a	a	a	a	a	a	a	a	a	a	a
	0.1 mM	ab	a	a	a	ab	a	a	a	a	a	a	a
	1 mM	a	a	a	a	a	a	a	a	a	a	a	a
Spermidine	ANOVA	$p < 0.001$ *** $p < 0.001$ ***		$p < 0.001$ ***	$p < 0.001$ ***	$p < 0.001$ ***	$p < 0.001$ ***	$p < 0.001$ ***	$p < 0.001$ ***	$p < 0.001$ ***	$p < 0.001$ ***	$p < 0.001$ ***	$p < 0.001$ ***
	H ₂ O	b	b	b	b	b	b	b	b	b	b	b	b
	0.001 mM	a	a	a	a	a	a	a	a	a	a	a	a
	0.01 mM	a	a	a	a	a	a	a	a	a	a	a	a
	0.1 mM	ab	ab	ab	ab	ab	ab	ab	a	a	a	ab	ab
	1 mM	a	a	a	a	a	a	a	a	a	a	a	a
Spermine	ANOVA	$p < 0.001$ *** $p < 0.001$ ***		$p < 0.001$ ***	$p < 0.001$ ***	$p < 0.001$ ***	$p < 0.001$ ***	$p < 0.001$ ***	$p < 0.001$ ***	$p < 0.001$ ***	$p < 0.001$ ***	$p < 0.001$ ***	$p < 0.001$ ***
	H ₂ O	b	b	b	b	b	b	bc	bc	bc	bc	bc	bc
	0.001 mM	a	a	a	a	a	a	a	a	a	a	a	a
	0.01 mM	a	a	a	a	a	a	a	a	ab	ab	ab	ab
	0.1 mM	a	a	a	a	a	a	ab	ab	ab	a	ab	ab
	1 mM	b	b	b	b	b	b	c	c	c	c	c	c
Proline	ANOVA	$p < 0.001$ *** $p < 0.001$ ***		$p < 0.001$ ***	$p < 0.001$ ***	$p < 0.001$ ***	$p < 0.001$ ***	$p < 0.001$ ***	$p < 0.001$ ***	$p < 0.001$ ***	$p < 0.001$ ***	$p < 0.001$ ***	$p < 0.001$ ***
	H ₂ O	b	b	b	b	a	b	b	b	b	b	b	b
	0.001 mM	b	b	c	c	b	c	c	c	c	c	c	c
	0.01 mM	b	b	c	c	b	c	c	c	c	c	c	c
	0.1 mM	a	a	a	a	ab	ab	ab	ab	ab	ab	ab	ab
	1 mM	a	a	a	a	a	a	a	a	a	a	a	a

Note: multiple comparison according Dunn & Sidák's approach after ANOVA

Blue colour	Significantly higher size compared to control
Red colour	Significantly lower size compared to control

Table S2. Continued.

75 mM NaCl

		Day 1		Day 2	Day 3		Day 4		Day 5		Day 6		Day 7
		10:00 h	16:00 h	16:00 h	10:00 h	16:00 h	10:00 h	16:00 h	10:00 h	16:00 h	10:00 h	16:00 h	10:00 h
Putrescine	ANOVA	$p < 0.001$ ***	$p < 0.001$ ***	$p < 0.001$ ***	$p < 0.001$ ***	$p < 0.001$ ***	$p < 0.001$ ***	$p < 0.001$ ***	$p < 0.001$ ***	$p < 0.001$ ***	$p < 0.001$ ***	$p < 0.001$ ***	$p < 0.001$ ***
	H ₂ O	b	b	b	b	b	b	b	b	b	b	b	b
	0.001 mM	a	a	a	a	a	a	a	a	a	a	a	a
	0.01 mM	a	a	a	a	a	a	a	a	a	a	a	a
	0.1 mM	a	ab	ab	a	a	a	a	a	a	a	a	a
	1 mM	ab	ab	ab	a	a	a	a	a	a	a	a	a
Spermidine	ANOVA	$p < 0.001$ ***	$p < 0.001$ ***	$p < 0.001$ ***	$p < 0.001$ ***	$p < 0.001$ ***	$p < 0.001$ ***	$p < 0.001$ ***	$p < 0.001$ ***	$p < 0.001$ ***	$p < 0.001$ ***	$p < 0.001$ ***	$p < 0.001$ ***
	H ₂ O	b	b	b	b	b	b	b	b	b	b	b	b
	0.001 mM	a	a	a	a	a	a	a	a	a	a	a	a
	0.01 mM	a	a	a	a	a	a	a	a	a	a	a	a
	0.1 mM	a	a	a	a	ab	a	a	a	a	a	a	a
	1 mM	a	a	a	a	a	a	a	a	a	a	a	a
Spermine	ANOVA	$p < 0.001$ ***	$p < 0.001$ ***	$p = 0.1118$	$p < 0.001$ ***	$p < 0.001$ ***	$p < 0.001$ ***	$p < 0.001$ ***	$p < 0.001$ ***	$p < 0.001$ ***	$p < 0.001$ ***	$p < 0.001$ ***	$p < 0.001$ ***
	H ₂ O	b	b	a	b	b	b	b	b	b	b	b	b
	0.001 mM	a	a	a	a	a	a	a	a	a	ab	ab	ab
	0.01 mM	ab	a	a	a	a	ab	ab	ab	ab	ab	ab	ab
	0.1 mM	a	a	a	a	a	a	a	a	a	a	a	a
	1 mM	a	a	a	a	a	a	a	ab	ab	ab	ab	ab
Proline	ANOVA	$p < 0.001$ ***	$p < 0.001$ ***	$p < 0.001$ ***	$p < 0.001$ ***	$p < 0.001$ ***	$p < 0.001$ ***	$p < 0.001$ ***	$p < 0.001$ ***	$p < 0.001$ ***	$p < 0.001$ ***	$p < 0.001$ ***	$p < 0.001$ ***
	H ₂ O	b	b	a	b	b	b	b	b	b	b	b	b
	0.001 mM	c	c	b	b	b	bc	bc	bc	bc	bc	bc	bc
	0.01 mM	bc	bc	a	b	b	c	c	c	c	c	c	c
	0.1 mM	ab	ab	a	ab	ab	ab	ab	ab	ab	ab	ab	ab
	1 mM	a	a	a	a	a	a	a	a	a	a	a	a

Note: multiple comparison according Dunn & Sidák's approach after ANOVA

Blue colour	Significantly higher size compared to control
Red colour	Significantly lower size compared to control

Table S2. Continued.

150 mM NaCl

		Day 1		Day 2	Day 3		Day 4		Day 5		Day 6		Day 7
		10:00 h	16:00 h	16:00 h	10:00 h	16:00 h	10:00 h	16:00 h	10:00 h	16:00 h	10:00 h	16:00 h	10:00 h
Putrescine	ANOVA	$p < 0.001$ ***	$p < 0.001$ ***	$p < 0.001$ ***	$p < 0.001$ ***	$p < 0.001$ ***	$p < 0.001$ ***	$p < 0.001$ ***	$p < 0.001$ ***	$p < 0.001$ ***	$p < 0.001$ ***	$p < 0.001$ ***	$p < 0.001$ ***
	H ₂ O	b	b	b	b	b	b	b	b	b	b	b	b
	0.001 mM	a	a	a	a	a	a	a	a	a	a	a	a
	0.01 mM	ab	ab	ab	ab	ab	a	ab	ab	ab	a	ab	ab
	0.1 mM	ab	ab	ab	ab	a	a	a	a	a	a	a	a
	1 mM	a	a	a	a	a	a	a	a	a	a	a	a
Spermidine	ANOVA	$p < 0.001$ ***	$p < 0.001$ ***	$p < 0.001$ ***	$p < 0.001$ ***	$p < 0.001$ ***	$p < 0.001$ ***	$p < 0.001$ ***	$p < 0.001$ ***	$p < 0.001$ ***	$p < 0.001$ ***	$p < 0.001$ ***	$p < 0.001$ ***
	H ₂ O	b	b	b	b	b	b	b	b	b	b	b	b
	0.001 mM	a	a	a	a	a	a	a	a	a	a	a	a
	0.01 mM	a	a	a	a	a	a	a	a	a	a	a	a
	0.1 mM	a	a	a	a	a	a	a	a	a	a	a	a
	1 mM	a	a	a	a	a	a	a	a	a	a	a	a
Spermine	ANOVA	$p < 0.001$ ***	$p < 0.001$ ***	$p < 0.001$ ***	$p < 0.001$ ***	$p < 0.001$ ***	$p < 0.001$ ***	$p < 0.001$ ***	$p < 0.001$ ***	$p < 0.001$ ***	$p < 0.001$ ***	$p < 0.001$ ***	$p < 0.001$ ***
	H ₂ O	b	b	b	b	b	b	b	b	b	b	b	b
	0.001 mM	b	b	b	b	b	b	b	b	b	b	b	b
	0.01 mM	a	a	a	a	a	a	a	a	a	a	a	a
	0.1 mM	a	a	a	a	a	a	a	a	a	a	a	a
	1 mM	a	a	a	a	a	a	a	a	a	a	a	ab
Proline	ANOVA	$p < 0.001$ ***	$p < 0.001$ ***	$p < 0.001$ ***	$p < 0.001$ ***	$p < 0.001$ ***	$p < 0.001$ ***	$p < 0.001$ ***	$p < 0.001$ ***	$p < 0.001$ ***	$p < 0.001$ ***	$p < 0.001$ ***	$p < 0.001$ ***
	H ₂ O	a	a	a	a	a	a	a	a	a	a	a	a
	0.001 mM	b	b	b	b	b	b	b	b	b	b	b	b
	0.01 mM	ab	ab	b	ab	ab	b	b	b	b	b	b	b
	0.1 mM	b	b	b	b	b	b	ab	ab	ab	ab	ab	b
	1 mM	ab	ab	b	b	ab	ab	ab	ab	ab	ab	ab	ab

Note: multiple comparison according Dunn & Sidák's approach after ANOVA

Blue colour	Significantly higher size compared to control
Red colour	Significantly lower size compared to control